Study of the physiological function of carnitine palmitoyltransferase 1C enzyme

Patricia Carrasco Rodríguez

UNIVERSITAT DE BARCELONA

Facultat de Farmàcia

Departament de Bioquímica i Biologia Molecular

STUDY OF THE PHYSIOLOGICAL FUNCTION OF CARNITINE PALMITOYLTRANSFERASE 1C ENZYME

Patricia Carrasco Rodríguez

2012

UNIVERSITAT DE BARCELONA

Facultat de Farmàcia

Departament de Bioquímica i Biologia Molecular
Programa de doctorat de Biotecnologia

STUDY OF THE PHYSIOLOGICAL FUNCTION OF CARNITINE PALMITOYLTRANSFERASE 1C ENZYME

Memòria presentada per Patricia Carrasco Rodríguez per optar al títol de doctor per la Universitat de Barcelona.

Dra. Núria Casals Farré
Directora de tesi
Universitat Internacional de Catalunya

Dra. Dolors Serra Cucurull
Tutor de tesi
Universitat de Barcelona

Patricia Carrasco Rodríguez
Doctoranda

A MI FAMILIA Y AMIGOS.

Nunca consideres el estudio como una obligación, sino como una oportunidad para penetrar en el bello y maravilloso mundo del saber.

Mai consideris l'estudi com una obligació, sinó com una oportunitat per penetrar en el bell i meravellós món del saber.

Never consider the study as an obligation but as an opportunity to enter the beautiful and wonderful world of knowledge.

Betrachte das Studium nicht als Verpflichtung, sondern als Möglichkeit in die wunderbare und schöne Welt des Wissens einzutauchen.

Albert Einstein

AGRADECIMIENTOS

El camino ha sido duro, pero gracias a todos vosotros, este trabajo ha sido posible. Por ello, me gustaría agradecer a:

Mis compañeras de la facultad, a Paula, Rocio, Montse, Laura y Mónica, por los buenos momentos que pasamos en prácticas y en el bar.

A mi directora de tesis, Núria, por confiar en mí y darme la oportunidad de poder realizar la tesis bajo su dirección y así empezar en el fantástico mundo de la investigación. Gracias por todo lo que me has enseñado y por tener la puerta siempre abierta para resolver cualquier problema. A Pep, por sus consejos, sus críticas, y sus ánimos durante toda la tesis. Gracias también a Agustín y aunque ya no esté entre nosotros, a Núria Durany, por darme la oportunidad de entrar en la UIC.

Al Dr. Fausto García Hegardt, por quien siento un gran respeto y admiración, gracias por sus consejos y sus aportaciones. Gracias a vosotras también, Guille y Dolors, por vuestros consejos, por vuestra disponibilidad, por los ánimos y por todas las gestiones realizadas durante mi tesis. Muchísimas gracias a ti también Laura, por tus consejos y tu ejemplo del saber hacer, por tu capacidad de ayudar siempre a los demás y por estar ahí siempre que te lo he pedido, muchísimas gracias. A todos los del lab de Farmacia, a todos los del inicio, al David, Toni, Irene, Assia, Chandru y Yolanda, los cuales me dejaron sorprendida en mis primeros seminarios de grupo. A los de la etapa actual, a Paula y Pep por su amistad y apoyo y a Joan, Mida, Mar, Iván y Kamil, por compartir semana tras semana nuestro trabajo.

Gracias a Mara, por darme la oportunidad de realizar los experimentos de conducta en su laboratorio, sin los cuales, esta tesis no hubiese sido posible. Gracias a ti Ignasi, por todo lo que me enseñaste, por tu ayuda, tu buen humor, y tus consejos. A ti también Jerome, por pasar esas Navidades conmigo haciendo conducta y por todo lo que me ayudaste.

Gracias a ti Amparo, por darme la oportunidad de poder hacer una estancia fuera, por presentarme un día en tu laboratorio y abrirme sus puertas. Gracias también a toda la gente del laboratorio, a Mathias, Helge, Aycan, Eva, Sylvia, Julia, Florian, Marta, Miriam, Susanne, Ricarda y Ioanna, gracias por acogerme tan bien en vuestro laboratorio y ayudarme en todo lo que necesité. Gracias!

A toda la gente que conocí en Frankfurt, sin los cuales mi estancia allí hubiese sido más dura y los que han contribuido en parte a la creación de este manuscrito, gracias por sus consejos, sus correcciones, sobretodo dar las gracias a Angel y Tine, que sin dudarlo me prestaron su ayuda para las correcciones, gracias también a Marcos Medina por su ayuda, su apoyo y su amistad y, así como a Andrea, Madhu, Christian, Fiona, Eike y Jordi, por estar siempre ahí y ayudarme con el inglés!

A todos los de la UIC, mil gracias! Gracias por estar siempre, siempre ahí, en los momentos buenos y no tan bueno. Gracias por llevarme amigos y no compañeros, gracias por las terapias de grupo y por hacer que estos años de tesis sean inolvidables. Decir que os echaré de menos a cada uno de vosotros. A los yeast´s group, a Sara y Samuel, a Naty, decirle que voy a echar de menos por sus piropos diarios, a Sandra, por su sonrisa y su apoyo durante toda la tesis, por preocuparse de mi en cada momento. A la cap del laboratorio, Marta, por su alegría y por estar siempre ahí para ayudarme en todo lo que necesitaba. A los Durany-Pitch, gracias a Alex, Aloa, Mónica, os echaré de menos en los desayunos y en meriendas y a Tània, mi compañera de escritorio durante todos estos años, Tània, gracias por todo tu apoyo, por los consejos científicos y por tu amistad. A los del grupo del Maher, a Carles, Jordi, Esther y a los que se fueron, Dani y Marc. Y por último, a los mi grupo, a Helena y Macarena, las nuevas incorporaciones del grupo, a Jordi por su amistad y su ayuda con el HPLC y a mi flor, Sara, la que me

alegra el día, te voy a echar muchísimo de menos. Y a los que ya no están en él, a Adriana y sobretodo a Esther, de la que he aprendido muchísimo ya que además de ser una gran madre, es una gran científica, gracias por todo tu apoyo durante toda la tesis y sobretodo en la parte final.

Y bueno, por últimos que decir, todo este Trabajo no lo hubiese podido hacer sin la ayuda de mi familia, gracias a mis padres, por su excelente educación y por su esfuerzo para que esto haya sido posible, gracias por haber dedicado toda la vida a cuidarnos. Y que decir de mi hermana, la cual ha seguido mis pasos, y estoy segura de que se convertirá en una excelente científica, con la que comparto todas las alegrías y las penas día a día, gracias por tu alegría. Y por último, agradecerte a ti, Paco, mi medio biólogo, por todo tu cariño, tu apoyo y por toda tu paciencia a lo largo de estos años. Gracias por tu tozudez, porque sin ella, nunca me hubiese ido a hacer una estancia fuera. Gracias por estar siempre a mi lado.

"Cuando veas tus metas cumplidas y tus sueños hechos realidad, no te sientes a contemplar lo que has logrado. Es hora de buscar nuevas metas y de soñar aun más"

TABLE OF CONTENTS

INTRODUCTION

CHAPTER 1 : INTRODUCTION

1.1 CARNITINE ACYLTRANSFERASES

Mitochondria fatty acid oxidation (FAO) is essential for energy homeostasis in situations that require simultaneous glucose sparing and major supply, such as prolonged fasting or exercise. Fatty acids are catabolized mostly in the mitochondria through the β-oxidation pathway. The transport of fatty acids is performed by a group of enzymes with acyltransferase activity (carnitine acyltransferase family) and a transporter in the inner mitochondrial membrane (McGarry, J.D. 1989). Different enzymes belong to the carnitine acyltransferase family, each of them having specificity for a determinate length of the fatty acyl group used as a substrate:

- Carnitine acetyltransferase (CrAT or CAT) uses acetyl-CoA as a substrate (Bieber, L.L. 1988).
- Carnitine octanoyltransferase (CrOT or COT) facilitates transport of fatty acids (C8-C10) from peroxisomes to mitochondria (Ferdinandusse, S. 1999).
- Carnitine palmitoyltransferases (CPTs) 1 and 2 facilitate the transport of long chain fatty acids (C16-C20) to the mitochondrial matrix where they will be β-oxidated (McGarry, J.D. 1989).

1.1.1 Carnitine palmitoyltransferases 1

Long chain fatty acyls can be used to obtain energy through the β-oxidation into the mitochondria or they can be used for the synthesis of complex lipids in the endoplasmic reticulum.

Whether long chain fatty acids (LCFA) are used to the β-oxidation, they cannot enter into the mitochondria by simple diffusion, contrary to medium or short chain fatty acids, therefore, consecutive trans-esterification reactions are required (Figure 1).

The first component of this system is the carnitine palmitoyltransferase 1 (CPT1), an integral transmembrane of the mitochondrial outer membrane that catalyzes the transfer of acyl moieties from CoA to carnitine. The acylcarnitine product can traverse the inner membrane by means of a carnitine-acylcarnitine translocase (CACT). CPT2, on the matrix side of the inner membrane, reverse the reaction, retransferring the acyl-group to CoA-SH. The acyl-CoA then undergoes β-oxidation and ultimately yiels acetyl-CoA (Zammit, V.A. 2008; Rufer, A.C. 2009).

The reaction catalyzed by CPT1 is the key regulatory site controlling the flux through β-oxidation, by virtue of its inhibition by malonyl-CoA, an intermediate in fatty acid biosynthesis (McGarry, J.D. 1980). This reaction is not only central to the control of fatty acid oxidation, but it also determines the availability of long chain acyl-CoA for other processes, notable the synthesis of complex lipids.

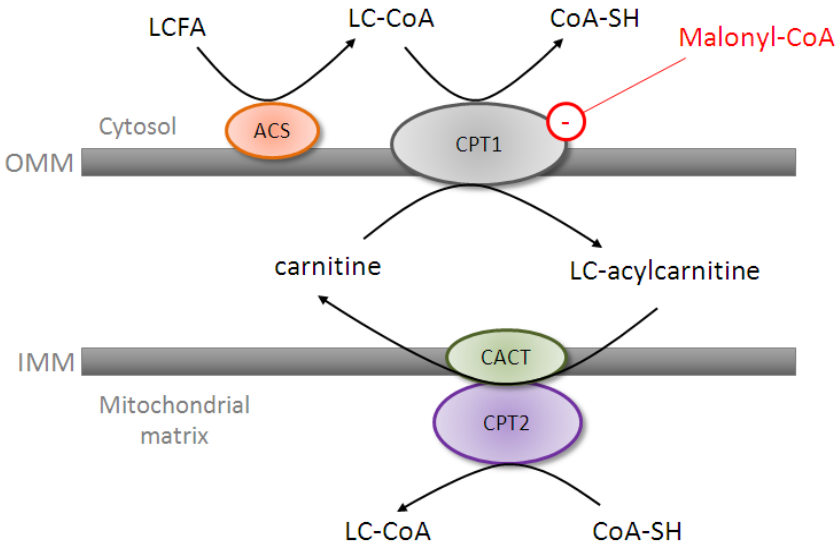

Figure 1: LCFA translocation into the mitochondria by the carnitine palmitoyltransferase system. LCFA (long chain fatty acids) are activated to LC-CoA by the action of the acyl-CoA synthetase (ACS). Transport of LC-CoA from the cytosol to the mitochondrial matrix involves the conversion of LC-CoA to acylcarnitines by CPT1, translocation across the mitochondrial inner membrane by the carnitine acylcarnitine translocase (CACT) and reconversion to LC-CoA by CPT2. The physiological inhibition of CPT1 enzymes by malonyl-CoA is also represented (in red). OMM: outer mitochondrial membrane; IMM: inner mitochondrial membrane.

While CPT2 is the same protein bodywide (Demaugre, F. 1990), three tissue-specific isoforms of CPT1s have been identified in mammals:

- **CPT1A** is the most widely expressed and the most extensively studied isoform. It is so-called liver isoform or L-CPT1. It is found in liver, kidney, lung, spleen, intestine, ovary and brain (McGarry, J.D. 1997).
- **CPT1B** is the second isoform to be discovered. It is highly expressed in skeletal muscle, heart, adipose tissue and testis. This isoform is also called M-CPT1 (Esser, V. 1996; Yamazaki, N. 1995).
- **CPT1C** is the most recently discovered (Price, N. 2002) and it is specific from the brain, although shows lower levels of protein in testis, ovary, small intestine, and colon. It has high homology sequence with the other isoforms although its function and regulation are not well defined.

In this study, all three genes and isoforms will be referred using capital letters. A, B and C will be used to specify each isoform.

1.1.1.1 CPT1A and CPT1B

CPT1A and CPT1B have been extensively studied since they were cloned for the first time. The identity in amino acid residues is high (62%), but both isozymes present different kinetic and regulatory properties: CPT1A displays higher affinity for its substrate carnitine (Km ≈ 30 µM) and long chain fatty acyls (Km for palmitoyl-CoA ≈ 40-150 µM), while CPT1B shows lower affinity for the substrate (Km ≈ 500 µM) although presents more affinity for long chain fatty acyls-CoA. The sensibility to the physiological inhibitor, malonil-CoA is 30 to 100 times higher in CPT1B (IC_{50} ~ 0.03 µM) than the liver pisoform, CPT1A (IC_{50} ~ 2.5 µM) (Esser, V. 1996; McGarry, J.D. 1997; Zammit, V.A. 2008). This differential sensitivity to the

reversible inhibitor of the enzyme is probably involved in the finer regulation of fatty acid oxidation in heart and skeletal muscle, in comparison to liver (Table 1).

CPT1A and CPT1B are encoded in different chromosomes and exhibit different tissue distribution. The primary structures predicted from cDNAs show a high degree of homology with calculated molecular masses of 88.15 KDa (773 amino acids) and 88.27 KDa (772 amino acids) for the liver and skeletal muscle isoforms, respectively (Table 1).

	CPT1A	CPT1B
Amino acids	773	772
Mass	88 kDa	88 kDa
Malonyl-CoA IC_{50}	2.5 µM	0.03 µM
Carnitine K_m	30 µM	500 µM
Human chromosome locus	11q13	22q13.3

Table 1: Characteristics of mitochondrial CPT1 enzymes (Table modified from McGarry, J.D. 1997).

Both isoforms are located in the outer mitochondrial membrane with two transmembrane domains (TM1 and TM2) and the N- and C-termini facing the cytosolic side (Fraser, F. 1997; Zammit, V.A. 2008). It has been demonstrated that residues within the N-terminal domain of CPT1A (comprised among amino acid position 1-150), including both transmembrane domains and a downstream region, contain key information for directing the enzyme to its target localization (Cohen, I. 1998; Cohen, I. 2001).

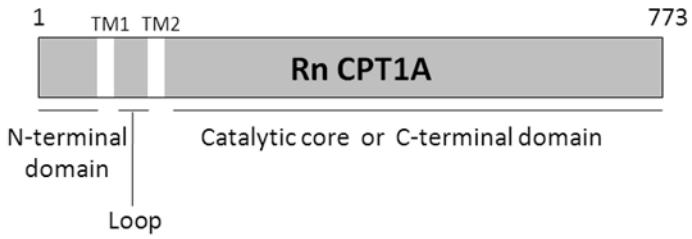

Figure 2: Schematic representation of the structural domains of rat CPT1A sequence. TM1 (residues 48-75) and TM2 (residues 103-122) represent domains traversing the outer mitochondrial membrane. N- and C-terminal domains are facing the cytosol and the loop region is oriented towards the intermembranous space.

In addition, the amino acid residues that are critical for catalytic activity or malonyl-CoA sensitivity have been identified for both enzymes, and three-dimensional structures have been predicted (Figure 3) based on the carnitine acetyltransferase (CAT), carnitine octanoyltransferase (COT) and carnitine palmitoyltransferase 2 crystals (CPT2) (Lopez-Vinas, E. 2007).

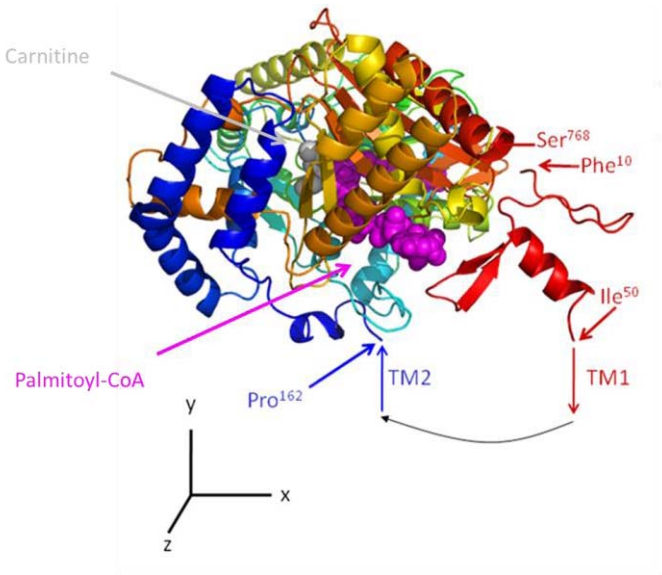

Figure 3: Structural model of rat CPT1A. A proposed model for CPT1A is shown in the ribbon plot representation. The putative sites for carnitine (gray) and palmitoyl-CoA (magenta) are indicated. A frontal view of the model in which residues flanking the modeled region have been highlighted [regions modeled: from Phenilalanine 10 to Isoleucine 50 (in blue) and from Proline 162 to Serine 768]. In this model, the hypothetic position of transmembrane domains 1 and 2 (TM1, TM2), and the loop region between them, have been represented by red, blue and black arrows respectively.

The most important residue for the catalysis in CPT1A is His^{473} because when it is mutated, catalytic activity is abolished (Morillas, M. 2001). It has also been shown that mutations in Glu^{26} and Lys^{561} decrease malonyl-CoA sensitivity, confirming that interactions between the N- and C-terminal domains are critical for malonyl-CoA binding and sensitivity (Lopez-Vinas, E. 2007).

1.1.1.1.1 Physiological regulation of CPT1A and CPT1B in liver and muscle

CPT1 is tightly regulated by its physiological inhibitor malonyl-CoA, and thus CPT1 is the most physiologically important regulatory step in mitochondrial fatty acid oxidation (McGarry and Foster, 1980). This process allows the cell to signal the relative availability of lipid and carbohydrate fuels in liver, heart, skeletal muscle, and pancreatic β-cells (Zammit, V.A. 1999).

In the liver, malonyl-CoA acts as a key metabolite which ensures that fatty acid oxidation and *de novo* fatty acid synthesis do not occur simultaneously. In case of carbohydrate feeding (high insulin), hepatic lipogenesis is active, the concentration of malonyl-CoA rises, CPT1 is suppressed and newly formed LC-CoA are directed into esterification products (triacylglycerides, TAG) forming very-low density lipoproteins (VLDL). VLDLs are then transported to adipose tissue for storage (McGarry, J.D. 1997). Conversely, in ketotic states (low insulin) carbon flow through glycoslysis diminishes, malonyl-CoA levels fall and fatty acid synthesis comes to a halt. In this context, CPT1 is highly activated and incoming free fatty acids (FFA) readily undergo β-oxidation with accelerated production of ketone bodies (McGarry, J.D. 1980; McGarry, J.D. 1989).

In the case of non lipogenic tissues such as heart and skeletal muscle, malonyl-CoA acts mainly as a signaling intermediate. Malonyl-CoA concentration fluctuates with feeding and fasting, as in liver (McGarry, J.D. 1983). Thus, the flux of synthesis and turnover of malonyl-CoA mediates the fatty acid oxidative potential of muscle (Wolfgang, M.J. 2006). During fasting, malonyl-CoA levels decrease and

CPT1 activity increases the entry of fatty acids into the mitochondria producing a high oxidative rate in muscle. On the other hand, CPT1 inhibition mediated by increases in malonyl-CoA levels produced during feeding decreases the β-oxidation rate. Notably, muscle expresses a mitochondrial bound acetyl-CoA carboxylase (ACC2) that produces malonyl-CoA, but contains little or no fatty acid synthase (FAS). Therefore, malonyl-CoA levels must be cleared through enzymatic activities other than FAS. It has been shown that muscle expresses malonyl-CoA decarboxylase (MCD) in abundance (McGarry, J.D. 1980), thus MCD decreases malonyl-CoA levels in this tissue. The flux of synthesis and turnover of malonyl-CoA mediates the fatty acid oxidation potential of muscle (Wolfgang, M.J. 2006).

1.1.1.1.2 The role of CPT1 in the regulation of food intake and energy homeostasis

Hypothalamic nuclei are responsible for integrating multiple signals (informing about energy status from different peripheral tissues through neuronal and hormonal signals, like insulin, leptin, ghrelin or adipokines) and for responding to changes in energy status by altering the expression of specific neuropeptides (NPY, AgRP, POMC, CART) to adjust food intake to whole body energy demands (Lopez,M. 2008). Restriction of food intake leads to increased firing of a specific subpopulation of neurons, and induces the expression of the hypothalamic orexigenic neuropeptides: neuropeptide Y (NPY) and agouti-related protein (AgRP) mRNAs, and decreases expression of the hypothalamic anorexigenic neuropeptides: proopimelanocortin (POMC) and cocaine-amphetamine-regulated transcript (CART). In combination, these changes provoke increased food intake and reduced energy expenditure. When fasted animals are re-fed, the inverse response occurs (Hu, Z. 2003).

Neurons involved in monitoring the amount of available fuel in the body and thus modulating energy intake and expenditure, must have the ability to sense these conditions through various signals. Different hypothesis have been proposed about the nature of these signal. Recent developments support the lipostatic hypothesis. This hypothesis states that signals proportional to the amount of body fat modulate the amount of food eaten at each meal to maintain whole-body energy balance, via both humoral action and nutrient signaling. The humoral signals proposed to date include leptin and ghrelin, endocannabinoids, insulin, among others. Nutrient signalling energy status can be glucose, circulating free fatty acis or amino acids (Horvath, T.L. 2008). There are evidences supporting each of them:

1. There are glucose-specific sensing mechanism involving ATP, one being the AMPK pathway (described below) and an ATP independent mechanism mediated by glucokinase (Ainscow, E. K. 2002).
2. It has been reported that intracerebroventricular (icv) injection of oleate inhibits food intake (Obici, S. 2002). Other fatty acids did not have any effect on feeding behavior. The physiological source of brain fatty acid is unknown. It is possible that fatty acids are derived from the blood through the leaky blood barrier in the region of the arcuate nucleus of the hypothalamus (a region responsible for monitoring energy status). Alternatively, hypothalamic fatty acids may be of endogenous origin derived from either phospholipid turnover or de novo biosynthesis. It has been shown that hypothalamic neurons possess the metabolic machinery for fatty acid synthesis (Kim, E.K. 2002; Gao, S. 2003).
3. Administration of low doses of leucine in the third ventricle reduced food intake signicantly in rats (Morrison, C.D. 2007). The reduction of food intake is due to the activation of the mammalian target of rapamycin (mTOR) pathway (Cota, D. 2006).

Neurons have developed mechanism to monitor energy availability in the extracellular space. One of these mechanism includes an increase in AMPK activity when AMP/ATP ratio increases, for example during fasting. It is widely accepted that changes in the phosphorilation state of AMPK, an AMP-activated protein kinase, affects the phosphorilation state and activity of ACC, thus affecting feeding

behavior (Kahn, B.B. 2005). It has been shown that activation of AMPK in the hypothalamus, using adenoviruses expressing constitutively active AMPK, is sufficient to increase food intake and body weight whereas repression of hypothalamic AMPK activity, induces anorexia (Minokoshi, Y. 2004). Additionally, alterations in AMPK activity are associated with the corresponding changes in orexigenic and anorexigenic neuropeptide expression (Kim, E.K. 2004).

Both ACC isoforms (ACC1, cytosolic and ACC2, anchored to the outer mitochondrial membrane) are found in hypothalamic neurons and are known to be phosphorylated and thereby inhibited by AMPK. Therefore, activation of AMPK reduces the flux of substrates in the fatty acid biosynthetic pathway and reduces malonyl-CoA levels, which in turn will induce CPT1 activity activating the entry of fatty acids into the mitochondria for β-oxidation (Lopez, M. 2007)

Humoral signal, like leptin and ghrelin, act through similar targets (the hypothalamic AMPK/malonyl-CoA/CPT1 axis) but have opposite effects (figure 4) (Wolfgang, M.J. 2007, Gao, X.2007; Lopez, M. 2008) Centrally administered leptin inhibits hypothalamic AMPK activity, which in turn switches on fatty acid synthesis pathway and decreases oxidation, leading to suppression of food intake (Minokoshi, Y. 2004). Central administration of ghrelin decreases hypothalamic de novo fatty acid synthesis and increases fatty acid oxidation through selective activation of AMPK and CPT, respectively. Pharmacological or genetic inhibition of AMPK or CPT1 blunted ghrelin feeding-promoting effects (Lopez, M. 2008). The effects of ghrelin on hypothalamic mitocondrial respiration and on food intake have been shown to be mediated by UCP2. Fatty acid β-oxidation promotes generation of reactive oxygen species (ROS), which together with fatty acids, promote UCP2 transcription and activity. UCP2 activity neutralizes ROS, enabling continuous CPT-promote fatty acid β-oxidation (Horvath, T. L. 2009)

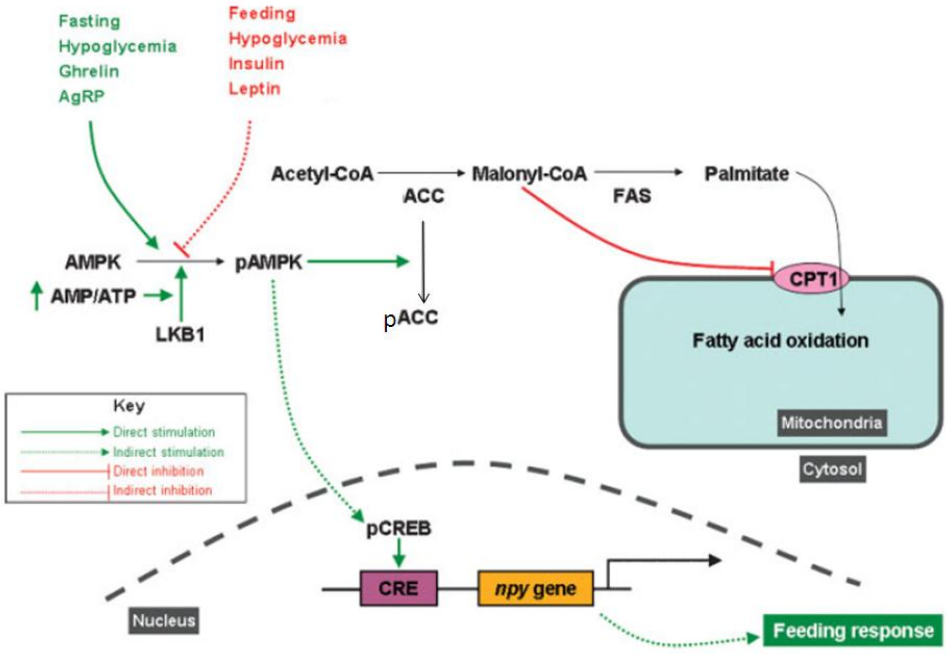

Figure 4: Mechanisms of AMPK regulation in the brain. In the hypothalamus, positive energy balance signals inhibit AMPK phosphorylation, whereas negative energy balance signals stimulate AMPK phosphorylation and activation. These signals are integrated and progress through alterations in the LKB1 pathway. A series of metabolic events (such as modulation of fatty acid synthesis) and gene transcription events (such as npy gene) is initiated, eventually leading to an inhibition or stimulation of the feeding response. (Modified from López, M. 2007).

In fact, affecting hypothalamic CPT1 activity also modifies feeding behaviour. Evidence shows that pharmacologic inhibition of CPT1 in the CNS of rodents, results in reduction of food intake and loss of

body weight (Obici, S. 2003). In the mentioned work, Rossetti and colleagues decreases the activity of CPT1A by administering to rats a ribozyme-containing plasmid designed specifically to decrease the expression of this enzyme, or by icv infusion or pharmacological inhibitors (TDGA or ST1326). They found that either genetic or biochemical inhibition of CPT1 activity was sufficient to substantially decrease food intake and endogenous glucose production in peripheral tissues. These results indicate that changes in the rate of lipid oxitation in selective hypothalamic neurons signaled nutrient availability to the hypothalamus, which in turn modulates feeding behavior, and the endogenous input of nutrients into the circulation (Obici, S. 2003).

It can not be discarded that the effects on feeding behavior are mediated by malonyl-CoA instead of being CPT1 activity itself or the acyl-CoA levels.

In fact, increasing evidence has implicated malonyl-CoA as a possible mediator in the hypothalamic pathway that indicated energy status and mediates the feeding behavior of rodents:

1. **FAS inhibition**: The main evidence stems from the observation that potent pharmacological inhibitors of FAS (C75 and cerulin) suppress food intake causing substantial weight loss in obese as well as lean mice (Loftus, T.M. 2000). The reduction of food intake is rapid (<2h) and dose-dependent and occurs either by intraperitoneal (ip) or icv administration of the inhibitors, being the icv delivery of C75 effective at much lower levels, consistent with a CNS site of action (Loftus, T.M. 2000; Hu, Z. 2003). In addition, icv injection of C75 rapidly increases the concentration of malonyl-CoA in the hypothalamus. Concomitant with the rise in malonyl-CoA, neurons in arcuate nucleus are activated (Gao, S. 2003) followed by down-regulation of key orexigenic and up-regulated of anorexigenic peptides in the hypothalamus (Loftus, T.M. 2000; Hu, Z. 2003). However, prior injection of an ACC inhibitor, which block malonyl-CoA formation, blunts the C75-induced rise in hypothalamic malonyl-CoA concentration and prevents the suppression of food intake (Hu, Z. 2003). These result suggest that levels of malonyl-CoA play a key role by acting both as a substrate of FAS and as an inhibitor of CPT1.

2. **Genetic manipulation of MCD**: Other studies have shown that delibery of viral MCD expression vector into the ventral medial hypothalamus of mice by bilateral stereoractic injection increases food intake and body weight gain and reverses the C75-mediated suppression of food intake (Hu, Z. 2005). Similar effects were obtained when injecting a viral MCD vector in the medial basal hypothalamus of rat. These findings indicate that nutritional modulation of the hypothalamic abundance of malonyl-CoA is required to restrain food intake, and that a primary impairment in this central nutrient-sensing pathway is sufficient to disrupt energy homeostasis and induce obesity.

3. **Physiological levels of malonyl-CoA in the hypothalamus**: It has also been observed that nutritional and physiological perturbations also markedly alter hypothalamic malonyl-CoA concentration and food intake. In the fasted state (that produces hunger) hypothalamic malonyl-CoA concentration is low (0.1-0.2 μM), whereas re-feeding after fasting (that produces satiation) causes malonyl-CoA levels to rise to 1-1.4 μM (Hu, Z. 2003)

1.1.1.2 A new brain expressed isoform: CPT1C

Performing *in silico* database searches based on human CPT1A cDNA nucleotide or protein sequence, a new gene was identified. CPT1C is apparently, a recent gene duplication, because it is only found in mammals (Price, N. 2002). This new gene was designated CPT1C due to its high similarity to the other isoforms of CPT1. Searches of human genome sequence data revealed that CPT1C is found on a region of chromosome 19 (band 19q13.33).

It is suggested that CPT1C most likely adopts the same membrane topology as the other CPT1 isoforms, with two transmembrane segments and C- and N-terminal segments exposed on the cytosolic face. In contrast to the other CPT1 isoforms, the new isozyme contains an extended tail (of approximately 30 aa) at the C-terminal end (Figure 5).

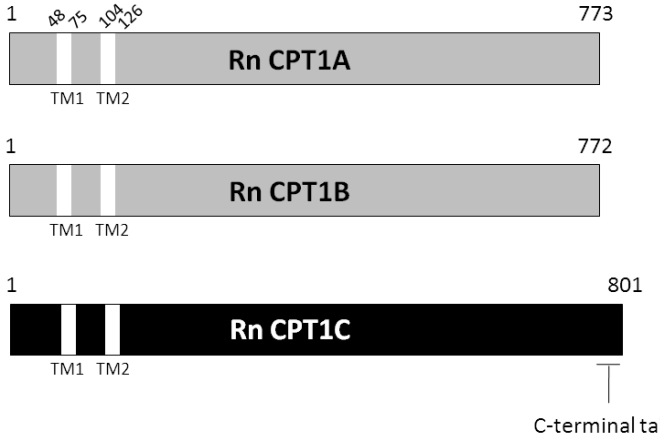

Figure 5: Schematic representation of rat (Rn) CPT1A, CPT1B and CPT1C showing the extended C-terminal tail of CPT1C. Transmembrane domains (TM1 and TM2) and the amino acid positions from the begining to the end are also shown.

The analysis of amino acid sequence similarity and identity percentage among different isoforms revealed that CPT1C is more similar to CPT1A than to CPT1B (Table 2) (Wolfgang, M.J. 2006).

	CPT1A vs. CPT1C	CPT1B vs. CPT1C	CPT1A vs. CPT1B
% Identity	52.4	50.6	62.3
% Similarity	69.6	66.3	77.7

Table 2: Comparison of amino acid sequence among three isoforms of CPT1 enzymes. Amino acid sequence identity and similarity comparison between different CPT1 isoforms was performed *in silico*. CPT1C has higher degree of similarity to CPT1A than to CPT1B. (From Wolfgang, M.J. 2006).

The 3-D structure of CPT1C was constructed by homology modeling thanks to the existing model of CPT1A (Esther Gratacòs Thesis). The model proposed for CPT1C enzyme is shown in figure 6. In the ribbon plot representation, the putative sites for carnitine (white) and palmitoyl-CoA (magenta) are indicated.

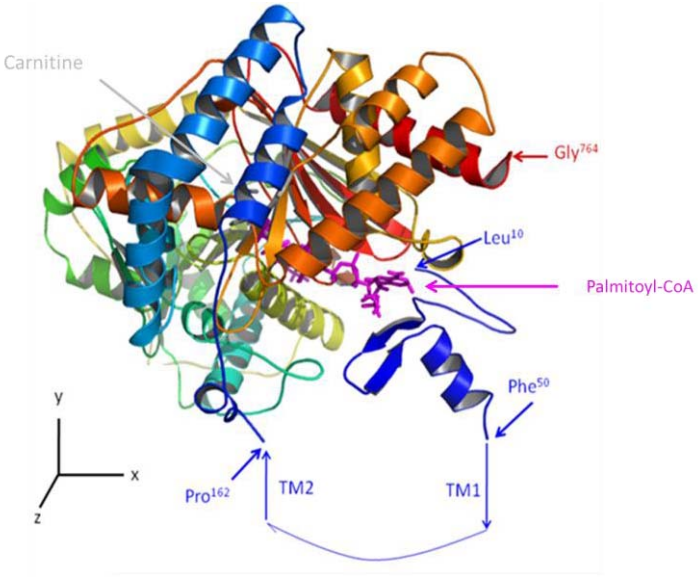

Figure 6: Structural model of rat CPT1C. A proposed model for CPT1C is shown in the ribbon plot representation. The putative sites for carnitine (white) and palmitoyl-CoA (magenta) are indicated. A frontal view of the model in which residues flanking the modeled region have been highlighted (regions modeled: from Leucine 10 to Phenylalanine 50 (in blue) and from Proline 162 to Glycine 764). In this model the hypothetic position of transmembrane domains 1 and 2 (TM1, TM2), and the loop region between them, have been represented by blue arrows. (From Esther Gratacòs Thesis).

All residues implicated in carnitine and palmitoyl-CoA binding are well conserved in CPT1C, with some conservative and semi-conservative changes which do not apparently influence the activity of this isoenzyme.

It is important to notice that residues that are involved in the catalysis of the reaction in CPT1A, are also conserved in CPT1C sequence. Looking at the 3-D model, the important residues for catalysis (His^{473}) and the residues forming the substrates channel have the same spatial distribution as in CPT1A model (Figure 7).

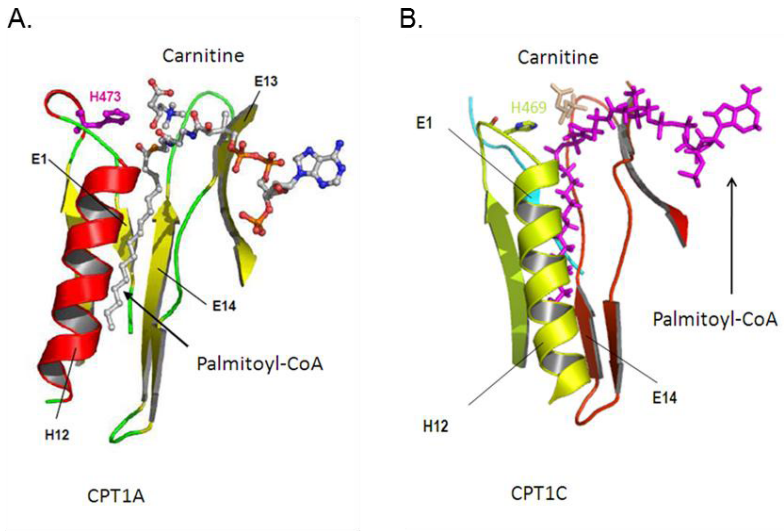

Figure 7: Comparison of residues forming the hydrophobic channel where palmitoyl-CoA accommodates in CPT1A (A) and CPT1C (B) models. Relative position of the hydrophobic channel for docking palmitoyl-CoA, formed by alpha helix 12 and the beta sheet 14. Catalytic histidine and carnitine are also shown. (From Esther Gratacòs Thesis).

The data provided by this 3-D structure model of CPT1C suggest that this isoenzyme would be able to catalyze the conversion of palmitoyl-CoA into palmitoylcarnitine.

Moreover, recent data about sequence analysis of the CPT1C mRNA (Lohse, I. 2011) describe the existence of a conserved uORF (upstream open reading frames) element in the 5´UTR of CPT1C mRNA. The analysis sequences revealed that CPT1C is the only CPT1 member that contains an uORF element. The presence of uORF elements within mRNA 5´UTR can affect the levels of translation initiation in the main open reading frame (mORF). Eukaryotic ribosomes generally only initiates once per mRNA, so the presence of an uORF element, normally inhibits the translation of the mORF and may lead to mRNA decay. Therefore, although they are short sequences, they play critical roles in physiology changes. They show that the regulation of uORF within the 5´UTR maintains low basal expression of CPT1C during unstressed conditions and they are important in the translational induction for expression during conditions of reduced energy availability. The transcriptional regulation levels through uORF elements suggests that CPT1C protein levels must rapidly change to fulfil its role and that this regulation can be impacted by cellular energy availability and AMPK activity (important enzyme involved in the regulation of food intake and homeostasis energy).

1.1.1.2.1 Protein localization

Looking for CPT1C EST sequences from other species, no orthologous sequences were found in species other than mammals, while the other isoforms are expressed in organisms like birds, fishes, reptiles, amphibians or insects. This result suggests that CPT1C has a specific function in more evolved brains (Price, N. 2002; Sierra, A.Y. 2008).

Expression studies indicate that CPT1C is located exclusively in the central nervous system, with homogeneous distribution in all brain areas although there are extremely high levels of mRNA concentrated in discrete areas that have been implicated in appetite control or feeding behavior, including the hippocampus and the paraventricular, arcuate, and superchiasmatic nuclei (Figure 8) (Price, N. 2002; Dai, Y. 2007).

Morevoer, the mRNA expression pattern resembles that of FAS (fatty acid synthetase) or acetyl-CoA carboxylase 1 (ACC1) (enzymes related to biosynthesis) rather than CPT1A or ACC2 (enzymes related to β-oxidation) (Sorensen,A. 2002).

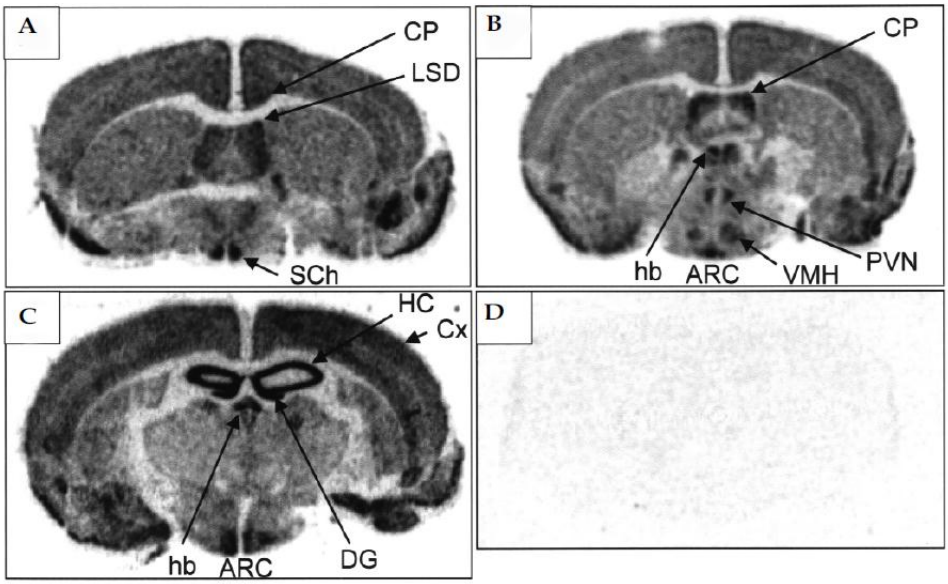

Figure 8: Detection of CPT1C mRNA transcripts in mouse brain by *in situ* hybridization. (A–C) Sections moving towards the posterior of the brain, probed with ^{35}S-labeled antisense probe. A. A section containing dorso-lateral septal (LSD) and suprachiasmatic (SCh) nuclei. B. An oblique section containing lateral ventricular choroid plexus (CP), paraventricular (PVN) and arcuate nuclei (ARC), and ventromedial hypothalamus (VMH). C. An oblique section through the hippocampus (HC), habenulae (hb), and ARC. D. Hybridization of a sense probe. The figures show scanned autoradiographs. DG, dentate gyrus; Cx, cerebral cortex. (From Price, N. 2002)

1.1.1.2.1.1 Expression of CPT1A, B and C in different regions of the rat brain

The expression of CPT1A mRNA is much greater (12 ± 2-fold) than CPT1B throughout the brain with the sole exception of the cerebellum, where there is 8.4 ± 0.8 times greated CPT1B mRNA expression compared with all other regions of the brain. CPT1C mRNA is twice the level of CPT1B mRNA in the cerebellum. When CPT1A mRNA is compared with CPT1C mRNA, CPT1A is significantly greater (1.7 ± 0.2 fold) in all regions of the brain. The expression of CPT1A mRNA in the hypothalamus is 1.3 ± 0.2 times higher compared with average expression in other regions of the brain. There is also some difference in expression of CPT1A in the cerebellum (1.3 ± 0.08 times the average expression). Neither CPT1A nor CPT1B differ greatly in other brain regions (Lavrentyev, E.N. 2004).

Moreover, it is described that during fasting there are a minor changes in expression of mRNAs encoding the CPT1 isoforms. For example CPT1A expression increases in the medium basal hypothalamus 1.35 ± 0.08 times in fasting animals. In addition both CPT1A and CPT1B in the motor cortex are increased 1.3 ± 0.2-fold and 1.4 ± 0.2 times, respectively (figure 9).

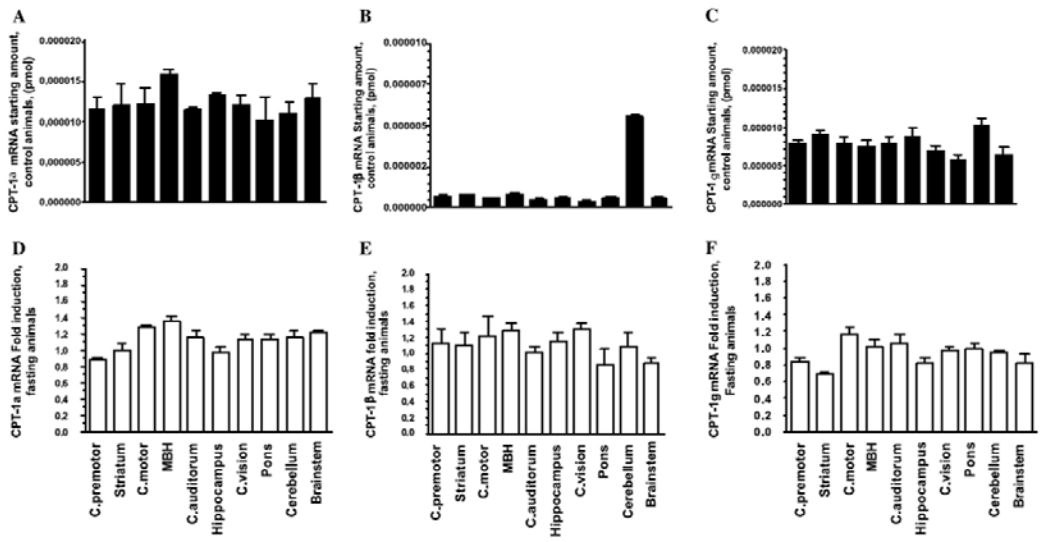

Figure 9: Expression of CPT1 isoforms mRNA within different rat brain regions by control and fasted. **A.B.C**. Quantification of CPT1A (A), CPT1B (B), CPT1C (C) mRNA by RTQ-PCR in the brain regions of control animals. Data have been normalized to 18S RNA. **D,E,F.** CPT1A (D), CPT1B (E), y CPT1C (F) mRNA fold induction by fasting. (From Lavrentyev, E.N. 2004).

1.1.1.2.2 Cellular localization

To identify the cell types expressing CPT1C in the brain, co-localization studies with a neuronal marker (Neuronal Nuclei, NeuN), or an astrocyte marker (Glial Fibrillary Acidic Protein, GFAP) were performed by our group. Figure 10 shows co-labeling of CPT1C with NeuN confirming that CPT1C is expressed mainly in neurons (Figure 10C). No co-localization was detected between CPT1C and GFAP indicating that CPT1C is not present in brain astrocytes (Figure 10D) (Sierra, A.Y. 2008; Dai, Y. 2007). It is unknown whether CPT1C colocalizes with other glial cells.

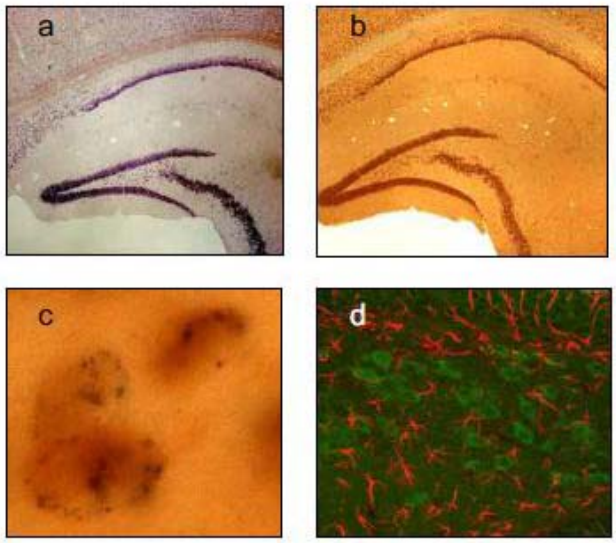

Figure 10: Co-localization studies of CPT1C mRNA with NeuN and GFAP proteins in brain sections. Brain sections were processed using *in situ* hybridization with CPT1C antisense Riboprobe (a) or immunocytochemistry with NeuN primary antibodies and biotinylated secondary antibodies (b) or both methods (c). (d) Mouse adult brain sections were processed by double immunocytochemistry with CPT1C antibodies (green stain) and GFAP (red stain). (From Sierra, A.Y. 2008).

1.1.1.2.3 Subcellular localization

CPT1C has a high sequence similarity to CPT1A and CPT1B isoforms. Therefore, it is expected that CPT1C has the same intracellular localization as the other two isoforms, CPT1A and B, the outer mitochondrial membrane (Price, N. 2002).

To study the intracellular localization of CPT1C, different strategies were designed by our group. The first aproach was to transfect fibroblast with pCPT1A-EFGP or pCPT1C-EGFP. They show different fluorescence pattern, cells transfected with pCPT1A-EFGP express a punctuate manner while cells transfected with pCPT1C-EGFP show a reticular manner, indicating a different subcellular localization between the isozymes (Sierra, A.Y. 2008). The second approach to verify the subcellular localization of CPT1C in the endoplasmic reticulum was co-localization studies with mitoTracker, a potential-sensitive dye that accumulates in mitochondria or with antibodies against calnexin, an ER integral protein. As shown figure 11, CPT1C is localized in the ER membrane and not in mitochondria. It is also described that the N-terminal region of CPT1C contains a putative microsomal targeting signal responsible for ER localization (Sierra, A.Y. 2008).

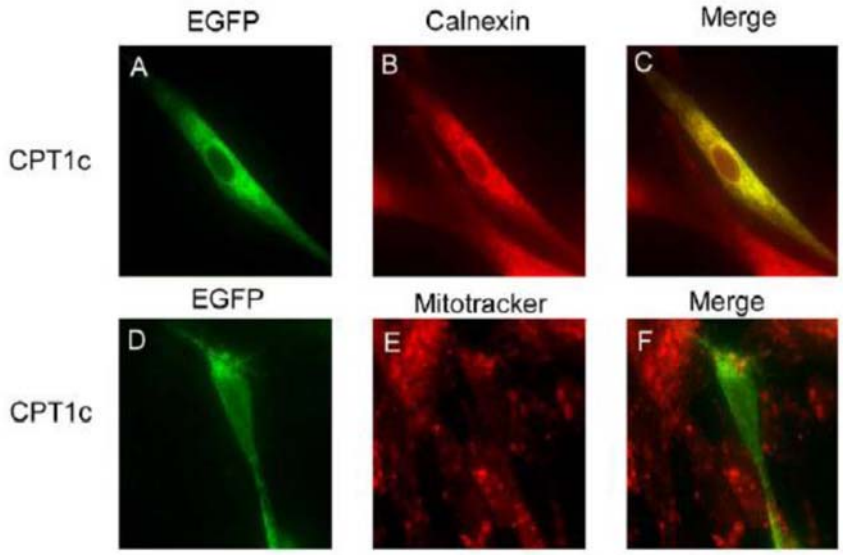

Figure 11: Co-localization studies of CPT1C in mitochondria and ER. Fibroblasts were transfected with pCPT1C-EGFP (panels A to F) and incubated with anti-calnexin as primary antibody (panel B and C) or stained with mitotracker (panels E and F) . Images were taken with a confocal microscope. (From Sierra, A.Y. 2008)

1.1.1.2.4 Enzyme activity

Analysis of the amino sequence of CPT1C reveals that all important residues for carnitine acyltransferase activity are conserved in CPT1C, as well as the malonyl-CoA binding site.

Despite this, when CPT1 radiometric activity assays were performed, no catalytic activity was found in CPT1C enzyme (Price, N. 2002; Wolfgang, M.J. 2006; Wolfgang, M.J. 2008). Probably, due to the fact that they used isolated mitochondrias instead of microsomes (Figure 12).

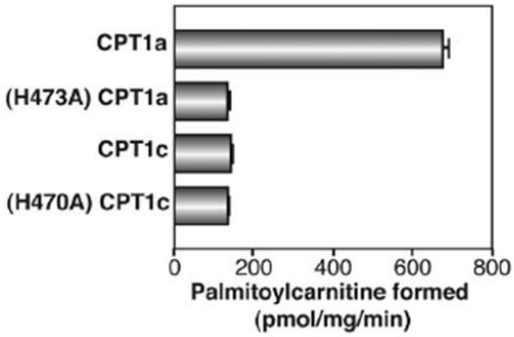

Figure 12: Mitochondria from 293 T cells transfected with expression vectors from CPT1A, CPT1A (H473A) (inactive mutant), CPT1C or CPT1C (H470A) (inactive mutant) were used in carnitine acytransferase assays with palmitoyl-coA (75 µM) as a substrate. (Modified from Wolfgang, M.J. 2006).

It is also demonstrated that CPT1C has the abilty to bind malonyl-CoA with a K_D similar to that of CPT1A (K_D value ≈ 0.3 µM). It is suggested that CPT1C regulates malonyl-CoA availability in the brain (Price, N. 2002; Wolfgang, M.J. 2006).

1.1.1.2.5 Physiological function of CPT1C

1.1.1.2.5.1 Role of CPT1C in the regulation of energy homeostasis

In order to elucidate the role of this isozyme in vivo, two groups developed a mouse with targeted deletion of CPT1C gene (Wolfgang, M.J. 2006; Gao, X.F. 2009).

The first CPT1C knockout (CPT1C-KO) mouse model was developed by the group of Dr. Lane and colleagues (Wolfgang, M.J. 2006). CPT1C-KO mice showed no apparent developmental abnormalities or alterations in any organ size, and they did not show differences in body temperature when they were compared with wild type littermates. When they were fed with a standard laboratory chow (SC), CPT1C-KO mice showed a reduction in whole body weight (of approximately 15%) and a decrease in food intake (by ≈25%) (Figure 13).

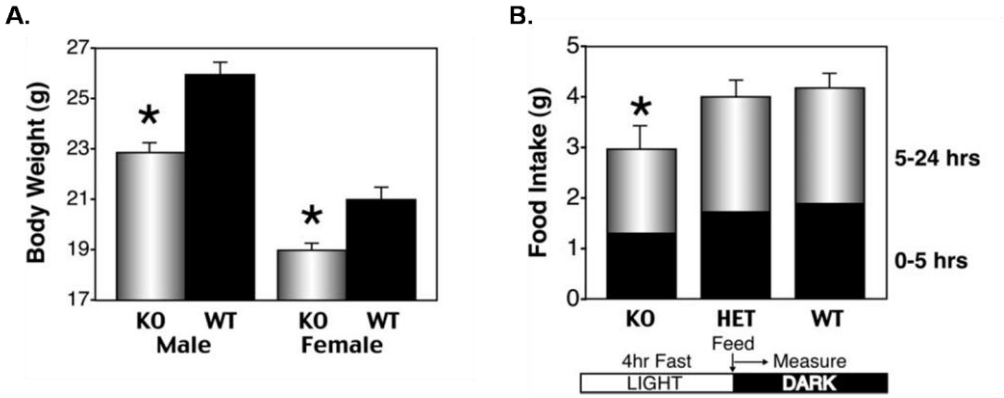

Figure 13: CPT1C KO mice are hypophagic and have a lower body weight than WT mice. *A*. Body weight is significantly lower in CPT1C KO males (*, $P < 0.0001$; $n = 10$ per group) and females (*, $p < 0.005$; $n = 10$ per group). B. CPT1C KO mice exhibit lower food intake than WT or heterozygous littermates (*, $p < 0.05$; $n = 6$ per group) after a short (4-h) fast just before the dark cycle (Modified from Wolfgang, M.J. 2006).

Moreover, when mice were fed with a high fat diet (HFD, 45% high fat), CPT1C-KO mice were more susceptible to obesity (increased weight gain despite reduced food intake) (Figure 14), became mildly insulin-resistant and showed lower peripheral energy expenditure (Wolfgang, M.J. 2006).

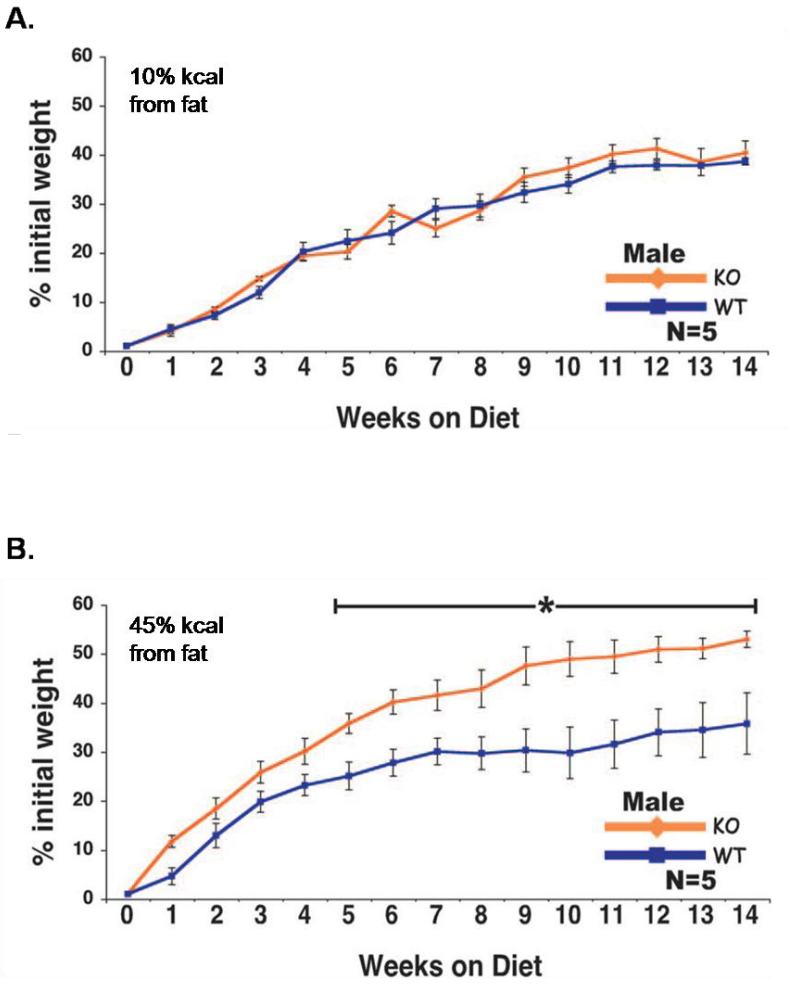

Figure 14: CPT1C KO mice are more susceptible to the effect of a high-fat diet. Male WT and CPT1C-KO mice (*n* = 5 per group) were fed with a control diet (10% of total kcal from fat; 1 kcal = 4.18 kJ) (*A*) or with a high-fat diet (45% of total kcal from fat) (*B*) for 14 weeks. Animals were weighed weekly at 14h 00 min. Initial body weights (average grams) were as follows: WT, 25.9 g; KO, 22.9 g (*, $p < 0.05$) (Modified from Wolfgang, M.J. 2006).

The other CPT1C-KO mouse model developed by Dr. Wu and colleagues (Gao, X.F. 2009) displayed a similar phenotype to that of the previous model. In addition, they found that the liver and the muscle expression of genes promoting fatty acid oxidation (such as CPT1A, CPT1B, PdK4, Acadm) were markedly decreased in CPT1C-KO mice on a high fat diet compared to WT mice. In line with these results, CPT1 activity and palmitate oxidation in liver and muscle were also lower in CPT1C-KO mice fed with high fat diet (Figure 15). Moreover, CPT1C-KO mice fed with a high fat diet had impaired glucose tolerance, which were attributable to the elevated hepatic gluconeogenesis and the decrease in the glucose uptake by the skeletal muscle.

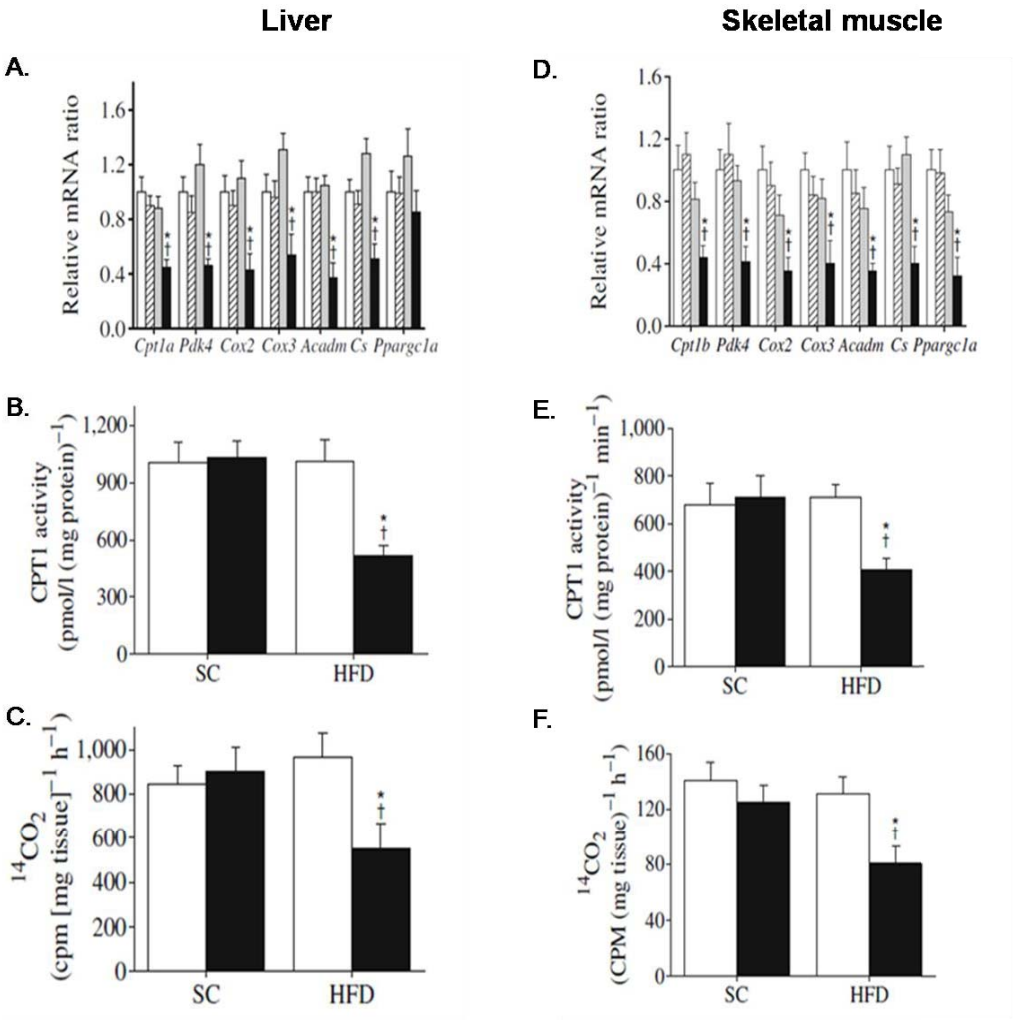

Figure 15: Expression of some oxidative genes, analyzed by real-time PCR, CPT1 activity and fatty acid oxidation in liver (A, B,C) and skeletal muscle (D,E, F) (n=5-6). Liver (A) and soleus muscle (D) expression of some oxidative genes. White bars, standard chow (SC) WT; hatched bars, SC KO; gray bars, HFD WT; black bars, HFD KO. Liver (B) and muscle (E) CPT1 activity and liver (C) and muscle (F) fatty acid oxidation. Wh ite bars, WT; black bars, KO. Values are means ± standard error of the mean. *p < 0.05 compared with WT mice on HFD; †p < 0.05 compared with KO mice on SC (Modified from Gao, X.F. 2009).

Contrary to the CPT1C deletion results, over-expression of CPT1C in the hypothalamus of WT mice by adenoviral vector, protects mice from weight gain when they were fed with a high fat diet despite no differences in daily food intake were found between the groups (Dai, Y. 2007).

Taken together these results suggest that CPT1C is protective against the effect of fat feeding on body weight and that CPT1C is necessary for the regulation of energy homeostasis.

1.1.1.2.5.2 Molecular mechanism by which CPT1C is regulating energy homeostasis

Recently, new data from our group, in collaboration with the group of Dr. Lopaschuk (Gao, S. 2011) show the molecular mechanism by which CPT1C is regulating food intake and satiety.

Adenoviral overexpression of CPT1C in the arcuate nucleous (Arc) of hypothalamus, increases food intake and simultaneously, induces an increase in the levels of the Arc orexigenic neuropeptide Y (NPY),

an important mediator in central control of feeding. Moreover, we related CPT1C to ceramide levels, showing that CPT1C over-expression in the Arc, increases ceramide levels in this nucleous under fasting conditions (Figure 16A), while CPT1C deletion causes a reduction in ceramide levels (Figure 16B).

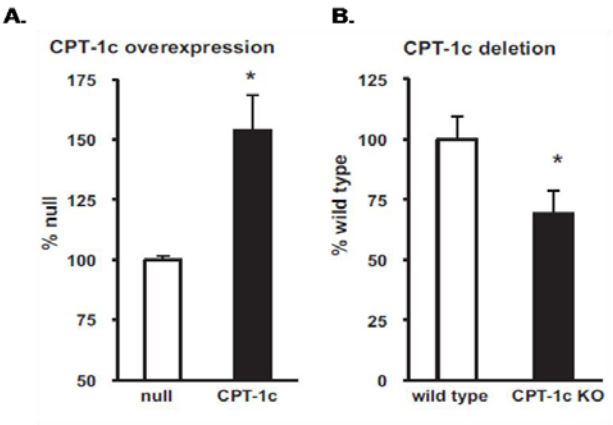

Figure 16: Ceramide levels in the Arc. A.The Ade-CPT1C or Ade-GFP (null) was delivered into the Arc of rats. The rats were killed following 8h food deprivation and ceramide levels in the Arc were measured. B. CPT1C deletion: The CPT1KO mice and their wild type littermates were killed under ad libitum fed conditions. The ceramide levels in the mediobasal hypothalamus encompassing the Arc were measured. (Modified from Gao, S. 2011).

Finally, myriocin (an inhibitor of the *de novo* biosynthesis of ceramide) was infused into the Arc. We found that myriocin administration prevents the increase in the ceramide levels induced by CPT1C or MCD (malonyl-CoA decarboxylase catalyzes the conversion of malonyl-CoA into acetyl-CoA and carbon dioxide; and malonyl-CoA is the physiological inhibitor of CPT1. Therefore MCD over-expression increases CPT1 activity) (Figure 17). Moreover, the overexpression of MCD or CPT1C into the Arc increases rebound feeding, which is blocked by myriocin. Same result is shown with the orexigenic peptide, NPY, its effect is blocked by myriocin. These results show that CPT1C controls food intake through the regulation of the *de novo* synthesis of ceramide.

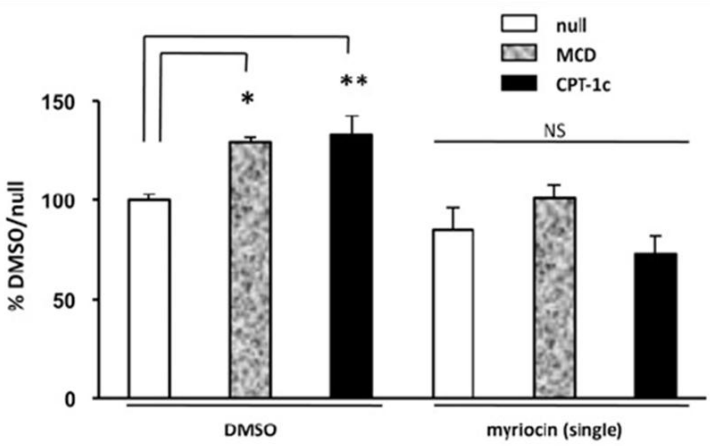

Figure 17: Ceramide *de novo* biosynthesis mediates CPT1C actions on food intake and body weight. The rats with Arc overexpression CPT-1C (n = 12), or GFP (null, n = 16) received a single intra-Arc infusion of myriocin (4 µg in DMSO) before the dark cycle and food was removed. Eight hours later, some rats were killed and were then used for ceramide assay. (Modified from Gao, S. 2011).

1.1.1.2.5.3 Over-expression of CPT1C in mouse brain

Other group developed a transgenic mouse that over-expressed CPT1C specifically in brain in order to know, the effect of the enhanced expression of CPT1C in the brain (Reamy, A.A. 2011). These mice present a dramatic inhibition of postnatal growth accompanied by a postnatal profound microencephaly, 2-3 fold decreased in wet brain weight compared to their control littermates. Moreover, the body weights of adult CPT1C-TgN mice are significantly lower than WT mice although there are not effects in the organ weight like kidney, liver or spleen of CPT1C-TgN mice compared to the control. The histological examination of the brain shows that all the major brain structures are present in CPT1C-TgN mice but the size is smaller. Therefore, it seems that CPT1C over-expression produces a decrease in brain size causing a remarkable microencephaly.

Moreover, when transgenic mice were fed with a low fat diet, long chain fatty acids were clearly depleted in brain. Surprisingly, CPT1C-TgN mice fed with a low fat diet (10% Kcal from fat) gained more weight than control mice, increasing their adiposity, and showed a marked increase in glucose and insulin during fasting.

By contrary, when they were fed with a high fat diet (60% Kcal from fat), they had reduced body weight gain and increased peripheral metabolism becoming resistant to obesity. These results confirm the role of CPT1C in energy homeostasis.

1.1.1.2.5.4 CPT1C is involved in cell survival and tumor growth

Finally, another recent study identifies CPT1C as a gene expressed and up-regulated in tumors in response to metabolic stress (Zaugg, K. 2011). They demonstrate that CPT1C is frequently expressed in human lung tumors and protects cancerous cells from death induced by glucose deprivation or hypoxia. Furthermore, CPT1C expression facilitates energy production, obtains ATP from fatty acids oxidation and provides advantages that enhance cell growth under poor nutrient supply. By contrary, CPT1C depletion reduces ATP production, alters fatty acids homeostasis, and heightened sensitivity to hypoxia or glucose deprivation producing a reduction in the growth of tumors in vivo. These findings propose CPT1C as a new potential target in the treatment of hypoxic tumors based on manipulating fatty acid metabolism.

1.2 CERAMIDES

Sphingolipids constitute a class of lipids defined by eighteen carbon amino-alcohol backbones, which are synthesized in the ER from non-sphingolipid precursors. Modification of this basic structure is what gives rise to the vast family of spingolipids that play significant roles in membrane biology and provide many bioactive metabolites that regulate cell function, such us regulating signal transduction pathway, directing protein sorting, and mediating cell-to-cell interaction and recognition (Degroote, S. 2004; Marchesini, N. 2007). Different combinations of sphingoid long chain bases, fatty acids and head group moieties lead to a large number of sphingolipids and glycosphingolipids.

Ceramide is the central core in sphingolipid metabolism, it is involved in the regulation of signal transduction processes, induced cell cycle arrest and promote apoptosis (Obeid, L.M. 1993), a form of programmed cell death. Also, ceramide plays an important role in the regulation of autophagy, cell differentiation, survival, senescence (Venable, M.E. 1995), diabetes, insulin resistance, neurodegenerative disorders, atherosclerosis and inflammatory response (Hannun, Y.A. 1996).

Over the past decade, sphingolipid metabolites including ceramide (Cer), sphingosine (Sph), and sphingosine 1-phosphate (S1P) have emerged as bioactive lipids, being a new class of lipid biomodulator of various cell functions, like proliferation, growth, migration, differentiation, senescence and apoptosis (Cuvillier, O. 2001; Hannun, Y.A. 2000; Kolesnick, R.N. 1998; Kolesnick, R. 2002; Luberto, C. 2002; Malisan, F. 2002; Pettus, B.J. 2002; Spiegel, S. 1998; Spiegel, S. 2003; Tettamanti, G. 1994).

1.2.1 Synthesis of sphingolipids

Sphingolipids metabolism mainly occurs in eukaryotes, but is also found in the Sphingomonas bacterial genus. The metabolic pathways of simple and complex sphingolipids are shown in figure 18 and 19. It is clear from these figures that the metabolites are interconvertible and this makes complex to determine the specific role of each one.

The pathway of sphingolipid metabolism has a unique metabolic entry point (serine palmitoyl transferase; SPT), which forms the first sphingolipid in the *de novo* synthesis pathway, and a unique exit point, S1P lyase, which breaks down S1P into non-sphingolipid molecules. *De novo* sphingolipid synthesis begins at the cytosolic leaflet of the ER where a set of four enzyme groups coordinately generate ceramides of different acyl chain lengths from non-sphingolipid precursors.

Briefly, sphingolipids are synthesized *de novo* from the condensation of the amino acid serine and palmitoyl-CoA to form 3-ketodihydrosphingosine, a reaction catalyzed by a serine palmitoyltransferase (SPT). This is then reduced to form of dihydrosphingosine (sphinganine), which is acylated by dihydroceramide synthases (CerS) to form dihydroceramide. In mammals, six genes that encode (dihydro)ceramide synthase have been identified, CerS1-6 (Mizutani, Y. 2005; Mizutani, Y. 2006; Riebeling, C. 2003), each isoform shows substrate preference for specific chain length fatty acyl-CoAs and that each CerS can produce different dihydroceramide/ceramide species profiles. For example, CerS1 shows significant preference for stearoyl-CoA as a substrate and generate predominantly C18-ceramide species, whereas CerS2 utilizes C20-C26 acyl-CoA species and is one of the major CerS responsible for very long chain ceramide species. CerS5 and 6 both prefer palmitoyl-CoA as a substrate and generate predominantly C16-ceramide species. Finally, CerS3 prefers middle and long chain acyl-

CoAs (Mizutani, Y. 2005; Lahiri, S. 2005). Ceramide is generated by the action of dihydroceramide desaturase. It is responsible for converting the dihydrosphingosine backbone within ceramide into a sphingosine backbone. The process of the *de novo* pathway of sphingolipid biosynthesis starts in the endoplasmatic reticulum and continues in the Golgi apparatus (Figures 18). Ceramide is transported from the ER to the Golgi thanks to vesicular transport or through the ceramide transfert protein (CERT).

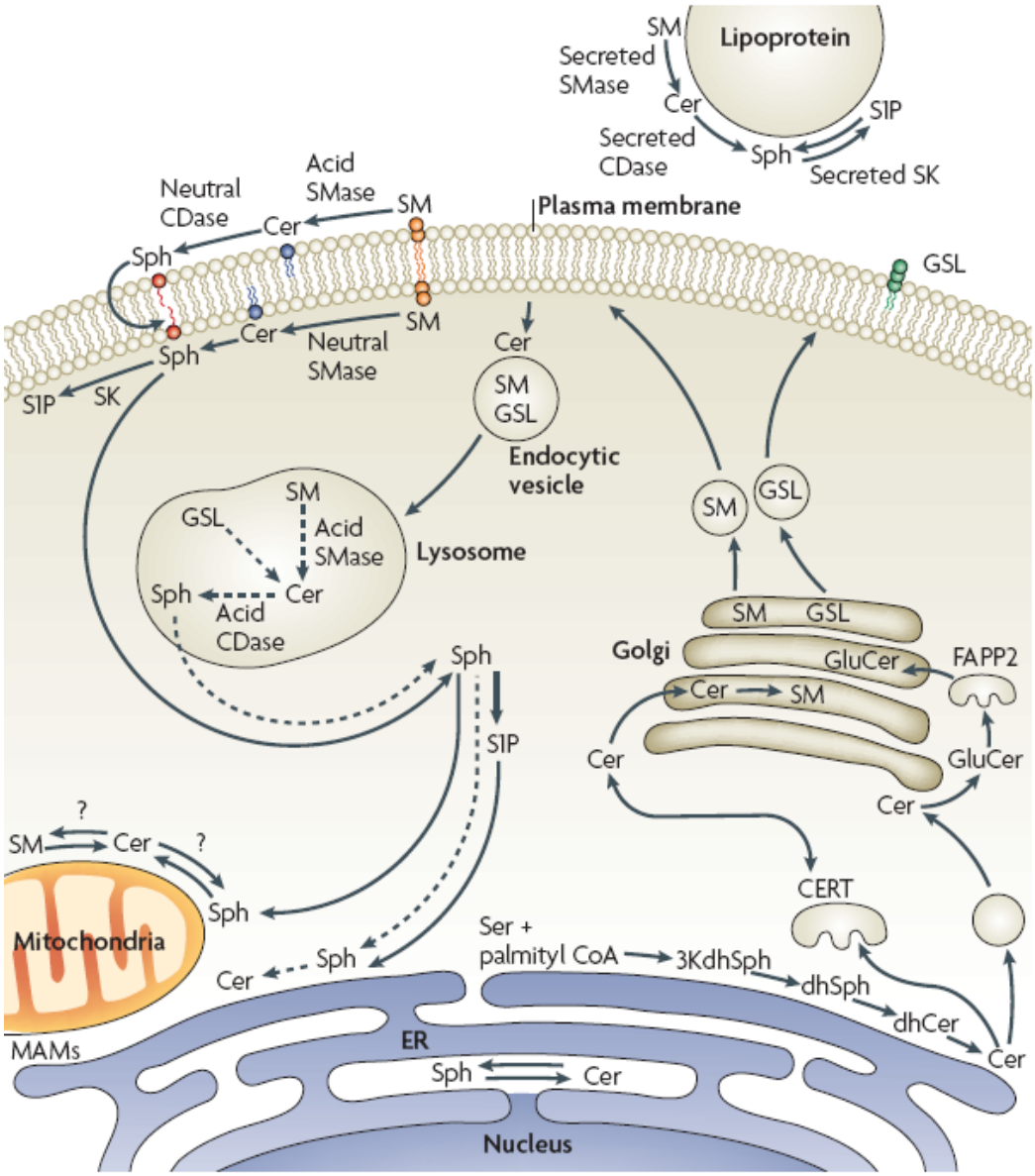

Figure 18: Compartmentalization of pathway of sphingolipid metabolism. De novo synthesis of sphingolipids occurs in the endoplasmatic reticulum (ER) and possibly in ER-associated membranes, such as the perinuclear membrane and mitochondria-associated membranes (MAM). Ceramide (Cer) formed in this compartment is transported to the Golgi, which is the site of synthesis of sphingolmyelin (SM) and glucosylceramide (GluCer), with the latter serving as the precursor for complex glycosphingolipids (GSLs). Transport of Cer to the Golgi occurs either through the action of the transfer protein CERT, which specifically delivers Cer for SM synthesis, or though vesicular transport, which delivers Cer for the synthesis of GluCer. In turn, transfer of GluCer for GSL synthesis requires the action of the recently identified transport protein FAPP2. GluCer appears to be synthesized on the cytosolic side of the Golgi, and requires flipping to the inside of the Golgi for the synthesis of complex GSLs, possibly with the aid of the ABP transporter, P-glycoprotein (also known as MDR1). Delivery of SM and complex GSLs to the plasma membrane appears to occur by vesicular transport. Acid sphingomyelinase (SMase) that is present in the outer membrane leaflet or neutral SMases in the inner leaflet of the bilayer can metabolize SM to Cer and subsequently other bioactive lipids. Cer is hydrolysed by acid CDase to form sphingosine (Sph). Subsequence dephosphorylation by S1P phosphatases in the ER would recycle the salvaged Sph to Cer. The salvage pathway is shown by the dashed arrows. KdhSph, 3-keto-dihydrosphingosine; dhCer, dihydroceramide; dhSph, dihydrosphingosine; S1P, sphingosine-1-phosphate (Modified from Hannun, Y.A. 2008).

Ceramide is also produced by hydrolysis of sphingomyelin by sphingomyelinases (SMases). There are three types of SMases based upon their pH optimum: acid, alkaline and neutral sphingomyelinase. Although all three forms of SMases catalyze a similar reaction, these three groups of enzymes are evolutionarily unrelated and have different subcellular distributions. Alkaline is exclusively expressed in the intestine and liver. Acid and neutral SMases are ubiquitously expressed and serve as the major regulator of sphingomyelin catabolism in most of tissues. Acid sphingomyelinases are found in lysosomes, whereas neutral sphingomyelinases exhibit both cytosolic and plasma membrane bound forms like endoplasmatic reticulum (Hannun, Y.A. 1994). Ceramide can be phosphorylated by ceramide kinase (CK) to ceramide 1-phosphate (C1P), or utilized for the synthesis of sphingomyelin or glycosphingolipids. This pathway provides rapid increase of cellular ceramide levels in response to diverse stimuli (Goni, F.M. 2002; Levade, T. 1999; Marchesini, N. 2004).

Ceramide can also be broken down by ceramidases (CDase) to sphingosine, and some ceramidases can catalyze the reverse reaction and to function as a ceramide synthase (CerS) (el Bawab, S. 2002). Sphingosine (Sph) is converted to sphingosine 1-phosphate (S1P) by a family of sphingosine kinases (SPhKs).

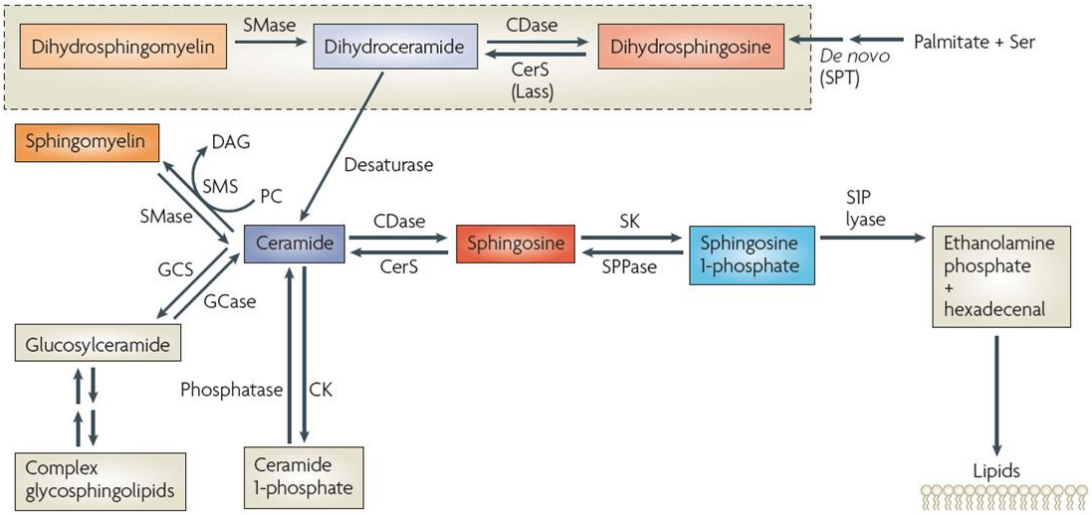

Figure 19: Sphingolipid metabolism and interconnection of bioactive sphingolipids. Ceramide is considered to be the central hub of sphingolipid metabolism, and is synthesized *de novo* from the condensation of palmitate and serine to form 3-keto-dihydrosphingosine (not shown). In turn, 3-keto-dihydrosphingosine is reduced to dihydrosphingosine followed by acylation by (dihydro)-ceramide synthase (also known as Lass or CerS). Ceramide is generated by the action of desaturases. From here, ceramide can be converted to other interconnected bioactive lipid species. The only exit pathway from the sphingolipid pathways is mediated by sphingosine-1-phosphate (S1P) lyase, which metabolizes S1P. Both ceramide and dihydroceramide have been shown to be bioactive and, in fact, >50 distinct molecular species may be classified as ceramide. Each may have its own separate metabolic network, resulting in unprecedented levels of complexity in sphingolipid signalling. In this figure, only a pathway for a generic ceramide and a generic dihydroceramide (shown in the dotted outline box) are depicted. It does not show the multiplicity or subcellular localization of these pathways. CDase, ceramidase; CK, ceramide kinase; DAG, diacylglycerol; GCase, glucosyl ceramidase; GCS, glucosylceramide synthase; PC, phosphatidylcholine; SK, sphingosine kinase; SMase, sphingomyelinase; SMS, sphingomyelin synthase; SPPase, sphingosine phosphate phosphatase; SPT, serine palmitoyl transferase (Modified from Hannun, Y.A. 2008).

1.2.2 Ceramide function in the neurons

1.2.2.1 Roles for sphingolipids metabolism in synaptic activity

Sphingolipid metabolism is a dynamic process that modulates the formation of several bioactive metabolites including ceramide, ceramide-1-phosphate, sphingosine and sphingosine 1-phosphate. It is becoming increasingly recognized that these sphingolipids play critical and complex roles in regulating neuronal excitability. The biophysical properties of sphingolipids play important roles in the regulation of membrane shape, endo- and exocytotic events, and vesicles and protein trafficking; several lipid species also function as second messengers that regulate neuronal functions including pre- and post-synaptic processes involved in synaptic plasticity (Stahelin, R.V. 2009; Day, C.A. 2009; Swartz, K.J. 2008; Owen, D.M. 2009).

At the pre-synaptic terminal, docking and fusion of synaptic vesicles with the plasma membrane are regulated by a highly conserved family of SNARE proteins such as synaptobrevin in vesicles and syntaxin and SNAP-25 at the plasma membrane. Recent findings have demonstrated that the formation of the SNARE complex, synaptic vesicle fusion and exocytosis are regulated by sphingosine. Synaptobrevin adheres tightly to synaptic vesicles through electrostatic and hydrophobic interaction of the cytoplasmic part of synaptobrevin with the vesicular membrane. Sphingosine activates synatobrevin by neutralizing interactions of synaptobrevin with phospholipids thus allowing synaptobrevin to engage syntaxin/SNAP-25, resulting in SNARE assembly, vesicle fusion and transmitter release (Darios, F. 2009). These results are consistent with an earlier report that identified ceramidase (catalyze the deacylation of ceramide to produce a free fatty acid and sphingosine) as an important regulator of synaptic vesicle exocytosis (Rohrbough, J. 2004).

Sphingosine can be rapidly converted into S1P by sphingosine kinase 1 (SK1), and this more soluble product has also been implicated in regulation of transmitter release. SK1 is formed in the pre-synaptic terminal in an activity-dependent manner, and S1P applied to hippocampal neurons promotes transmitter release that is dependent on the S1P receptor (Kajimoto, T. 2007; Bajjalieh, S.M. 1989). Ceramide, thanks to its fusogenic properties, is also involved in neurotransmitter release, promoting vesicle fusion with the plasma membrane (Numakawa, T. 2003; Jeon, H.J. 2005; Blochl, A. 1996).

Ceramide is emerging as an important regulator of synaptic function and has been implicated in synapse formation, transmitter release and plasticity (Brann, A.B. 1999; Wheeler, D. 2009; Ping, S.E. 1998; Furuya, S. 1998; Ito, A. 1995). Early evidence for the regulation of synaptic activity by ceramide was provided by experiments that used synthetic cell-permeable short (C2-C6) ceramide analogs to demonstrate that ceramide could directly increase excitatory post-synaptic currents without affecting paired-pulse facilitation (Furukawa, K. 1998; Coogan, A.N. 1999; Fasano, C. 2003). Interestingly, these ceramide-associated enhancements of excitatory currents were often transient and followed by sustained depression of excitatory post-synaptic currents (Yang, S.N. 2000; Furukawa, K. 1998; Coogan, A.N. 1999). One mechanism by which ceramide may be involved regulating synaptic activity is by controlling the spatial and temporal location of receptors at postsynaptic sites. In neurons, the sphingomyelin-, ceramide- and ganglioside-rich membrane regions known as lipid rafts have been identified as important sites for the docking and insertion of both NMDA and AMPA subtypes of glutamate receptors. For instance, disrupting lipid raft by removal of cholesterol from membrane inhibits NMDA receptor currents and calcium flux, increasing the basal internalization rate of AMPA receptors (Hering, H. 2003; Frank, C. 2004; Abulrob, A. 2005).

1.2.2.2 Role of sphingolipids in survival and differential neurons

It is known that ceramide plays a role in neuronal apoptosis, but under certain conditions, it may promote cell survival and differentiation.

It is believed that ceramide may have biphasic action, with lower concentrations promoting cell differentiation and increasing concentrations contributing to cell death. Indeed, it is suggested in the literature that low levels of ceramide may be necessary for neuronal differentiation. For example, in neuroblastoma cells, the accumulation of ceramide is required for neuritogenesis, with ceramide returning to basal levels after the complete differentiation (Riboni, L. 1995).

The effects of ceramide on hippocampal neuron survival depend on the developmental neuronal stage and the concentration of ceramide used. For example, both cell permeable ceramide analogs (like C_2 ceramide and C_6 ceramide) and exogenous sphingomyelinase protect sympathetic neuronal cultures from the death (Ito, A. 1995). Low dose of ceramide application also protects against excitotoxic, oxidative, or β-amyloid-induced injury in hippocampal neurons (Goodman, Y. 1996). Other important effects of ceramide in hippocampal neurons include modulation of ion currents, neurotransmitter release and synaptic transmission (Yang, S.N. 2000).

1.3 SYNAPTOGENESIS

Synaptogenesis is a complex process in which specialized sites of communication between neurons, also called functional synapses, are formed. The formation of synapses in vertebrates occurs over a prolonged developmental period. Synaptogenesis begins in the embryo and continues into early postnatal life, but also occurs in the adult organism, where it is thought to contribute significantly to memory formation and learning.

During development, synapse formation is coupled to neuronal differentiation and the establishment of neuronal circuits. Correct connections have to be formed, often initially transient, between the presynaptic axon and postsynaptic dendrites. The process of synaptogenesis involves multiple molecules that influence not only the timing and location of synapse formation, but also determine the specificity and stability of the contact. Some of these molecules are soluble and act at a distance, guiding axons to their correct receptive fields, while also promoting neuronal differentiation and maturation.

In vertebrates, most of the synapses are chemical synapses transducing electrical signals from the axon into chemical signals in form of neurotransmitters, which are released from vesicles at the presynaptic terminal. Neurotransmitters diffuse through the synaptic cleft activating neurotransmitter-gated ion-channels situated at the postsynaptic site and converting the chemical signal back into an electrical impulse. Two categories of synapses are found in the nervous system, namely inhibitory and excitatory synapses. They are so called due to their effect on the membrane potential of the postsynaptic target and differ significantly with regard to their structure and molecular organization. For example, inhibitory synapses are localized directly at dendritic shafts whereas the postsynaptic site of an excitatory synapse is more commonly situated on a short dendritic protrusion named spine.

Glutamatergic synapses use glutamate as a neurotransmitter, which acts on AMPA- and NMDA-type (Ca^{2+}-channel) glutamate receptors expressed at the postsynaptic target site. The functional properties of a synapse change when the organism develops due to presynaptic and postsynaptic modifications. The probability of transmitter release decreases and a larger number of transmitter-filled vesicles accumulate at the presynaptic terminal. The kinetics of the synaptic response change with the type of neurotransmitter receptor expressed at the postsynaptic site and its subunit composition, which is different in young premature synapses, compared those, which are stabilized and mature. During development, most synapses are initially void of AMPA receptors but possess functional NMDA receptors. The early activity of the latter is important for the formation of the developing contact. Once the synaptic contact is established, NMDA-receptor activity can induce the insertion of AMPA receptors leading to fully functional synapses (Constantine-Paton, M. 1998). Moreover, even later on in the mature organism, synapses are found in different regions of the brain that still express only functional NMDA but lack AMPA receptors at the synaptic surface. These synapses are referred to as ‘silent synapses’ because, at normal resting membrane potentials, they remain functionally silent with no measurable current flow. Similarly, these synapses can be ‘unsilenced’ by NMDA-receptor activity that induces the recruitment of AMPA receptors to the postsynaptic site. The observations, that activity induces the delivery and insertion of AMPA receptors, led to the idea that AMPA-receptor trafficking might be one of the key mechanisms of synaptic plasticity. Soon after, it was reported that additional AMPA receptors are indeed inserted to the synapse to increase synaptic transmission during some forms of plasticity, termed as long-term-potentiation (LTP). As mentioned before, different receptor subunits can influence in the synaptic properties because they differ in the ligand-sensitivity, conductance and in their interaction with intracellular molecules. For example, the subunit composition of NMDA receptors changes during development. NMDA receptors consist of at least one NR1 subunit and different types of NR2 (NR2A-D) subunits. Initially, in the developing brain, the NR2B and NR2D subunits are the most prominent but are partially replaced by NR2A subunits when the organism

matures (Monyer, H. 1994). Later on, the subunit composition determines the localization of NMDA receptors in mature synapses: NR2A-containing NMDA receptors are concentrated at synaptic sites whereas NR2B-containing receptors localize at both synaptic and extrasynaptic sites. Furthermore, as expected, the subunit composition of synaptic AMPA receptors changes during maturation and activity, as will be described more in detail in a later section.

1.3.1 Dendritic spines

Spines were first observed more than 100 years ago by the Spanish neuroscientist Santiago Ramón y Cajal (Ramon y Cajal, S. 1981) using the Camillo Golgi "reazione near" protocol (the "black reaction" or the Golgi staining). He was the first to describe spines as small protrusions emerging from branched projections of a neuron, namely dendrites, and suggested that these are in fact, contact sites between neurons (Figure 20).

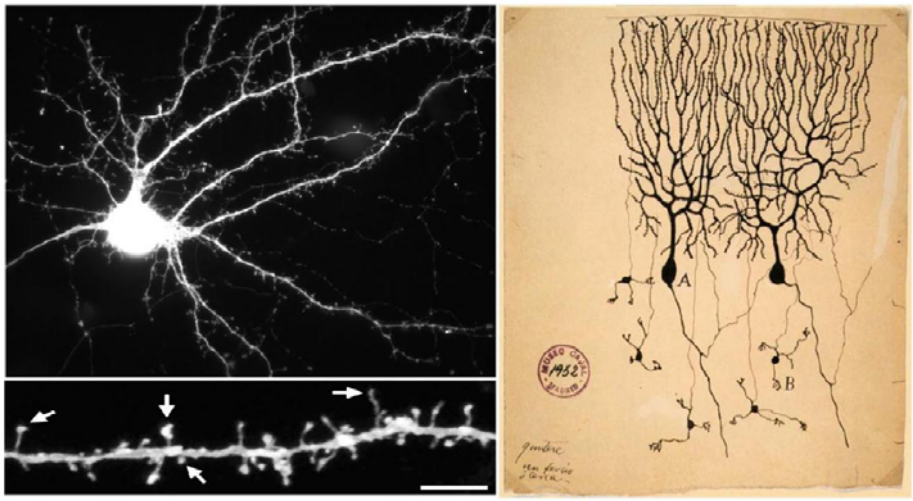

Figure 20: Dendritic spines. Left. After 14 days in culture an YFP-labeled hippocampal neuron shows a highly developed dendritic tree covered with spines of various shape and size (large picture). The enlargement of a dendrite (Harms,K.J. 2007) highlights the shape variations of spines from stubby spines, long and thin spines, to mushroom spines with defined spine heads (scale bar 5µm). Right. Drawing from the 20th century by Santiago Ramón y Cajal of neurons in the pigeon cerebellum. Denoted are purkinje cells.

Today, dendritic spines are defined as small structures (0.5-2 µm in length) emerging from the dendrite via a thin neck, or shaft, ending in a bulbous enlargement, the spine head (volume ranging from 0.01 μm^3 to 0.8 μm^3), which serves as the site of synaptic contact. Spines have been divided into several types such as thin, stubby, cup-, or mushroom-shaped (figure 21) (Lippman, J. 2005). However, the arbitrary classification of spines into these four categories underestimates the great heterogeneity of spine morphology, which is apparent even a single dendrite because the dendritic spines are dynamic structures able to change their size, form and shape on a time scale of minutes (Dunaevsky, A. 1999; Parnass, Z. 2000).

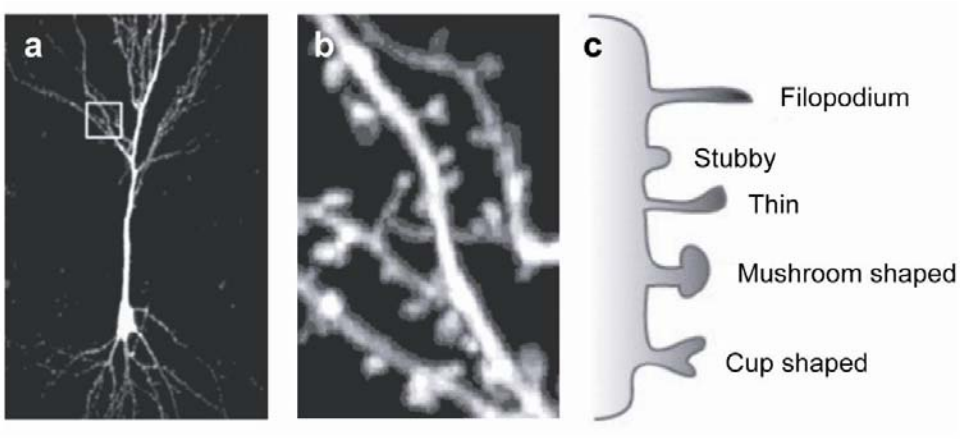

Figure 21: Morphology of dendritic spines. A. A pyramidal neuron in hippocampal slice culture transfected with green fluorescent protein (GFP) imaged with two-photon microscopy. Dendrites are covered by small protrusions: the dendritic spines. B. High magnification image of a hippocampal dendrite demonstrating the diversity in the morphology of dendritic spines. Most dendritic spines, however, have a narrow neck and an enlarged head. C. A schematic representation of morphological classifications of dendritic spines (modified from Lippman and Dunaevsky; 2005).

Dendritic spines are found at a linear density of 1-10 spines per µm of dendritic length in mature neurons. Most excitatory synapses in the mature mammalian brain occur on spines, and a typical mature spine has a single synapse located at its head. So, dendritic spines represent the main unitary postsynaptic compartment for excitatory input (Tsay, D. 2004) and it is known that it is the size of the spine head that correlates with synaptic strength (Schikorski, T. 1997; Matsuzaki, M. 2001).

The site of contact between spine and a presynaptic terminal is marked by the postsynaptic density (PSD), an electron dense thickening of the postsynaptic membrane. The PSD contains the molecular machinery that links synaptic transmission to various signaling cascades and cytoskeletal components. Unlike the dendritic shaft, the spine head is highly enriched in actin filaments (Fifkova, E. 1982; Matus, A. 1982), which mediate spine shape changes and motility (Fischer, M. 1998). Some dendritic spines also contain smooth endoplamatic reticulum, which is an internal store of calcium and also in the largest spine takes the form of a specialized organelle called “spine apparatus” (Gray, E.G. 1963). In addition, poliribosomes and protein translation machinery are often anchored at the base of spines (Ostroff, L.E. 2002).

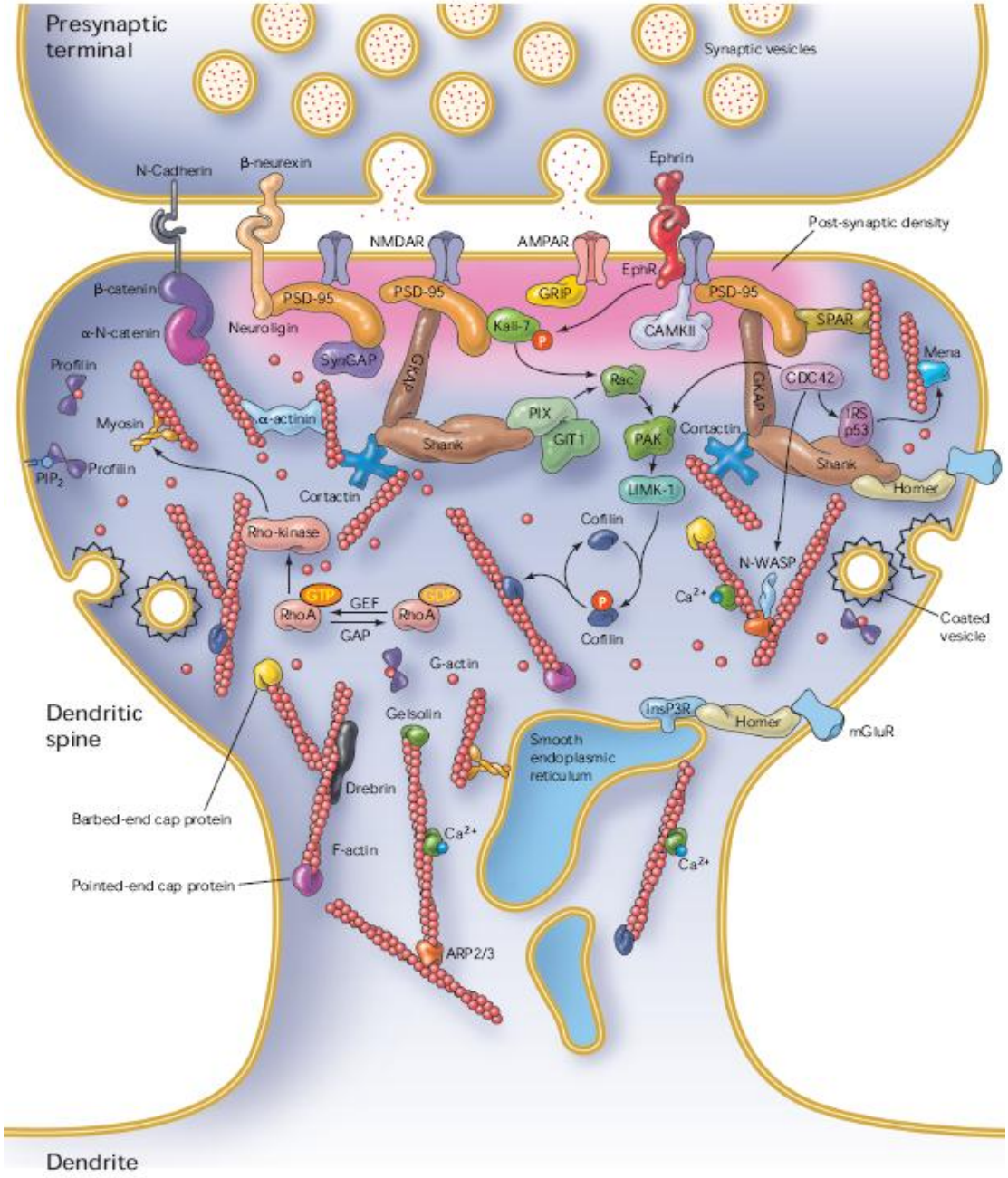

Figure 22: Some important components of dendritic spines: Spines are small membrane protrusions at synaptic junctions that use the excitatory neurotransmitter glutamate, which is released from synaptic vesicles clustered in the presynaptic terminal. Across from these glutamate release sites, _-amino-3-hydroxy-5-methyl-4-isoxazolepropionic acid (AMPA) and *N*-methyl-D-aspartate (NMDA) subtypes of glutamate receptors are clustered at the postsynaptic active zone within a dense matrix called the postsynaptic density (PSD; pink). Beyond the PSD lie subregions of spine membrane that contain G protein-coupled glutamate receptors (mGluR) and endocytic zones for recycling of membrane proteins. Receptors, in turn, connect to scaffolding molecules, such as PSD-95, which recruit signaling complexes (e.g., regulators of RhoGTPases, or protein kinases). Actin filaments provide the main structural basis for spine shape. Via a network of protein interactions, actin filaments indirectly link up with the neurotransmittter receptors and other transmembrane proteins that regulate spine shape and development, including Eph receptors, cadherins, and neuroligins. Actin-regulatory molecules such as profilin, drebrin, cofilin, and gelsolin control the extent and rate of actin polymerization. These, in turn, they are regulated by signaling cascades through engagement of the transmembrane receptors (Modified from Calabrese, B. 2006).

1.3.1.1 From filopodia to spines

By definition, filopodia are thin, long (>2 µm), highly motile dendritic protrusions with short life spans. In general, young neurons possess more filopodia-like protrusions whereas older cells are more abundant in mature dendritic spines (Dailey, M.E. 1996). Put into numbers, the proportion of filopodia-like protrusions declines from 60% in two-week-old mice to less than 2% in 4-5 month old animals (Grutzendler, J. 2002; Zuo, Y. 2005). These filopodia-like protrusions are not simply lost in older animals but have, most likely, transformed into thin or mushroom-like spines (Majewska, A.K. 2006). It is noteworthy, that only a small percentage of these short-lived protrusions actually transforms into spines (<2 µm), while the vast majority disappear within two days of formation (Zuo, Y. 2005). However, not every spine seems to arise from a filopodia-like transition stage. Other studies have confirmed the direct emergence of spines from the dendrite without a filopodia-like precursor (Engert, F. 1999). In vivo live-imaging studies have shown that most excitatory synapses form on dendritic filopodia, transforming them into spines while the synaptic contacts are stabilized. Hence, filopodia formation and spine motility have been implied as important processes during synaptogenesis (Fiala, J.C. 1998; Ziv, N.E. 1996). However, whether derived from filopodia-like precursors or directly from the dendrite – when newly developed protrusions become more stable, their volume increases and synapses form (Knott, G.W. 2006). The volume increase is mainly governed by an enlargement of the spine head which can then accommodate enlarged postsynaptic structures (Holtmaat, A. 2006).

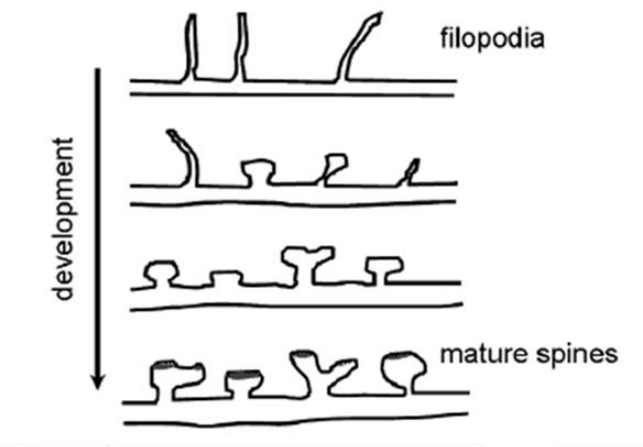

Although there are several hypotheses about the spine formation, the process is not clear. It seems that filopodia probably function to maximize the chance encounter between a developing axon and a target dendrite. Once contact is made, either physically via cell-cell adhesions or chemically via locally released signals, a synapse can be initiated and proceed through appropriate maturations steps. Several molecular families, including receptors, scaffolding proteins, and regulators of the cytoskeleton have been shown to regulate spine numbers and shape.

1.3.2 AMPA receptors

AMPA receptors are a subclass of ionotropic glutamate receptors that mediate fast excitatory neuronal transmission in the mammalian central nervous system (CNS). The two other members of this group include NMDA receptors, crucial for the induction of specific forms of plasticity including long-term potentiation (LTP) and long-term depression (LTD) (Bear, M.F. 1994), and kainate receptors that play important roles in the modulation and plasticity of the synaptic response (Lerma, J. 2006).

AMPA receptors are hetero-tetramers composed of different combinations of the subunits GluR1, GluR2, GluR3 or GluR4, being the most prominent subunit, GluR2 (Nakanishi, S. 1992). These subunits combine in different stoichiometries to form ion channels with distinct functional properties (Hollmann, M. 1994).

The subunit composition of AMPA receptors changes during development and upon neuronal activity. In the mature hippocampus most AMPA receptors are composed of either GluR1-GluR2 or GluR2-GluR3 subunits, whereas GluR4-containing receptors occur mainly during early postnatal stages (Wenthold, R.J. 1996; Zhu, J.J. 2000). Each subunit possesses a large extracellular N-terminal domain, three membrane-spanning domains (TM1, TM3 and TM4), a hairpin that contributes to the pore (M2), and a cytoplasmic C-terminal domain. The four subunits have very similar extracellular and transmembrane domains, but differ in their cytoplasmic tail which provides the subunit-specific interaction with scaffold proteins that bind signaling proteins (for example, kinases, phosphatases) as well as cytoskeletal proteins (for example, actin) (Collingridge, G.L. 2004; Kim, E. 2004; Nicoll, R.A. 2006).

The GluR1, GluR4 and an alternative splice form of GluR2 (GluR2L) have long cytoplasmatic tails. In contrast, the predominant splice form of GluR2, GluR3 and alternative splice form of GluR4 that is primarily expressed in cerebellum (GluR4S) has shorter, homologous cytoplasmatic tails. The C-terminal tail determines the binding of the subunits to specific interacting proteins as well as the modes of the receptors by protein phosphorylation (Song, I. 2002). Expression of the receptor subunits is developmentally regulated and is brain region specific. All four AMPAR subunits also occur in two alternatively spliced versions, flip and flop, that are encoded by exons 14 and 15 (Sommer, B. 1990), and form part of the extracellular ligand-binding domain (LBD). This splicing event is regulated both developmentally and regionally and influences the pharmacologic and kinetic properties of the channel. The flop versions generally desensitize much more rapidly than the flip forms in response to glutamate (Sommer, B. 1990). Furthermore, the flop channels are less responsive to the pharmacological agent cyclothiazide, which blocks desensitization.

AMPARs are also regulated by RNA editing, a process involving enzymatic deamination of ribonucleotides in prespliced mRNA. For example, in adult brain, GluR2 is subjected to RNA editing such that the genomic glutamine (Q) codon for residue 607 can be replaced by the arginine (R) codon. This edited GluR2 controls various AMPAR properties including Ca^{2+} permeability, channel conductance, kinetics and receptor affinity for glutamate, and subunit assembly into a functional receptor (Hollmann, M. 1991; Burnashev, N. 1992). The genetically encoded uncharged glutamine (Q) is changed to a positively-charged arginine (R) that increases the activation energy necessary for calcium to enter into the cell. During development, unedited GluR2 (Q) subunits are abundant whereas in the adult CNS nearly one hundred percent of the GluR2 subunits are edited. Besides, the arginine residue has been shown to control channel composition and, in turn, channel conductance. The R-edited GluR2 is retained unassembled in the endoplasmic reticulum (ER) supporting the formation of GluR2 hetereo-tetrameres over homo-tetramers and restricting the functionally critical number of R-subunits in AMPA-receptor tetramers (Greger, I.H. 2003).

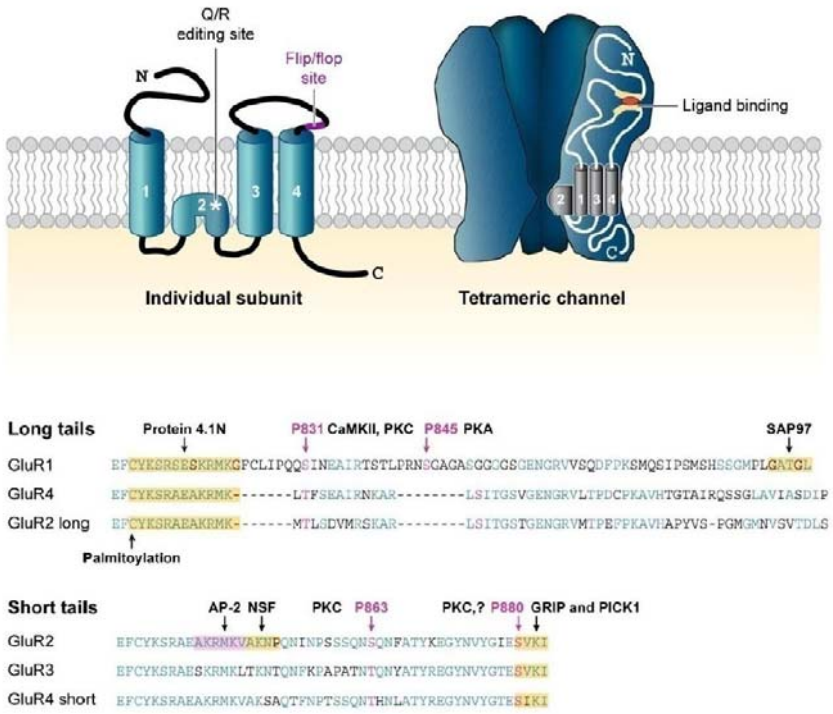

Figure 23: Structure and composition of the AMPA receptor (Shepherd and Huganir, 2007). The individual subunits are composed of four transmembrane domains, a large extracellular N-terminal domain and a subunit-specific cytoplasmic C-terminus. Post-translational modifications are indicated: The Q/R - RNA-editing controls the heteromeric assembly and conductance, the flip/flop splice variants determine the desensitization properties. The channel consists of four subunits, which are usually two dimers of a subunit such as GluR1 and -2 or GluR2 and -3. AMPA receptors C-termini differ in their amino acid sequence determining their interaction partners. Various phosphorylation sites and binding partners are highlighted. Protein abbreviations: AP-2 - adaptor protein-2; CaMKII - calcium/calmodulin-dependent protein kinase II; GRIP - glutamate receptor–interacting protein; NSF - N-ethylmaleimide-sensitive fusion protein; PICK1 - protein interactingwith C kinase 1; PKA - protein kinase A; PKC - protein kinase C; SAP97 - synapse-associated protein 97.

1.3.2.1 AMPA-receptor trafficking

1.3.2.1.1 Vesicular/Cytoskeletal trafficking

During neuronal development, packets of receptors and scaffolding proteins travel along dendrites (Gerrow, K. 2006; Washbourne, P. 2002). The trafficking of these packets is microtubule dependent, and transport is an active process involving motor proteins such as dynein and kinesin (Hirokawa, N. 2005). Although dendrites contain microtubules along which most cargo is transported, dendrites are also enriched in actin, especially in spines. Myosin, the main actin-dependent motor proteins, have recently implicated in AMPAR transport.

1.3.2.1.2 Exocytosis

It is unclear whether AMPARs are first inserted into the extrasynaptic plasma membrane or directly into synapses. One possibility is that AMPARs first are inserted into the membrane in the soma at extrasynaptic sites and then travel out into dendrites via lateral diffusion in the plasma membrane until they finally reach the synapses and become anchored in the PSD. Another possibility is that AMPARs are

trafficked intracellularly into dendrites via the cytoskeleton-associated motors and then directly inserted at synaptic sites. And a third possibility is that AMPARs are synthesized in dendritic compartments and then inserted directly into synapses.

Many studies have shown that plasma membrane insertion of AMPARs is independent on the subunit composition of the receptor. Upon neuronal activity and NMDA receptor activation, GluR1-containing receptors (GluR1-GluR2 heteromers) are added to the synaptic surface increasing synaptic transmission. In contrast, GluR2 containing receptors, including GluR2-GluR3 heteromers and GluR2 homomers, cycle continuously between synaptic and non-synaptic pools independently of neuronal activity, replacing pre-existing receptors (Hayashi,Y. 2000). The permanent cycle, under basal conditions and independent of neuronal activity, allows a fast control of the synaptic receptor density. The current model suggests that GluR2-GluR3 receptors preserve the total number of AMPA receptors by continuous cycling, whereas the GluR1-GluR2 receptors are added to the synapse increasing the total number of receptors in an activity-dependent manner. Understanding the regulation of AMPA-receptor trafficking is therefore of great importance with regards to synaptic plasticity.

1.3.2.1.3 Synaptic targeting and membrane diffusion

AMPARs are concentrated at synapses, where they are precisely localized to efficiently mediate the response to glutamate released from presynaptic terminals. A variety of molecules have been found to associate with AMPA receptors thus controlling their systematic trafficking. Besides controlling trafficking, intracellular molecules interact with AMPA receptors to regulate their stabilization and their electrophysiological properties. These processes seem to be, to a great extent, controlled through interactions between the intracellular carboxy (C)-tails of AMPA receptors and the effector proteins. Many of these effector proteins contain PDZ-domains (postsynaptic density 95, PSD-95; drosophila discs large, Dlg; zonula occludens-1, ZO-1), which interact with the PDZ-binding motif of AMPA receptors located at the C-terminus of the subunit, and forms a functional scaffolding complex.

The GluR1 subunit carries a group I PDZ-motif and specifically interacts with the synapse-associated protein 97 (SAP97), a member of the membrane-associated guanylate kinase family (MAGUK), or with the reversion-induced LIM gene (RIL). SAP97 is essential for the transport of the subunit from the endoplasmic reticulum to the cis golgi and dissociates from the receptor at the plasma membrane (Leonard, A.S. 1998; Sans, N. 2001). RIL might control actin-dependent AMPA-receptor trafficking (Schulz et al., 2004). Furthermore, GluR1 interacts with the cytoskeletal protein 4.1N that links AMPA receptors with actin to mediate their surface expression (Shen, L. 2000). In contrast, both GluR2 and GluR3 carry a group II PDZ-motif and interact with glutamate-receptor-interacting protein (GRIP1), AMPA-receptor-binding protein (ABP; also known as GRIP2) and protein interacting with C kinase 1 (PICK1) (Dong, H. 1997; Xia, J. 1999). Although these molecules bind the same site in AMPA receptors, their binding is differently regulated. This allows them to function in distinct aspects of AMPA-receptor trafficking, membrane insertion or endocytosis, and the stabilization at the synaptic membrane. Disruption of GRIP1 and ABP binding to GluR2 leads to accelerated AMPA-receptor endocytosis at synapses (Osten, P. 2000) revealing a membrane stabilizing role of these two molecules. Phosphorylation of serine 880 (ser880) in GluR2, induced upon receptor activation, leads to the dissociation of GRIP1/ABP but allows the binding of PICK1 and subsequently its endocytosis (Chung, H.J. 2000; Matsuda, S. 1999). Regulating the endocytosis of AMPA receptors is only one of the multiple roles of PICK1 during receptor trafficking. Indeed, PICK1 functions in the removal of AMPA receptor from the synaptic surface during LTD, in constitutive trafficking under basal conditions as well as in the recycling of internalized receptors (Hanley, J.G. 2008; Hanley, J.G. 2005).

Another group of PDZ-domain-containing molecules that bind AMPA receptors are the family of transmembrane AMPA receptor regulatory proteins (TARPS) including stargazing, γ-3, γ-4 and γ-8. TARPs show discrete and complementary expression patterns in both, neurons and glia cells in the brain (Tomita, S. 2003). They facilitate the transport of AMPA receptors from the ER to the plasma membrane and control their expression at the synapse (Ziff, E.B. 2007). Furthermore they assist in the correct folding of the receptors, and affect their channel kinetics as well as their rectification properties. Through their interaction with PSD-95, they link AMPA receptors to the postsynaptic density which appears to be crucial for the synaptic targeting of AMPA receptors (Tomita, S. 2005).

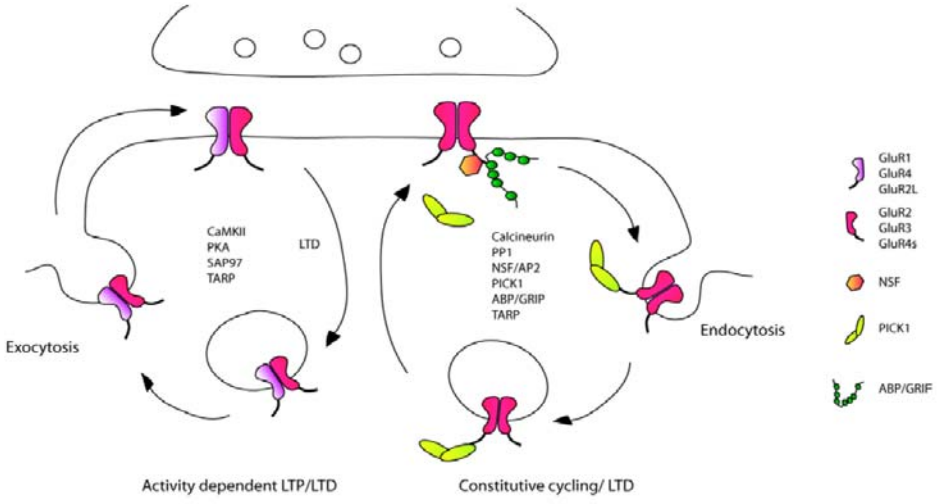

Figure 24: Trafficking of synaptic AMPA receptors (adapted from Bred and Nicoll 2003). AMPA receptors containing subunits with a long cytoplasmic tail (GluR1, GluR4 or GluR2L) are delivered to the synapse upon activity. Some evidence suggests that they are inserted in extra synaptic membrane sites and move laterally to the synapse. Proteins thought to be involved in the delivery include CaMKII, PKA, SAP97, and TARPs. In contrast, receptors containing only short tails cycle constitutively between the synapse and intracellular pools. Proteins like calcineurin, PP1, NSF/AP2, PICK1, and ABP/GRIP regulate different steps during constitutive cycling and LTD. Abbr.: CaMKII- calcium/calmodulin kinase II; PKA- protein kinase A/cAMP dependent protein kinase; TARPS- transmembrane AMPA receptor regulatory proteins; PP1- protein phosphatase 1; NSF- N-ethylmaleimide-sensitive fusion protein; AP2- clathrin adaptor protein 2; PICK1- protein interacting with C kinase 1; ABP- AMPA receptor binding protein; GRIP- glutamate receptor interacting protein.

Beside PDZ-containing proteins, the cytoplasmic tail of GluR2 interacts with N-ethylmaleimide-sensitive fusion protein (NSF), an ATPase known to play an essential role during membrane fusion (Nishimune, A. 1998). The ATPase action of NSF helps to dissociate PICK1 from GluR2 thus facilitating the delivery of AMPA receptors to the cell membrane. Furthermore, NSF allows the binding of GRIP1/ABP resulting in the membrane stabilization of AMPA receptors. Therefore, NSF is crucial in limiting the endocytosis of AMPA receptors and to maintain constitutive cycling at a constant rate and hence to maintain a constant level of receptors at the synaptic membrane (Hanley, J.G. 2002).

1.3.2.1.4 Endocytosis

Clathtin-mediated endocytosis is a general mechanism of membrane protein regulation, and the core endocytic protein machinery is highly conserved in most species and cell types (Mousavi, S.A. 2004). So, postsynaptic endocytosis of receptors is mediated by a similar repertoire of proteins, although perhaps via specific protein isoforms. Dynamin 2 and 3 are mostly postsynaptic and are localized to the PSD via their interaction with the postsynaptic scaffolding proteins Shank and Homer, respectively (Okamoto, P.M. 2001). Endocytosis of AMPARs is similar to the simulated endocytosis of G protein-couple receptors in that processes occurs via clathrin-coated pits and require dynamin.

After internalization, AMPARs are sorted either within early endosomes to a specialized recycling endosome compartment that allows quick reinsertion to the surface or to late endosomes and lysosomes that allow degradation (Ehlers, M.D. 2000; Lee, S.H. 2004).

1.3.2.1.5 Recycling

Recent studies suggest that recycling endosomes contain a pool of AMPARs that is a source for the rapid insertion of receptors. Activation of NMDA receptor can regulate the kinetic of recycling and significantly affect the relative amount of receptors that are maintained intracellularly versus on the surface (Park, M. 2004). This enhancement of recycling also provides additionally lipid membrane, which is critical for the structural growth and expansion of dendritic spines during long term potentiation (LTP) (Park, M. 2006).

1.3.2.1.6 Degradation

Little is known about how AMPARs are degraded at synapses, but some studies suggest a role for the ubiquitin/proteasome system (UPS) (Colledge, M. 2003; Patrick, G.N. 2003).

OBJECTIVES

CHAPTER 2 : OBJECTIVES

2.1 GENERAL OBJECTIVE:

- To determine the molecular and physiological function of CPT1C enzyme.

2.1.1 Specific objectives

1. To identify CPT1C activity and characterize its kinetic parameters in cultured mammalian cells.
2. To determine whether CPT1C is involved in the *de novo* ceramide synthesis pathway.
3. To study CPT1C expression along mouse brain development and in the peripheral nervous system.
4. To characterize the implication of CPT1C in the motor and cognitive behavior.
5. To study CPT1C function in dendritic spine morphology and in the trafficking of AMPA receptor at the plasma membrane of hippocampal neurons.

EXPERIMENTAL PROCEDURES

CHAPTER 3 : EXPERIMENTAL PROCEDURES

3.1 MOLECULAR BIOLOGY

3.1.1 Microbiology

3.1.1.1 Bacterial strains

The *Escherichia coli (E.Coli)* strains used in this study is DH5α for plasmid propagation. (DH5α: F^-/endA1 glnV44 thi-1 recA1 relA1 gyrA96 deoR nupG Φ80d*lacZ*ΔM15 Δ(*lacZYA-argF*) U169, hsdR17(r_K^- m_K^+), λ–) .

It was grown in autoclaved LB agar plates made from Pronadisa powder (Luria Agar, #1552.00) with the antibiotic necessary for plasmid selection.

3.1.1.1.1 Preparation and transformation of competent *E.Coli*

Plasmid DNA can be introduced into competent bacteria by the process of transformation.

3.1.1.1.2 Obtaining of competent E. coli

Competent cells are those cells which have been treated to increase their capacity to introduce a circular exogenous DNA. They were obtained by concentration through successive washes in water and 10% glycerol.

Competent cells were prepared in the laboratory following the next protocol:

1. A single colony of *E. coli* cells was inoculated into 5 ml LB medium with the appropriate antibiotic and grown o/n at 37°C with moderate shaking.
2. The next day, 500 ml of LB plus antibiotic was inoculated with the 5 ml preinocul and grown for approx. 2h in the shaker at 37°C to an OD_{600} of 0.5-0.6.
3. Cells were then chilled on ice for 10 min and centrifuged at 1,600 x *g* for 15 min at 4°C (centrifugation stopped without brake).
4. Cells should be kept at 4°C for the subsequent steps.
5. After that, the pellet was immediately resuspended in 10 ml of sterile and ice-cold $CaCl_2$.
6. Centrifuge again at 1,100 x *g* for 5 min at 4°C.
7. Resuspend the pellet in 10 ml of sterile and ice-cold $CaCl_2$.
8. Centrifuge again at 1,100 x *g* for 5 min at 4ºC.
9. Discard the supernatant and resuspend the pellet in 2 ml $CaCl_2$.
10. Put 100 µl aliquots are stored at -80°C.

$\underline{CaCl_2}$: 60 mM $CaCl_2$, 15% glycerol, 10mM PIPES pH 7. Filter the solution and store at 4°C.

3.1.1.1.3 Bacterial transformation protocol

The transformation process consists of introducing the plasmid DNA into the competent bacterial cells for later amplification, plasmid purification or protein expression.

Plasmid DNA was introduced by the heat-shock method as follows:

1. Thaw competents *E. coli* cells (DH5α) on ice.
2. Add 1-5 µl of DNA in each transformation tube.
3. Add 50-100 µl competent cells in a 13 ml polystyrene tube (Sarstedt, #55.468.001). To transform a DNA construct use 30-50 µl of competent cells. In order to transform a ligation use 100 µl of competent cells. Mix by pipetting up and down only once.
4. Incubate the tubes on ice for 30 min.
5. Heat-shock the cells for 1 min at 42°C.
6. Put tubes back on ice for 2 min.
7. Add 1 ml of LB (with no antibiotics). Incubate tubes for 1 hour at 37°C with vigorous shaking (250rpm).
8. Spin down briefly in a microcentrifuge. Remove supernatant and resuspend the cell pellet with 100 µl of LB medium in the tube by softly pipetting.
9. Plate out the suspension on an LB agar plate containing the appropriate antibiotic and incubate the plates up-side-down overnight at 37°C.
10. Pick colonies about 12-16 hours later.

3.1.1.1.4 Plasmid vectors

3.1.1.1.4.1 pIRES2-EGFP:

The pIRES2-EGFP plasmid vector (BD Biosciences, #6029-1) is a vector of approx. 5.3 kbp designed to translate the protein cloned into the multiple cloning site and the enhanced green fluorescent protein (EGFP) from a single bicistronic mRNA. The vector contains the SV40 origin of replication for expression in mammalian cells. It also contains the Kanamycine/Neomycin resistance gene for bacterial or mammalian cells selection and a suitable origin of replication for bacterial propagation.

3.1.1.1.4.2 pIRES-EGFP-CPT1C:

From base pair 1 to 2403 of rat CPT1C cDNA sequence (also excluding stop codon) was amplified using primers F1bisRnCPT1C and R5RnCPTca that introduced BamHI sites at each end. Primer reverse sequence also introduced base pairs to maintain the reading frame with EGFP.

3.1.1.1.5 Bacterial culture

Bacterial strains were cultured in LB medium (Luria-Bertrani Broth) in the presence of the appropriate antibiotic. When cells were grown in a solid medium, 2% of agar was added to the LB medium.

In the case of the bacterial strains and vectors used in this study, the antibiotics ampicillin and kanamycine were used.

Solid LB medium: LB medium plus 2% (w/v) agar. It is autoclaved immediately. When the temperature is about 50°C, 100 mg/L ampicillin/kanamycine is added and the medium is distributed into 10-cm plates with 30 ml of medium each. Plates are stored at 4°C.

3.1.1.1.6 Plasmid DNA preparation

Plasmid DNA was obtained from bacterial cultures that contain the plasmid of interest by growing them in LB medium with the appropriate antibiotic and the later purification of the plasmid DNA from the cell lysate.

Minipreparations of plasmid DNA were obtained using the *Minipreps DNA Purification System* (Promega, #A1330) where the yield of high-copy-number plasmids obtained were about 3-5 µg DNA per millilitre of the original bacterial culture. When higher amounts of plasmid DNA were needed, the *QUIAGEN Plasmid Maxi kit* (QUIAGEN, #12163) was used. In this case up to 500 µg DNA could be obtained.

Minipreparations were obtained from 2 ml LB medium with the appropriate antibiotic which has been inoculated with a single colony of *E. coli* cells and grown overnight (o/n) at 37°C with moderate shaking. For the maxipreparations, 500 ml of LB medium with the appropriate antibiotic was inoculated with the 2 ml preinocul and grown o/n at 37°C with moderate shaking. In both cases cells were harvested by centrifugation and lysed with NaOH and SDS. The precipitate formed contains the bacterial genomic DNA, proteins, cell debris and SDS. The bacterial RNA was degraded by the action of RNAse. Then, the plasmid was purified from the supernatant using ion-exchange resin columns. After that, the DNA was washed and eluted, and it was pure enough for enzymatic modifications, PCR, sequencing, etc.

For future preparation of plasmid DNA, a stab of each construct was prepared as follows: 1 ml aliquot from the 500 ml maxipreparation inoculum was mixed with 500 µl of 50% sterile glycerol and stored at -80°C.

3.1.2 DNA and RNA resolution and purification

3.1.2.1 DNA preparation from mouse tail

The DNA for genotyping was prepared from mouse tail of about 0.1-0.5 cm length. The tails were boiled at 95°C in 100 µl 50 mM NaOH for 45 min using the termoblock machine and thoroughly vortex afterwards. If it is necessary, this step is repeated until the tails are properly dissolved. To neutralize the lysates, 10 µl of 1.5 M Tris pH 8.3 was added, mixed by vortexing and centrifuged down for 30 sec. 2 µl of the samples was used for genotyping.

3.1.2.2 DNA amplification

3.1.2.2.1 Polymerase chain reaction (PCR) for mouse genotyping

The polymerase chain reaction (PCR) is used to amplify a segment of DNA that lies between two regions of known sequence.

A master mix for 25 µl reaction volume was done for each sample:

Master mix Components	Volume
DNA	2 µl
dNTPs (2,5 mM each)	0.4 µl
Primer 1 (100 µM)	0.5 µl
Primer 2 (100 µM)	0.5 µl
10x Taq pol buffer	5 µl
Taq Polymerase	0.5 µl
Distilled H2O	16.1 µl

Primers used for the PCR:

- KOF9: 5´- GAG TCA GCC ATG ACC CGA CTG TTG-3´
- KOR1: 5´-CCG GTA GAA TTG ACC TGC AGG GGC-3´
- KOR9: 5´-CGC TAA AGC CCA GAC AGA ACA CAC-3´

Two separate reactions were done to identify mice genotype. KOF9-KOR9 primers were used to identify WT band and KOR1-KOR9 primers for CPT1C-KO band.

The DNA samples (2 µl) were placed into 96 well PCR reaction tubes, the master mix was prepared and added, and the tubes were placed into the PCR machine to run the appropriate program. Samples were run in 2% agarose gel.

PCR program used for genotyping was the following:

Segment	Cycles	Temperature	Time
1	1	94°C	1 min
2	35	94°C	45 sec
		62°C	45 sec
		72°C	45 sec
3	1	72°C	5 min
4	1	10°C	Forever

3.1.2.3 DNA resolution in agarose gels

To separate different sized DNA fragments or/and to determine their length and amount, DNA samples were run on agarose gels of 1-2% and separated by electrophoresis. Low melting temperature agarose (Genaxis, #GX12420) was dissolved in 1x TAE buffer by microwaving, mixed with 0.5 µg/ml ethidium bromide to visualize the DNA, poured into an electrophoresis gel chamber and cooled to RT while polymerizing.

DNA samples were mixed with 1X loading buffer loaded into the gel pockets and separated for approximately 30-45 min at 100-200V depending on the gel size. A picture of the gel was taken in the transilluminator on UV light.

1x TAE electrophoresis buffer: 40 mM Tris-acetate pH 8.3, 1 mM EDTA.

10x sample loading buffer: 0.42% bromophenol blue, 0.42% xylene cyanol FF, 50% glycerol in bidistilled water.

3.1.2.4 DNA and RNA quantification

3.1.2.4.1 DNA and RNA spectrophotometric quantification

RNA and DNA were quantified in a spectrophotometer measuring the absorbance at 260 and 280 nm in 1 ml quartz cuvettes. The reading at 260 nm allows calculation of the concentration of nucleic acid in the sample. An OD of 1 corresponds to approximately 40 µg/ml for single-stranded DNA and RNA, and 50 µg/ml for double-stranded DNA. The ratio between the readings at 260 and 280 nm (OD_{260}/OD_{280}) provides an estimate of the purity of the nucleic acid. Pure preparations of RNA and DNA have OD_{260}/OD_{280} values higher than 1.6 and 1.8, respectively.

Therefore, the RNA or DNA concentrations in a sample could be given as:

RNA (µg/µl) = OD x 40/v

DNA (µg/µl) = OD x 50/v

Where OD is the absorbance at 260 nm and v is the µl of RNA or DNA diluted in 1 ml of water and quantified in the spectrophotometer.

3.1.2.5 RNA isolation

Total RNA isolation from tissue was performed using Trizol Reagent (Life Technologies, #15596) following manufacturer's instructions. Tissue was homogenized 25 times on ice, using the loose pestle of a Douncer with 1ml of Trizol Reagent per 50-100 mg of tissue.

The protocol was performed as follows:

- Separation:
    1. Incubate the mix during 5 min at 15-30°C to allow the correct dissociation of the nucleoproteins.
    2. Add 0.2ml of cloroform per each ml of Trizol.
    3. Shake the tube during 15 sec and incubate 15-30°C during 3 min.
    4. Centrifuge at 12000 x g during 15 min at 2-8ºC. A phase separation is done:
        - Down phase phenol-cloroform
        - Interphase
        - Aquost phase: where RNA is found.

- Precipitation:
    1. Transfer the aquous phase to a new eppendorf.

2. Add 0.5ml of isopropilic alcohol per each ml of Trizol.
3. Incubate at 15-30°C during 10 min.
4. Centrifuge at 12000 x g during 10 min at 2-8°C.

- Cleaning:

1. Remove the supernatant.
2. Add 1 ml of ethanol 75% RNAase free per each ml of Trizol to clean the pellet.
3. Vortex and centrifuge at 7500 x g during 5 min at 2-8°C
4. Dry the pellet and dissolve in H_2O DEPC (40µl).
5. Incubate the mix at 60°C during 10 min.

3.1.2.6 cDNA synthesis

Reverse Transcription (RT reaction) is a process in which single-stranded RNA is reverse transcribed into complementary DNA (cDNA) by using total cellular RNA, a reverse transcriptase enzyme (Moloney Murine Leukemia Virus Reverse Transcriptase: M-MLV RT (Invitrogen, #28025-013)), a primer, dNTPs and an RNase inhibitor. Three types of primers can be used for RT reaction: oligo (dT) primers, random (hexamer) primers and gene specific primers with each having its pros and cons.

The PCR reaction used for cDNA synthesis was:

Component	Volume/well (20 µL)	Final concentration
Buffer 5X	4 µl	1X
DTT 0.1M	2µl	10mM
dNTPs 10 mM each	1 µl	500 µM
Random 50ng/µl	5 µl	250 ng
RNAasa out 40U/µl	0.5 µl	20U
MLV-RT 200U/µl	1 µl	200U
RNA	---	2 µg
H2O DEPC	---	Up 20 µl

The reaction was put in the Thermocycler machine following the manufacture´s instructions.

3.1.2.7 Real time PCR

Real time PCR is a combination of a conventional PCR plus a fluorimeter that determine the fluorescence produced by the amplification tube long the reaction. For real time PCR analysis, Taqman® Gene expression assays were used (Applied Biosystem).

The protocol used for the reaction was:

Component	Volume/well (20 µL)	Final concentration
TaqMan 2X	10 µl	1X
20X Assay on demand	1µl +1µl	1X
cDNA	9µl (2 µl cDNA + 6 µl H2ODEPC)	--
Total	20 µl	--

Taqman probes used for the experiment were the followings:

- CPT1C: Mn00463970_m1
- CPT1A: Mn00550438-m1
- CPT1B: Mn 00487200-m1
- Pdk4: Mn 01166879-m1

Relative abundance of mRNA was calculated after normalization to GADPH mRNA.

3.1.3 Protein quantification and detection

3.1.3.1 Cell and tissue lysis

Cells or tissue were lysed in chilled lysis buffer (containing freshly added phosphatese inhibitor cocktail and kinase inhibitor cocktail (Roche)). Cells were placed on an ice tray, washed once with cold PBS and collected from the culture dish in the appropriate volume of lysis buffer (e. g. 500 µl/ 10 cm Ø dish) using cell scraper (Sarsted). Tissue was homogenized in chilled lysis buffer using a glass homogenizer (B.Braun, Melsulneg AG). Lysates were collected in tubes on ice and fixed on a spinning wheel at 4°C for minimum 10 minutes to let the lysis proceed. Thereafter, the lysates were cleared from cell debris by centrifugation at 4°C (10 minutes from cell lysates, 45 minutes for homogenized tissue) and the protein content was determined.

3.1.3.2 Bradford method for protein quantification

Protein levels were measured according to the manufacturer's instructions (BioRad protein assay, #500-001 MT), using BSA (Sigma, #P0834) as a protein standard in the range of 2-25 µg/ml. BSA standard stock was prepared in water at 0.1 mg/ml and the absorbance of the blank, standard curve or the samples were measured at 595 nm in a spectrophotometer with plastic cuvettes in a total volume of 1 ml.

3.1.3.3 Protein separation and Western blot assay

SDS-PAGE electrophoresis was used to separate proteins by their molecular weight using different percentages depending on the predicted weight of the protein to be analyzed.

When Western blot was not being performed, the gel at the end of the electrophoresis was stained with Bio Safe Coomassie (BioRad, #161-0786) to evaluate the protein content of the sample.

When Western blot was to be performed, the proteins in the gel were transferred to Immobilon PVDF membranes (Millipore, #IPVH 00010). The side of the membrane in contact with the gel was marked to identify the side where proteins were, for later antibody incubation and detection. The transference was performed at 4°C for 3h at 300 mA. Once it was finished, membrane was immersed in blocking solution for 1h and the gel was stained with Bio Safe Coomassie to determine the degree of transferred protein.

2x Protein Loading Buffer: 130 mM Tris-HCl pH 6.8, 6% SDS, 15% β-mercaptoethanol, 20% sucrose and 0.05% bromophenol blue. It is prepared freshly at the moment of use.

5x Electrophoresis buffer : 25 mM Tris, 250 mM glycine and 0.1% SDS. It is stored at room temperature.

Transfer buffer: 12 mM Tris, 20% methanol and 96 mM glycine. It is stored at 4°C.

3.1.3.3.1 Blocking the membrane:

Non-specific binding sites were blocked by immersing the membrane in blocking solution, 5% (w/v) of nonfat dried milk in TBS-T for 1h on an orbital shaker at room temperature. After this time, membrane was rinsed and washed three times for 10 min in TBS-T on an orbital shaker.

3.1.3.3.2 Primary antibody incubation:

Incubations were done overnight at 4°C on an orbital shaker. After this time, membranes were rinsed and washed three times for 10 min in TBS-T on an orbital shaker. The first antibody could be reused by storing it at -20°C.

Primary antibodies used were:

- **Anti CPT1A**: rabbit CPT1A specific polyclonal antibody against amino acids 317-430 of the rat liver CPT1A (Prip-Buus). Diluted 1/1.000 in blocking solution.
- **Anti CPT1B**: sheet CPT1B specific polyclonal antibody against amino acids 259-760 of the rat muscle CPT1B (Farmacia,UB). Diluted 1/1.000 in bloquing solution
- **Anti CPT1C**: rabbit CPT1C specific polyclonal antibody against the last 14 amino acids of the *Mus musculus* sequence of CPT1C (Sigma Genosys). Diluted 1/500 in blocking solution.
- **Anti Tubulin:** mouse tubulin monoclonal antibody (Sigma, #T5201). Diluted 1/1.000 in blocking solution.
- **Anti GluR2:** rabbit (Upstate, # AB1768-25µg) Diluted 1/1.000 in blocking solution.

3.1.3.3.3 Secondary antibody incubation:

Incubations were performed for 1h at room temperature on an orbital shaker. After this time, membranes were rinsed and washed three times for 10 min in TBS-T on an orbital shaker.

Secondary antibodies were detected using ECL reagent (Amersham Biosciences, #RPN 2106).

Secondary antibodies used for the experiments were:

- **Donkey anti- rabbit HRP IgG** (Amersham Biosciences, ref. NA 9340) was used for detecting CPT1A or CPT1C primary antibodies. A dilution of 1/5.000 in blocking solution was used.
- **Donkey anti-sheep HRP IgG:** was used for detecting CPT1B primary antibodies. A dilution of 1/5.000 in blocking solution was used.
- **Sheep anti-mouse HRP IgG** (Jackson immunoresearch, #515-035-003): was used for detecting tubulin primary antibodies. A dilution of 1/10.000 in blocking solution was used.

TBS-T: 0.1% Tween20 in 1X TBS (20 mM Tris, 137 mM NaCl, 3.9 mM HCl). It is stored at room temperature.

3.1.3.3.4 Reprobing membranes

Following ECL detection the membranes may be stripped of bound antibodies and reprobed several times. The membranes were stored wet and wrapped in a refrigerator (2–8°C) after each immunodetection.

The complete removal of primary and secondary antibodies from the membrane was possible following the protocol outlined below.

1. Submerge the membrane in stripping buffer (100 mM 2-Mercaptoethanol, 2% SDS, 62.5 mM Tris-HCl pH 6.7) and incubate at 50°C for 30 minutes with occasional agitation.
2. Wash the membrane for 3 × 10 minutes in TBS-T at room temperature using large volumes of wash buffer.

3.2 CELL BIOLOGY

3.2.1 Cell lines and maintenance

3.2.1.1 Cell lines

3.2.1.1.1 HEK293 cell line

This cell line derived from human embryonic kidney, was grown at 37°C with 5% CO_2 in complete medium composed of Dulbecco´s Modified Eagle (DMEM, Gibco, #41965-039) containing 4,500 mg/L glucose and suplemented with 10% (v/v) heat inactivated FBS, 2mM glutamine and penicillin/streptomycin (100 U/ml / 100 µg/ml). The maintenance culture was passaged once a week and the medium was changed every 2-3 days. To passage HEK293 cells, it was not necessary to trypsinise them. Cells were first washed in PBS preheated to 37°C and then detached by simply up and down pippetting with medium preheated to 37°C and spread as desired. For experiments cells were grown until confluence.

3.2.1.1.2 PC12 cell line

Cell line PC12, derived from a pheocromocytoma of the rat adrenal medulla, was grown at 37°C with 5% CO_2 in Kaighn's modification of Ham's F12 medium (F12K) (Invitrogen, #21127-022) containing 15% Horse serum (HS) (Gibco, #16050-122) and 2.5% FBS, 2 mM glutamine and penicillin/streptomycin (100 U/ml / 100 µg/ml). The medium was changed every 2-3 days.

All solutions used for cell culture were sterilized by autoclaving at 121°C for 30 min or by filtering them through a 0.22 µm filter (Millipore, #SLGP33R3).

3.2.1.2 Basic procedures in cell culture

3.2.1.2.1 Counting the cells

Cells were counted in a Neubauer chamber. One drop of cells resuspended in medium was placed between the coverslip and the chamber. Cells from one large square (which contains 16 small squares) were counted and multiplied by 10,000 to calculate the number of cells per ml.

3.2.1.2.2 Freezing the cells

First cells were detached with medium. Then, they were centrifuged at 1,200 rpm for 5 min and resuspended in 1.5 ml of medium plus 150 µl of DMSO in a 1.5 ml cryogenic tube. DMSO is a cryoprotector agent that physically protects the cells from the forming ice crystals, changes in osmotic pressure or fast freezing. However the 10% DMSO used to freeze the cells is toxic at 37ºC, so cells must be frozen immediately at -80°C in a recipient with isopropanol and stored in liquid N_2 the following day.

3.2.1.2.3 Thawing the cells

Cells were stored in the cryogenic tube were thawed in a 37°C water bath. Then, they were diluted in 10 ml of medium and centrifuged at 1,200 rpm for 5 min to eliminate medium with DMSO. After that, cells were resuspended in the desired volume of medium and seeded. Medium was changed the next day.

3.2.2 Primary hippocampal cell culture

Hippocampal primary cells were obtained from E17 mouse embryos of C57BL/6J wild-type and CPT1C-KO mouse.

3.2.2.1 Coverslip (CVS) treatment

CVS were treated with nitric acid (Fluka) in a glass beaker at RT overnight. The next day, the CVS were washed 3-4 times with H_2O, left with changes of fresh H_2O on a rocker 4 times for 30 minutes to briefly remove the acid and they were spread separately on Whatman paper to dry. Dry CVS were baked to sterilize in the oven at 165°C.

3.2.2.2 Coating of the CVS

The CVS were placed into 24-well plates (Costar) and coated with 1 mg/ml poly-D-lysine (Sigma, #P7886-1G) in Borate-Buffer (400 µl/well), which has been sterilized by passing through a 0.22 µm pore size filter after poly-D-lysine dissolvement, at 37°C for minimum 5 hours. Then the CVS were washed 3 times with distilled sterile H_2O, left in the hood to dry and coated with 5µg/ml laminin in PBS (400µl/well) for minimum 2 hours at 37°C. Excessive laminin was washed off 3 times with PBS, the wells were filled with 400 µl NB medium and placed into the incubator for pH and temperature equilibration.

3.2.2.3 Isolation of hippocampal neurons

4 ml of serum medium (SM) and Neurobasal medium (NB) each was filled in dishes and placed into the incubator; trypsin was put into the water bath to warm up. The embryos of pregnant E17 mouse were taken, the heads were cut off and collected in a 35mmØ dish filled with chilled dissection medium (DM).

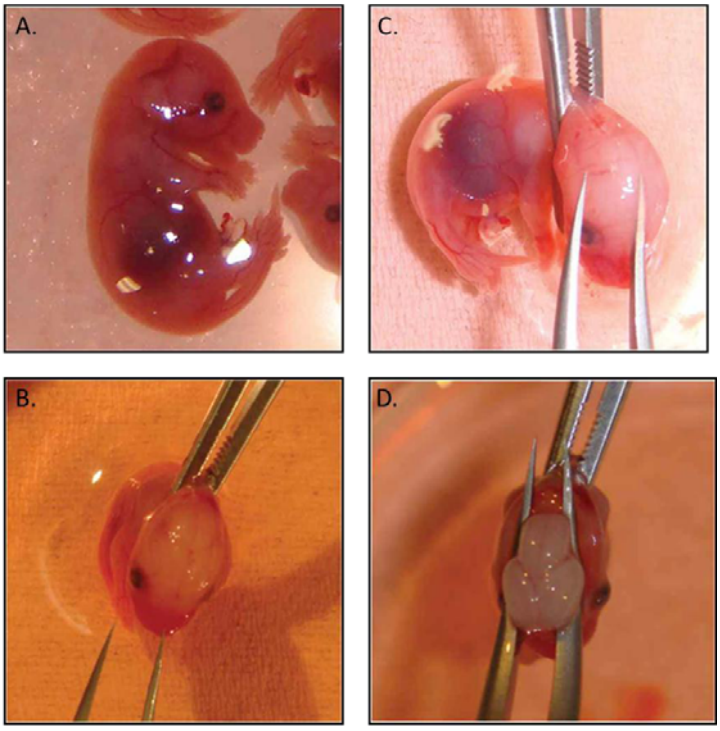

Figure 25: Collecting brains from E16.5 embryos. A. E16.5 embryo removed from the uterus. B. Hold the embryo at the neck while inserting the sharp tip of a bent Dumont no. 7 forceps above the nose. C. Push the forceps forward underneath the bone to open the skull untel the rear of the head. C. To remove the brain, press the opened forceps gently against the skull, thereby moving the bone down- and sidewise. Close the forceps beneath the brain and transfer brain into fresh HBSS. (Modified from Fath, T. 2009).

Carefully the skulls were opened, the brains removed and transfered into a fresh dish of 35 mm Ø filled with chilled DM. The two cortices halves of each brain was then separated from the brain steam, the meninges were removed and the hippocampi were cut out of each cortex half. The hippocampi were collected in a 15 ml tube on ice filled with 10 ml DM. When all hippocampi were isolated, the DM was carefully replaced by 1-2 ml prewarmed trypsin and the tube placed into the water bath for 20 min at 37ºC. Meanwhile, a Pasteur pipette was flamed to decrease the diameter of the tip. The trypsin was removed after 20 min and the hippocampi washed 3 times with prewarmed SM to stop the reaction. The tissue was homogenized in 1.5 ml SM using the fire-polished Pasteur pipette by pipetting up and down 20-30 times, it was carefully avoided to make bubbles (neurons do not like oxygen). Cells were collected by centrifugation for 5min at 650 rpm, the supernatant removed and the cells resuspended in warm NB medium using the fire-polished Pasteur pipette. Cell number was determined using a Neubauer counting chamber, there after the cells were plated on the CVS in 24-well plates with prewarmed medium at desired density. Low density cultures require 75.000 cells/well (24 well/plate). In 6 well/plate 200.000 cells per well are plated.

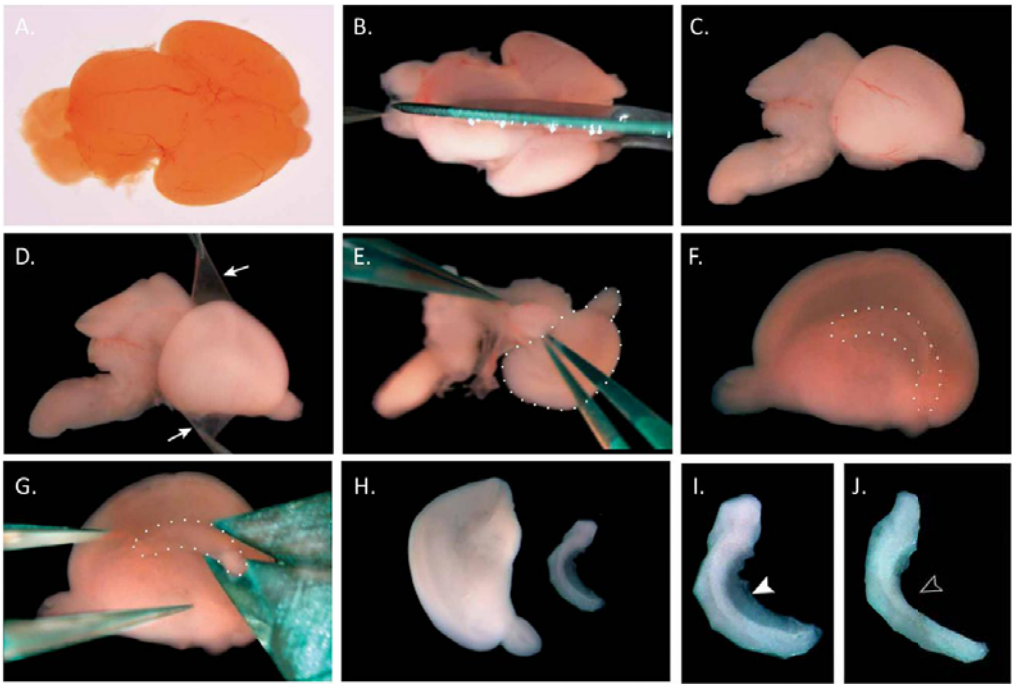

Figure 26: Dissection of hippocampus from embryonic E16.5 brains. A. The E16.5 mouse is **B.** cut intothe halves via the midline sagittal section. **C.** The halves are placed such that the cortex is facing up. **D.** Meninges (arrows) are removed from the hemispheres with Dumont no. 5 froceps by gently pulling. **E.** While holding the brainstem, the cortex (cx) is flipped outward and clipped off the midbrain. **F.** The hippocampus (hip) is visible on the inner surface of the forebrain. **G.** The hippocampus is removed with a microscissor. **H.** Cortex (cx) and hippocampus (hip) are separated**. I and J.** The fimbriae (arrowhead) on the concave side of the hippocampus are removed (open arrowhead)(Modified from Fath, T. 2009).

3.2.2.4 Media and supplements for primary cell culture

3.2.2.4.1 Borate buffer

Dissolve 1.55 g of boric acid and 2,375 g of borax in 500 ml distilled water, adjust to pH 8.5 and store at 4°C. For coating of plate and cover slips, dissolve Poly-D-Lysine (1 mg/ml) in borate buffer and sterilize by filtration.

3.2.2.4.2 Neurobasal medium (NB)

Neurobasal medium (Invitrogen, #21103-049)	500 ml
B27 supplement (Invitrogen, #17504-044)	10 ml
L-Glutamine, stable 200 mM (PAA, #M11-004)	1.25 ml

Store at 4°C. For low density and hippocampal neuron cultures add 10% conditioned neurobasal medium.

3.2.2.4.3 Serum medium (SM)

DMEM (Invitrogen, #61965-026)	100 ml
FBS, heat inactivated (Invitrogen, #F-7524)	10 ml

Sterilize by passing through a 0.22 µm-pore sized filter and stored at 4°C. FBS is kept in aliquots of 10 ml at -20°C.

3.2.2.4.4 Dissection medium

HBSS (Invitrogen, #24020-091)	500 ml
Penicilin/Streptomycin (Invitrogen, #15070-063)	5 ml
1M Hepes (Invitrogen, #15630-056)	3.5 ml
L-Glutamine 200 mM (PAA, #M11-044)	5 ml

Store at 4°C and keep on ice during dissection.

3.2.3 Development of a CPT1C knock out mouse

In order to study the physiological role of CPT1C enzyme, a knock-out (KO) mouse for the enzyme was generated in collaboration with the *Centre de Biotecnologia Animal i Teràpia Gènica (CBATEG)* at the *Universitat Autónoma de Barcelona (UAB).*

3.2.3.1 Strategy to generate CPT1C Knock-out mouse (CPT1C-KO)

The generation of CPT1C knockout mice (CPT1C-KO) was through a genetic mutation introduced by homologous recombination. A construct for CPT1C deletion was generated using the pPNT vector. A 2.0 kb genomic fragment from intron 9 to intron 11 of the mouse CPT1C gene was cloned into pPNT vector downstream of the neo cassette as the 5' flank. A 1.9 kb genomic fragment from intron 15 to exon 19 of the mouse CPT1C gene was cloned into pPNT vector upstream of the neo cassette as the 3' flank. The neo cassette was in the opposite transcriptional orientation to the CPT1C gene and was used for a positive selection for homologous recombination. Figure 27 shows a schematic representation of the targeted loci of the mouse CPT1C and the pPNT vector used for CPT1C-KO generation. Exons are depicted as shaded boxes and the arrow indicates the position of the catalytic histidine of the enzyme.

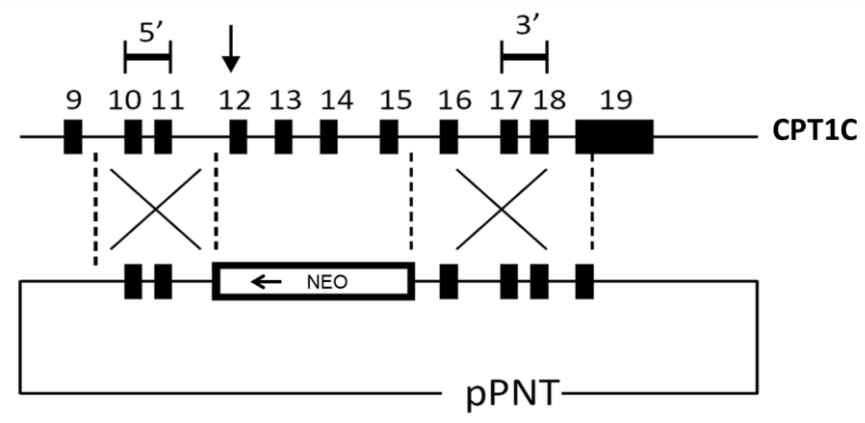

Figure 27: Generation of CPT1C-KO mice. Schematic representation of the targeted loci of the mouse CPT1C and the pPNT vector used for the generation of CPT1C-KO mice. A 2.0 kb genomic fragment from intron 9 to intron 11 of the mouse CPT1C gene was cloned into pPNT vector downstream of the neo cassette as the 5' flank. A 1.9 kb genomic fragment from intron 15 to exon 19 of the mouse CPT1C gene was cloned into pPNT vector upstream of the neo cassette as the 3' flank. The neo cassette was in the opposite transcriptional orientation to the CPT1C gene. Exons are depicted as shaded boxes. The arrow indicates the position of the catalytic histidine of the enzyme.

The targeting construct was electroporated into 129SvEv embryonic stem cells (ESC) and the two positive ESC clones obtained during the analysis were expanded and verified for correct recombination with PCR amplification and non-radioactive Southern blot analysis.

In the PCR analysis, two specific primer pairs were used to verify the correct recombination. For 5´insertion: 5'- GAGATCAGCAGCTCTTGTTCCAC-3 and' 5'-CACTACACGGATTCCAGGGTGGG-3' were used, for the 3´insertion: 5'-CCGGTAGAATTGACCTGCAGGGGC-3' and 5'GGGGCTCACAAGTTGGGTGG

AGGATG-3´ were used. In figure 28A, amplification of 3´ end was used to identify wild type (WT), heterozygous (HT) and CPT1C-KO mice. PCR results were analyzed in 2% agarose gel.

Positives clones were also analyzed using a non-radioactive Southern blot. Analysis of genomic DNA from ESC or mouse tail was digested by *Xho*I, *EcoR*I or *EcoR*I/*Xba*I restriction site enzymes. PCR DIG Probe Synthesis Kit (Roche) was used to generate a 900 bp DIG labeled 3' and a 500 bp DIG labeled 5' external probes. DIG Easy Hyb (Roche) was used as hybridization solution, following the protocol recommended by the manufacturer. In figure 28B a non-radioactive Southern blot for the 5´end genotype detection was used, showing a 5 kb and 7Kb band for WT and CPT1C-KO mice, respectively.

After knockout ES cell lines were identified, they were cultured to expand, and microinjected into C57BL/6 mouse blastocysts. Then the blastocysts were transferred into foster mothers. The mice born from these procedures were referred to as chimeras, as they were composed of cells derived from the C57BL/6 embryo and the 129/SV ES cells. C57BL/6 mice have a black coat while 129/SV mice have an agouti coat. By examining the coat of chimeric mice, we could estimate the percentage of cells derived from 129/SV ES cells. In order to maximize the chances of generating excellent chimeric mice, multiple ES cell lines were injected.

We selected the best chimeric mice and mate these mice to C57BL/6 mice in order to transmit the knockout allele through the mouse germ line. Then, DNAs from the tail biopsies were extracted and analyzed by either Southern blot analyses or PCR to identify heterozygous mice in between the knockout allele. Then, the heterozygous knockout mice were intercrossed to generate homozygous knockout mice.

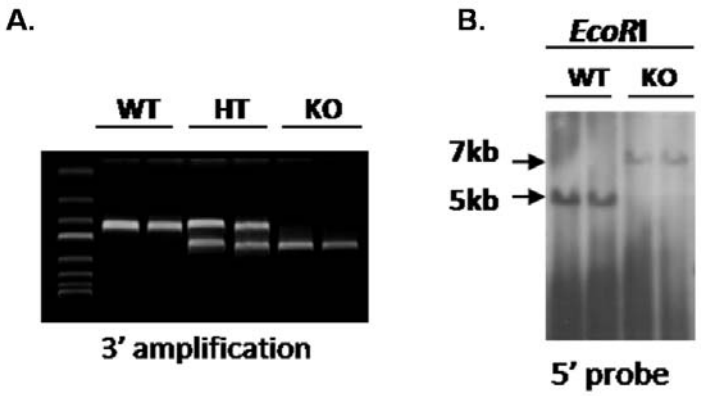

Figure 28: Generation of CPT1C-KO mice. A. PCR amplification and B. Southern blot analysis of genomic DNA from mice tails. A. PCR analysis was performed using the following primer pairs: (1) 5'-GAGATCAGCAGCTCTTGTTCCAC-3' and 5'-CACTACACGGATTCCAGGGTGGG-3' for the 5' insertion, and (2) 5'-CCGGTAG AATTGACCTGCAGGGGC-3' and 5'-GGGGCTCACAAGTTGGGTGGAGGATG-3' for the 3' insertion. B. For Southern blot analysis genomic DNA obtained from ESC or mouse tail was digested by *EcoR*I. PCR DIG Probe Synthesis Kit (Roche) was used to generate a 500 bp DIG labeled 5' external probe. DIG Easy Hyb (Roche) was used as hybridization solution, following the protocol recommended by the manufacturer.

3.2.3.2 Analysis of CPT1C expression in CPT1C-KO mouse

Next step was to confirm the lack of expression of functional protein in CPT1C-KO mouse.

CPT1C mRNA and protein levels from samples of WT, HT and CPT1C-KO mice were checked by real time PCR and western blot, respectively.

Figure 29A shows that no CPT1C mRNA levels were observed in CPT1C-KO mice, showing a complete deficiency of CPT1C in CPT1C-KO mice. Moreover, moderate levels of CPT1C mRNA were found in heterozygous (HT) animals respect to the WT mice.

Same result was confirmed by western blot assay (Figure 29B). 80 µg of brain protein and polyclonal anti-CPT1C antibodies were used. We determined that CPT1C was absent in homozygous knockout mice, and heterozygous animals exhibited moderate levels of CPT1C expression compared to WT mice.

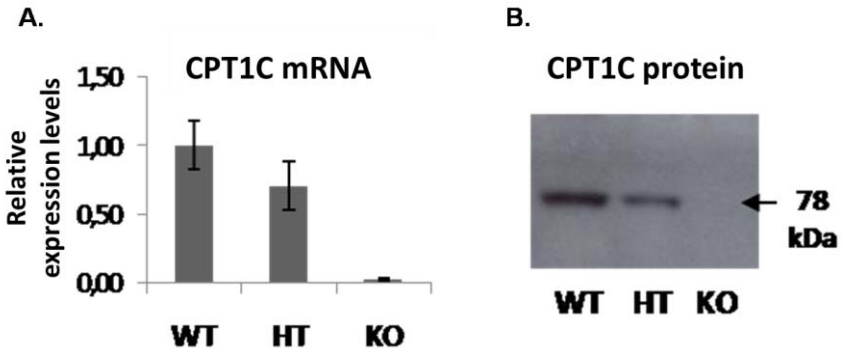

Figure 29: Generation of CPT1C-KO mouse. A. qRT-PCR determination and B. Western blot analysis for measuring the CPT1C expression in brain from WT, HT and KO mice. Data are presented as mean ± standard error (s.e.m). n=3

3.2.4 Transfection protocol

Transfection is the process of introducing foreign genetic material into cultured mammalian cells using non-viral methods. Transfection usually involves opening of transient pores in the cell membrane to allow the uptake of the genetic material desired. This process can be performed using the calcium phosphate method, electroporation or by mixing a cationic lipid with the genetic material to produce liposomes, which fuse with the cell membrane and introduce their cargo inside the cells. This last method was the chosen one for our studies and transient transfections were realized with two different commercially available transfection reagents.

For transfection were used two methods:

- ***Cell lines Metafectene (Biontex*)**: transfecting 1 µg of DNA and using 2 µl of transfection reagent for each well of a 24-well tray. The cells were incubated with the transfection reagent and the DNA for 6 h, and after this time, the medium was replaced by new complete medium.

- ***Primary cultures effecten transfection reagent (Qiagen, # 301425)*** The protocol used for 24 wells plated was:

    1. Incubate the cells under their normal growth conditions (37°C and 5% CO_2). The dishes should be 40–80% confluent on the day of transfection.
    2. The day of transfection, dilute 0.2 µg DNA dissolved in TE buffer, pH 7 to pH 8 with the DNA-condensation buffer, Buffer EC, to a total volume of 60 µl.
    3. Add 1.6 µl Enhancer and mix by vortexing for 1 s.
    4. Incubate at room temperature (15–25°C) for 2–5 min then spin down the mixture for a few seconds to remove drops from the top of the tube.
    5. Add 5 µl Effectene Transfection Reagent to the DNA-Enhancer mixture. Mix by pipetting up and down 5 times, or by vortexing for 10 s.
    6. Incubate the samples for 5–10 min at room temperature (15–25°C) to allow transfection-complex formation.
    7. While complex formation takes place, gently aspirate the growth medium from the plate, and wash cells once with PBS 1X. Add 350 ml fresh growth medium (can contain serum and antibiotics) to the cells.
    8. Add 350 ml growth medium (can contain serum and antibiotics) to the tube containing the transfection complexes.
    9. Mix by pipetting up and down twice, and immediately add the transfection complexes drop-wise onto the cells in the dishes. Gently swirl the dish to ensure uniform distribution of the transfection complexes.
    10. The cells were incubated with the transfection reagent and the DNA for 4 h, and after this time, the medium was replaced by new complete medium.

3.2.5 Transduction protocol

3.2.5.1 Virus formation

Two adeno-associated virus (AAV) vectors, serotype 1, AAV1-GFP, AAV1-CPT1C were constructed by AMT company to drive cell expression of GFP and CPT1C respectively. Vector plasmids carry the transgene expression cassette including: the cytomegalovirus promoter; the cDNA sequence of GFP and the rat CPT1C (Price, N. 2002); the woodchuck posttranscriptional regulatory element (WPRE, acc #AY468 486) to enhance transcription (Grimm,D. 1998). Novel tools for production and purification of recombinant adenoassociated virus vectors (Hum Gene Ther 9: 2745-2760); and the bovine growth hormone polyadenosine transcription termination signal [bGH poly(A)] (bases 2326-2533 GenBank acc #M57764). The expression cassette is flanked by two inverted terminal repeats (ITRs) derived from AAV serotype 2. AAV1 vectors are produced in insect cells using baculovirus (Dentin, R. 2004). The vector preparations used in this study had titers of $1x10^{12}$ and $2.5x10^{12}$ genome copies (gc)/ml for AAV1-GFP and AAV1-CPT1C, respectively.

3.2.5.2 Transduction protocol

AAV1-CPT1C virus infection was performed at 7DIV in cells cultured in six-well plates. Medium was removed and kept apart to be after re-used. 0.5 ml of neurobasal medium without B27 and containing 0.5 mM Glutamine and AAV1 at a concentration of 100,000 viruses per cell (as described in Royo, N.C. 2008 for AAV transduction in hippocampal cultured neurons) was added to each well and let for 2 hours. Then, 1.5 ml of the pre-conditioned medium kept apart was added and let for 7 days more. Then, they were removed for analysis of CPT1C expression and ceramide levels. Myriocin (Sigma, # M1177) treatment was performed 8 hours before cells recollection.

3.2.6 Immunocytochemistry

After transfection and stimulation, cells and neurons grown on cover slips were fixed with 4% paraformaldehyde (PFA), 4% sucrose in PBS for 12 minutes on an ice tray (4°C). The cells were rinsed twice with PBS and incubated with 50 mM NH_4Cl in PBS for 10 minutes at 4°C to remove excessive PFA. The NH4Cl was rinsed off twice with cold PBS before the cells were permeabelized for 5 minutes with ice cold 0.1% Triton X-100 in PBS. After washing the cells 3 times for 5 minutes with PBS, the cells were blocked for 30 minutes at RT in blocking solution (2% bovine serum albumin, 4% donkey and/or 4% goat serum (Jackson Immuno Research)), and thereafter incubated with primary antibodies for 60-90 minutes at RT, or over night at 4°C. The samples were washed thoroughly with PBS 1X, 3 times 5 minutes and incubated with secondary antibodies for 60 minutes at RT protected from light. Finally, the cover slips were washed 3 times for 5 minutes with PBS, once with H_2O by dipping them into a water filled dish, and mounted on slides using the Gel/Mount anti-fading medium (Biomeda corp.). Images were acquired using a digital camera (SpotRT; Diagnostic Instruments) attached to an epifluorescence microscope (Zeiss).

3.2.6.1 Primary antibodies used in the study

Antibody	Concentration	Reference
Anti-GluR2 extracellular	1:500	Upstate, #MAB397
Anti-PSD-95, mouse	1:200	Sigma, #P246-100UL
Anti-Synapsin1, mouse	1:200	Synaptic Systems, #106-001

3.2.6.2 Secondary antibodies used in the experiments were:

Antibody	Concentration	Reference
Goat anti-mouse Alexa488	1:200	Invitrogen, #A11029
Goat anti-rabbit Alexa488	1:200	Invitrogen
Donkey anti-mouse munx cy3	1.200	Dianova (Jackson) #715-165-151

3.2.7 Immunodetection in brain sections

Coronal sections (30µm) from adult mouse forebrains were incubated with primary antibodies against GFAP (1/500, Chemicon, #MAB360) and CPT1C (1/100) overnight at 4°C, washed three times in PBS 0.1 M and incubated for two hours with secondary antibodies coupled to fluorochromes Alexa 488 (for green fluorescence) and Alexa 568 (for red fluorescence) at a dilution 1/500. Sections were mounted with Mowiol and observed using a Confocal Leica TCS SP2 (Leica Lasertechnik GmbH, Mannheim Germany).

3.2.8 Antibody feeding assay

Hippocampal neurons from E17 mouse embryos were isolated and plated on coated coverslips Ø13 mm in 24-well plates. Briefly, hippocampal neurons at 15 DIV were blocked at 37°C for 10 minutes in blocking solution, incubated with the primary antibody anti mouse GluR2 extracellular (Upstate, #MAB397; 1:500,) for 18 minutes at 37°C, and washed with warm D-PBS$^{+}Ca^{2+}Mg^{2+}$. Cells were stimulated with 100 µM AMPA which was added in the last 10 minutes. After that, cells were fixed as described under the point immunocytochemistry, and incubated with Alexa Fluor 488 (Invitrogen, #A11029,) conjugated secondary antibodies for 2 hours at RT protected from light to detect pre-labeled surface remained receptors. After washing 3 times 5 minutes with PBS, the neurons were permeabelized for 4 minutes with ice cold 0.1% Triton X-100 in PBS, blocked again for 30 minutes and finally incubated with Cy3 (Dionova, Jackson, #715-165-151) conjugated secondary antibodies to visualize pre-labeled internalized receptors. Images were acquired using a digital camera (SpotRT; Diagnostic Instruments) attached to an epifluorescence microscope (Zeiss).

AMPA STIMULATION: AMPA (Sigma, #A0326) was dissolved in artificial cerebrospinal fluid (ACSF) and kept at -80°C in aliquots of 100 mM (1000x). Cells were stimulated in culture medium with 100 µM AMPA for 10 minutes at 37°C.

3.2.9 Histological staining

3.2.9.1 Animal´s perfusion

Mice were sacrified with CO_2 gas in a bag. Immediately after respiratory arrest, lay mouse on its back and open the thorax carefully to avoid excessive bleeding. Cut carefully through the rib cage and remove the diaphragm for access to the heart. Carefully insert syringe filled with 1X PBS into the left ventricle. Cut open the right ventricle for drainage, allowing the 1X PBS to be slowly (4 to 5 ml/min) but constantly perfused into the heart. If the perfusion is working well, blood-rich organs such as liver, spleen, and kidneys will turn grayish-white. Use 15 to 20 ml per mouse. After most of the blood has been flushed out, remove the syringe with 1X PBS and insert syringe filled with 4% PFA fixative (4°C) into the same puncture of the left ventricle. Slowly perfuse the mouse with <20 ml fixative at 4 to 5 ml/min. The start of the perfusion with 4% PFA is considered the starting point of the fixation process (t = 0). A sign of a good perfusion is a muscle tremor, best seen on the limbs and tail. Following perfusion, dissect out organs and tissues, transfer into well-labeled glass vials filled with 4% PFA fixative, and store at 4°C. After 24h, change the sample to 30% sucrose. Leave the tissue in sucrose during 48h and stored it at -80°C.

3.2.9.2 Cresyl fast violet (Nissl) stain

Histological analysis of WT and CPT1C-KO brain area: cerebellum, cortex and hippocampus were done following cresyl violet stain. Slices of 30 µm of coronal brain sections were used for the assay.

The protocol used is:

1. Take sections on slides to 95% alcohol.
2. Stain in cresyl violet solution (0.5 g cresyl violet + 100 ml distilled water), 10-20 minutes.
3. Wash in tap water.
4. Diffenciated in cresyl violet differentiator (100 ml alcohol + 250 ml Glacial acetic acid)
5. Dehydrate, clear in xylene and mount.

3.3 BIOCHEMISTRY

3.3.1 CPT1 activity assay

CPT1 activity assays were performed with mitochondrion or microsomal-enriched fractions from cell culture or extracted from mouse tissue. 20 µg of fresh mitochondrial or microsomal fraction were used for CPT1 activity assay.

3.3.1.1 Mitochondrial and microsomal purification

3.3.1.1.1 From cell culture

Cells were recovered by centrifugation at 1200 X g for 5 min at 4°C, washed in 1.5 ml of PBS, and resuspended in 2 ml of lysis buffer (250 mM sucrose, 10 mM Tris pH 7.4, 1 mM EDTA, supplemented with 1 mM phenylmethylsulfonyl fluoride, 0.5 mM benzamidine, 10 ng/mg leupeptin, and 100 ng/ml pepstatin). Cells were disrupted by Dounce homogenization (30 pulse with loose pestle and 30 pulses with tight pestle). Homogenates were centrifuged at 2.000 X g for 3 min at 4°C to remove cell debris. This crude extracted was further centrifuged at 10.000 X g for 30 min at 4°C to remove the mitochondrial fraction. Supernatant was centrifuged at 100.000 X g for 1h at 4°C to sediment the microsomal fraction. The concentration of the mitochondria and microsomal obtained were quantified by the Bradford assay and 20 µg protein was used for the CPT1 activity assay. Mitochondrial and microsomal pellet were resuspended in 2 ml of homogenization buffer B (420 mM Tris-HCl pH 7.2, 8 mM KCN, 60 mM KCl, 16 mM $MgCl_2$). Stored at 4°C. Pellets were inmmediately used in the carnitine palmitoyltransferase activity assay.

3.3.1.1.2 From tissue

Tissue was resuspended in 0.5-1 ml of lysis buffer (250 mM sucrose, 10 mM Tris pH 7.4, 1 mM EDTA, supplemented with 1 mM phenylmethylsulfonyl fluoride, 0.5 mM benzamidine, 10 ng/mg leupeptin, and 100 ng/ml pepstatin) and it was disrupted by Dounce homogenization (30 pulse with loose pestle and 30 pulses with tight pestle). Homogenates were centrifuged at 2.000 X g for 3 min at 4°C to remove cell debris. This crude extracted was further centrifuged at 10.000 X g for 30 min at 4°C to remove the mitochondrial fraction. Supernatant was centrifuged at 100.000 X g for 1h at 4°C to sediment the microsomal fraction. The concentration of the mitochondria and microsomal obtained were quantified by the Bradford assay and 20 µg protein was used for the CPT1 activity assay. Mitochondrial and microsomal pellet were resuspended in 2 ml of homogenization buffer B (420 mM Tris-HCl pH 7.2, 8 mM KCN, 60 mM KCl, 16 mM $MgCl_2$. Stored at 4°C.). Pellets were inmmediately used in the carnitine palmitoyltransferase activity assay.

3.3.1.2 CPTI activity assay

The substrates for the CPT1 activity assay were carnitine (Sigma, #C9500) and palmitoyl-CoA (Sigma, #P9716), and the reaction was done in the following direction:

carnitine + palmitoyl-CoA ⟶ palmitoyl-carnitine + CoA-SH

The procedure takes the advantage of the fact that the product of the reaction, palmitoyl-carnitine, is soluble in an organic medium. Deacylases convert the substrate acyl-CoA in acyl plus CoA-SH, generating ATP. This process would reduce the availability of the substrate palmitoyl-CoA in the reaction. Therefore, ATP is added to the reaction mix to minimize this process, by inverting the equilibrium of the deacylase reaction and by stimulating the reaction of the acyl-CoA synthetases and thus regenerating the substrate palmitoyl-CoA. KCN is added to avoid mitochondrial oxidation. Glutathione (GSH, reduced form) is used as a reduction agent instead of dithiothreitol (DTT) or dithioeritrol (DTE) because DTT and DTE have been shown to reduce malonyl-CoA sensitivity (Saggerson and Carpenter, 1982). Defatted BSA is added to protect mitochondria from the detergent effect of fatty acids. However, BSA concentration must not be higher than 0.1% because this could give a sigmoidal effect in the enzyme *v.s*. acyl-CoA kinetic (Prip-Buus et al, 1998). Finally, KCl is added because it increases enzyme activity (Saggerson, 1982).

The procedure for the CPT1 activity assay was as follows:

1. The reaction mix was prepared in a 1.5 ml tube kept on ice. Samples were done in triplicate.
2. The following amounts were per point:

CPT1 reaction mix/point

Bidistilled water	92.33 µl
4X CPT1 buffer	40 µl
1 mM palmitoyl-CoA	10 µl
80 mM ATP	10 µl
30% BSA	0.67 µl
25 mM GSH	2 µl
16 mM carnitine	5 µl
Total volume	160 µl

3. Protein samples were prepared on ice in 1.5 ml tubes by diluting the protein in 4x CPT1 buffer and by adjusting the volume with bd. water up to 40 µl. The blank contains bidistilled water instead of protein.

Protein samples

Protein	20 µg
4x CPT1 buffer	10 µl
Bidistilled water up to	40 µl

4X CPT1 buffer B: 420 mM Tris-HCl pH 7.2, 8 mM KCN, 60 mM KCl, 16 mM $MgCl_2$. Stored at 4°C.

4. One by one, 160 µl of the reaction mix was added to each protein sample. Samples were vortex-mixed and placed on a water bath at 30°C for exactly 5 min.

5. Reaction was stopped with the addition of 200 µl of 1.2 M HCl. Samples were vortex-mixed and placed on ice. The internal standard pamitoylcarnitine-d3 (200 ng·mL^{-1}) was added at that moment in each sample.

6. Extractions of the product of the reaction, palmitoyl-carnitine, were done by adding 600 µl of water-saturated butanol. Samples were vortex-mixed and centrifuged for 2 min at 13,000 rpm in a microcentrifuge.

7. 400 µl of the upper phase was added to another 1.5 ml tube with 200 µl of bidistilled water. Samples were vortex-mixed and centrifuged for 2 min at 13,000 rpm.

8. 250 µl of the upper phase was recovered and analyzed by HPLC–MS/MS. Values were given as means of three independent experiments performed. All protein concentrations were determined using the Bradford protein assay (Bio-Rad, USA) with bovine serum albumin as standard.

3.3.1.2.1 HPLC analysis

The HPLC system used is a Perkin-Elmer Series 200 (Norwalk, CT, USA) quaternary pump equipped with an autosampler. For the analysis of the extracts, an Atlantis HILIC Silica (Waters, Milford, USA) column (150 mm × 2.1 mm, 3.0 µm) was used. Isocratic separation was done with 200 mmol/L ammonium formate pH 3, acetonitrile and water at the proportions 5:86:9 (v/v) and a constant flow-rate of 200 L/min. To reduce the residual matrix effect reaching the mass spectrometer, a divert valve (Valco, Houston, USA) drained off the LC eluent. MS and MS/MS experiments were performed on an API 3000 triple quadrupole mass spectrometer (PE Sciex, Concord, Ont., Canada). All the analyses were performed using the Turbo Ionspray source in positive ion mode with the following settings: capillary voltage +4500V, nebulizer gas (N_2) 10 a.u., curtain gas (N_2) 12 a.u., collision gas (N_2) 4 a.u. The drying gas (N_2) was heated to 400°C and introduced at a flow-rate of 5000 cm^3/min. All the MS and MS/MS parameters were optimized by infusion experiments: individual standard solutions of acylcarnitines (1 ng/L) were infused into the mass spectrometer at a constant flow-rate of 5 L/min using a Model 11 syringe pump (Harvard Apparatus, Holliston, MA, USA). Full scan data acquisition was performed by scanning from *m/z 50 to 500 in a profile* mode and using a cycle time of 2 s with a step size of 0.1 u and a pause between each scan of 2 ms. In product ion-scan experiments MS/MS product ions were produced by collisionactivated dissociation (CAD) of selected precursor ions in the collision cell of the triple quadrupole mass spectrometer, and mass was analyzed using the second analyzer of the instrument. However, in precursor ion-scan experiments, Q1 gives information on all the possible precursors of the selected ion in Q3 of the triple quadrupole. Additional experimental conditions for MS/MS included collision energy (depending on the compound), CAD gas (N2) at 6 (arbitrary) units, and scan range, as necessary for the precursor selected. Precursor ion scan experiments were performed by scanning Q1 between 150 and 700 u. In all the experiments both quadrupoles Q1 and Q3 operated at unit resolution. MRM (multiple reaction monitoring) acquisition was done monitoring one transition for each compound (see Table 1) with a dwell time of 700 ms. The MRM mode was required because many compounds could present the same nominal molecular mass, and the combination of the parent mass and unique fragment ions was used to selectively monitor acylcarnitines. Internal standard palmitoylcarnitine-*d3 (*200 ng/ml) was added to samples before extraction to give a final concentration of 0.2g/ml. The same concentration was present in the standards used for quantification.

A graph plotting area of palmitoylcarnitine, stearoylcarnitine and oleoylcarnitine *ratios against* concentration of palmitoylcarnitine-*d3 ratios* is used for quantification.

3.3.2 Acyl-carnitine assay

3.3.2.1 Acyl-carnitine extraction protocol

The protocol was:

1. Cells were washed in cold 1X PBS buffer and gently collected with a pipette.
2. Centrifuged the cells at 700 X g for 5 min at 4°C and washed in PBS 1X.
3. After that, add to the pellet 200 µl of 0.2 M NaCl.
4. Rip the tissue with a Dounce in ice.
5. Take 20 µl of samples for Bradford protein assay.
6. To separate aqueous and lipid phases, add 750 µl of Folch reagent (cloroform: methanol, 2:1) and 50 µl of 0.1M KOH.
7. Vigorous vortex mixing.
8. The phases were separated by 15 min of centrifugation at 2000 X g at 4°C.
9. The top aqueous phase was removed and the lipid phase was washed in 200 µl of methanol/water/cloroform (48:47:3).
10. Vortex mixing.
11. Centrifuge at 700 X g for 5 min at 4°C.
12. Pass the organic lower phase (lipid extraction) to another tube and dried with a stream of N_2.

3.3.2.1.1 Quantification of acyl-carnitines by HPLC-MS/MS

Acyl-carnitines were analyzed via an LC-ESI-MS/MS System (API 3000 PE Sciex) in positive ionization mode described in Jáuregui, O. 2007. For the analysis of the extracts, an Atlantis HILIC Silica (Waters, Milford, USA) column (150mm×2.1 mm, 3.0 µm) was used. Quantification was done through multiple reaction monitoring (MRM) experiments using the isotope dilution method with deuterated palmitoyl carnitine (d3 palmitoylcarnitine) as internal standard (200 ng/mL). 10 µl of sample was injected in the LC-ESI-MS/MS system. MRM transitions were as follows: 400.4/85.2 for quantification of palmitoylcarnitine, 4001.4/341.4, 403.4/85.2 for quantification of d3-palmitoylcarnitine. Isocratic separation was done with 200 mmol/L ammonium formate pH 3, acetonitrile and water at the proportions 5:86:9 (v/v) and a constant flow-rate of 200 L/min. The method was linear over the range from 2 to 2000 ng/mL.

3.3.3 Ceramide assay

3.3.3.1 Ceramide extraction protocol

The protocol use for ceramide extraction was:

1. Add between 50-100 µl of PBS and sonicate at 100%, 0'6.
2. Take 20 µl of samples for Bradford protein assay.
3. Add 250 µl of methanol and 500 µl of cloroform (1:2) per tube, and 50 ng/ml ceramide C17 are used as internal standard. Incubate 1h at 48°C in the bath
4. Put the tubes at room temperature and add 50 µl of KOH 1M in water, sonicate and incubate at 37°C, 1h.
5. Sonicate again.
6. Separate the two phases by centrifugation at 2000 X g during 5 minuts.
7. Take the lower phase.

8. Wash with 200 µL of methanol: water: cloroform (48:47:3).
9. Centrifuge at 2000 X g during 5 minuts.
10. Pass the organic lower phase to another tube and dried with a stream of N_2.

3.3.3.1.1 Ceramide quantification by HPLC-MS/MS

Ceramides were extracted and analyzed via an LC-ESI-MS/MS System (API 3000 PE Sciex) in positive ionization mode. Their concentrations were measured by MRM experiments using the isotope dilution method C17:0 as internal standard (50 ng/ml). The method was linear over the range from 0.2 to 1000 ng/ml.

Dry sample was resuspended in 300 µl of mobile phase A. Then, 10 µl of sample was injected in the LC-ESI-MS/MS system.

The solutions used during the analysis were:

Mobile phase
Phase A: 74% MeOH, 25% H_2O , 1% HCOOH, 5mM $HCOONH_4$
Phase B: 99% MeOH, 1% HCOOH, 5mM $HCOONH_4$

Wash solution	
Seal Wash	80% MeOH, 20% H_2O
Weak Wash	80% MeOH, 20% H_2O
Strong Wash	50% MeOH, 50% H_2O

The gradient used was:

Time(min)	Flow Rate	%A	%B
1. Initial	0.800	100	0
2. 2.00	0.800	0	100
3. 5.50	0.800	0	100
4. 5.60	0.800	100	0
5. 6.50	0.800	100	0

MRM transitions were as follows:

Ceramide	MRM transition
C17:0 (S.I.)	552,90 / 264.40
C16:0	538,70 / 264.40
C18:0	566,70 / 264.40
C18:1	564,70 / 264.40
C20:0	594,70 / 264.40
C24:1	648,90 / 264.40

For the analysis of the extracts a Kinetex (2,6 µm 75x3 mm C18. p/n 00C-4462-Y0. s/n 556453-8) column was used.

3.4 BEHAVIORAL TEST

3.4.1 Animals

The mice were housed in a room with a 12:12 h light-dark schedule with lights on at 8:00 a.m., in controlled environmental conditions of temperature (22ºC ± 2°C) and humity (60%) with food and water ad libitum. Only males were tested in this study. The numbers of animals used for each test were 12 mice per group. Animals were tested at age of 11-12 weeks of age. All the behavioral testing was conducted by the same experimenters, in an isolated room and at the same time of day. The behavioral experimenters were blinded as to the genetic status of animals. All animal procedures met the guidelines of European Community Directive 86/609/EEC and were approved by the Local Ethics Committee.

3.4.2 Behavioral test

3.4.2.1 Neurological test (SHIRPA protocol)

It is a three stages protocol designed as a series of individual test that itself provides quantitative data about an individual performance. Such test specific performance is directly comparable between animals, over time, and between groups.

SHIRPA primary screen is a comprehensive semiquantitative routine testing protocol to identify and characterize phenotype impairments. Assessment of each animal began with the observation of undisturbed behavior in a cylindrical clear Perspex viewing jar (15 cm height, 11 cm diameter) for wild running or stereotypy.

Then the mice were transferred to an arena (56 x 34 cm) for the observation of the motor behavior and sensorial function. Animals underwent screening exams for visual acuity, vibrissae, corneal, and pinna responses to an approaching cotton swab, auditory (Preyer reflex), and vestibular function (contact righting reflex and negative geotaxis), grip strength, and body tone.

In the last part of the test, changes in excitability, aggression, general fear, vocalization and salivation, and piloerection (for analysis of autonomic function) were recorded.

The protocol used for this test was the following:

Test	Score
General Health	
Body position	completely flat
	lying on side
	lying prone
	sitting or standing
	rearing on hind legs
	repeated vertical leaping
Breathing	grasping, irregulat
	slow, shallow
	normal
	hyperventilation
Trembling	none
	mild
	marked
Trunk arching	absent
	present
Piloerection	none
	coat stood on end
Salivation	normal
	excessive
Sensory Reflexes	
Visual placing	nonne
	upon vibrasse contact
	before vibrasse contact 18 mm
Corneal reflex	none
	active single eye blink
	multiple eye blink
Pinna reflex	none
	active retraction, noderately brisk flick
	hyperactive, repetitive flick
Toe pinch	yes
	none
Righting reflex	yes
	gragging
Tail elevation	dragging
	horizontally extended
	elevated/strub tail
Preyer reflex	yes
	absent
Grip response	present
	upon nose contact
Reaching	none
	upon nose contact
	upon vibrasse contact
	before vibrasse contact 18 mm
	early vigorous extension 25 mm

Emotional Domain	
Irritability	none
	struggle during supine restraint
Fear	none
	freezes during transfer arousal
Startle response	none
	preyer reflex
	jump less than 1 cm
	jump more than 1 cm
Transfer arousal	come
	prolonged freeze, then slight movement
	extended freezem the moderate movement
	brief freeze (few seconds), then active movement
	momentary freeze, then swift movement
	no freeze, immediate movement
	extremely excited
Touch escape	no response
	mild (scape response to frim stroke)
	moderate (rapid response to light stroke)
	vigorous (escape response to approach)
Aggression	none
	provocked biting or attack
Motor Abilities	
Activity	none, resting
	casual scratch, groom, slow movement
	vigorous scratch, groom, moderate movement
	vigorous, rapid/dart movement
	extremely vigorous, rapid/dat movement
Negative geotaxia	none response
	incomplete response
	complete response

3.4.2.2 Motor test

3.4.2.2.1 Rotarod test

The performance of mouse was tested in the rotarod, a task that evaluates motor coordination and balance. The ability of each mouse to maintain balance on a rotation rod (5 cm diameter and 10 cm long) with a plastic dowel surface was assessed with a commercially available rotarod apparatus (Rotarod LE8500, Panlab SA, Barcelona, Spain).

The equipment consists of a rotating spindle that is able to maintain a fixed rotational speed (FRS) of 7, 10, 14, 19, 24, or 34 rpm and starting at 4 rpm to accelerate at a constant rate to 40 rpm over 1 min period. The equipment is provided with a magnetic plate to detect when a mouse has fallen off the rod. Mice were placed on the middle of the rotating rod, its body axis being perpendicular to the rotation axis, and its head against the direction of rotation. All animals were tested for acquisitions and maintenance of rotarod performance. The experimental design consists of two consecutive acquisition trials in which the number of trials required to learn to remain on the rod at the minimum speed (4 rpm) was recorded. After the mice passed one criterion test, a second session (Day 2) is performed in which two different tasks are performed:

a) Motor coordination and balance were assessed by measuring the latency to fall off the rod in consecutive trials with increasing fixed rotational speeds (FRS 7, 10, 14, 19, 24, and 34 rpm), and animals were allowed to stay on the rod for a maximum period of 1 min per trial and a resting period of 15 min was left between trials.

b) For the accelerating rod test, the rotation speed was increased during a single session of 1 min from 4 to 40 rpm. For each trial, the elapsed time until the mouse fell off the rod was recorded.

3.4.2.2.2 Paw print test

To examine the step patterns of the hind limbs during forward locomotion, mice were required to traverse a straight, narrow tunnel. These experiments, designed to evaluate the walking pattern of the mice, was adapted from previously published work (Costa et al., 1999). The hind paws of the mice were coated with black nontoxic waterproof ink.

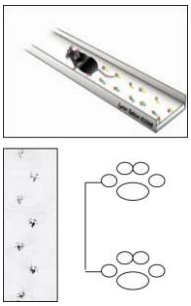

Animals were then place at one end of a long and narrow tunnel (10 x 10 x 70 cm), which they spontaneously enter and partially or totally transverse.

A clean sheet of white paper (35.5 cm long) was place on the floor of the tunnel to record the paw prints. Footprints made at the beginning and at the end, when the animals was initiating and finishing movement, were excluded from the analysis.

The use of a tunnel that is longer than the recording paper has proven to be a necessary measure to avoid artefacts generated by strain differences not directly related to alterations in motor function.

This task was repeated at least three times to obtain clear and visible footprint in 20 cm of sheet. Footprint patterns were analyzed for a minimum of five step cycles for each trial. A complete step cycle was defined as the distance from one pair of hind limb prints to the next.

3.4.2.2.3 Bar Hang Test

Neuromuscular strength was tested by the wire hang test. The mouse was placed on a wire cage lid and the lid is gently waved in the air so the mouse grips the wire. The lid was then turned upside down, approximately 6 inches above the surface of soft bedding material. Latency to fall onto the bedding and the used of the hindlimbs to climb to the bar were recorded, with 60 s cut-off time.

3.4.2.2.4 Grip- Force

The force exerted by the forelimbs was assessed with an adapted version (Costa, Walsh & Davisson, 1999) of the original procedure (Meyer, Tilson, Byrd, & Riley, 1979) to improve the reproducibility of the recordings. A force transducer was used to measures the peak force exerted by the forelimbs of the mouse as its grip was broken by the experimenter pulling the mouse away from the transducer by the base of the tail. The grasping ring was set up vertically, which cause the mouse to grasp more consistently to it. Most of the "human component" of the test was eliminated by using a gravity–driven system to produce a consistent 10N downward force onto the mouse´s tail. The system was activated manually when the mouse held firmly to the grasping ring of a digital push-pill strain gauge (Grip Strength Meter; BIOSEB, Chaville, France) Each trial was repeated three times, and the data were given as the mean $\pm SEM$ of the three values.

3.4.2.2.5 Locomotor activity test

Locomotor activity was measured by using actimetry boxes (45 X 45 cm; Harvard Apparatus) contained in a soundproof cupboard. Back and forward movements were monitored via a grid of infrared beams and used as an index of locomotor activity (counts). Counts were integrated every hour and added to obtain total locomotor activity for a 24 h period maintaining the 12:12 h light-dark schedule. The parameter measured in the study was the total distance travelled by the animals (cm).

3.4.2.3 Memory and learning test

3.4.2.3.1 Morris water maze Test

To test hippocampal-dependent spatial cognition, CPTC-KO mice were trained in the standard Morris water maze (MWM) with a hidden platform. 12 wild type and 12 CPT1C-KO mice were tested over 10 days (4 trials/session, 10 min inter- trial intervals).

The water maze test consisted of a circular pool (diameter, 1.20 m, height, 0.5 m). It was filled with a tepid water (17ºC) opacified by the addition of powdered milk (0.9 Kg). A white escape platform (15 cm diameter, height 24 cm) was located 1 cm below the water surface in a fixed position (NE quadrant, 22 cm away the wall).

In each trial, mice were placed at one of the starting locations in random order (north, south, east, west (N, S, E, W)), including permutations of the four starting points per session) and were allowed to swim until they located the platform. Mice fail to find the platform within 60s was placed on it for 20s (the same period of time as the successful animals). At the end of every trial the mice were allowed to dry for 15 min in a heated enclosure and are returned to their home cage.

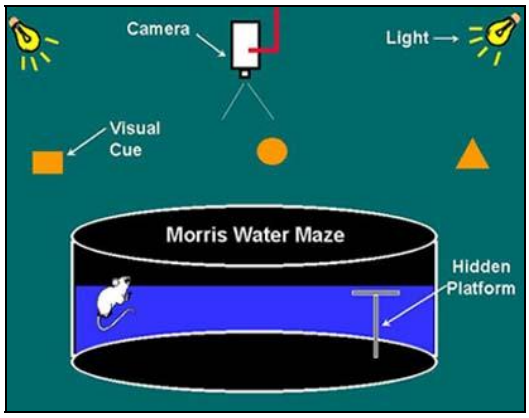

This test consists of several sessions with groups of differential targets:

- **Training session**: animals have to learn to the task.
- **Acquisition session**: the visuo-spatial learning is evaluated.
- **Cue session**: guided learning session in which motor or emotional dysfunctions are discarted.
- **Removal session**: the platform is removed and the visio-spatial memory is evaluated.
- **Reversal session**: the platform is located in another pool area. The cognitive flexibility (the ability to learn new things and forget the old ones) is evaluated in this session.

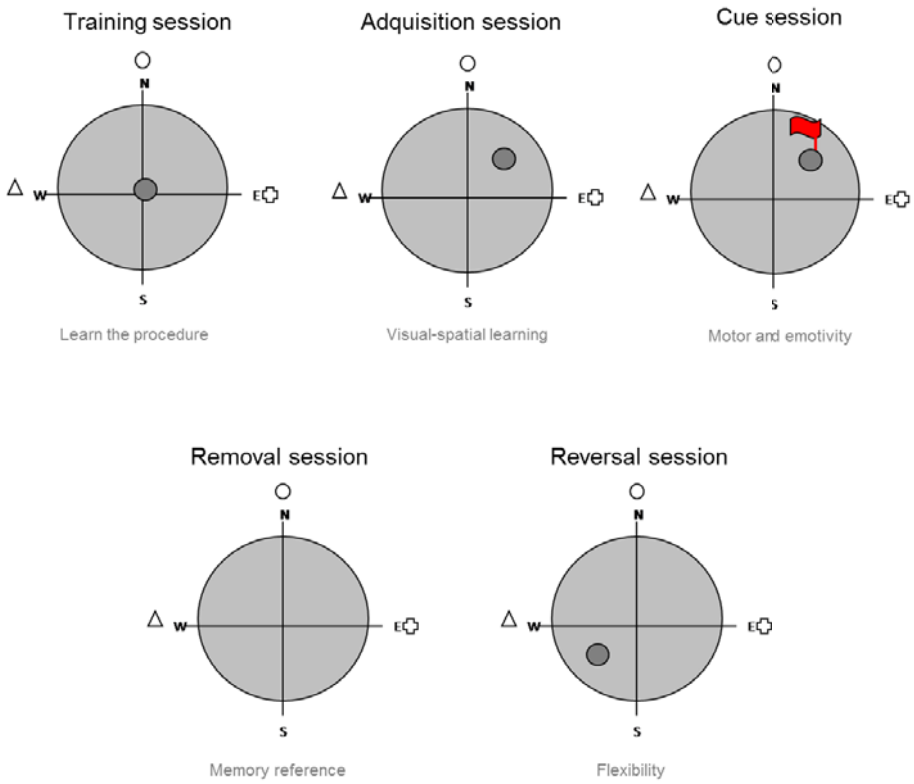

Figure 29: Parts of the Morris water maze test.

In the **training session**, the mice learn the task.

In the **acquisition session**, the platform was located in the north-east position and the mice must learn to use distal cues to navigate a direct path to the hidden platform when started from different, random locations around the perimeter of the tank. The latency to find the platform was evaluated along 10 sessions (days).

The **cue session** was performance to test the swimming speed and visual ability using the visible platform, elevated 1 cm above the water and its position was clearly indicated by a visible cue (black flag). White curtains with affixed black patterns to provide an arrangement of spatial cues surrounded the maze. This test was done twice.

To test if the mice remember the location of the platform, probe trials were performed. In the probe session the platform was removed and the mice are allowed to swim for 60 s. The time spent in the trained and non-trained quadrants as well as the number of platform annulus crossing during 60s were recorded.

Mice performed the **reversal learning session**. In this test the platform is changed to the opposite quadrant, south-west and the mice have to extinguish their initial learning of the platform´s position and acquire a direct path to the new goal position. Tracking patterns typically reveal that mice swim to the previous location first, then, begin to search in an arching pattern to reach the new goal. Even after multiple trials, mice do not entirely abandon their initial learning strategy and begin trial by starting to move towards the original platform position, then turn and swim more directly to the new goal.

All the trials were recorded and traced with an image tracking system (SMART, Panlab, Spain) connected to a video camera placed above the pool. Escape latencies, length of the swimming paths and swimming speed for each animal and trial were monitored and computed. Path length was defined as the total

distance swum from the start location to the target and latency as the total duration of the trial when the mouse was placed in the water until it located the escape platform.

3.5 DATA ANALYSIS

3.5.1 Immunofluorescence analysis

Images were acquired using a digital camera (SpotRT; Diagnostic Instruments) attached to an epifluorescence microscope (Zeiss) equipped with a 63X objective (Plan-Apochromat; Zeiss). All quantitative measurements are performed using MetaMorph software (Molecular Devices).

Quantification of AMPA-receptor and its internalization were based on fluorescence intensities. The percentage of internalized GluR2 (red fluorescence intensity) versus total GluR2 (red + green fluorescence intensity) was calculated for dendrite stretches of 100-200 µm imaged on at least 10 different transfected or treated neurons (n= 50-100). GluR2 in the dendritic spine surface was analyzed by counting the number and the area of clusters positive. One-way Anova post-hoc or Student's t tests were used to assess statistical significance of the quantifications (Microsoft Excel).

For the quantification of spine length, spine head area and protrusion number, approximately 100 dendrites from independent transfections were selected randomly. For each construct the number of protrusions on dendrite stretches of proximal 50 µm, and the area of the spines heads were quantified. The protrusion length was determined by measuring the distance between the tip and the base (n>500 protrusions). Protrusion (dendrite spines) morphology classification was done as: filopodia (only neck), mushroom (neck + head) and stubby (only head). Groups of protrusions were compared using Student´s t-test or one-way Anova post-hoc.

Synapse formation and number of mature synapses was analyzed by counting the number and the area of clusters positive for the pre-synaptic protein synapsin1, or the post-synaptic marker PSD-95 along dendrite stretches of approximately 100 µm.

3.5.2 Statistical analysis

Data are expressed as means ± SEM for at least three or four independent experiments performed in triplicate. Different experimental groups are compared either with the Student's *t* test or with the one-way ANOVA followed by Bonferroni's test for comparisons post hoc. Performance in rotarod and MWM test are compared using repeated measures ANOVA. Values of * $p<0.05$; ** $p<0.005$; *** $p<0.001$ are considered significant. All the analyses were performed using the statistical package SPSS.

RESULTS

CHAPTER 4 : RESULTS

4.1 ENZYMATIC CHARACTERIZATION OF CPT1C ENZYME

The enzymes of the carnitine palmitoyltransferase (CPT1) family are predominantly localized in the outer mitochondrial membrane in contrast, the isoform CPT1C is located in the endoplasmic reticulum of cells (Sierra, A.Y. 2008). Preliminary results from our group showed that palmitoyl-CoA is the substrate for CPT1C enzyme (Sierra, A.Y. 2008), although no CPT1 activity has been detected to date.

In the following experiments, our objectives will be the identification of CPT1C activity and the characterization of its kinetic parameters in PC12 and HEK 293T mammalian cells *in vitro* and *in vivo*.

4.1.1 CPT1C activity in PC12 and HEK293T microsomal cell fraction

The first aim of the study was to determine CPT1C activity in PC12 and HEK293T cells. Both were transfected with either a pIRES-CPT1C vector or an empty pIRES vector (serving as a control for endogenous activity) using Metafectene reagent (Biontex, Germany) with a transfection efficiency of approximately 80% (Figure 30).

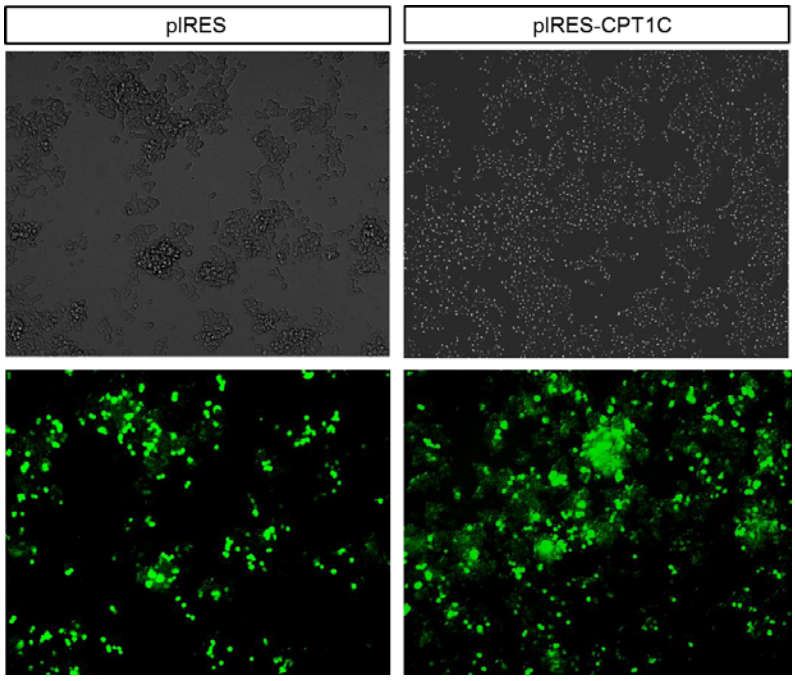

Figure 30: Transfection efficiency in PC12 cells transfected with pIRES empty and pIRES-CPT1C vector. 48h after transfection approximately 80% of the PC12 cells showed green fluorescence from EGFP expression encoded in pIRES vector. Images were taken with 40X magnification in a fluorescence microscope visualizing cells either with transmitted-light microscopy (upper images) or fluorescence microscopy (bottom images).

After 48 hours of transfection, cells were lysed and the microsomal enriched cell fraction was used to to characterize CPT1C over-expression and CPT1C activity.

To verify whether CPT1C over-expression could be detected in the microsomal enriched cell fraction after pIRES-CPT1C transfection, a western blot assay was performed. 40 µg of protein from microsomal or mitochondrion-enriched cell fraction from cells transfected with empty pIRES (Ø), pIRES-CPT1C (C) or pIRES-CPT1A (A) (used as mitochondrial control) was analyzed in 10% SDS-acrylamide gel. As shown in figure 31, CPT1C protein was over-expressed in cells transfected with pIRES-CPT1C, but the over-expressed protein was only detected in the microsomal cell fraction. For the determination of the correct separation of microsomal and mitochondrial cell fraction, the same PVDF membrane, once de-hybridized, was stained with a mouse anti-CPT1A antibody (1:1000) (used as a positive control of mitochondrial extracts). As it is shown in figure 31, CPT1A was not expressed in the microsomal fraction, implicating that the fractionation protocol will allow the observation of the specific CPT1C activity in microsomal fraction where no CPT1A contamination was detected.

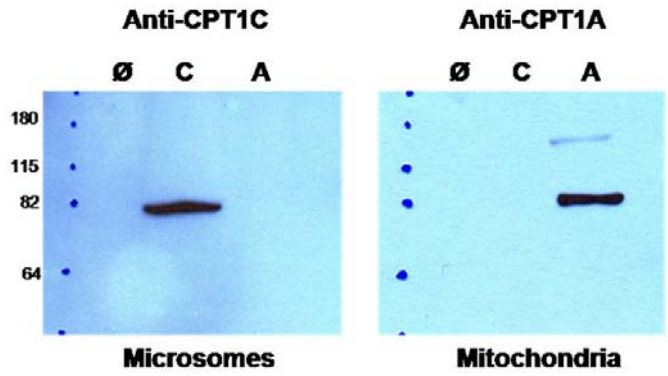

Figure 31: A. Western blot of transfected HEK293Tcells.Cells transfected with pIRES-CPT1C (C), empty pIRES (Ø) or pIRES-CP1A (A). 40 µg of microsomes or mitochondrion enriched cell fraction were loaded per lane in 10% SDS-acrylamide gel, for blotting detection anti-mouse CPT1C antibody (1:500) and anti-mouse CPT1A antibody (1:1000) were used.

After establishing CPT1C protein over-expression conditions and given the fact that there is a high sequence similarity between CPT1A and CPT1C at the protein levels, CPT1C should catalyze the same reaction as that of CPT1A. For that reason, CPT1 activity assay was performed following the same protocol described in material and methods (section 3.3.1) for the other CPT1 isoforms.

After over-expressing CPT1C with pIRES-CPT1C in PC12 and HEK293T cells, cells were harvested, lysed and microsomal enriched cell fractions were obtained. Then, CPT1 activity was determined by HPLC-MS/MS method described by Jauregui, O. 2007. The substrates included 1 mM palmitoyl-CoA and 16 mM carnitine. Palmitoyl-carnitine was the product, which was determined. 20 µg of protein from microsomal enriched cell fractions were assayed for 5 min at 30ºC, and the specific activity was calculated (nmoles palmitoyl-carnitine/mg protein · min). Microsomal enriched cell fractions of cells transfected with empty pIRES vector were used as a control to measure the endogenous CPT1 activity.

Microsomes from CPT1C over-expressing PC12 and HEK293 cells showed a significant increase of 0.57 or 0.13 nmols of palmitoyl-carnitine/mg of protein/min, respectively, when compared to control cells (endogenous activity) (Figure 32).

Cells	Plasmid transfection	n	Activity (nmols palmitoyl-carnitine / mg / min)	p	Absolute increase	% increase
PC12	Control	7	1.37 ± 0.81			
	CPT1c	7	1.94 ± 0.96	<0.05	0.57	41.6
293	Control	9	0.22 ± 0.11			
	CPT1c	9	0.35 ± 0.18	<0.05	0.13	59

Figure 32: Carnitine palmitoyl transferase activity in HEK293T and PC12 cells. Cells were transfected with pIRES-CPT1C or empty vector pIRES (control cells). 48h after transfection, cells were collected and 20 µg of microsomal fraction was assayed for CPT1 activity. The palmitoylcarnitine formed in the assay was determined by HPLC-MS/MS chromatography. Activity is presented as the mean ± the standard error (S.E.M). Willcoxon test for non-parametric paired samples was used. n. number of experiments. Absolute and percentatge (%) increases in CPT1C activity are compared to control cells.

This result indicates that CPT1C enzyme has low activity because CPT1C over-expression only produced a 50% increase of CPT1 activity. In contrast, CPT1A over-expression increased 4-5-fold CPT1 activity (data from Adriana Sierra´s Thesis).

4.1.2 Characterization of kinetic parameters of CPT1C enzyme

PC12 cells were used to check the kinetic parameters of CPT1C enzyme. Cells were transfected with pIRES-CPT1C vector following Metafectene Reaction protocol. 48h after transfection, a kinetic assay was performed. 20 µg of microsomal enriched cell fractions of CPT1C over-expressing cells were assayed with increasing concentrations of palmitoyl-CoA (from 5 to 300 µM with constant carnitine concentration) and increasing concentrations of carnitine (from 20 to 500 µM with constant palmitoyl-CoA concentration) for 5 min at 30ºC. Then, the specific CPT1 activity was determined by HPLC-MS/MS method. Kinetic parameters of CPT1C enzyme were calculated subtracting the activity of the empty pIRES (as a control of endogenous activity of microsomes).

Four independent experiments were carried through to determine CPT1 activity (nmol/min•mg protein) in applying concentrations of palmitoyl-CoA (left) or carnitine (right) (Figure 33A). In figure 33B, CPT1C and CPT1A kinetic parameters are shown. CPT1A kinetic parameters were obtained from a previous study of our lab. These results indicate that CPT1C displayed similar affinity for its substrates: carnitine and pamitoyl-CoA than CPT1A (Km for palmitoyl-CoA was 5-fold lower and for carnitine was 2-fold higher as compared to CPT1A). Vmax values for palmitoyl-CoA and carnitine in CPT1C were about 70-fold lower than those of CPT1A. As a consequence, CPT1C catalytic efficiencies for palmitoyl-CoA and carnitine were 320 and 25-fold lower than those of CPT1A, respectively.

A.

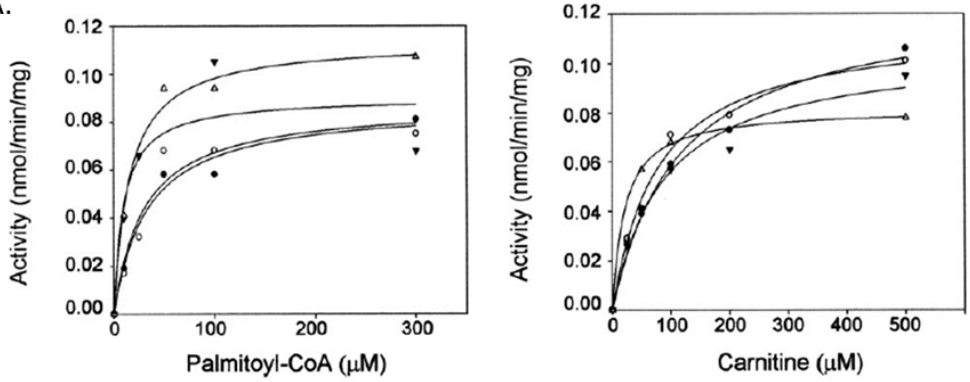

B.

Parameter	CPT1c	CPT1a
Km palmitoyl-CoA (mM)	25.35 ± 7.77	4.9 ± 0.3
Vmax palmitoyl-CoA (nmol/min/mg)	0.095 ± 0.012	6.3 ± 0.4
Catalytic efficiency palmitoyl-CoA (Vmax/Km)	0.004	1.28
Km carnitine (mM)	58.53 ± 21.31	127.0 ± 4.5
Vmax carnitine (nmol/min/mg)	0.090 ± 0.010	6.6 ± 0.8
Catalytic efficiency carnitine (Vmax/Km)	0.002	0.05

Figure 33: A. Kinetic analysis of CPT1C over-expressed in PC12 cells. 20 µg of microsomes were incubated with increasing concentrations of palmitoyl-CoA (left) and carnitine (right), and CPT1 activity was measured. **B. Kinetic parameters of CPT1C overexpressed in PC12 cells.** Microsomes of PC12 cells overexpressing CPT1C were assayed for activity with different palmitoyl-CoA and carnitine concentrations to calculate Km and Vmax values for both substrates. The results are the mean ± standard deviation of three experiments. CPT1A kinetic parameters were obtained from a previous study of other member of the lab.

This result indicates that CPT1C has similar affinity for its substrates: carnitine and palmitoyl-CoA than CPT1A, although it has a reduced catalytic efficiency as compared to the one of CPT1A.

4.1.3 CPT1C activity in the brain

In the next approach, the CPT1 activity was measured in the brain of fasted WT and CPT1C-KO mice *in vivo*. As it was previously observed in section 4.1.1: CPT1C activity in mammalian cells was low (see figure 32) therefore, any inhibition of the enzyme was avoided. It is well described that in the fasted state, CPT1 mRNA and CPT1 activity are increased, therefore fasting was the best condition for measuring CPT1C activity in the brain (Lavrentyev, E.N. 2004).

For that purpose, 20 µg of microsomal enriched cell fractions from the cortices of fasted CPT1C-KO and WT adult mice were used for the assay. Animals were fasted for 12h. Subsequently, the concentration of palmitoyl-carnitine, the product of CPT1 mediated reaction, was determined by HPLC-MS/MS chromatography.

No significant differences were found between WT and CPT1C-KO mice, as indicated in figure 34. In this study, CPT1 brain activity was calculated as nmols of palmitoyl-carnitine formed per minute and per mg of protein.

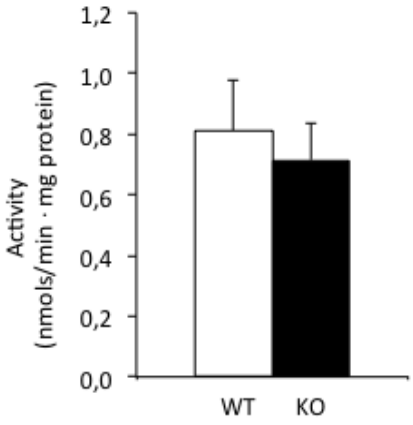

Figure 34: CPT1 activity in microsomes of brain cortex. 20 µg of microsomes from the cortices of fasted CPT1C-KO and WT adult mice were assayed by HPLC-MS/MS to measure CPT1 activity. Data are presented as mean of CPT1 activity values (nmols/mg protein/ min) ± standard error (S.E.M). The Student t-test was used. n=3.

These data suggest that CPT1C has a negligible activity in isolated microsomes from fasted mice. The data are in line with those described in the previous section (4.1.1), where low CPT1 activity was found in over-expressing CPT1C cell cultures.

4.1.4 Levels of acyl-carnitine in different brain areas

Since no differences were found in CPT1 activity *in vivo* between WT and CPT1C-KO mice, we decided to investigate whether CPT1C was active by measuring long chain acyl-carnitine levels in WT and CPT1C-KO mice.

For this study, three different types of long chain acyl-carnitine: palmitoyl-carnitine, stearoyl-carnitine and oleoyl-carnitine, from different brain areas were analyzed via HPLC-MS/MS chromatography. Samples were obtained from CPT1C-KO and WT mice in fed and fasting conditions (12 hours). Fasting is associated not only with decreased malonyl-CoA concentration but also with a pronounced decrease in sensitivity of CPT1 to inhibition by malonyl-CoA as well an increased CPT1 mRNA and CPT1 activity (Lavrentyev, E.N. 2004).

As it is represented in table 3, a decrease in the acyl-carnitine levels in CPT1C-KO mice were shown after fasting condition, revealing a higher significance in cerebellum, hippocampus and hypothalamus. In fed animals, no significant differences were detected between the groups, suggesting that CPT1C activity was higher in fasting.

Sample	Palmitoyl-carnitine	Stearoyl-carnitine	Oleoyl-carnitine
Cerebellum			
WT fast	1,47 [0,10]	2,78 [0,56]	2,45 [0,38]
KO fast	***0,76 [0,16]	*1,50 [0,15]	**1,10 [0,15]
WT fed	2,19 [1,10]	3,21 [1,61]	3,32 [0,50]
KO fed	1,71 [0,66]	2,53 [0,30]	2,44 [0,31]
Cortex			
WT fast	1,29 [0,20]	1,01 [0,16]	2,04 [0,45]
KO fast	1,37 [0,19]	0,93 [0,16]	1,58 [0,23]
WT fed	2,19 [0,26]	0,71 [0,05]	2,461[0,30]
KO fed	2,56 [0,25]	0,75 [0,05]	2,79 [0,27]
Hippocampus			
WT fast	5,02 [0,92]	2,79 [0,56]	7,52 [1,58]
KO fast	*2,80 [0,44]	*1,49 [0,15]	**2,77 [0,49]
WT fed	4,21 [0,67]	2,53 [0,45]	6,44 [1,00]
KO fed	5,34 [1,10]	1,93 [0,42]	6,75 [1,30]
Hypothalamus			
WT fast	1,94 [0,76]	1,93 [0,42]	2,71 [0,55]
KO fast	1,28 [0,25]	*0,91 [0,14]	1,83 [0,34]
WT fed	4,21 [0,57]	2,52 [0,49]	5,61 [0,80]
KO fed	5,14 [0,89]	3,10 [0,39]	6,19 [1,13]

Table 3: Acyl-carnitine levels in different regions of brain in fed and fasted animals. Acyl-carnitine levels were measured in different brain areas: cerebellum, cortex, hippocampus and hypothalamus from fed and fasted mice (12h food deprivation) by HPLC-MS/MS. Data were presented as a mean of acyl-carnitine levels (mmols of acyl-carnitine/ mg of protein) $\pm$ standard error. Standard error (S.E.M.) is included in brackets. n=6. * $p<0.05$, ** $p<0.005$, *** $p<0.001$. One-way Anova test followed by a Bonferroni post hoc test was applied.

This result indicates that CPT1C enzyme has CPT1 activity. Thus it is able to convert acyl-CoA into acyl-carnitine under conditions that require an increase in the fatty acid oxidation such as fasting conditions.

Under fasting conditions, when malonyl-CoA levels are lowered, CPT1 activity is decreased in CPT1C-KO mice as compared to WT mice. In order to find out if this decrease in the levels of acyl-carnitine is a result of the activity of the other two isoforms, CPT1A and B, we next characterized their expressions levels.

4.1.5 CPT1A and CPT1B mRNA levels in different brain areas

In order to know whether the decrease in the acyl-carnitine levels found in fasted CPT1C-KO mice was produced by the absence of CPT1C or by an alteration in the expression of other isoforms, mRNA levels of CPT1A and B were measured in different brain areas in fed and fasting conditions.

mRNA expression of CPT1A was measured in cortex, hippocampus, hypothalamus and cerebellum, while CPT1B was only measured in cerebellum due to its specific expression in this brain region. Expression levels of WT mice at *ad libitum* condition were used as reference value and GAPDH was used as a housekeeping gene to calculate the fold change in gene expression.

No differences between both genotypes either fasting or *ad libitum* conditions were found neither for CPT1A nor CPT1B expression (Table 4).

CPT1A	Ad libitum		Fasted	
	WT	KO	WT	KO
Cortex	1 ± 0.10	1.01 ± 0.23	1.01 ± 0.08	1.24 ± 0.30
Hippocampus	1 ± 0.16	0.99 ± 0.22	1.24 ± 0.23	1.02 ± 0.17
Hypothalamus	1 ± 0.12	1.03 ± 0.11	1.16 ± 0.12	0.89 ± 0.07
Cerebellum	1 ± 0.16	0.90 ± 0.13	0.87 ± 0.08	0.77 ± 0.15
CPT1B	Ad libitum		Fasted	
	WT	KO	WT	KO
Cerebellum	1 ± 0.10	1.59 ± 0.50	1.67 ± 0.19	1.56 ± 0.17

Table 4: Relative CPT1A and CPT1B mRNA expression levels present in different brain regions. CPT1A and CPT1B mRNA expression levels were measured by qRT-PCR using GAPDH as a housekeeping gene and the expression levels of WT mice at *ad libitum* condition were used as reference value. CPT1B expression was analyzed only in cerebellum because CPT1B is not expressed in other brain regions. Data are presented as mean ± S.E.M. n=4. No statistical differences were found between genotypes.

This result implicates that the reduction in the acyl-carnitine levels in CPT1C-KO mice was due to a null CPT1C activity itself, rather than a consequence of indirect down-regulation by CPT1A or CPT1B expression.

4.2 CPT1C AND THE CERAMIDE SYNTHESIS PATHWAY

Our group has recently reported that CPT1C regulates ceramide synthesis in the arcuate nucleus of the hypothalamus (Gao, S. 2011). So, the question arose whether CPT1C was also regulating ceramide levels in other brain areas.

4.2.1 Brain ceramide levels in WT and CPT1C-KO mice

In the first approach the ceramide levels from different brain regions such as cerebellum, hippocampus, striatum and motor cortex of fed and fasted CPT1C-KO and WT mice were determined.

As shown in figure 35, CPT1C-KO mice showed a reduction in ceramide levels in all brain regions analyzed in comparison to WT levels. Fasting increased ceramide levels in the cerebellum and the striatum of WT mice by two-fold over ceramide levels in the same regions in CPT1C-KO animal. In contrast, in the hippocampus and the motor cortex, ceramide levels in WT mice were not altered by fasting, but were clearly reduced in CPT1C-KO mice.

To summarize, CPT1C-KO mice have a decrease in ceramide levels in fasting conditions in comparison with the WT ones, mainly in the long chain ceramides (C16:0, C18:0 and C18:1) but not in the very long chain ones (C24:1). These data are indicative for a modulation or regulation of long chain ceramide levels by CPT1C activity in the brain.

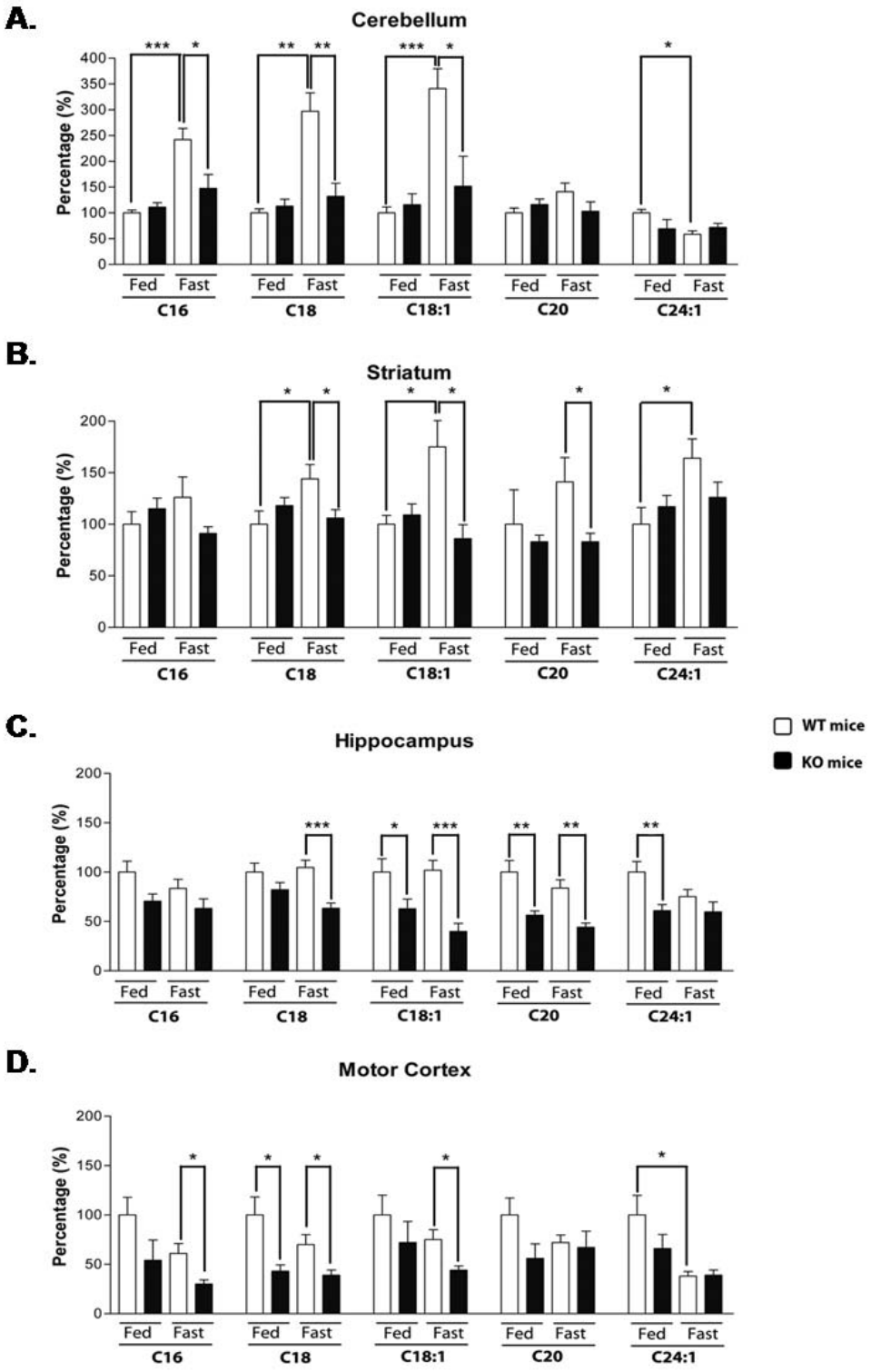

Figure 35: Brain ceramide levels. Different ceramide species were measured by HPLC-MS/MS in fed and fasting conditions of different brain areas. The percentage (%) of ceramide levels were normalized using the WT mice in fed condition representing 100%. Data are expressed as mean of percentage ± S.E.M. * p<0.05, ** p<0.005, *** p<0.001. An one-way Anova test followed by a Bonferroni post hoc test was applied (n=10).

4.2.2 The involvement of CPT1C in the *de novo* ceramide synthesis

The data provided by the previous experiment suggest the involvement of CPT1C in the ceramide synthesis. To date there are at least two known and distinct mechanism that lead to ceramide production.

First, endogenous ceramide can be generated *via de novo* pathway. In this pathway, serine and palmitoyl-CoA condense to form 3-ketosphinganine by serine palmitoyl transferase (SPT). This is followed by reduction of 3-ketosphinganine to sphinganine. Sphinganine is then N-acylated by ceramide synthases to finally produce dihydroceramide (dhCer) (Mandon, 1992).

Second, the generation of ceramide can be triggered by the action of sphingomyelinases (SMases), which hydrolyze sphingomyelin (SM) to yield ceramide and phosphorylcholine. Several SMases have been characterized and can be divided in two main groups referring to their pH optimum: acidic or neutral. Moreover they show differential subcellular localizations (Spence, 1983; Andrieu-Abaand Levade, 2002; Kolesnick, 2002; Ogretmen and Hannun, 2004; Bartke and Hannun, 2009), acidic SMases are exclusively localized in lysosomes while the neutral SMases are mainly expressed in the cytoplasmatic membrane although it could be also localized in the endoplasmic reticulum.

Taking into account that CPT1C is located in the endoplasmic reticulum, where *de novo* ceramide synthesis takes place, it was important to investigate whether CPT1C is involved in the regulation of this pathway.

In order to address this question CPT1C was over-expressed in primary hippocampal neurons using CPT1C adeno-associated viruses (AAV1-CPT1C). CPT1C over-expression was confirmed by western blot analysis. As it is showed in figure 36, CPT1C protein level was increased to four-folds in cells transduced with AAV1-CPT1C viruses as compared to control cells (transduced with AAV1-GFP).

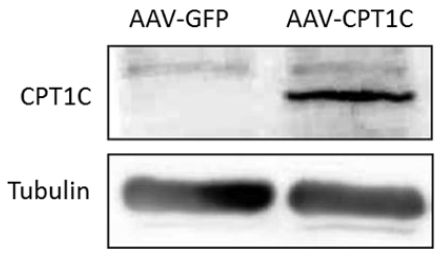

Figure 36: Western blot to confirm AAV1-CPT1C over-expression. 80 µg of protein from isolated hippocampal neurons transduced with AAV1-GFP and AAV1-CPT1C were loaded in 10% SDS-acrylamide gel and subjected to immunoblotting using anti-CPT1C and anti-tubulin antibodies.

After testing the system, AAV1-CPT1C virus infection was performed at 7DIV in hippocampal cells cultured in six well plates (300.000 cells per well), AAV1-GFP transfection served as a control. Medium was removed and stored for later use. 0.5 ml of neurobasal medium without B27 and containing 0.5 mM glutamine and AAV1 at a multiplicity of infection (MOI) of 1X 10^5 was added stand for 2 hours. Then, 1.5 ml of the pre-conditioned medium was added and left to stand for a further seven days. Then, cells at 14DIV were removed for analysis of ceramide levels by LC-ESI-MS/MS System (API3000 PE Sciex).

As shown in figure 37, CPT1C over-expressing cells revealed a two-fold increase in the ceramide levels in almost all types of ceramide in comparison to control cells. Saturated ceramides such as C16:0, C18:0 and C20:0 were the predominantly increased by CPT1C over-expression. Ceramide levels where normalized using the AAV1-GFP transduced cells representing 100% (control).

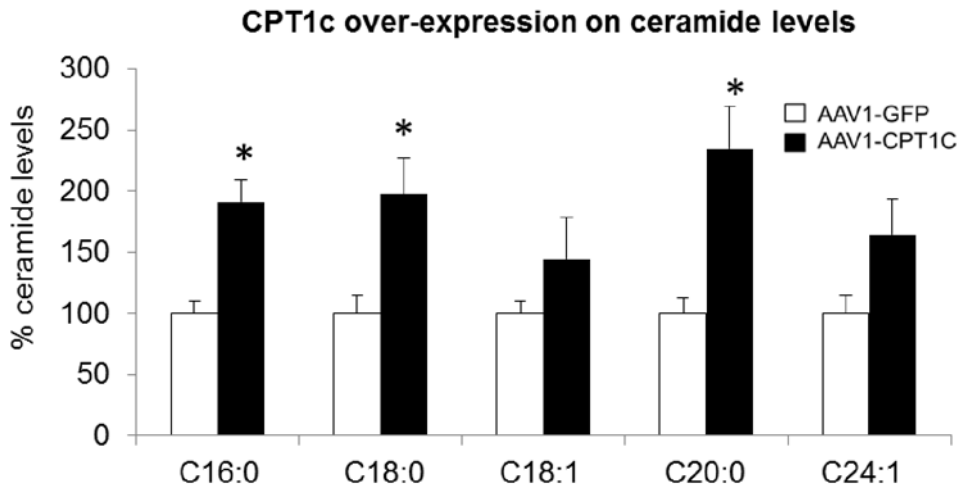

Figure 37: Ceramide levels in hippocampal neurons transfected with AAV1-CPT1C adenovirus. Levels of ceramide in hippocampal neurons transduced with AAV1-GFP (serving as a control) and AAV1-CPT1C at 7DIV. Cells were collected at 14DIV and analyzed via HPLC-MS/MS. Ceramide levels were normalized using the AAV1-GFP transduced cells representing 100%. Error bars are S.E.M.; * p< 0.05. The Student's t test was applied.

After confirming that CPT1C over-expression increases ceramide levels, we wondered whether this increment was through the *de novo* synthesis pathway.

Cells were transduced with AAV1-CPT1C or AAV1-GFP virus (serving as a control) at 7DIV. At 14DIV transduced cells were treated with 10 µM myriocin for 8 hours. Myriocin is a specific inhibitor for the serine-palmitoyl transferase, the first enzyme involved in the synthesis the *de novo* of ceramide. After the inhibitor incubation, cells were collected and ceramide extraction was performed.

The percentage of ceramide levels in cells transduced with AAV1-CPT1C respect to control cells (AAV1-GFP) is shown in figure 38 with or without myriocin treatment. The increase in the ceramide levels induced by CPT1C over-expression was blocked by myriocin (figure 38) further supporting that CPT1C regulates or facilitates the *de novo* synthesis of ceramide.

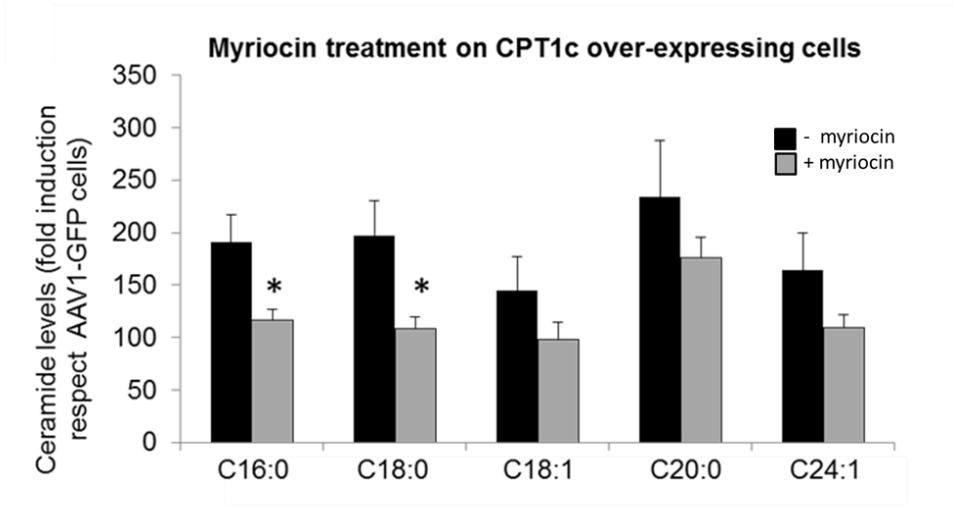

Figure 38: Ceramides levels after myriocin levels. Levels of ceramide in hippocampal neurons transduced with AAV1-GFP or AAV1-CPT1C at 7DIV and treated with 10 µM myriocin during 8h at 14DIV.Then, cells were collected and analyzed by HPLC-MS/MS. Data are represented as the percentage of ceramide levels in cells transduced with AAV1-CPT1C and treated with or without myriocin respect the control cells (AAV1-GFP). Error bars are mean $\pm$ S.E.M. * $p<0.05$. Student's t tests were used to assess statistical significance of the quantifications.

CPT1C is involved in the synthesis of ceramide through the *de novo* synthesis pathway.

4.3 CPT1C EXPRESSION

It is known that CPT1C enzyme is expressed in the central nervous system of the adult mouse. Thus, the questions arose whether this enzyme is exclusively expressed in the adult animal or by whether it is already up-regulated during brain development and whether CPT1C is additionally expressed in the peripheral nervous system (PNS).

4.3.1 CPT1C expression along mouse development

To study CPT1C expression during mouse development samples from the following embryonic and postnatal stages E15 (embryos at day 15), E19 (embryos at day 19), P0 (birth day), P21 (weaning) and adult mice were taken.

CPT1C mRNA expression and protein levels were measured by real time PCR and Western blot, respectively. In figure 39, CPT1C mRNA expression was present in preadult developmental stages of the animals. During mouse development CPT1C expression levels increased, being most abundant in the adult animal (figure 39A). Same results are shown by western blot analysis (figure 39B), where 80 µg of microsomal enriched cell fraction from total brain was run in a 8% SDS-acrylamide gel and later incubated with CPT1C antibody (1:500) or tubulin (as a loading control, 1:1000).

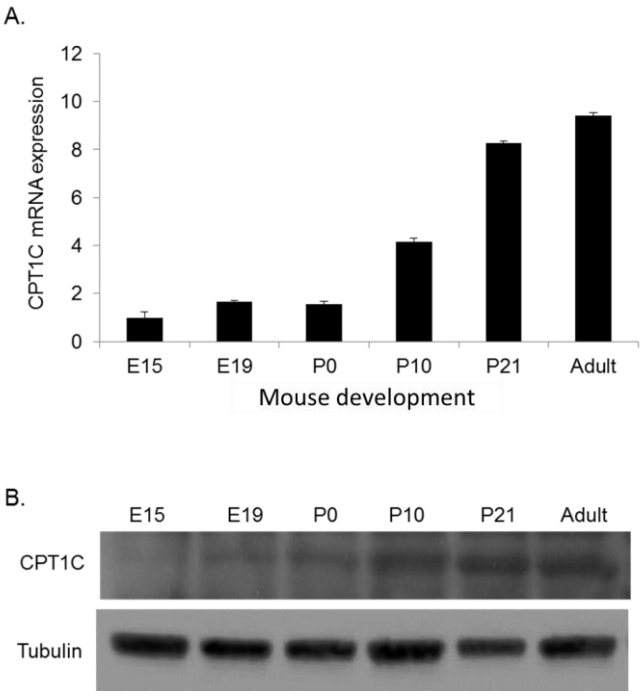

Figure 39: CPT1C expression along mouse development: A. CPT1C mRNA expression. B. CPT1C expression by western blot analysis. 80 µg of microsomal fraction from total brain from different stages of mouse development were run in 8% SDS-acrylamide gel. Anti-CPT1C antibody (1:500) and anti-tubulin (1:1000) antibodies were used.

Thus in conclusion CPT1C protein expression is present in early stage E15, is increased postnatally and reaches its expression peak in adulthood.

4.3.2 CPT1C is expressed in the peripheral nervous system.

In order to determine whether CPT1C is expressed in the peripheral nervous system, two different peripheral regions were analyzed: the ventral horn of the spinal cord (mainly composed of motor neurons) and the sensitive ganglions (mainly formed by sensitive neurons). Samples were kindly provided by Dr. Xavier Navarro from *Universitat Autónoma de Barcelona*.

CPT1C protein expression levels were determined by Western blot analysis. Samples of six rats were pooled and 80 µg of total protein from each sample was applied to a 10% SDS-acrylamide gel. After gel electrophoresis and blotting, membranes were incubated with CPT1C or tubulin (as a loading control) antibodies. Samples from WT cortices were used as a positive control for CPT1C expression.

Western blot analysis revealed that CPT1C is expressed in both regions, in the sensitive ganglion and in the ventral horn of spinal cord (figure 40). This implicates that CPT1C is indeed expressed in peripheral nervous system although at lower levels than in the brain. In addition, CPT1C seems to be stronger expressed in motor neurons than in sensory neurons.

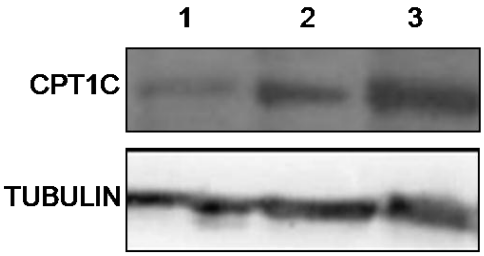

Figure 40: Western blot analysis of CPT1C expression in the peripheral nervous system. 80 µg of protein was run in 10% SDS-acrylamide gel. 1, Ganglion (the majority are sensitive neurons); 2, ventral horn of the spinal cord (the majority are motor neurons); and 3, brain cortices from WT mice.

In summary these results indicate that CPT1C is expressed during mouse development, being more abundant in the adult stage. Moreover, CPT1C expression could not only be detected in the central nervous system but in addition, is present in the peripheral nervous system, although the CPT1C expression levels in the PNS appear to be lower than in the brain.

4.4 STUDY OF THE BEHAVIORAL PHENOTYPE OF CPT1C-KO MICE

Most of the groups, who study CPT1C, are interested in the role of CPT1C in the hypothalamus, where its main function is the regulation of food intake and energy homeostasis. Since we were interested in knowing its functional role in other brain regions, for that reason, a set of behavioral tests was carried through comparing CPT1C-KO and WT mice.

In order to confirm that our model displays a similar basic phenotype to the ones previously described in the other CPT1C-KO models, in a first series of experiments the metabolic phenotype of our CPT1C-KO mouse model was characterized.

4.4.1 Metabolic phenotype analysis of the CPT1C-KO mice

Several parameters were measured in adult mice (14 weeks) fed with a normal rodent chow to assess the metabolic phenotype of CPT1C-KO mice.

Body weight of mice was measured before starting the experiment. Subsequently, food intake was evaluated using the weight transducer technology developed by Panlab. This technology allows the continuous assessment of the animal food consumption with highest accuracy and stability. Animals were kept individually in this cage during a week. Body temperature was measured using a rodent thermometer from Bioseb.

As shown in table 5, CPT1C-KO mice ate less than WT animals (~10%) although they had the same body weight in adulthood. No differences were found in body temperature between the genotypes.

	n	WT	KO
Food intake, in (g)	12	4.00 ± 0.11	3.62 ± 0.14 *
Body weight (g)	12	31.31 ± 0.66	34.06 ± 1.17
Body temperature (ºC)	8	35.25 ± 0.23	35.11 ± 0.20

Table 5: Metabolic parameters. Food intake, body weight and body temperature were measured in adult mice. A student t-test was performed. * $p<0.05$. n=12 or 8 mice.

This metabolic study revealed that CPT1C-KO mice eat less surprisingly retaining the same body weight. These data are indicative for an impaired energy homeostasis in CPT1C-KO mice as compared to WT mice.

Since no differences in body weight were observed between genotypes in the adult age group, body weight during postnatal mouse development from 1 week to 16 weeks after birth was investigated.

As shown in figure 41, no differences in body weight were found during the mouse development between CPT1C-KO and WT mice.

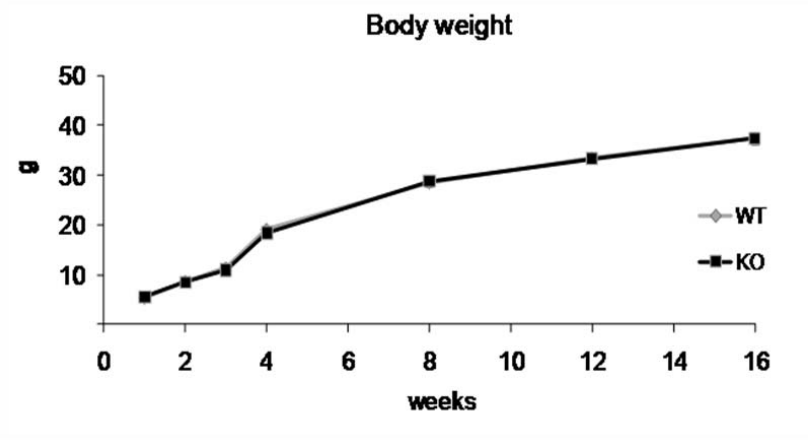

Figure 41: Body weight analysis during the postnatal mice development. Body weight was measured from the first week to 16 weeks after birth. n= 20. No differences were found between genotypes.

Importantly, our CPT1C-KO mouse model displays a similar basic phenotype to the one that has been previously described in the others CPT1C-KO mouse models (Wolfgang, M.J. 2006; Gao, X.F. 2009), thus confirming the role of CPT1C in regulation of food intake and energy homeostasis.

4.4.1.1 Peripheral metabolism studies in CPT1C-KO mice

Having the same body weight and body temperature than the WT mice, CPT1C-KO mice show alterations in the food intake. To address the question whether CPT1C also regulates peripheral tissue metabolism, CPT1 activity and expression of genes involved in fatty acid oxidation were measured in liver and muscle tissues of both genotypes.

4.4.1.1.1 CPT1 activity in liver and skeletal muscle

CPT1 activity was measured in muscle and liver samples from fasted animals. 20 µg from mitochondrion-enriched cell fractions from CPT1C-KO and WT fasted mice were assayed. Fasted mice were used because peripheral CPT1 activity is increased under this condition. Fasting is associated not only with decreased malonyl-CoA concentration but also with a pronounced decrease in sensitivity of CPT1 to inhibition by malonyl-CoA as well an increased CPT1 mRNA and CPT1 activity (Lavrentyev, E.N. 2004).

The product of CPT1 reaction, the palmitoyl-carnitine, was measured by HPLC-MS/MS chromatography. CPT1 activity was calculated as nmols of palmitoyl-carnitine formed by minute and mg of protein.

Results revealed that CPT1 activity in fasted CPT1C-KO mice was reduced by 20% and 40% as compared to WT mice in muscle and liver tissue, respectively (figure 42).

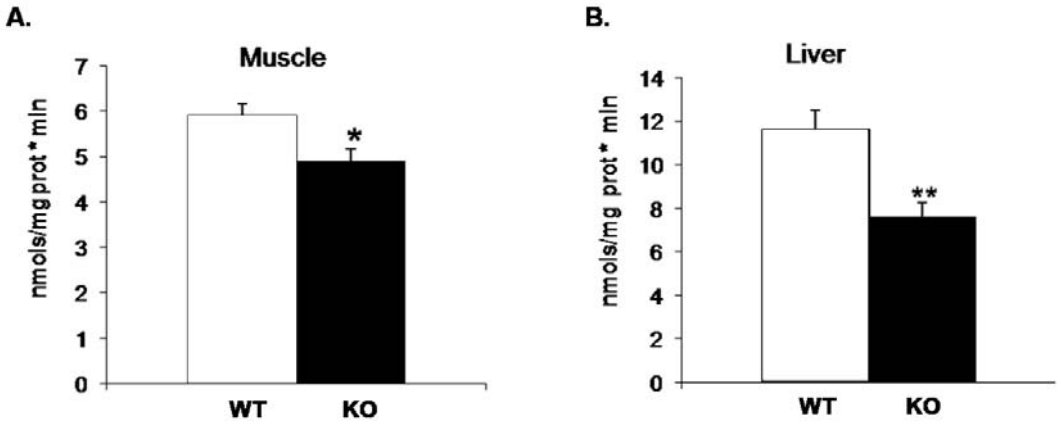

Figure 42: CPT1 activity in mitochondria from muscle (A) and liver (B) of mice. 20 µg from mitochondrion-enriched cell fraction from CPT1C-KO and WT fasted mice were assayed. Data are presented as mean ± S.E.M (n=4); * p<0.05, ** p<0,005. For statistical analysis a student t-test was applied.

This finding suggests that in CPT1C-KO mice, the peripheral fatty acid oxidation does not respond to central hypothalamic signals.

4.4.1.1.2 mRNA levels of fatty acid oxidation genes in liver and skeletal muscle

The decrease of CPT1 activity in fasted CPT1C-KO mice was indicative for a missregulation in the peripheral oxidation. Thus we asked whether this impaired peripheral oxidation resulted from a down-regulated expression of CPT1A and CPT1B isoforms.

mRNA expression of CPT1A from liver and CPT1B from skeletal muscle was measured from CPT1C-KO and WT mice in fasting and fed conditions. As a control of the fatty acid oxidation, the expression of *pdk*4 gene was measured. *Pdk*4 is a pyruvate dehydrogenase kinase, isozyme 4, which is regulated by nutrient deprivation (Sugden, M.C. 1993).

As shown in the figure 43, mRNA expression of CPT1A, CPT1B and *pdk*4 genes were markedly decreased in CPT1C-KO mice in fasting as compared to WT mice. No differences between genotypes were found in fed condition.

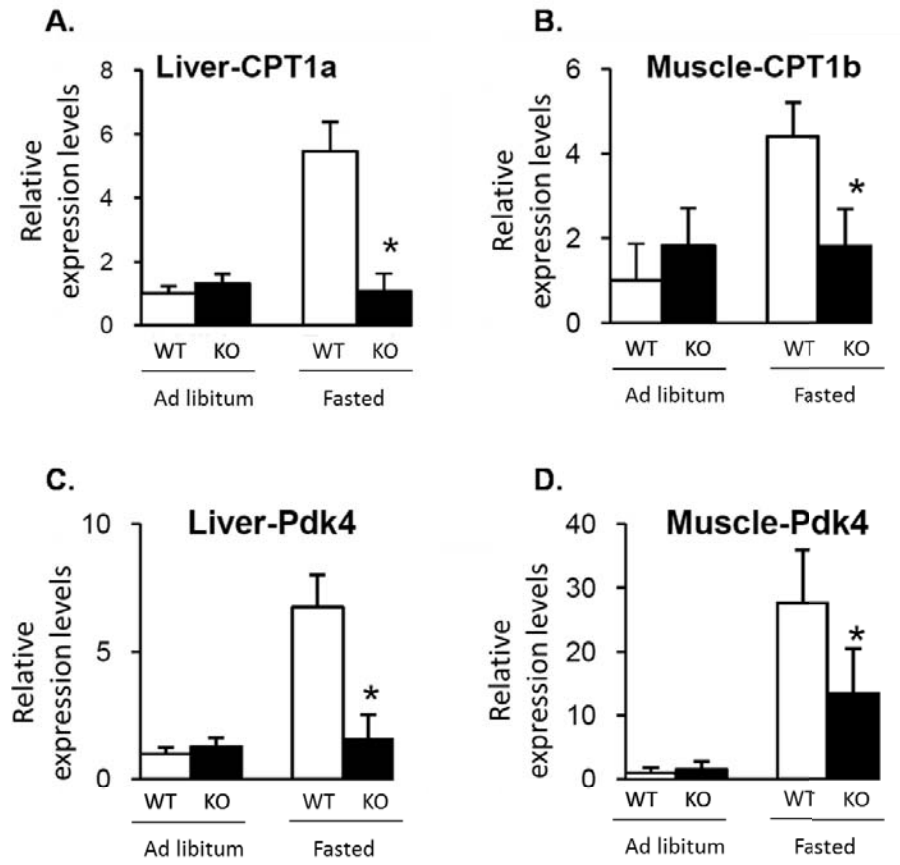

Figure 43: mRNA expression of CPT1A, CPT1B and pdk4 in liver and skeletal muscle. mRNA expression of CPT1A (A-B), CPT1B (C-D) and pdk4 (E-f) were measured by qRT-PCR in liver and skeletal muscle from fasted and fed mice. GAPDH was used as a housekeeping gene in all the cases. Error bars are the standard errors (S.E.M). An one-way Anova test followed by a post hoc test was applied. n=4.

The down-regulation of the oxidative genes in CPT1C-KO mice under fasting condition correlates with the decrease in CPT1 activity observed in peripheral tissues of CPT1C-KO mice.

Taken together, these results further support the notion that CPT1C-KO mice do not respond to hunger signals produced in the hypothalamus, which leads to a decrease in CPT1 activity in peripheral tissues such as muscle and liver.

4.4.2 Histological studies of brain areas of CPT1-KO mice

Histological studies were performed to investigate whether the lack of CPT1C results in gross alterations in brain regions like cerebellum, hippocampus or cortex in CPT1C-KO mice.

This technique required fixed brains. Brains were perfused through left ventricle with 50 ml of 0.1M PBS, pH 7.4, followed by 100 ml of cold 4% paraformaldehid (PFA) in PBS through a peristaltic bomb (30ml/min). Once perfused, brains were extracted and incubated in 30% sucrose in PBS for 24h. After that, 30 µm of coronal brain slices from WT and CPT1C-KO mice were further treated for luxol blue and cresyl violet stainings.

Cresyl violet staining of CPT1C-KO brain sections did not disclose gross histological abnormalities in the structure of any analyzed region of the brain (Figure 44).

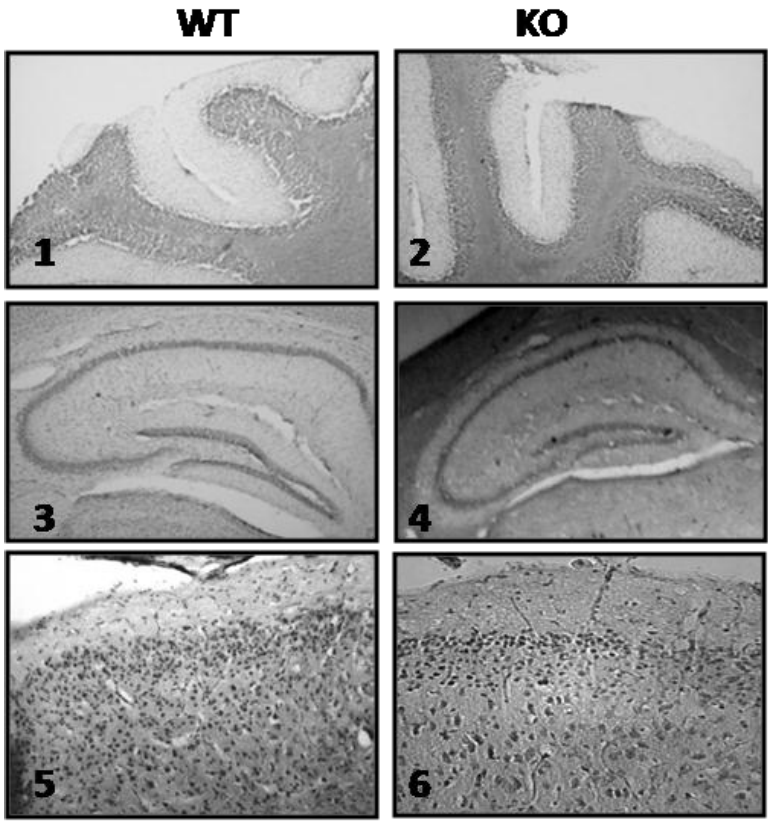

Figure 44: Histological analysis from CPT1C-KO and WT mouse brains. 30 µm coronal brain sections were stained with luxol blue and cresyl violet, in order to visualize the overall morphology of the cerebellum (1, 2), the hippocampus (3, 4) and the cortex (5, 6). No gross abnormalities were detected in the brains of CPT1C KO mice analyzed under the microscope.

4.4.3 Behavior studies in CPT1C-KO mice

As CPT1C is expressed not only in the hypothalamus but in all brain regions, various behavioral tests were performed to identify a putative role for CPT1C also in the other brain regions.

Before starting behavioral tests, a handling training was carried through for one week. In order to reduce the stress ans anxiety of the animal, the training consisted of picking up the mouse by its tail for habituation of animals to this kind of manipulation.

4.4.3.1 SHIRPA test

The SHIRPA test is a comprehensive semiquantitative routine testing protocol to identify and characterize phenotype impairments.

The assessment of each animal started with the observations of undisturbed behavior in a cylindrical clear Perspex viewing jar for wild running or stereotypy. In this part of the test, general health issues like breathing, trembling, salivation, etc. were measured. No differences between the two groups were observed in this part of the SHIRPA test.

Then, the mice were transferred to an arena for the observation of the motor behavior and sensorial function. In this part of the test, no significant differences between genotypes were detected in reflexes, sensory function, autonomous function or reactivity, but revealed that CPT1C-KO mice presented hypoactivity and a reduced escape response in the touch escape test (Table 6).

In summary behavioral Shirpa test showed no gross impairment in general neural function between CPT1C-KO and WT mice, although they are suggestive for some kind of motor dysfunction.

	WT (n=12)	KO (n=12)
General Health		
Body position	sitting or standing	sitting or standing
Breathing	normal	normal
Trembling	none	none
Trunk arching	present (50%)	present (50%)
Piloerection	none	none
Salivation	normal	normal
Sensory Reflexes		
Visual placing	upon vibrasse contact	before vibrasse contact 18 mm
Corneal reflex	active single eye blink	active single eye blink
Pinna reflex	active retraction, moderate brisk flick	active retraction, moderate brisk flick
Toe pinch	none	none
Righting reflex	yes	yes
Tail elevation	horitzontal extended	horitzontal extended
Preyer reflex	yes	yes
Grip response	present	present
Reaching	before vibrasse contact 18 mm	before vibrasse contact 18 mm
Emotional Domain		
Irritability	struggle during supine restraint	struggle during supine restraint
Fear	none	none
Startle response	just less that 1cm	just less that 1cm
Transfer arousal	no freeze, immediate movement	no freeze, immediate movement
Touch escape	**moderate (rapid response to light stroke)**	**mild (escape response to frim stroke)**
Aggression	none	none
Motor Abilities		
Activity	**vigorous, rapid/ dart movement**	**casual scratch, groom, slow movement**
Negative geotaxia	yes	yes

Table 6: SHIRPA test: Observational assessment of mice.

4.4.3.2 Motor test

As motor alterations were detected in CPT1C-KO mice by the SHIRPA test, more specific motor tests such as activity, strength or coordination were performed to characterize the motor behavioral phenotype of CPT1C-KO mice.

4.4.3.2.1 Circadian global activity: Actimetry test

The first test performed was the actimetry test. In this test the circadian global activity was directly assessed in the animal homecage (IR Actimeter, Panlab, Barcelona, Spain) through long periods (>24h). The activity parameters (locomotion, exploration) were evaluated using automatized procedures (photocell beams and video-tracking system).

CPT1C-KO mice showed strongly reduced locomotor activity throughout the circadian period (24h) as revealed by the actimetry test. The reduction of locomotor activity was more prominent during spontaneous activity in the dark period, when the animal is usually more active (figure 45). Moreover, this hypoactivity also affected the animals during the first two hours after entering a new cage. This behavior is called “the exploratory activity” and animals normally increase this activity to spot a new environment.

Below the line, when total activity was averaged during all the cycles (over the entire 24h period), the total locomotor activity was significantly reduced to 70% in CPT1C-KO mice (**WT**: 51.6 ± 6.4 x10^3 cm/s; **KO**: 35.9 ± 2.1 x10^3 cm/s; p<0.05; n=12; Student´s t-test.)

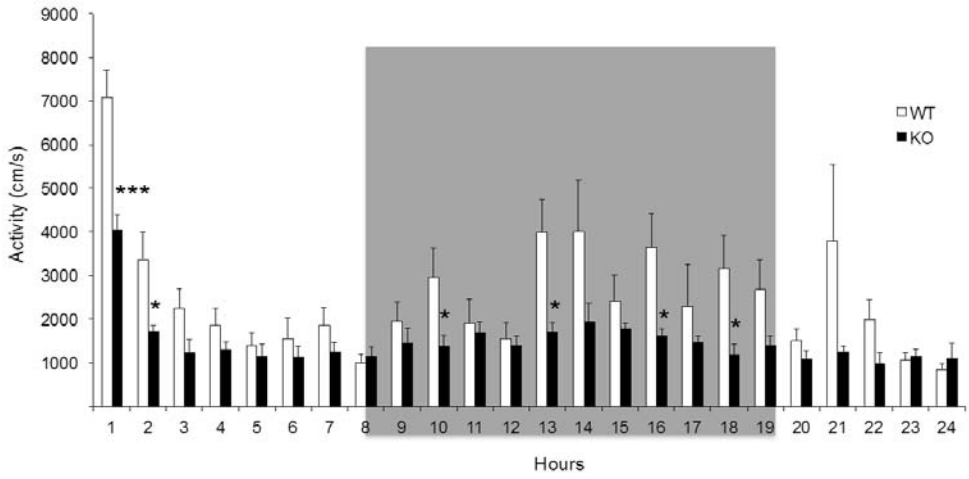

Figure 45: Circadian activity (actimetry) during a 24-h cycle. Locomotor activity measured in actimetry boxes. Grey rectangle represents dark hours. Data are represented as mean ± S.E.M. *p<0.05, ***p<0.001 (n=12). A student´s t-test was applied.

4.4.3.2.2 Coordination test: rotarod and paw print tests

To address the question whether CPT1C-KO mice displayed altered the motor coordination, the rotarod and paw print tests were applied.

Rotarod test is a performance test based on a rotating rod with forced motor activity being applied from 4 to 34 rpm. Rotarod performance test measures parameters such as the latency to fall from the wheel.

The length of time that a given animal stays on this rotating rod is a measure of their balance, coordination, physical condition, and motor-planning. Before starting the test, mice were trained on the rotarod at the minimum rotational speed, 4 rpm.

Rotarod test, when performed at low speed (4 rpm), revealed no significant difference between CPT1C-KO and WT mice. However, at higher rotation speed, CPT1C-KO mice performed significantly worse than WT mice, as it is manifested by their shorter latency to fall [repeated measures ANOVA F(1.21)=24.89, p=0.000] (Figure 46).

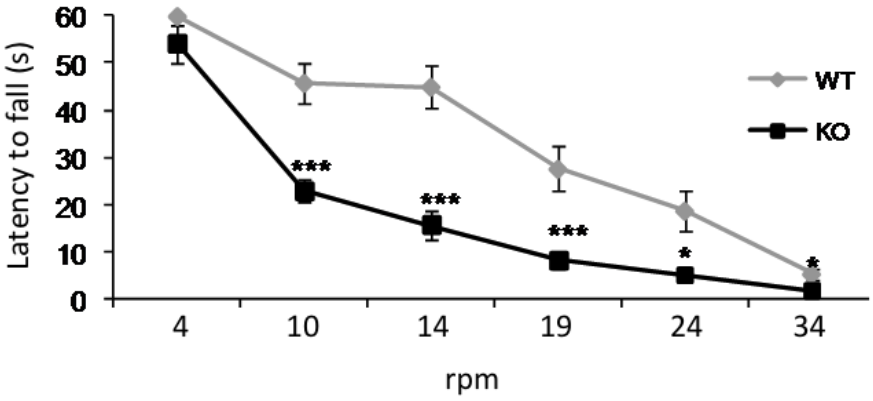

Figure 46: Rotarod test. Performances review on the rotarod during consecutive trials with increasing rotational speeds (4, 10, 14, 19, 24 and 34 pm). Data are represented as mean ± S.E.M; * p<0.05, *** p<0.001 (n=12). For statistical analysis the ANOVA test repeated measures was applied. n=12 mice. rpm= revolutions per minute.

Moreover, when the mice were submitted to a more coordination-demanding task (accelerating rod test), where the rotation speed was increased from 4 to 40 rpm during a single session of 1 min, the performance of CPT1-KO mice were less than the WT mice, confirming the motor and coordination dysfunction observed in the rotarod test (figure 47).

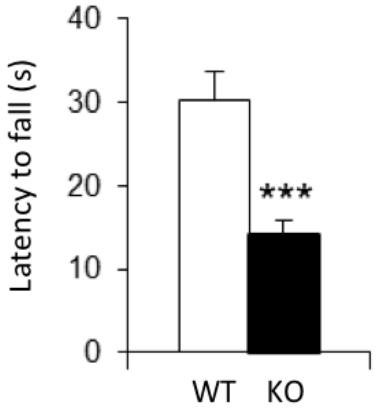

Figure 47: Accelerating rod for motor coordination and balance. Rotation speed was increased from 4 to 40 rpm during a single session of 1 min. Data are represented as mean ± S.E.M. *** p<0.001 (n=12). A student t-test was applied.

Next test was the paw print test, in which the walking pattern was examined. The hindpaws of the mice were painted with black nontoxic waterproof ink. Animals were then placed at one end of a long and narrow tunnel, where they spontaneously enter and leave. Footprints made at the beginning and at the end were excluded from the analysis. This task was repeated at least three times.

CPT1-KO mice showed a significant reduction in stride length (distance between each step) over a 20 cm distance (figure 48). This result showed a defective coordination between the movements of the hindlimbs.

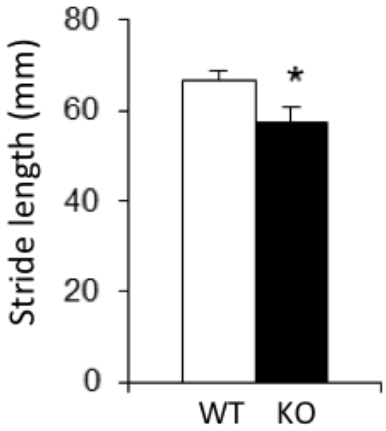

Figure 48: Paw print test. Distance between two steps of the same limb is measured of WT and CPT1C-KO mice over a distance of 20 cm. Mean ± S.E.M. n=12 * p<0.05. A student´s t-test was applied.

Since CPT1C-KO mice showed a decrease in the distance between the prints and less latency to fall in the rotarod and acceleration test than WT mice, these data further support that these mice have impaired motor coordination.

4.4.3.2.3 Muscular force: grip strength and bar hang test

The muscular force was measured through the grip strength in the forelimbs. A force transducer was used to measure the peak force exerted by the forelimbs of the mouse. Each trial was repeated three times, and the data were given as the mean of the three values.

CPT1C-KO mice showed a significant reduction in the vertical force compared with the controls (figure 49). Body weight between the groups was the same, so differences found in mouse force were not caused by differences in the body weight (**KO**: 39.5 ± 2.64 g; **WT**: 37.8 ± 1.33 g; p=0.541).

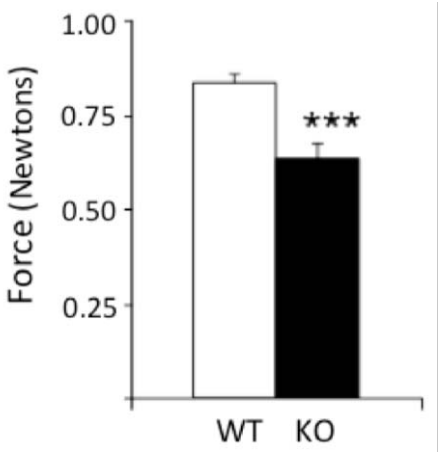

Figure 49: Grip strength test: Grip strength meter measures the forelimbs grip strength. Data are represented as mean ± S.E.M; The Student´s t-test was applied. *** p<0.001. n=12.

Next experiment to measure neuromuscular strength was the bar hang test. In this test, mouse was gripping the bar with forepaws and the latency to fall out and the latency to use the hindlimbs to climb up the bar were measured with 60 seconds (sec) cut off time.

This series of experiments disclosed that the latency to fall was significantly shorter for CPT1C-KO mice as compared to WT latency, 41.83 and 60 sec, respectively. Moreover, 66.7% of CPT1C-KO mice fell while any of WT mice fell (Table 7).

In addition, 100% of WT mice used their hindlimbs to climb up to the bar whereas only 66.7% of CPT1C-KO mice performed the same way. Furthermore, those CPT1C-KO mice that were able to use their hindlimbs, spent much more time with the task than WT mice (42.58 sec for CPT1C-KO mice and 6.33 sec for WT mice).

	WT (n=12)	KO (n=12)	p
Latency to fall (sec)	60.00±0.00	41.83±6.91	**
Fall (%)	0	66,7	***
Latency to use hindlimbs (sec)	6.33±3.29	42.58±7.48	***
Use 1 hindlimb (%)	100	66.7	*

Table 7: Bar hang test. The test was performed for 60s. Data are represented as mean ± S.E.M. * p<0.05, ** p<0.005, *** p<0.001. The student´s t-test was applied. n=12

Taken together, these results show that, CPT1-KO mice are hypoactive and exhibit clear deficits in motor function, especially in coordination skills and strength.

4.4.3.2.4 Food intake inside the cage

To analyze whether CPT1C-KO mice have a reduced food intake either due to alteration in the homeostatic energy or due to motor problems to get the food in the cage, the food was placed inside the cage. Food consumption was measured every day during 4 days.

As shown in figure 50, CPT1C-KO mice consumed significantly less food than WT mice.

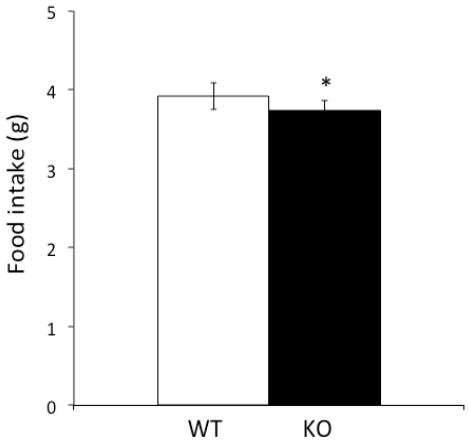

Figure 50: Food intake inside the cage. Food was placed inside the cage and food intake was measured every day. Data are represented as mean ± S.E.M. * p<0.05. Student t-test. n=12

This result suggests that CPT1C-KO mice show alterations in food intake that are not caused by motor dysfunction but by alterations in homeostatic metabolism.

4.4.3.3 Memory and learning test: Morris water maze test

To measure hippocampus dependent spatial navigation memory and learning in mice, the Morris water maze test (MWM) was performed.

The water maze consists of a circular pool, with an escape platform located 1cm below the water surface in some pool position. In each trial, mice were placed at one of the starting locations in random order: north (N), south (S), east (E) and west (W) and they were allowed to swim until they located the platform. Mice failed to find the platform within 60 seconds. White curtain with affixed black pattern to provide an arrangement of spatial cues surrounded the maze. All the trials were recorded and traced with an image tracking system (SMART, Panlab) connected to a video camera placed above the pool.

During the first part of the Morris water maze (MWM) test, mice had to learn to swim. In the pre training test, mice have to learn that climbing to the platform permits leaving the pool. After that, mice proceed with the acquisition test.

The **MWM acquisition test** consists in measuring the latency of the mouse to find the platform along the 10 sessions (days). In this part of the test, the platform was localized in the north-east (NE) of the swimming pool and the animal had to learn to use distal cues to navigate a direct path to the hidden platform when started from different, random locations around the perimeter of the tank.

As it is represented in figure 51, an important learning impairment was detected in CPT1C-KO mice as shown by the increased latencies to reach the platform, although the ability of the CPT1C-KO mice to reach the hidden platform improved along the last acquisition sessions.

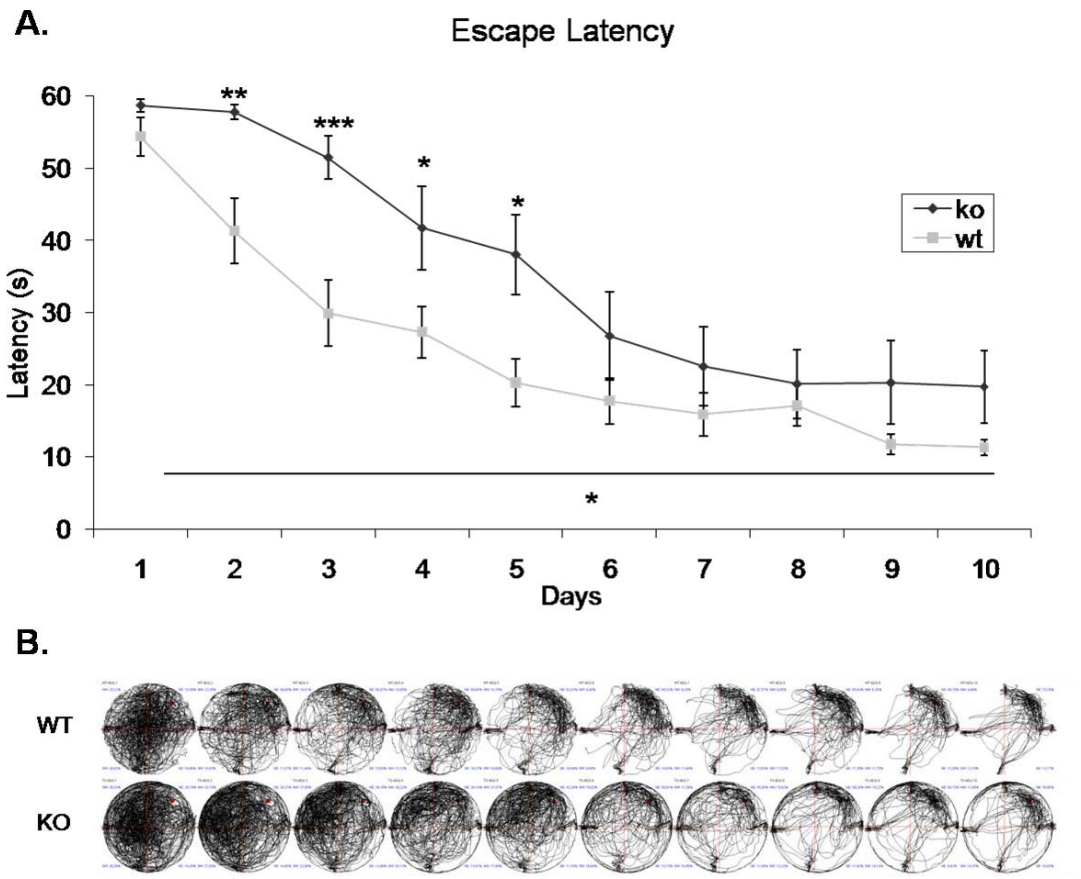

Figure 51: Morris water maze task test. A. The time required to reach the hidden platform. Mean ± SEM, over the ten testing days is indicated. n=12. Repeated measures ANOVA revealed significantly different performances between the two genotypes. B. Diagram

The learning curves from WT and CPT1C-KO mice differed significantly from WT mice [repeated measures ANOVA F(1.22)=6.726, p=0.017 values for CPT1C-KO, respectively], is not until session 8 that CPT1C-KO mice spent the same time as WT mice to reach the platform. This implicates that the lack of CPT1C produces alterations in the spatial learning mechanism.

In order to test whether the alteration in learning observed in CPT1C-KO mice was consequence of motor impairment, swimming speed and floating were measured during all the MWM tests. In figure 52 swimming speed and floating mean of the ten days of acquisition test are represented and no difference between groups was observed, suggesting that the delay of CPT1C-KO mice in finding the hidden platform was not a result of their motor impairment.

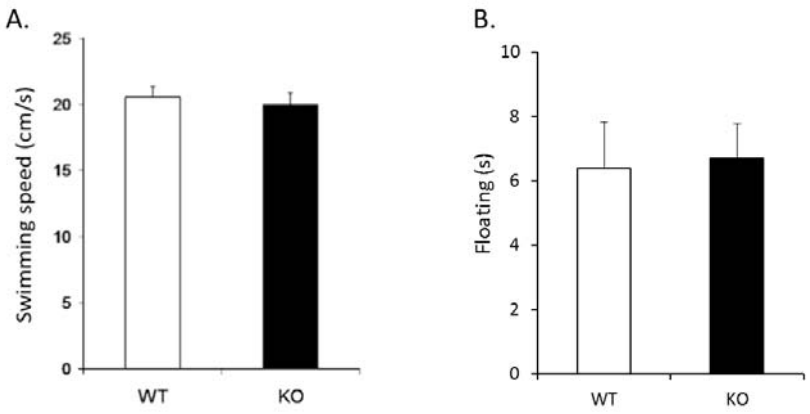

Figure 52: A. Swimming speed. Swim speed was measure during the acquisition sessions in the MWM test. **B. Floating**. Data are represented as mean ± S.E.M. Student´s t-test. n=12

Next part of the test was the **cued session**, where the goal was to find a visible platform (black flag). This test was two times repeated. The escape latency of CPT1C-KO mice was similar to the one of WT mice (Figure 53) indicating that CPT1C-KO mice have the same basic abilities (such as intact eyesight, motor ability (swimming) and the same motivation (escape from the water) as WT mice.

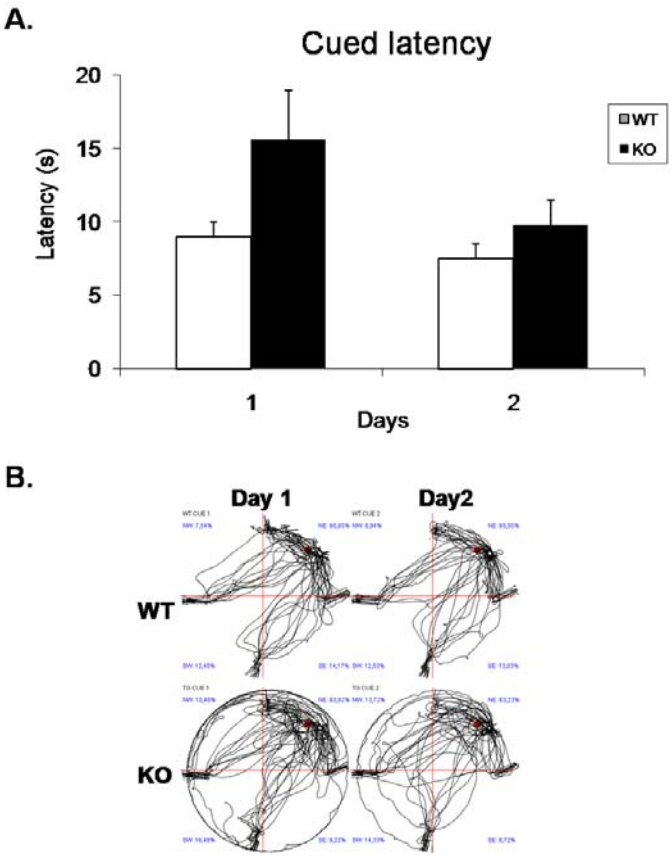

Figure 53: Cued session. A. Escape latency (mean + SEM) of WT and KO mice in the visible platform task over two testing days. One-way ANOVA revealed no significant difference between both groups. B. Diagram

These parts of the MWM test were specifically related to learning problems since swimming speed remained unaffected. Moreover in the cued session, where the goal was to find a visible platform, no differences were detected in the latency to reach the platform when it was visible implicating no motivational deficits.

In order to **test visuospatial memory**, in the removal test the platform was removed and the percentage of time spent in each quadrant was measured. No significant differences between genotypes were detected in the preference for the trained quadrant, which indicates that once the platform position was learnt, it was equally retained in CPT1C-KO and WT mice (Figure 54).

This observation support the conclusion that CPT1C-KO mice indeed remember the location of the platform and its deficits are limited to the learning phase.

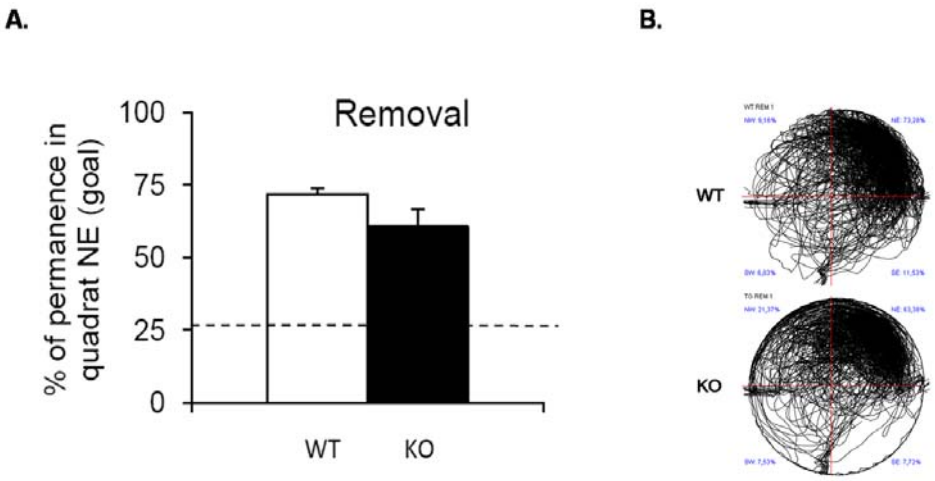

Figure 54: Removal test: A. Percentage of permanence spent in the target quadrant (NE) during the removal session; discontinuous lines represent the chance level in this session. Data are represented as mean ± S.E.M; Student´s t-test. n=12

In the **reversal test** (Figure 55) the platform was placed in another quadrant (in the opposite site, south-west), and another set of four trials per day for 4 additional days was performed. This test evaluates the cognitive flexibility of the mice, though their ability to learn a new platform position. No significant differences were observed between genotypes in the percentage of time spent in the previously trained quadrant (NE). However, measuring the time spent in the new goal quadrant (SW), CPT1C-KO mice spent less time in the new goal quadrant (SW). This reinforced the concept of a hippocampal-dependent learning deficit in CPT1C-KO mice.

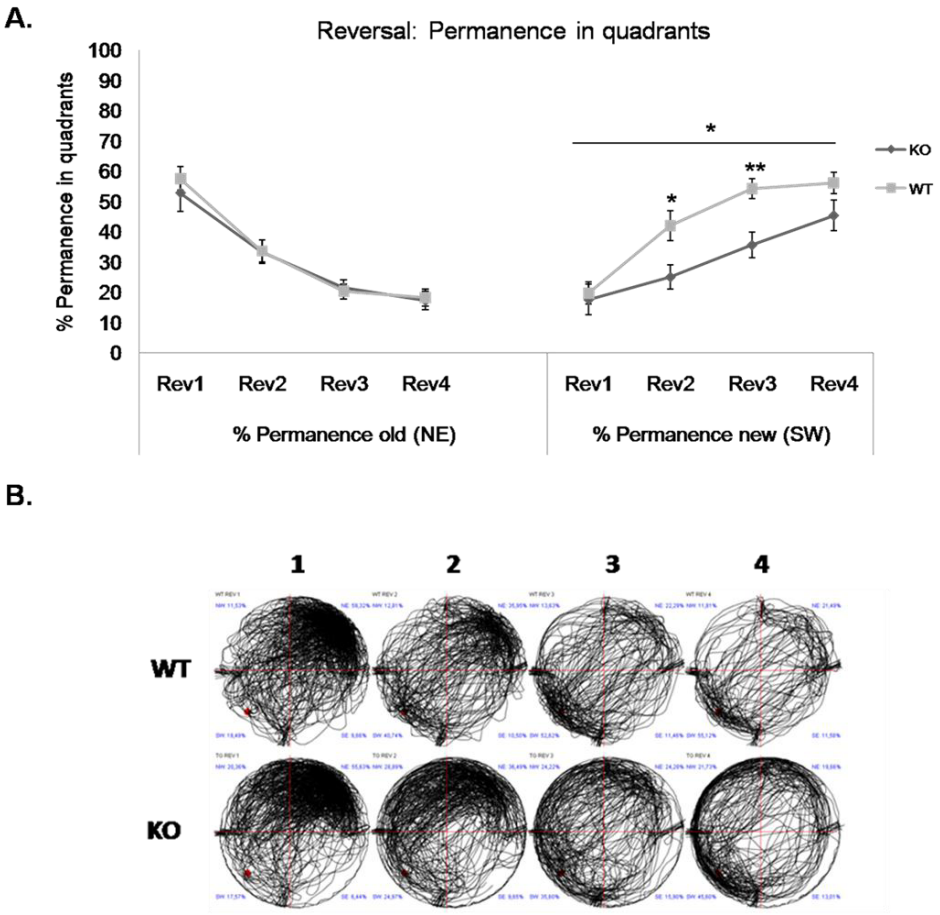

Figure 55: Reversal test. A. Percentage of permanence spent in the old target quadrant (NE) and in the new target quadrant (SW) along 4 days. Data are represented as mean ± S.E.M. * $p<0.05$, ** $p<0,005$, repeated measures ANOVA test. n=12. B. Diagram Rev means reversal.

Taken together, CPT1C-KO mice show an impaired learning efficiency as compared to WT animals without affecting memory or cognitive flexibility.

4.5 STUDY OF CPT1C FUNCTION IN THE HIPPOCAMPAL NEURONS

4.5.1 CPT1C is located in the ER of dendritic spines

It was previously described that CPT1C was highly expressed in the hippocampus (Price, N. 2002). In order to determine the precise expression pattern of the protein, we performed brain section and incubated them with anti-CPT1C and GFAP (glial fibrillary cidic protein, an astrocyte marker) antibodies. Figure 56 shows that CPT1C (in green) is expressed in pyramidal neurons of hippocampus (figure 56).

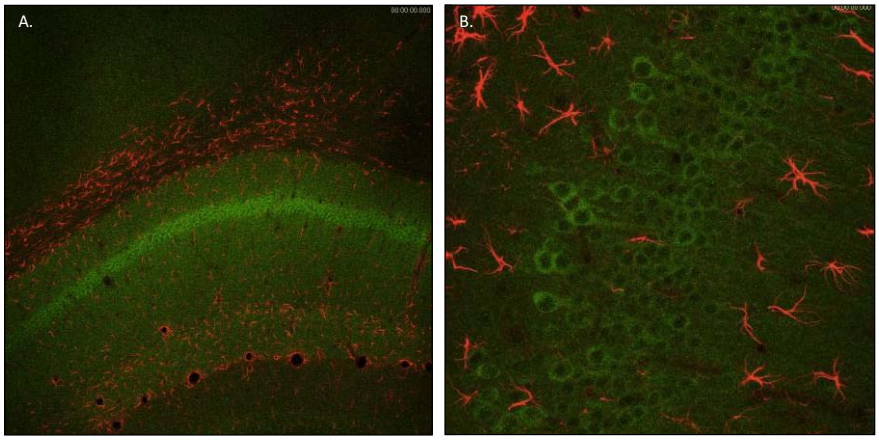

Figure 56: CPT1C location in hippocampal neurons. A. Hippocampus. B. CPT1C is present in pyramidal neurons of hippocampus. Brain sections were doble immnodetected with anti-CPT1C antibody (green, 1:100) and anti-GFAP antibody (red) (1:500, glial fibrillary acidic protein (Chemicon, #MAB360))

To analyze the detailed localization of CPT1C in hippocampal neurons, we performed neuronal primary cultures and transfected them with pIRES-CPT1C-EGFP, a plasmid that encodes CPT1C fused to the N-terminal region of EGFP (green fluorescence protein). Figure 57A shows that CPT1C is located throughout the neuron, including neuronal bodies and dendrites. Detailed photos of dendrites demonstrate that CPT1C is present mainly in shaft but also in spines (figure 57A).

Finally to confirm that sub-cellular localization of endogenous CPT1C was the ER, cultured neurons were transfected with pDs-ER-Red2 (Clontech) that stains the ER red, and subsequently immunodetected endogenous CPT1C with anti-CPT1C antibody (green). Figure 57B shows that CPT1C is localized in ER of hippocampal neurons.

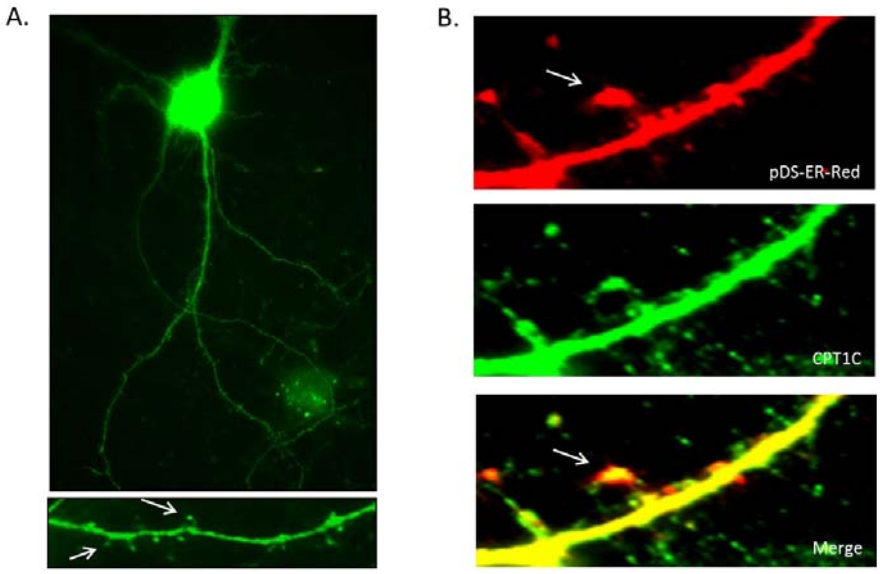

Figure 57: **A. Hippocampal cultured neurons were transfected with pIRES-CPT1C-EGFP at 11 DIV and visualized at 15 DIV**. Image shows that CPT1C is present in neuronal body, dendritic shaft and spines**. B. Hippocampal neurons were transfected with pDS-ER-Red to stain the ER**. At 15DIV, cells were transfected with pDS-ER-Red to stain the ER (red) and inmunodetected with CPT1C antibodies (green). The merge image (yellow) demonstrates that CPT1C is located in the ER.

4.5.2 Dendritic spine density and morphology

Spine morphogenesis and synapse formation are known to be important processes in the developing brain and in memory and learning process. In accordance with the previous observation in the Morris water maze test, where CPT1C-KO mice showed impaired learning process, spine density and cell morphology were measured to determine the role of CPT1C in the formation of dendritic spines.

To visualize the dendritic protrusions, hippocampal neurons were isolated from embryonic day 17 embryos of CPT1C-KO and WT mice. Cells were maintained in cultures and at 13 days in vitro (DIV) neurons were transfected with green fluorescent protein (EGFP) two days prior to the experiment. After that, at 15DIV, cells were fixed and dendritic protrusions were analyzed. Spine maturation was assayed by measuring spine length, the number of spines with heads and the spine head area. As it is described in the literature, spine maturation in hippocampal neurons culture occurs by 14DIV, depending on cell density. During the process of spine maturation, filopodia-like dendritic protrusions acquire a typical mushroom-like shape with bulbous heads and short dendritic shafts (Ethell and Yamaguchi, 1999).

As it is shown in figure 58, the mean protrusion density was not altered between CPT1C-KO and WT mice, 6.0 ± 0.2 and 6.6 ± 0.26 protrusions per 10 µm of the dendrite, respectively (Figure 58A). Regarding the dendritic spine morphology, CPT1C-KO and WT neurons showed a clearly different pattern in the protrusion lengths (figure 58B,C) with an increase in the protrusion length of CPT1C-KO neurons of approximately 20% longer compared to WT ones. Moreover, 56.79 % ± 2.97 of the protrusions were shorter than 1 µm in CPT1C-KO neurons compared to 87.05 % ± 1.69 in control neurons (WT). CPT1C-KO neurons showed remarkably more filopodia-like protrusions than the WT control cell (Figure 58D). The formation of spine heads was considered to be an indicator of maturity. The number of mature spines (mushrooms and stubbies) per 10 µm of dendrites was lower in CPT1C-KO than in WT neurons (Figure 58E, F). CPT1C-KO neurons had less mature spines (56.79 % ± 2.97) (mushroom and stubby) compared to WT cells (87.05 % ± 1.69). Moreover, the average size of the heads was similar in both cases: 0.23 μm^2 ± 0.005 and 0.22 μm^2 ± 0.006, for CPT1C-KO and WT, respectively. This data lead to the conclusion that CPT1C-KO neurons have less mature spines, although they have the

same maturity than WT ones. Taken together, these results clearly demonstrate the role of CPT1C in the dendritic spine maturation.

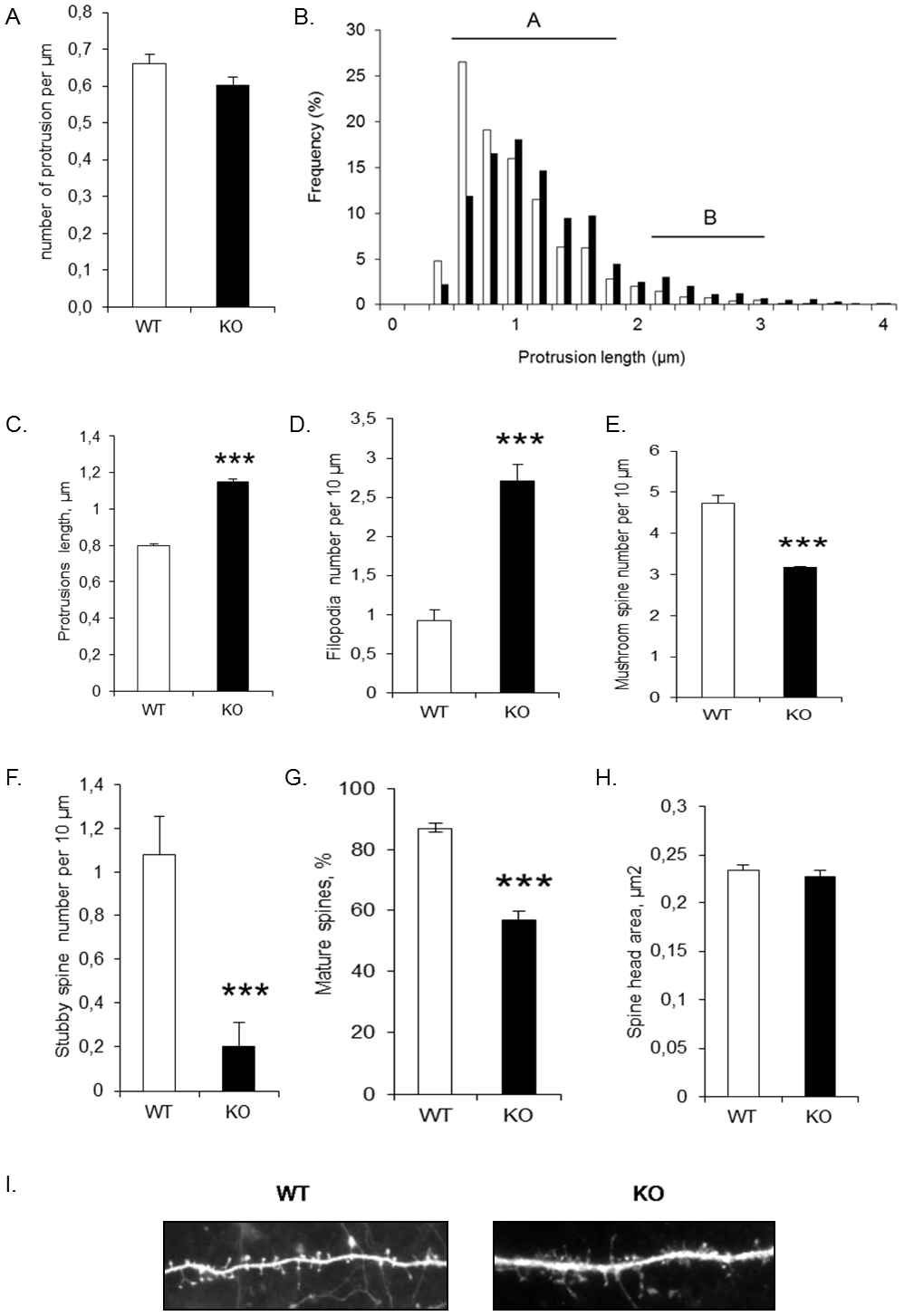

Figure 58: Dendritic spine density and morphology. Hippocampal neurons transfected (13DIV) with pEGFP (control) and fixed at 15DIV. Protrusions were analyzed two days after transfection. The spine morphogenesis was assayed by analysis of protrusion density (A), protrusion length (B and C, Group A represents spines and group B represents dendritic filopodia based on the length) types of spines per 10 µm: filopodia (only neck, D), mushroom (neck plus head, E) and stubby (only head, F) and by percentage of mature spines (E, mushroom+stubby) relative to total number of protrusions. Maturity of spine was measure by spine head area (G). For the quantification of spine length, protrusion number and type, approximately 100 dendrites from independent transfections were selected randomly. Student's t tests were used to assess statistical significance of the quantifications. (Error bars are S.E.M. * $p<0.05$; ** $p<0.005$; *** $p<0.001$). I. A representative image of the dendritic spine of WT, CPT1C-KO transfected with pEGFP fluorescence.

4.5.2.1 Rescue the phenotype of the CPT1C-KO dendritic spine morphology adding C6-ceramide to the culture medium

Previous results show that CPT1C promotes spine maturation. Moreover, CPT1C is also involved in ceramide synthesis. It was previously described that depletion of sphingolipids and cholesterol resulted in a loss of dendritic spines and enlargement of the remaining ones (Hering, H. 2003). Therefore, we wanted to prove whether CPT1C over-expression or ceramide treatment were able to rescue dendritic spine morphology in CPT1C-KO mice.

In a first approach CPT1C was over-expressed in CPT1C-KO neurons. Hippocampal neurons at 10DIV were transfected with pIRES-CPT1C-EGFP, a plasmid that encodes CPT1C fused to the N-terminal region of EGFP (green fluorescence protein). pIRES-CPT1C-EGFP vector expresses both CPT1C and GFP protein, which allowed the visualization of CPT1C over-expressing cells in green. We then analyzed these neurons for the morphology of dendritic protrusion four days after transfection. Over-expression of CPT1C on CPT1C-KO cultures reduced filopodia density and increased the percentage of mature spines to values similar to WT cultures (figure 59B), again confirming the requirement of CPT1C for efficient spine maturation.

In a second approach C6-ceramide was added to the culture medium. Short chain ceramides, like N-hexanoyl-D-erythro-dihydrosphingosine (C6 ceramide), are water soluble and cell membrane permeable and thus can be easily delivered to cells (Ghidoni, R. 1999) leading to the synthesis of complex ceramide. It is described in the literature that C6 ceramide at low concentrations promotes neuronal differentiation (Toman,R.E. 2000).

To test this hypothesis, hippocampal neurons from E17 embryos of CPT1C-KO and WT mice were treated with 1.5 µM C6 ceramide at 5DIV. It is shown in the literature that ceramide promote cell survival and dendritic outgrowth in the immature stages of hippocampal neuron, by contrary, in mature neurons, the treatment produce cell death even at a low concentration (Mitoma, J. 1998). For that reason, the treatment was done in immature hippocampal neurons (5DIV). Later, cells were transfected with the EGFP vector at 13DIV and two days later, cells were fixed (15DIV) and the dendritic spines were analyzed.

As observed in figure 59, the average of the protrusion length was reduced from 1.43 µm ± 0.03 to 1.17 µm ± 0.03 in the CPT1C-KO cells treated with the exogenous C6 ceramide. Consequently, the proportion of filopodia-like protrusions decreased from 2.3 µm ± 0.18 to 0.45 µm ± 0.07 in the CPT1C-KO cells treated with C6 ceramide, while the percentage of mature spines increased by 40% in the treated ones (Figure 59A). So, exogenous ceramide reversed the CPT1C KO phenotype by decreasing immature filopodia and restoring mature spine density almost to control levels.

Indeed, CPT1C over-expression or C6 ceramide treatment resulted in a reduction of long filopodia-like protrusions leading to an increased number of mature spines with characteristically short dendritic shafts.

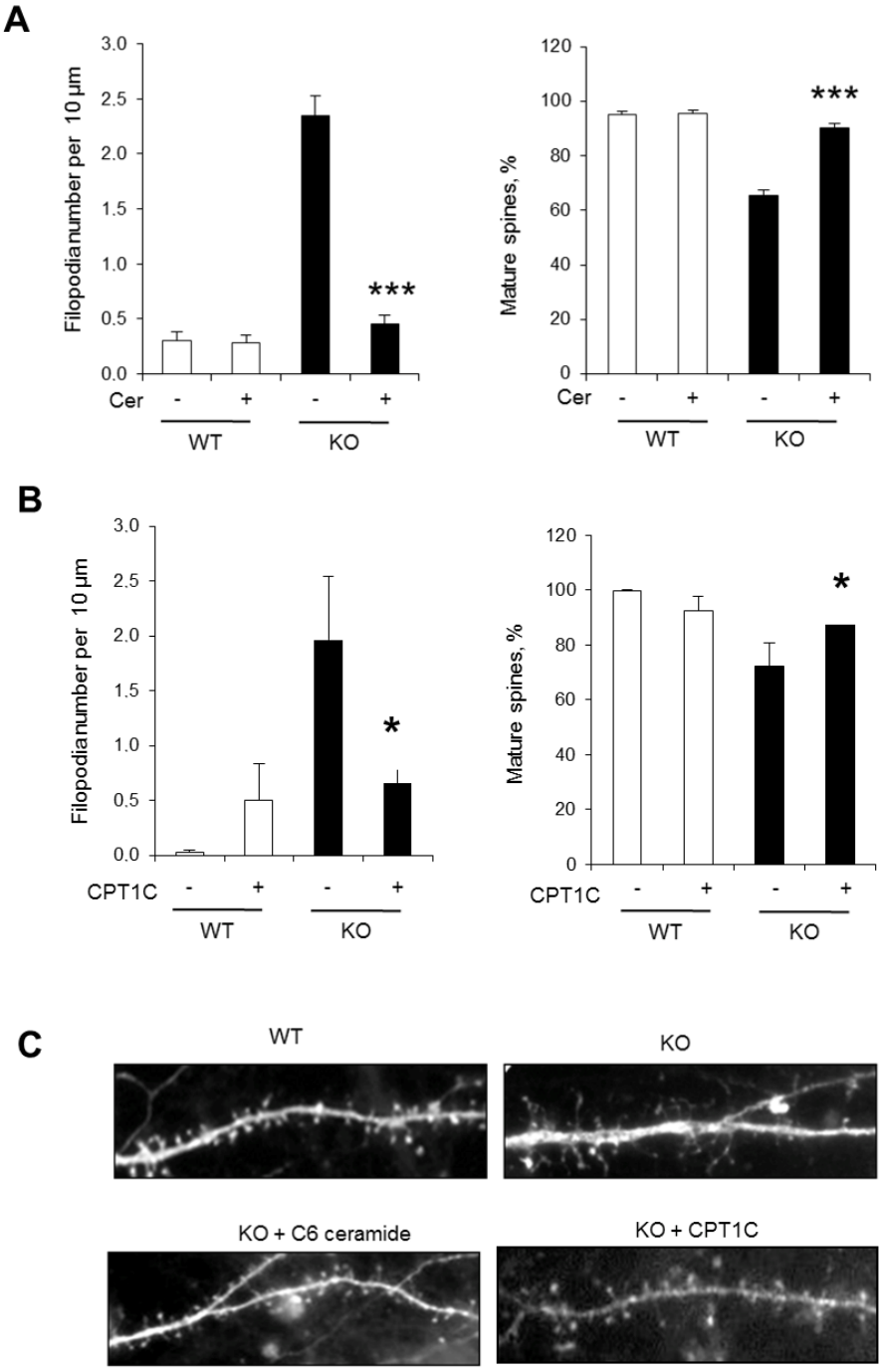

Figure 59: Rescue of CPT1C-KO phenotype on spine morphology by CPT1C expression or ceramide treatment. A. Hippocampal neurons treated with 1.5 µM C6-ceramide at 7DIV and transfected with GFP at 13DIV, fixed and analyzed for the morphology of dendritic protrusions at 15DIV. **B.** Hippocampal neurons were transfected with pIRES-CPT1C at 10DIV and analyzed at 14DIV. pIRES-CPT1C vector expresses both CPT1C and GFP protein, which allow visualize in green the cells overexpressiong CPT1C. For the quantification of filopodia length, matures spines number and percentage, approximately 100 dendrites from independent transfections were selected randomly. ANOVA post hoc was used to assess statistical significance of the quantifications. (Error bars are S.E.M. * p<0.05; ** p<0.005; *** p<0.001. **C.** A representative image of a dendritic spine of WT, CPT1C-KO, CPT1C-KO mice treated with C6-ceramide and CPT1C-KO mice transfected with pIRES-CPT1C-EGFP transfected with EGFP vector, which contains the fluorescent GFP protein.

These results indicate that CPT1C regulation of spine maturation is mediated by ceramide.

4.5.3 Synaptic markers

Spine maturation during development and synaptic remodeling occur when synaptic contacts are stabilized. In cultured hippocampal neurons, spine morphogenesis goes hand-in-hand with the establishment of synaptic contacts and consequent synapse formation. During the process of spine maturation, filopodia-like dendritic protrusions acquire a typical mushroom-like shape with bulbous heads and short dendritic shafts and most of excitatory (glutamatergic) synapses in the hippocampus are formed on spines. Deletion in CPT1C protein resulted in impaired spine maturation. Therefore, our question was, whether CPT1C-KO neurons do not make matures spines, do they make synapses?

To analyze synapse formation, we examined the distribution of pre- and post-synaptic proteins such as synapsin I and PSD-95, respectively. Hippocampal neurons at 15DIV from CPT1C-KO and WT mice were used to detect synapses using immunofluorescence staining. Synapse density was determined by counting the numbers of PSD-95 or synapsin1 positive clusters along different dendrite stretches. The numbers were normalized to a dendrite stretch of 100 µm.

Quantification disclosed no significant changes in the number of PSD-95 and synapsin I clusters between the genotypes, indicating the same level in synapse maturation (figure 60).

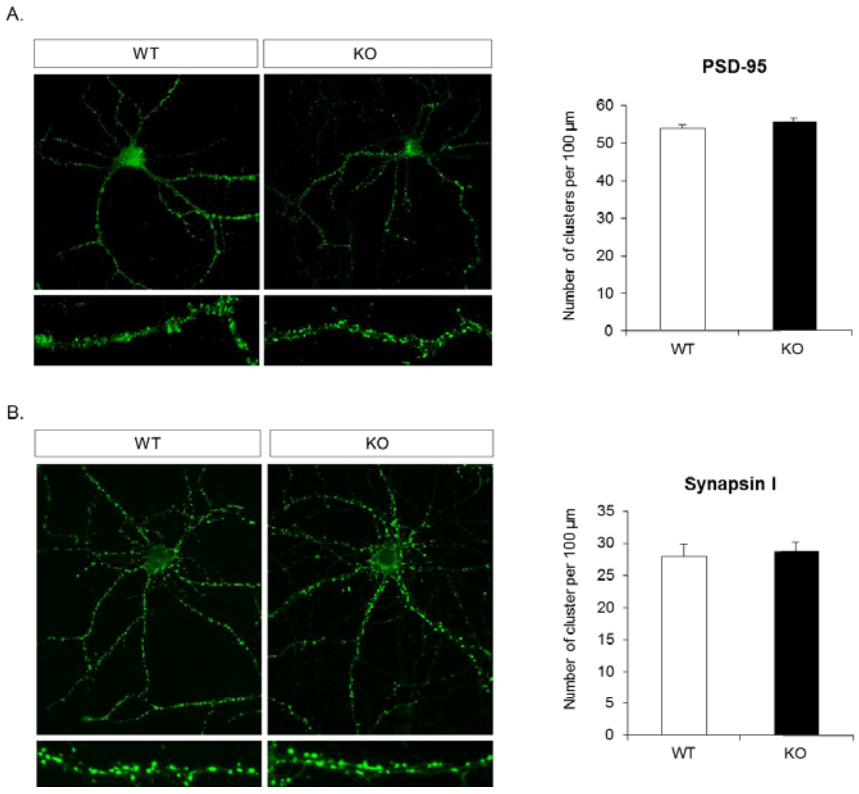

Figure 60: Analysis of the distribution of synaptic markers. Cultured hippocampal neurons from WT and CPT1C-KO mice at 15DIV were immunostained, using antibodies against the post- and pre-synaptic markers PSD-95 (A) or synapsin1 (B), respectively. Quantification of the number of PSD-95 or Synapsin1 positive puncta per 100 µm.

Lack of CPT1C does not affect the number of clusters for PSD-95 and synapsin I in hippocampal neurons at 15DIV.

4.5.4 Levels of AMPA receptors in hippocampal neurons

Dendritic spines usually receive most of the excitatory synapses in hippocampal neurons. To determine whether a reduction of mature spines in CPT1C-KO neurons reflects the failure to form excitatory synapses, AMPA receptor quantity and trafficking were examined.

In addition to spine morphology, CPT1C might regulate other processes associated with synaptic plasticity. The number of active AMPA receptors at the postsynaptic site determines the strength and responsiveness of the synaptic contact and AMPA-receptor trafficking is a key process involved in long-term potentiation (LTP) and long-term depression (LTD). It is known that LTP is controlled by the incorporation of additional AMPA receptors into the active synapse, whereas, during LTD, AMPA receptors are removed from the postsynaptic sites by endocytosis (Bredt and Nicoll, 2003). Therefore, in the following study we investigated whether the plasticity defects seen in CPT1C-KO is caused by a miss-regulation of AMPA-receptor trafficking.

Different approaches were used to study AMPA-receptor and its trafficking. We studied the subunit GluR2 of AMPA receptor because it is one of the most abundant in the AMPA receptor family. We performed the western blot analysis to determine the total level of GluR2 and a biochemical technique of surface inmunofluorescence staining to detect changes in the number of receptors present at the cell surface. A complementary immunofluorescence method we called “antibody feeding assay” was used to track receptor molecules moving in and out of the plasma membrane (Essmann, C.L. 2008).

4.5.4.1 Total levels of GluR2 subunit of AMPA receptor

Total quantity of GluR2 was measured by western blot analysis. 80 µg of total lysates of hippocampus of WT and CPT1C-KO mice were run in an 8 % SDS-acrylamide gel. Figure 61 shows CPT1C-KO mice had lower levels of GluR2 subunit than WT mice.

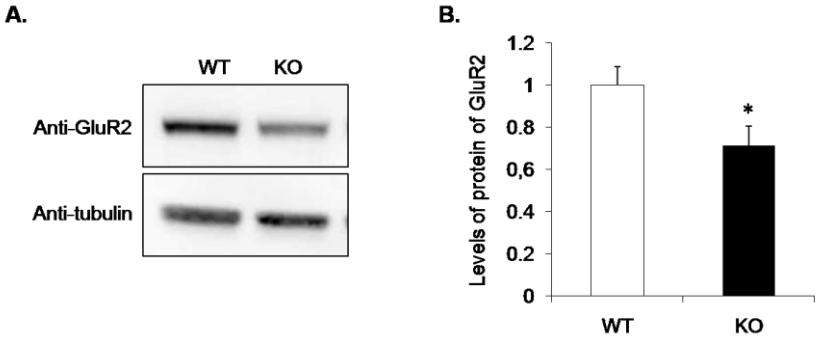

Figure 61: Western blot analysis of GluR2 subunit in hippocampal tissue. A. A representative image of GluR2 levels in hippocampal wild type (WT) and CPT1C-KO (KO) mice. B. Relative quantification of GluR2 levels in different hippocampal samples of WT and CPT1-KO mice (n=5) using ImageJ program. Student’s t-tests were used to assess statistical significance of the quantifications. Error bars are S.E.M. * $p<0.05$; ** $p<0.005$; *** $p<0.001$.

Total level of GluR2 was reduced in CPT1C-KO neurons. Next we questioned whether the GluR2 levels on neuronal membrane surface was reduced and if their trafficking was impaired.

4.5.4.2 Levels of GluR2 subunit on the cell surface

To further investigate the role of CPT1C on surface expression of AMPA receptor at synapses, we performed surface staining of GluR2 and the number of receptors present at the cell surface.

Immunofluorescence assay against the extracellular domain of GluR2 protein was carried through in hippocampal neurons of WT and CPT1C-KO mice at 14DIV.

Intensity fluorescence per cluster and surface area of each cluster was measured using the Image J program. CPT1C-KO had a significantly reduced number of GluR2 along the dendrite (fluorescence intensity/area) and the number of GluR2 receptors per synapse (cluster) was also diminished (Figure 62).

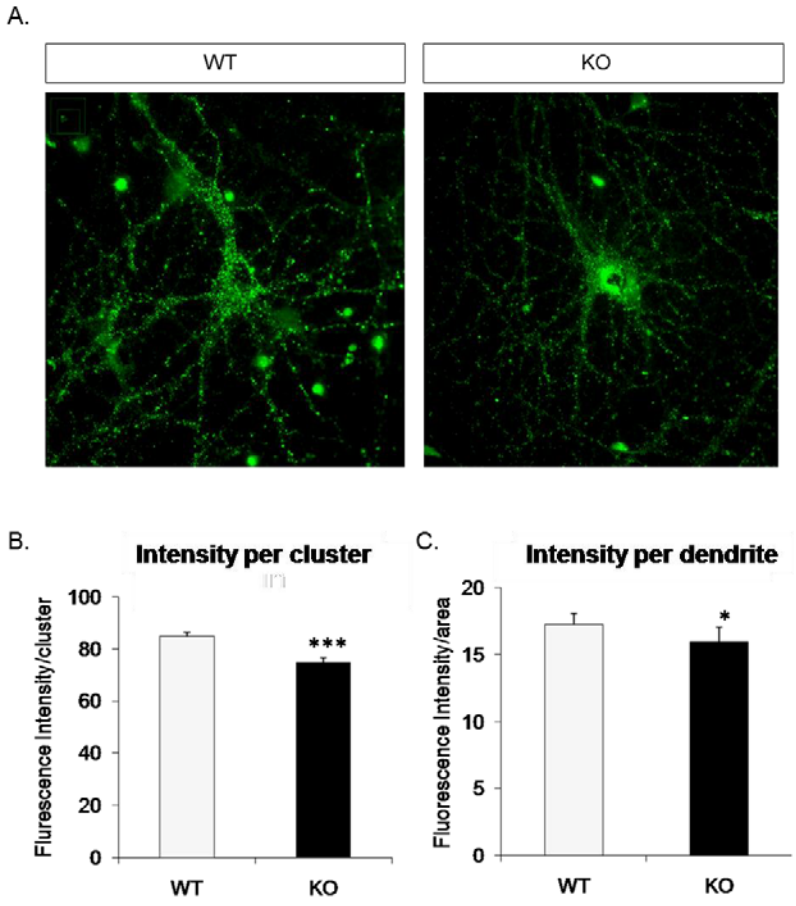

Figure 62: Extracellular GluR2 staining in hippocampal neurons. At 14DIV hippocampal neurons were incubated with extracellular GluR2 antibody. A. Representative image of extracellular GluR2 staining in WT and CPT1C-KO. B. Fluorescence intensity per cluster was measured in more than 100 random dendrites using ImageJ program. C. Fluorescence intensity per area was measured using ImageJ program in random dendrites. (Error bars are S.E.M. *p<0.05; *** p<0.001). n=3 independent experiments. Willcoxon test for non-parametric paired samples was used.

In conclusion these data suggest that CPT1C-KO neurons express lower levels of AMPA receptors at the cell surface than WT neurons.

4.5.4.3 Trafficking of AMPA receptor in hippocampal neurons

Previous results showed that CPT1C deletion produces a decrease in the expression of GluR2 subunit at the cell surface, so next step was to analyze whether CPT1C deficiency was interfered with the AMPA receptor trafficking.

Hippocampal neurons were isolated from WT and CPT1C-KO E17 embryos and subsequently cultivated. At 14 DIV, they were stimulated with 100 μM AMPA for 10 minutes resulting in increased AMPA-receptor internalization.

Trafficking of AMPA receptor was analyzed using the "antibody feeding assay', an immunofluorescence technique (Essmann, C.L. 2008). A specific primary antibody (anti-GluR2) was applied to the cells to label the surface pool of AMPA receptors. Thereafter, the cells were stimulated with AMPA to allow receptor internalization followed by fixation with PFA. AMPA-receptors retained on the cell surface were detected with a green-fluorescent labeled antibody. Following permeabilization, a red-fluorescent labeled antibody was used to target internalized receptor during the experiment. Representative images of each condition are shown in figure 63.

The internalization levels were quantified as percentage of internalized GluR2 versus total GluR2 staining (Figure 63). In control conditions, the basal level of AMPA-receptor internalization was about 40% in both cases, showing no significant differences between the genotypes.

Stimulation with 100 μM AMPA for 10 minutes led to a strong AMPA-receptor internalization detectable as intense red signal (internalized GluR2) and weak green signal (remnant surface receptors). So, cells treated with 100 μM AMPA for 10 minutes showed an increase in the GluR2 receptor internalization in both genotypes being significantly much higher in the CPT1C-KO neurons that in WT ones.

These data are indicative for an impaired trafficking of AMPA receptors in the CPT1C-KO mice, strongly suggesting a role for CPT1C in the regulation of glutamate receptor trafficking.

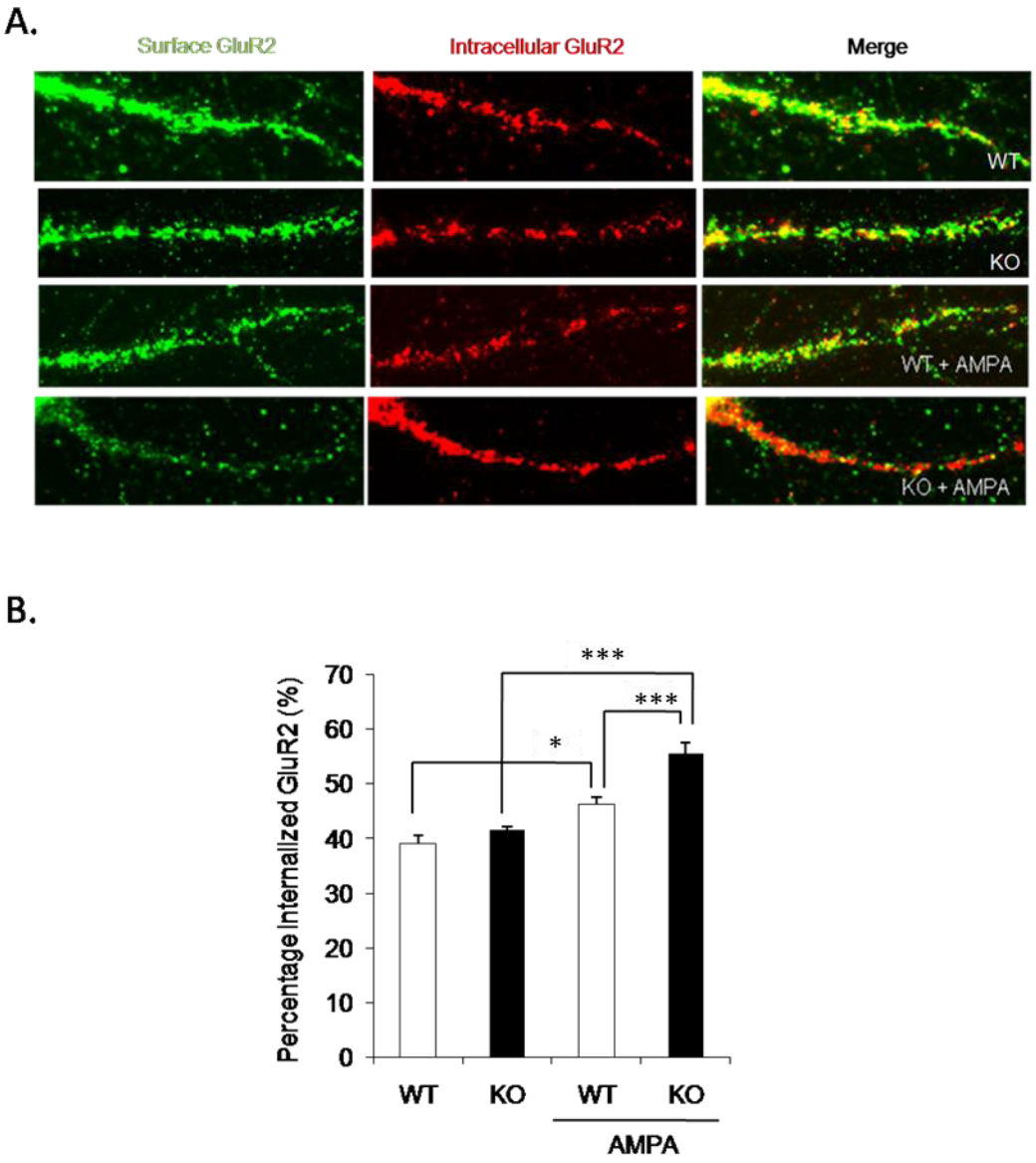

Figure 63: Endocytosis of AMPA receptor under AMPA stimulation were visualized and quantified by the antibody feeding assay. A. Neurons at 15DIV were labeled with primary antibodies (anti-GluR2), stimulated, fixed and incubated first with a secondary antibody (labeled in green), recognizing surface retained receptors. Then a secondary antibody (labeled in red) was applied after permeabilization to detect internalized receptors. B. Quantification of GluR2 internalization based on fluorescence intensities, pictured as the percentage of internalized GluR2 (red) versus total GluR2 (red + green) (Mean ±S.E.M; *p<0.05***p<0.001)

This result demonstrates CPT1C-KO neurons have an alteration in the trafficking of AMPA receptor.

DISCUSSION

CHAPTER 5 : DISCUSSION

CPT1C is an enzyme expressed in the endoplasmic reticulum of neurons located in all the brain regions (Dai, Y. 2007; Sierra, A.Y. 2008), but until now, it has been only reported to participate in the control of energy homeostasis. Therefore, its intriguing cellular location and its unknown function, makes its study attractive.

The present work shows that CPT1C has a completely different function from CPT1A and B, describing the role of CPT1C in an anabolic pathway instead of a catabolic one. We demonstrated that CPT1C regulates the *de novo* synthesis of ceramide in the ER of neurons.

At physiological level, we demonstrate for the first time that CPT1C is involved in spatial learning and motor function. Moreover, we observe that the lack of CPT1C produces an alteration in the maturation of dendritic spines, which is reverted by ceramide treatment. Thus, this is the first time that CPT1C or ceramide synthesis has been directly involved in spine morphogenesis.

5.1 CPT1C HAS A LOW CARNITINE PALMITOYLTRANSFERASE 1 ACTIVITY

Carnitine palmitoyltransferase 1 enzymes play a critical role in fatty acid metabolism. Given the fact that neurons do not use fatty acids for energy obtention, the identification of a third brain specific putative CPT1 gene was exciting and intriguing. Moreover, CPT1C is highly expressed in all the brain areas of mammalian species.

It is known that there is high sequence similarity between CPT1C and the other two isoforms, and the information obtained by the three-dimensional model shows that CPT1C can catalyze the same reaction with the same characteristics as CPT1A and B. So far no group had been able to measure its activity. We were able to measure CPT1C specific activity and our results showed that catalytic activity of CPT1C is very low, 100-fold lower compared to the other isoforms, even so, it has similar affinity for the substrates: palmitoyl-CoA and carnitine than the isoform CPT1A.

The fact that the other groups (Price, N. 2002; Wolfgang, M.J. 2006) did not find CPT1C activity could be due to the fact that they measured CPT1C activity in mitochondria. It was not until 2008, when our group demonstrated that CPT1C was located in the endoplasmic reticulum and not in mitochondria (Sierra, A.Y. 2008). Furthermore, the method that they used to determine CPT1C activity was a radiometric method. Perhaps, this method is not sensitive enough to detect the low CPT1C activity. Our group developed a more sensitive method to determine the catalytic activity of CPT1C enzyme in microsomes (Jauregui, O. 2007). This method is based on the HPLC-MS/MS and produces reliable and accurate measurements of the concentration of palmitoyl-carnitine in biological samples, with a sensitivity limit of 0.48 ng/ml which corresponds to a specific activity of 0.0045 nmols· mg^{-1}·min^{-1} in our test conditions. In the radiometric assay, the sensitivity limit (calculated as the deviation of ten blank points) corresponds to a specific activity of 0.4 nmols· mg^{-1}· min^{-1}. This indicates that our method is 100 times more sensitive than the radiometric one, and it allowed us to measure the low CPT1C activity.

The fact that CPT1C enzyme has low activity could be attributed to several hypotheses, among which:

- One hypothesis is that CPT1C needs to be attached to some cell structural protein to have activity. As we worked with isolated microsomes to measure the enzimatic activity, perhaps, we were eliminating the optimal environment for CPT1C to be active, and therefore, we could not observe its real activity.

- Another hypothesis is that the physiological role of CPT1C is to act as a malonyl-CoA or acyl-CoA sensor rather than being an enzyme. Having this role and under certain conditions, in the absence of malonil-CoA or presence of acyls-CoA such as fasting or other situations of energy depletion, it could change its conformation and by the interaction with other proteins, would activate certain metabolic pathway (discussed below).

All these hypotheses have been considered and our results support the biosynthetic role of CPT1C, but the other hypothesis has not been completely discarded.

5.2 MOLECULAR FUNCTION OF CPT1C ENZYME

5.2.1 CPT1C is involved in the *de novo* synthesis of ceramide

Although the exact biochemical function of CPT1C has not been described in the present study, our data demonstrate that CPT1C regulates ceramide metabolism. We saw a decrease in ceramide levels in all the brain areas analyzed in CPT1C-KO mice with respect to WT mice. In cerebellum and striatum, fasting increased ceramide levels in WT mice but not in CPT1C-KO animals, showing the same levels as in the fed conditions. In contrast, in hippocampus and motor cortex, ceramide levels in WT mice were not affected by fasting, but they were clearly reduced in CPT1C-KO with respect to WT. It has been described in the literature that ceramide levels in fasting or fed conditions are regulated in different ways depending on the analyzed area. These results are in line with our findings in which it seems that different brain areas are regulated in different ways. Moreover, it has been demonstrated that an increase in the ceramide levels in the brain produces cognitive and motor impairment (de la Monte, S.M. 2010). Consequently, the reduction in the ceramide levels observed in CPT1C-KO mice could produce the dysfunction in learning process and motor impairment seen in the CPT1C-KO mice.

One of the most relevant contributions of this Thesis is the confirmation that CPT1C facilitates the *de novo* synthesis of ceramide. We had previously described it in the ARC nucleus of hypothalamus (Gao, S. 2011), and now we demonstrate it in hippocampal cultured neurons. We do not elucidate the molecular mechanism by which CPT1C regulates ceramide levels, but based on our data, we propose two possible hypotheses:

The first hypothesis is that due to the fact that CPT1C is located in the ER, where serine-palmitoyltransferase (SPT) and ceramide synthase (CerS) reside and because CPT1C has very low activity, it is possible that CPT1C interacts physically with other membrane proteins such as SPT or CerS to modulate their activity. Then, under fasting conditions or reduction of malonyl-CoA levels, CPT1C might change its conformation and activate SPT or CerS enzymes and as a consequence, increase the *de novo* synthesis of ceramide (figure 64).

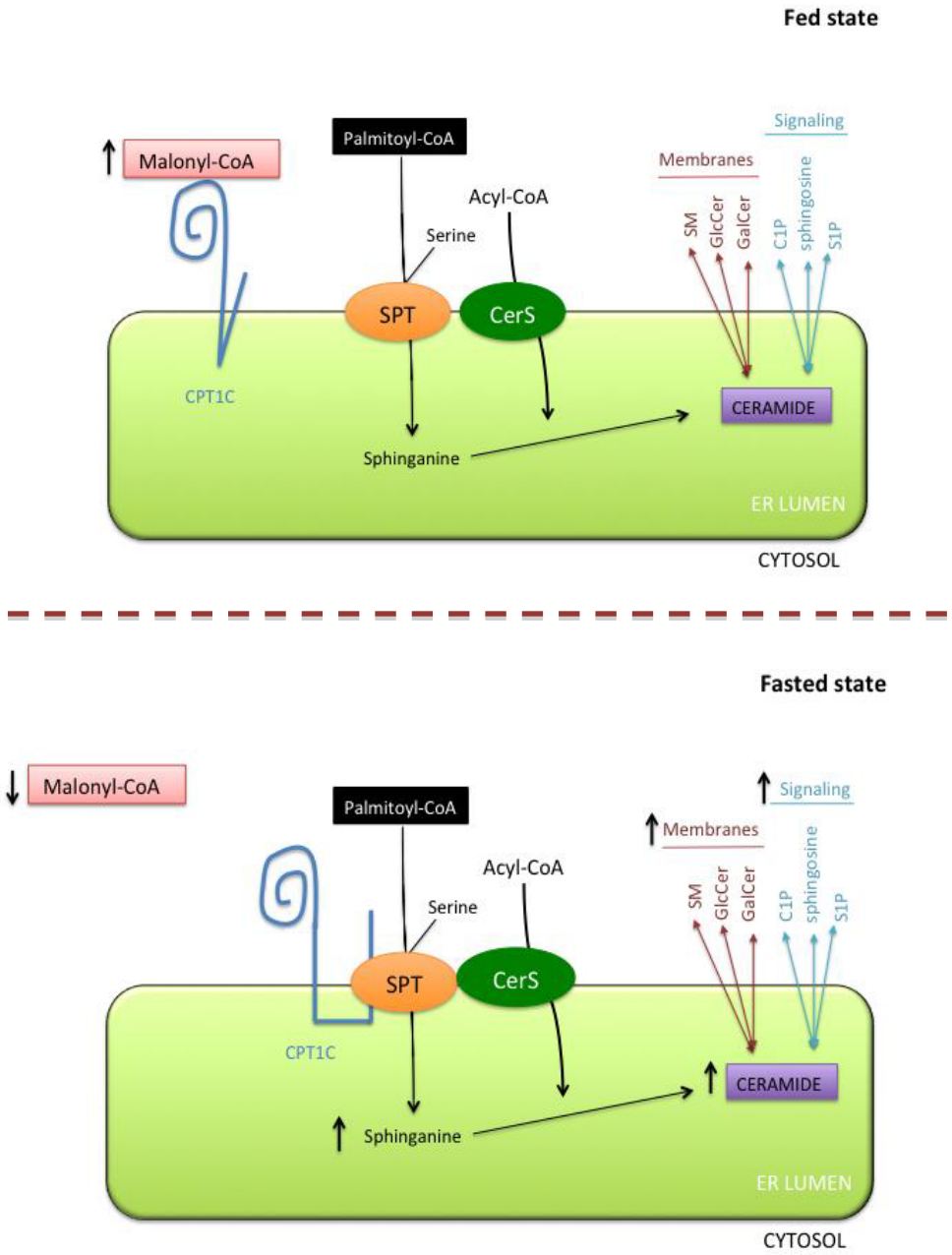

Figure 64: Theoretical function of CPT1C in the *de novo* synthesis of ceramide: CPT1C activates SPT or CerS enzyme. Ceramide synthesis begins with the condensation of palmitoyl-CoA and serine through the action of serine-palmitoyltransferase (SPT), an enzyme located in the ER membrane. The presence of CPT1C could modulate the activity and/or the conformation of SPT or CerS increasing ceramide synthesis in fasting. In fed state, CPT1C is inhibited by malonyl-CoA and SPT and CerS have the normal activity. SM, sphingomyelin; GlcCer, glucosylceramide; GalCer, galactosylceramide; C1P, ceramide 1-phosphate; S1P, sphingosine 1-phosphate; CerS, ceramide synthase.

The second hypothesis is that CPT1C could facilitate the entry of acyl-CoAs to the lumen of ER, preventing them from being used in other metabolic pathways in the cytosol, and providing substrates for the *de novo* synthesis of ceramides. Supporting this hypothesis is the existence of some carnitine-dependent acyl-CoA transporters across ER membrane (Arduini, A. 1994; Abo-Hashema, K.A. 1999; Gooding, J.M. 2004), therefore CPT1C could act as a possible transporter. However, the possibility that CPT1C transports acyls-CoA into the lumen of the ER as a way of increasing ceramide synthesis seems

implausible, due to the fact that SPT and CerS have their catalytic sites facing the cytosol not in the ER lumen, and therefore, *de novo* synthesis of ceramide occurs at the cytosolic face of the ER (figure 65).

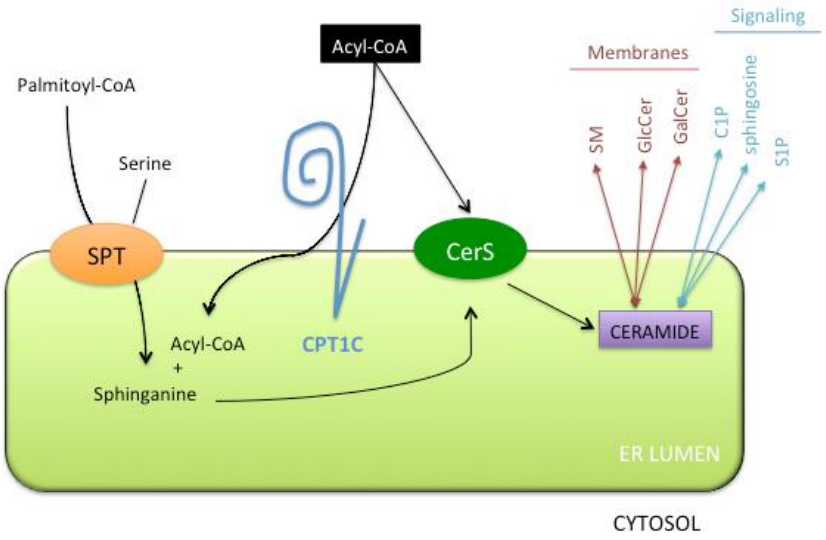

Figure 65: Theoretical function of CPT1C in the *de novo* synthesis of ceramide: CPT1C facilitates the entrance of acyl-CoAs into the lumen of ER, preventing them from being used in other metabolic pathways in the cytosol. SM, sphingomyelin; GlcCer, glucosylceramide; GalCer, galactosylceramide; C1P, ceramide 1-phosphate; S1P, sphingosine 1-phosphate; CerS, ceramide synthase.

5.3 PHYSIOLOGICAL ROLES OF CPT1C ENZYME

5.3.1 CPT1C is involved in food intake and peripheral metabolism

CPT1C is widely expressed throughout the central and peripheral nervous system indicating a broader role in neurometabolism (Wolfgang, M.J. 2006).

It is described in the literature that when CPT1C-KO mice are fed with a standard lab chow, they eat less food than WT animals and they also present lower rates of peripheral fatty acid oxidation after fasting conditions. When they are fed with high fat diet, they are more susceptible to obesity and diabetes than WT mice in contrast, CPT1C over-expression protects the animals from obesity (Wolfgang, M.J. 2006; Dai, Y. 2007; Gao, X.F. 2009). It seems that CPT1C-KO mice miss the capacity to sense the increase in circulating non-esterified fatty acid (NEFA) caused by high fat diet or by fasting, in the hypothalamus (Cnop, M. 2008; Finn, P.F. 2006) and thus fail to send information to peripheral tissues. Our results demonstrated the same results observed in the literature, where peripheral tissues of CPT1C-KO animals do not respond to the central hypothalamic signals. This indicates that CPT1C is an important enzyme in controlling the outflow in neural metabolic information to whole body energy homeostasis. Furthermore, during fasting, malonyl-CoA signal is rapidly communicated to skeletal muscle and liver, where fatty acid β-oxidation and the expression of the genes relevant to this process, are up-regulated and, this signal appears to be transmitted by the sympathetic nervous system (SNS). The facts that CPT1C is located in the PNS and that the lack of CPT1C produces a reduction in the β-oxidation in muscle

and liver, suggest that CPT1C might regulate the response to nutrients in the axis between the CNS and the PNS.

Besides, a correlation cause-effect has been demonstrated between CPT1C activity and the expression of orexigenic or anorexigenic neuropeptides, where hypothalamic over-expression of CPT1C increases food intake in mice (Gao, S. 2011). In this work, we show that CPT1C is involved in the regulation of food intake, although further experiments should be performed to clarify CPT1C participation in the appetite control. However, numerous studies suggest that CPT1A is the main isoform involved in the regulation of food intake. In 2003, Rossetti´s group demonstrated that genetic inhibition of hypothalamic CPT1A resulted in decreased levels of agouti-related protein, neuropeptide Y and anorexia (Obici, S. 2003). Some years later it was demonstrated that two contraposed hormones, leptin and ghrelin, exerted their hypothalamic effects, in part, through the AMPK-ACC-malonyl-CoA-CPT1 pathway (Gao, S. 2007; Lopez, M. 2008). Sabrina Diano´s group reveals that mitochondrial fatty acid oxidation is necessary for ghrelin´s anorexic action (Andrews, Z.B. 2008).

Taking into account that CPT1C has 100 times lower enzymatic activity than CPT1A and does not participate in mitochondrial fatty oxidation because of its ER location, suggests that CPT1C does not participate directly in the appetite control, but it might be involved in sequestering malonyl-CoA. The capacity of CPT1C to bind malonyl-CoA has been previously demonstrated (Wolfgang, M.J. 2006). Thus, we hypothesize that hypothalamic CPT1C binds malonyl-CoA and it reduces the availability of intracellular malonyl-CoA to bind CPT1A. Therefore, the deficiency of CPT1C lets more malonyl-CoA available and, as a result, CPT1A activity decreases and in consequence, food intake is reduced. Clearly, additional rigorous experimentation is needed to validate this hypothesis.

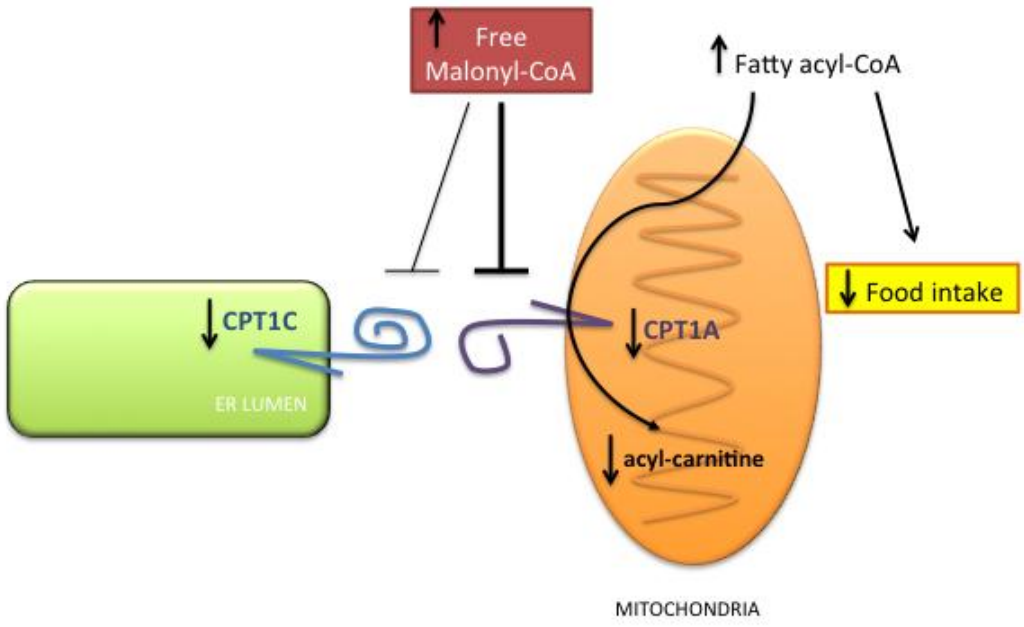

Figure 66: Hypothetical function of CPT1C in food intake. Malonyl-CoA is the product of the acetyl-CoA carboxylase catalyzed carboxylation of acetyl-CoA and serves as the basic chain elongation unit for fatty acid synthase (FAS). Inhibition of CPT1 by malonyl-CoA ensures that fatty acid oxidation and fatty acid synthesis does not occur concomitantly in cell types where both processes coexist. We hypothesize that CPT1C does not participate directly in the appetite control, but it might be involved in sequestering malonyl-CoA. We hypothesize that hypothalamic CPT1C binds malonyl-CoA and it reduces the availability of intracellular malonyl-CoA to bind CPT1A. So, the deficiency of CPT1C provides more malonyl-CoA available and, as a result, CPT1A activity decreases and in consequence, food intake is reduced.

5.3.2 CPT1C-KO mice have motor alterations and learning impairment

Our work shows that CPT1C has others physiological roles apart from the regulation of food intake and energy homeostasis. In addition to homeostatic problems, CPT1C deficient mice present pronounced motor deficits, like de-coordination, unbalance and muscle weakness. Considering that CPT1C-KO mice failed in all motor tests performed, it is suggested that several regions of brain involved in motor skills are affected. The finding of altered ceramide levels in cerebellum, striatum and motor cortex clearly implicates these areas in the motor dysfunction phenotype. Furthermore, the fact that CPT1C is also expressed in peripheral nervous system, defines new locations where CPT1C deficiency can be responsible for motor impairment. Altered acyl-carnitine levels found in cerebellum indicates that it is one of the principal areas implicated in motor dysfunction and probably, in coordination and gait alteration. On the other hand, reduced fatty acid oxidation present in muscles of CPT1C-KO mice, could generate muscle weakness and be the cause of altered bar hang and grip strength tests. Myopathy, hypotony and muscle weakness are typical features of fatty oxidation defects, which manifest predominantly during endurance-type activity or under fasting conditions (van Adel, B.A, 2009).

All these motor deficiencies are probably the cause of the hypoactivity found in CPT1C-KO mice. Nevertheless, we cannot discard hypothalamic contribution in this role. Leptin, ghrelin and other hormones, which are involved in food intake and energy homeostasis, have been described to modulate daily physical activity, and defects in their signaling produce hypo or hyperactivity. As CPT1C-KO mice present hypoactivity not only during the time of food ingest but also in a new environment (exploratory activity), it induces us to think that hypoactivity is consequence of their weakness and de-coordination problems.

In relation to cognition, CPT1C deficient mice also present spatial learning impairment, as seen in the Morris Water Maze tests. We saw a clear delay in the acquisition phase, in this part of the test the mouse had to learn where the platform was hidden due to its spatial orientation. Although they eventually learnt and remembered the location of the platform, they took longer to learn where it was located. It was not until the session number eight where CPT1C-KO mice took the same time as the wild type animals to find the platform. It is important to emphasize that motor deficiencies found in CPT1C-KO mice do not affect swimming velocity or motivation, and that longer acquisition times correspond to learning deficiencies and not to motor impairment.

On the other hand, memory and cognitive flexibility (ability to modify behavior in an increasingly demanding cognitive task) were not altered in CPT1C-KO mice, represented by removal (remember the localization of the platform) and reversal test (forget an old task and learn a new one). These results indicate that CPT1C deficiency affects the process of consolidating new information, but not retention or extinction. This phenotype could be directly related to the impairment in dendritic spine maturation found in CPT1C-KO mice and with the intact spine head area of matures spines found in both genotypes. It is accepted that spine-volume changes regulate new memory acquisition by enlarging and stabilizing smaller spines while the existing-memory persistence depends on changing volumes of larger spines (Kasai, H. 2010). In addition, in human patients and most animal models of mental retardation, dendritic spines tend to be abnormally small and immature.

Spatial impairment found in CPT1C-KO mice suggests that hippocampus is affected, as confirmed by the decrease in the palmitoyl-carnitine levels found in that region. Cognitive flexibility, which is not altered in CPT1C-KO mice, has been associated to the correct function of prefrontal cortex; a region where we did not find altered acyl-carnitine levels.

There are some papers that relate hypothalamus to the tasks of the hippocampus, for example, leptin, a satiety hormone secreted by the white adipose tissue. Its administration induces improvement in

learning and memory performance and provides hippocampal long term potentiation (Harvey, J. 2007). Same role is also played by ghrelin, an orexigenic hormone released from the stomach when it is empty. In the hippocampus, ghrelin is involved in the spine morphology, in the generation of long-term potentiation and locomotion. Ghrelin knockout animals show a smaller number of spine synapses (Carlini, V.P. 2002; Diano, S. 2006). Published data from our group suggest that CPT1C-KO mice do not respond to leptin pathway (Gao, S. 2011), so it could indicate a relationship between hippocampus and hypothalamus and be related to the alteration in dendritic spine morphology, motor and learning impairment in CPT1C-KO mice. Moreover, it has also been demonstrated that high fat diet, which promotes obesity, impairs some forms of hippocampus dependent memory formation, and this process is associated with low ghrelin levels. The adverse effects of high fat diet on learning and memory have been associated with impaired hippocampal synaptic plasticity and neurogenesis, suggesting that hippocampus may be particularly sensitive to changes in dietary energy intake (Lindqvist, A. 2006; Farr, S.A. 2008). These results suggest that the alteration in the metabolic phenotype observed in CPT1C-KO mice could be affecting the hippocampus dependent learning and motor skills.

At the behavioral level, we demonstrate for the first time the involvement of CPT1C in motor function and cognition, which opens the possibility for CPT1C mutations to be the cause of some human motor and cognition disabilities of unknown etiology.

5.3.3 CPT1C is involved in dendritic spine maturation

Dendritic filopodia is thought to serve as the precursor of dendritic spines during neuronal development and neuronal contact formation (Dailey, M.E. 1996; Ziv, N.E. 1996; Dunaevsky, A. 1999; Marrs, G.S. 2001). During development long thin filopodia protrudes are replaced by shorter spines with well-defined heads and short necks forming the mature spines. However, the molecules that regulate filopodia extension and their maturation to spines remain largely unknown.

Our results implicate CPT1C in the dendritic spine maturation: the lack of CPT1C resulted in severely impaired spine development. These hippocampal neurons appeared to have increased filopodia-like protrusions compared to control cells, giving them a ´hairy´ phenotype. In absolute numbers, the increase in filopodia in CPT1C-KO mice corresponds with the decline in mature spine number, without altering the overall density of dendritic protrusions. This indicates that CPT1C is not necessary for the formation of new protrusions; however, it is necessary for the conversion of filopodia into mature spines.

It has been described that some pathologies have one common feature in these developmental conditions, which is a failure to convert filopodia to dendritic spines, leaving the adult dendrites in an immature state. Lots of developmental disorders resulting in abnormal synaptic transmission and serious defects in learning and memory, such as fragile-X mental retardation, Angleman syndrome, etc, have been attributed to defects in spine formation (Marin-Padilla, M. 1972; Hering, H. 2001; Zoghbi, H.Y. 2003).

Thus, alterations in dendritic spine shape are suspected to be morphological manifestations of behavioral changes. Spine formation, stabilization and/or removal are one of the key components during plasticity and serve as a basis for learning and memory. Larger spines produce large synaptic currents and they are persistent and stable (memory) compared to small spines, which are transient. Furthermore, learning involves enlargement of small spine head and their conversion to be large and

stable. As we saw above, CPT1C is involved in the maturation of dendritic spine but not in their formation. Moreover, the head areas results indicate that those were mature spines, they had the same level of maturation as WT neurons. So, these results could explain that CPT1C-KO mice had alterations in learning but not in memory.

Stabilization of hippocampal spines also requires assembly of pre and postsynaptic elements. PSD-95 is necessary to stabilize the spine and it is correlated with spine morphogenesis and maturation (El-Husseini, A.E. 2000) and with the clustering of presynaptic vesicle protein (Okabe, S. 2001). Synapsin 1, a predominant synaptic vesicle protein, is also correlated. Our results showed no difference in the number of PSD-95 or synapsin I cluster between both genotypes, although we expected a decrease in the number of clusters in CPT1C-KO mice because they showed less mature spines than WT mice. However, it is described in the literature that PSD-95 is also expressed in immature neurons before synaptogenesis and determines dendrite outgrowth and branching in immature neurons but it is not completely cleared up (Okabe, S. 2001; Prange, O. 2001). Therefore, it could suggest that most of the cluster-type filopodia containing PSD-95 clusters may represent the transitional stage into mature spines rather than temporal snapshots of mature spines. In addition, it seems that the lack of CPT1C shifted the distribution of dendritic protrusions from mature to more immature filopodia-like spines and, as a result, a reduced number of mature synaptic contacts were apparent. More studies about cluster size should be done to clarify if CPT1C-KO mice have less or the same number of synaptic contact as the WT mice.

Moreover, one of the main biosynthesis pathways related to the cytoplasmatic face of the ER is the synthesis of sphingolipids, which are important constituents of membrane, and in neurons, their synthesis increases during neurite outgrowth (Araki, W. 1997). Sphingolipids composition also determines membrane fluidity and shape, important for chlatin-mediated endocytosis in synaptic vesicle recycling (Marza, E. 2006; Darios, F. 2006; Ben Gedalya, T. 2009). We suggest that CPT1C could regulate the synthesis of ceramide, the precursor of sphingolipids, and the alteration in the ceramide synthesis found in CPT1C-KO mice could be the cause of altered dendritic spine shape.

Our results show that the effect of CPT1C on dendritic spines is mediated by ceramide. Ceramide addition to the cultures media at low concentration reversed the CPT1C-KO phenotype and induced spine maturation. It is believed that ceramide may have biphasic actions, with lower concentrations promoting cell differentiation and with increasing concentrations contributing to cell death (Riboni, L. 1995) and ceramide also plays growth-supportive roles in hippocampal neurons at immature stages of development. Therefore, ceramide regulates the fate of hippocampal neurons, depending on its concentration and on the development stage.

Recent studies demonstrate the importance of ceramide in dendritic spines formation, in learning and memory process and in the synaptic strength. A recent paper describes the presence of a new long-chain acyl-CoA synthetase (ACSL4) isoenzyme that localizes specifically in ER of neurons. Its deficiency increases the percentage of filopodia and reduces the percentage of mature spines. (Meloni, I. 2009). This highlights the importance of fatty-acid metabolism in spinogenesis and indicates that ACSL could provide the substrate necessary for ceramide synthesis in the ER of neurons. Other study that correlates ceramide with the formation of dendritic spines is Hering, H. 2003. The authors report that coupled inhibition of cholesterol and ceramide synthesis causes alterations in the density and morphology of dendritic spines. The mechanism by which ceramides regulate spine maturation is unknown. However, ceramide binds to and regulates the activity of enzymes and signaling proteins such as kinases, phosphatases or membrane receptors (Breslow, D.K. 2010). One example is protein phosphatase 1 (PP1), which is activated by ceramide (Chalfant, C.E. 1999) and has been implicated in the conversion of filopodia into mature spines (Terry-Lorenzo, R.T. 2005). In addition, ceramide is the building block of all cellular sphingolipids, which in addition to cholesterol, are essential components of lipid rafts. All these phenomena are necessary for synapse stability and maturation of dendritic spines.

5.3.4 CPT1C is involved in the stabilization of AMPA receptor at the cell surface of neurons contributing to the regulation of AMPAR trafficking.

Synaptic transmission from excitatory nerve cells in the mammalian brain is largely mediated by AMPA receptors located at the surface of dendritic spines. The abundance of postsynaptic AMPA receptors correlates with the size of the synapse and the dimensions of the dendritic spine head (Matsuzaki, M. 2001). There is a direct link between AMPA receptors and spine formation and growth, although the molecular mechanism that coordinates AMPA receptor delivery and spine morphogenesis are unknown.

In hippocampus, most of AMPA receptors are composed of GluR1-GluR2 or GluR2-GluR3 subunits; GluR2 homomers are rare. GluR1 containing receptors are predominantly situated at synapse and it is inserted into synapses in an activity dependent manner, whereas GluR2 containing receptors cycle continuously between synaptic and non-synaptic pools, thus preserving the total number of AMPA receptor. A role for GluR2 in spine morphogenesis could explain the close correlation between AMPA receptor content of synapsis and the size and shape of dendritic spines. Moreover, lacking of GLuR2 (constitutive trafficking) display reduced synaptic transmission (Mainen, Z.F. 1998; Meng, Y. 2003) and showed major motor impairment and memory and learning abnormalities that preclude behavioral studies (Gerlai, R. 1998; Jia, Z. 1996) GluR2 lacking exhibited robust internalization throughout the dendritic spine in response to AMPA application.

One crucial factor for synaptic plasticity is the number of active AMPA receptor at the cell surface and its trafficking. In accordance with this, our immunofluorescence assay showed that the surface AMPA receptor (GluR2) is less abundant in CPT1C-KO mice although its internalization levels are higher than WT mice. It is likely that CPT1C could participate in the stabilization of AMPA receptor at the cell surface of neurons contributing to the regulation of AMPA-receptor trafficking, perhaps through lipid rafts (discuss below).

Moreover, ceramide can also be generated by the action of a family of sphingomyelin-catabolizing enzymes, the sphingomelinase. There are three classes of sphingomyelinase, which based on their optima pH are categorized as neutral, acidic and alkaline sphingomylinases. Three neutral sphingomyelinases (nSMase) have been identified but is the nSMase2 which is highly enriched in the neurons of hippocampus and it is important for regulating synaptic activities related to memory (Wheeler, D. 2009). Mice administered GW4869 (a specific inhibitor of nSMasa2) did progressively decrease latency to locate the hidden platform with repeated training trial during acquistion tasks, suggesting that they had difficulties in learning to use spatial cues to navigate the pool but is not critical for episodic-like memory required for repeated reversal tasks (Tabatadze, N. 2010). This result is in accorcondance with our results in which the lack of CPT1C produces a reduction in ceramide levels and an impairment in learning task or process.

Based on our data, in which we saw that CPT1C is involved in the dendritic spine maturation through ceramide synthesis, we propose another possible function of CPT1C enzyme. We hypothesize that CPT1C could be regulating the synthesis or the pool of sphingolipids needed for the lipid raft formation. Lipid microdomains rich in sphingolipids and cholesterol, also known as lipid rafts, have been demonstrated and functionally assessed in neurons (Tsui-Pierchala, B.A. 2002). A growing number of signaling receptors, complexes and ionic channels have been proposed as putative lipid raft components that contribute to dendritic morphology and synaptic transmission (Hering, H. 2003). Various glutamate receptors (NMDA and AMPA) and postsynaptic scaffolding proteins including postsynaptic density protein (PSD-95), ionic channels, adhesion proteins and elements of SNARE complex have been reported

to localize to lipid rafts (Hering, H. 2003). Rafts are also involved in membrane trafficking, and also play a role in the endocytosis of proteins from the cell surface and in intracellular sorting (Nichols, B.J. 2001).

The lack of CPT1C could cause a reduction in the ceramide levels producing a disruption of lipid rafts and/or in the bioactive lipids, leading to the instability of surface AMPA receptors, the loss of dendritic spines maturation and motor and cognitive dysfunction.

5.4 CONCLUDING REMARKS AND FUTURE DIRECTIONS

The different approaches proposed in this work were all focused to elucidate the possible role of CPT1C in the neurons, specifically in the synaptic transmission. Its ER location, the low activity found in the enzyme and its role in the synthesis of ceramides suggest that CPT1C might play a different role than the other CPT1 isoforms. The diverse of impairments observed, due to the lack of CPT1C in mice, indicates that CPT1C participates in a general and an important function in neurons.

Results from this work show that CPT1C has other physiological roles apart from the regulation of food intake and energy homeostasis. We demonstrate that the molecular function of CPT1C is the fine-tune regulation of the *de novo* synthesis of ceramide in neurons, which is necessary for spine maturation during brain development. At behavioral level, we demonstrate for the first time the involvement of CPT1C in learning and in motor skills.

Therefore, in the future, more studies should be performed to clarify the role of CPT1C in the ER of neurons. For example, experiments to explain whether CPT1C increases the entry of acyl-CoA into the ER or if it is a simple sensor of malonyl-CoA that activates the proteins involved in the *de novo* synthesis of ceramides. Finally, we should elucidate whether the ceramides synthesized by CPT1C have signaling or structural (such as lipid rafts) function.

Finally, to conclude, we propose the next diagram in which it is described the hypothetical pathway of CPT1C function in the ER of neurons. We suggest that in CPT1C enzyme, by some unknown mechanism, increases *de novo* synthesis of ceramide. Then, maybe through the signaling lipids or by lipid rafts, sphingolipids produce changes in the synaptic transmission: increasing dendritic spine maturation and the anchoring of AMPA receptor at the synaptic plasma membrane. Therefore, the disruption of this pathway produces learning and motor impairment.

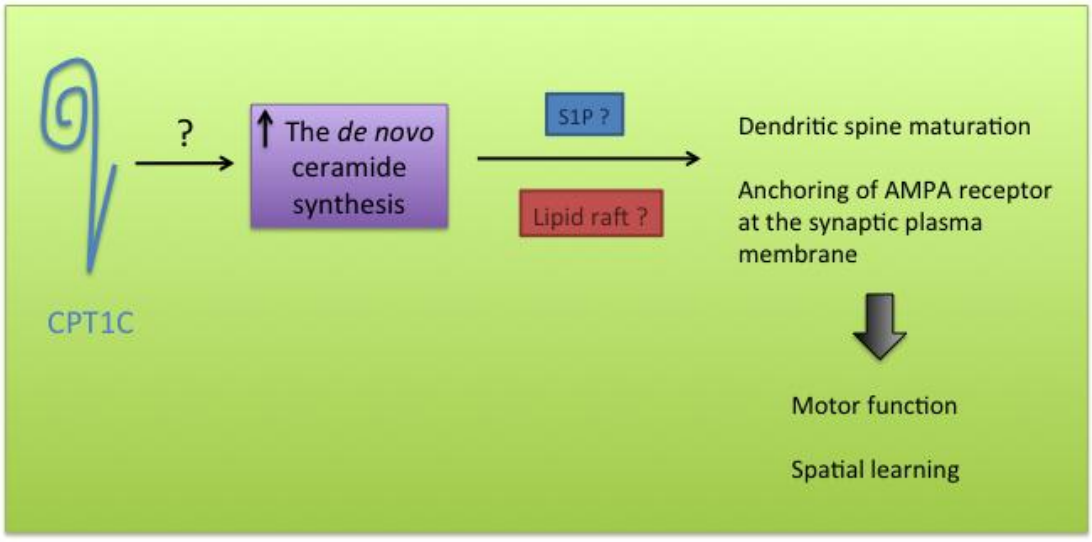

Figure 67: Hypothetical pathway of CPT1C function in the ER of neurons: CPT1C enzyme by some unknown mechanism increases *de novo* synthesis of ceramide. Then, maybe through the signaling lipids or by lipid rafts, sphingolipids produce changes in the synaptic transmission: increasing dendritic spine maturation and the anchoring of AMPA receptor at the synaptic plasma membrane. The the disruption of this pathway produces leaning and motor impairment.

CONCLUSIONS

CHAPTER 6 : CONCLUSIONS

1. CPT1C enzyme has lower carnitine palmitoyltransferase 1 activity than CPT1A, showing a reduced catalytic efficiency for carnitine and palmitoyl-CoA.

2. CPT1C-KO mice show low levels of acyl-carnitines and ceramides with respect to the wild type ones, indicating that CPT1C-KO mice have alterations in the lipid metabolism.

3. CPT1C activates the *de novo* synthesis of ceramide in primary cultures of hippocampal neurons.

4. CPT1C protein expression increases along the mouse development and reaches its expression peak in adulthood.

5. CPT1C is also present in the peripheral nervous system, although its levels appear to be lower than in the brain.

6. The lack of CPT1C does not produce any gross morphological alteration in the structure of cortex, hippocampus or cerebellum.

7. CPT1C deficiency produces impairment in spatial learning without affecting memory or cognitive flexibility.

8. CPT1C-KO mice are hypoactive and exhibit clear deficits in motor function, especially in coordination skills and strength.

9. The lack of CPT1C produces an alteration in the maturation of dendritic spines, increasing filopodia density and reducing mushroom and stubby spines, without altering the protrusion density.

10. Ceramide levels regulated by CPT1C enzyme control dendritic spine maturation in the primary culture of hippocampal neurons.

11. At the post-synaptic level, CPT1C is involved in the trafficking of AMPA receptor due to the fact that CPT1C deficiency reduces the number of AMPA receptors (GluR2 subunit) at the cell surface and increases their internalization.

ABBREVIATIONS

CHAPTER 7 : ABBREVIATIONS

#: reference

%: percentage

ºC: degree celsius

µ: micro

µm: micrometer

µM: micromolar

3-D: three-dimensional

aa: amino acid

AAV: adeno-associated virus

ABP: androgen-binding protein

ACC: acetyl-CoA carboxylase

ACSF: artifitial cerebrospinal fluid

ACSL: acyl-CoA synthetase

AMP: adenosine monophosphate

AMPA:(S)-α-Amino-3-hydroxy-5-methyllisoxazole-4-propionic acid

AMPAR: AMPA receptor

AMPK: AMP-activated protein kinase

ARC: arcuate nuclei

ATP: Adenosine-5´-triphosphate

BD: binding domanin

bp: base pairs

BSA: bovine serum albunin

C16:0: palmitic acid

C18:0: stearic acid

C18:1: oleic acid

C1P: ceramide 1 phosphate

C24:1: nervonic acid

CACT: carnitine-acylcarnitine translocase

CAT or CrAT: carnitine acetyltransferase

CDase: ceramidase

cDNA: complementary DNA

Cer: ceramide

CerK/CK: ceramide kinase

CerS: ceramide synthase

CERT: ceramide transport protein

cm: centimeter

CNS: central nervous system

CoA: coenzyme A

COT or CrOT: carnitine octanoyltransferase

CPT1: carnitine palmitoyltransferase 1

CPT1C-KO: CPT1C knockout mouse

CPT2: carnitine palmitoyltransferase 2

C-terminus: carboxy terminus

DAG: diacylglycerol

DEPC: diethylpyrocarbonate

dhCer: dyhydroceramide

dhSph: dihydrosphingosine

DIV: days in vitro

DMEM: Dulbecco´s modified Eagle´s medium

DMSO: dimethyl sulfoxide

DNA: deoxyribonucleic acid

DNase: deoxyribonuclease

dNTPs: 2´-deoxynucleosides 5´-triphosphate

DTE: dithioeritritol

DTT: dithithreitol

E. Coli: Escherichia coli

E: embryonic day

ECL: electrochemical luminescence

EDTA: ethylenediamine-tetra acetic acid

EGFP: enhanced green fluorescent

ER: endoplasmic reticulum

ESC: embryonic stem cell

EST: expressed sequence tag

FAO: fatty acid oxidation

FAS: fatty acid synthase

FBS: fetal bovine serum

FFA: free fatty acids

g: grams

GalCer: galactosylceramide

GFAP: Glial fibrillary acidic protein

GFP: green fluorescent protein

GlcCer: glucosylceramide

GluR1-4: glutamate receptor subunit

GRIP: glutamate receptor binding protein

GSH: glutathione, reduced form

GSL: glycosphingolipids

h: hour

HEK: human embryonic kidney

HFD: high fat diet

HT or HET: heterocygotous

IC: immunocytochemistry

ICV: intracerebroventricular injection

Ig: immunoglobulin

IMM: inner mitochondrial membrane

IP: intraperitoneal

IPTG: isopropyl-β-D-thiogalactoside

Kbp: kilo base pair

Kcal: kilocalories

K_d: dissociation constant

KDa: Kilo Dalton

K_m: michaelis constant

KO: knock out

m: liter

LB: Luria bertani broth

LC-CoA: long chain fatty acyl-CoA

LCFA: long chain fatty acids

LTD: long term depression

LTP: long term potentiation

m: mili

M: molar

mA: miliamperes

MAGUK: membrane associated guanylate kinase

MAM: mitochondrial associated membranes

MCD: malonyl-CoA decarboxylase

mg: miligrams

min: minute

ml: milliliter

Mm: mus musculus

MOI: multiplicity of infection

MRM: multiple reaction monitoring

mRNA: messenger RNA

MSC: multiple cloning site

MWM: Morris water maze

n: nano

N: number

NE: north-east

NEFA: non-esterified fatty acid

Neo: neomycin

NeuN: neuronal nuclei

NFD: normal fat diet

NMDA: N-methyl-D-aspartic acid

NPY: neuropeptide Y

NR: NMDA receptor subunit

NSF: N-ethylmaleimide sensitive factor

nSMase: sphingomyelinase neutral

o/n: over night

OD: optical density

OMM: outer mitochondrial membrane

P: postnatal

PAT: palmitoyl-acyl transferase

PBS: phosphate buffered saline

PCR: polymerase chain reaction

Pdk4: pyruvate dehydrogenase kinase

PDVF: polyvinylidene fluoride

PDZ: postsynaptic density 95, PSD-85; discs large, Dlg; zonula occludens-1, ZO-1

PFA: paraformaldehyde

pH: potential hydrogenni

PICK: protein interacting with PKC

PKA: protein kinase A

PKC: protein kinase C

PNS: peripheral nervous system

POMC: proopiomelanocortine

PP1: phosphatase 1

PSD: post synaptic density

PSD-95: post synaptic density protein

PUFA: polyunsaturated fatty acid

Rev: reversal

RNA: ribonucleic acid

RNAsas: ribonuclease

RPM: revolution per minute

RT: reverse transcription

RT: room temperature

S.D:standard desviation

S.E.M: standard error of means

S1P: sphingosine 1 phosphate

SAP97: synapse associated protein 97

SC: standard chow

SDS: sodium dodecyl sulfate

sec: second

SK: sphingosine kinase

SM: shpingomyelin

SMasa: sphingomyelinase

SMS: sphingomyelin synthase

SNAP-25: Synaptosomal-associated protein 25

SNARE: soluble NSF attachment protein

SNS: sympathetic nervous system

Sph: sphingosine

SPT: serine palmitoyltransferase

SW: south-west

TAE: Tris (hydroxymethyl) aminomethane acetate salt

TAG: triacylglycerol

TBS: tris buffered saline

TBS-T: tris buffered saline- tween-20

TE: Tris-EDTA

TM: transmembrane domain

U: units

UCP2: uncoupling protein 2

uORF: upstream open reading frame

UTR: untranslated region

UV: ultraviolet

V: voltage

V: volume

VLDL: very low density lipoproteins

w/v: weight/volume

WB: western blot

WT: wild type

RESUMEN

CHAPTER 8 : RESUMEN

8.1 INTRODUCCIÓN

8.1.1 Carnitina palmitoiltransferase 1

Los ácidos grasos de cadena larga pueden ser utilizados para obtener energía a través de la β-oxidación en la mitocondria o pueden ser utilizados para la síntesis de lípidos complejos en el retículo endoplasmático. Los ácidos grasos de cadena larga (LCFA) por si solos, no pueden entrar en la mitocondria para ser β-oxidados, necesitan una serie de reacciones consecutivas de trans-esterificación para poder hacerlo (Figura 1).

El primer componente de este sistema es la carnitina palmitoiltransferasa-1 (CPT1), una proteína transmembrana localizada en la membrana externa de la mitocondria, que cataliza la transesterificación de ácidos grasos desde el CoA a la carnitina. El producto acilcarnitina puede atravesar la membrana interna por medio de una carnitina-acilcarnitina translocasa (CACT). La CPT2, localizada en la matriz de la membrana interna, realiza la reacción reversa, volver a transferir el grupo CoA al ácido graso. Posteriormente, el acil-CoA entra en la β-oxidación donde acabará produciendo acetil-CoA (Zammit, V.A. 2008; Rufer, A.C. 2009).

La reacción catalizada por CPT1 es el sitio clave de regulación, ya que controla el flujo a través de la β-oxidación, y también por su capacidad de ser inhibida por el malonil-CoA, un intermediario en la biosíntesis de ácidos grasos (McGarry, J.D. 1980).

Existen tres isoformas específicas de tejido de CPT1s:

- **CPT1A**: es la isoforma más estudiada. También llamada isoforma hepática y es designada como CPT1L. Se encuentra en hígado, riñón, pulmón, bazo, intestino, ovario y cerebro (McGarry, J.D. 1997).

- **CPT1B**: fue la segunda isoforma en ser descubierta. Está altamente expresada en el músculo esquelético, corazón, tejido adiposo y testículos. Esta isoforma también es llamada CPT1M (Esser, V. 1996; Yamazaki, N. 1995).

- **CPT1C**: descubierta en el 2002 (Price, N. 2002) y se expresa únicamente en cerebro. Presenta una alta homología de secuencia con las otras isoformas, aunque su función es todavía desconocida.

8.1.1.1 CPT1A y B

Las enzimas CPT1A y B han sido ampliamente estudiadas. La similitud entre sus residuos de aminoácidos es alta (62%), pero ambas isoenzimas presentan propiedades cinéticas y reguladoras muy diferentes: CPT1A muestra una mayor afinidad por su sustrato, la carnitina (Km ≈ 30 μM) y por los aciles-CoA de cadena larga (Km para el palmitoil-CoA ≈ 40-150 μM). CPT1B muestra una menor afinidad por su sustrato carnitina (Km ≈ 500 μM), aunque presenta más afinidad por los aciles-CoA de cadena larga. La sensibilidad a su inhibidor fisiológico, el malonil-CoA es de 30 a 100 veces mayor en CPT1B (IC50 0,03 μM) que en CPT1A (Esser, V. 1996; McGarry, J.D. 1997; Zammit, V.A. 2008) (Tabla 1).

CPT1A y B están localizadas en la membrana externa mitocondrial, con dos dominios transmembrana (TM1 y TM2) y el dominio N- y C-terminal hacia el lado citosólico (Fraser, F. 1997; Zammit, V.A. 2008). Se ha demostrado que los residuos del dominio N-terminal de CPT1A (compuesto entre los aminoácidos 1-150), e incluyendo los dos dominios transmembrana y una región *downstream*, contienen la información clave para dirigir la enzima a su localización subcelular (Cohen, I. 1998, Cohen, I. 2001) (figura 2).

Además, los residuos de aminoácidos esenciales para la actividad catalítica o la sensibilidad al malonil-CoA, han sido identificados. Gracias a la predicción de las estructuras tridimensionales a partir de los cristales existentes para la carnitina acetil transferasa (CAT), la carnitina octanoil transferasa (COT) y la carnitina palmitoiltransferasa dos (CPT2) (López-Viñas, E. 2007) (figura 3), se ha visto que el residuo más importante para la catálisis de CPT1A es la His^{473}, ya que cuando ésta está mutada, la actividad catalítica es abolida (Morillas, M. 2001). También se ha demostrado que las mutaciones en Glu^{26} y Lys^{561} disminuyen la sensibilidad al malonil-CoA, lo que confirma que las interacciones entre los dominios N-y C-terminal son esenciales para la unión y la sensibilidad al malonil-CoA (López-Viñas, E. 2007).

8.1.1.1.1 Regulación fisiológica de CPT1A y CPT1B en hígado y músculo

CPT1 está estrechamente regulada por su inhibidor fisiológico, el malonil-CoA, y por lo tanto, CPT1 es el paso de regulación más importante en la oxidación mitocondrial de ácidos grasos (McGarry y Foster, 1980).

En el hígado, el malonil-CoA actúa como un metabolito clave que asegura que la oxidación y la síntesis *de novo* de ácidos grasos no se produzcan de forma simultánea. En el caso de la ingesta de carbohidratos (alta insulina) es la lipogénesis hepática la que está activa, elevando así, la concentración de malonil-CoA, y suprimiendo CPT1. Los nuevos aciles-CoA formados, son dirigidos a productos de esterificación (triglicéridos, TAG) los cuales forman las lipoproteínas de muy baja densidad (VLDL). Los VLDL son transportados al tejido adiposo para su almacenamiento (McGarry, J.D. 1997). Por el contrario, en los estados cetónicos (bajos de insulina) el flujo de carbono a través de la glucolisis disminuye, caen los niveles de malonil-CoA y la síntesis de ácidos grasos se detiene. En este contexto, CPT1 está muy activa y los ácidos grasos libres (AGL) son dirigidos hacia la β-oxidación para la producción acelerada de cuerpos cetónicos (McGarry, J.D. 1980, McGarry, J.D. 1989).

En el caso de tejidos no lipogénicos como el corazón o el músculo esquelético, el malonil-CoA actúa principalmente como un medio de señalización. La concentración de malonil-CoA varía con la alimentación y el ayuno (McGarry, J.D. 1983). Durante el ayuno, los niveles de malonil-CoA disminuyen y la actividad CPT1 aumenta la entrada de los ácidos grasos a la mitocondria, produciendo una tasa de oxidación alta en el músculo. Por otro lado, la inhibición de CPT1 mediada por el aumento de los niveles de malonil-CoA producidos por ejemplo durante la lactancia, disminuyen la tasa de β-oxidación (Wolfgang, M.J. 2006).

8.1.1.1.2 Papel de CPT1 en la regulación de la ingesta de alimentos y la homeostasis energética

Los núcleos hipotalámicos son los responsables de la integración de múltiples señales (información sobre el estado energético a partir de diferentes tejidos periféricos a través de señales neuronales y hormonales, como la insulina, la leptina, la grelina, o adipoquinas) y de responder a los cambios energéticos mediante la modulación de la expresión de neuropéptidos específicos (NPY, AgRP, POMC, CART) para ajustar la ingesta de alimento a la demanda energética del cuerpo (López, M. 2008). La restricción de la ingesta de alimentos permite el aumento de una subpoblación específica de neuronas, e induce la expresión de los neuropéptidos hipotalámicos orexigénicos como el neuropéptido Y (NPY) y

la proteína relacionada con agouti (AgRP), y disminuye la expresión de los neuropéptidos hipotalámicos anorexígenos: proopimelanocortina (POMC) y la transcriptasa relacionada con la cocaína y amfetamina (CART). En conjunto, estos cambios provocan un aumento de la ingesta y una reducción en el gasto energético. Cuando los animales en ayunas vuelven a comer, se produce la respuesta inversa (Hu, Z. 2003).

Las neuronas implicadas en el control del gasto energético deben tener la capacidad de detectar estas condiciones a través de diversas señales. Diferentes hipótesis han sido propuestas sobre la naturaleza de estas señales. Datos recientes apoyan a la hipótesis lipoestática.

Esta hipótesis dice que señales que son proporcionales a la cantidad de grasa del cuerpo modulan la cantidad de comida ingerida en cada comida para así poder mantener el balance energético a través de la acción humoral y a través de la señalización nutricional. Las señales humorales propuestas hasta la fecha incluyen los endocannabinoides, la leptina, la grelina y la insulina, entre otros y los nutrientes señalizadores del estado energético podrían ser la glucosa, los ácidos grasos libres circulantes o los aminoácidos (Horvath, T.L. 2008). Hay evidencias que apoyan cada una de ellas, por ejemplo a nivel de ácidos grasos, se ha visto que la inyección intracerebroventricular (icv) de oleato inhibe la ingesta de alimentos (Obici, S. 2002). Otros ácidos grasos no tuvieron ningún efecto sobre la conducta alimentaria. La fuente fisiológica de ácidos grasos en el cerebro es desconocida, pero puede ser que los ácidos grasos que provienen de la sangre atraviesen la barrera hematoencefálica llegando al núcleo arcuato del hipotálamo (región responsable de la supervisión del estado energético). Por otra parte, los ácidos grasos hipotalámicos pueden ser de origen endógeno o derivados del intercambio de fosfolípidos o de la biosíntesis de novo. Se ha demostrado que las neuronas hipotalámicas poseen la maquinaria metabólica necesaria para la síntesis de ácidos grasos (Gao, S. 2003).

Las neuronas han desarrollado mecanismos para controlar la disponibilidad de energía en el espacio extracelular. Uno de estos mecanismos incluye un aumento en la actividad de AMPK cuando la relación AMP/ATP aumenta, como por ejemplo durante el ayuno. Es un hecho ampliamente aceptado que cambios en el estado de fosforilación de la enzima AMPK, una proteína activada por AMP quinasa, afecta al estado de fosforilación y de actividad de la enzima ACC, lo que afecta al comportamiento alimentario (Kahn, B.B. 2005). Se ha demostrado que la activación de la AMPK en el hipotálamo, utilizando adenovirus que expresan constitutivamente la AMPK activa, es suficiente para aumentar la ingesta de alimentos y el peso corporal, mientras que la represión de la actividad de AMPK hipotálamica, induce a la anorexia. Además, alteraciones en la actividad de AMPK están asociadas con cambios en la expresión de neuropéptidos orexigénicos y anorexigénicos.

Ambas isoformas de ACC (ACC1, citosólica y ACC2, anclada a la membrana mitocondrial externa) se encuentran en las neuronas hipotalámicas y se sabe que son fosforilas por AMPK y por lo tanto son inhibidas. La activación de la AMPK reduce el flujo de sustratos en la vía biosintética de ácidos grasos y por lo tanto reduce los niveles de malonil-CoA, que a su vez, inducen la actividad de CPT1 activando así la entrada de ácidos grasos a la mitocondria para ser β-oxidados (López, M. 2007).

Las señales humorales, como los efectos opuestos de la leptina y la grelina, actúan a través de dianas similares (el eje AMPK hipotalámica/malonyl-CoA/CPT1), pero tienen efectos opuestos (Figura 4) (Wolfgang, M.J. 2007, Gao, X. 2007, López, M. 2008). La leptina administrada centralmente inhibe la actividad de la AMPK hipotálamica, que a su vez disminuye la oxidación, lo que lleva a la supresión de la ingesta de alimentos. La administración central de grelina, disminuye en el hipotálamo la síntesis de novo de ácidos grasos y aumenta la oxidación de ácidos grasos a través de la activación selectiva de la AMPK y de la CPT1, respectivamente (López, M. 2008). Los efectos de la grelina sobre la respiración mitocondrial y la ingesta de alimentos se ha demostrado que está mediada por la UCP2. La oxidación de ácidos grasos promueve la generación de especies reactivas de oxígeno (ROS), que junto con los ácidos

grasos, promueven la transcripción y la actividad de la UCP2. La actividad de la UCP2 neutraliza ROS, lo que permite promover la continua oxidación de ácidos grasos por CPT1 (Horvath, T.L. 2009)

De hecho, modificando la actividad CPT1 hipotalámica también se modifica el comportamiento alimenticio. Se ha observado que la inhibición farmacológica de la CPT1 en el SNC de roedores, resulta en una reducción de la ingesta de alimentos y una pérdida de peso corporal (Obici, S. 2003). En la cita anterior, Rossetti y colegas disminuyen la actividad de CPT1A mediante la administración icv de una ribozima que contiene un plásmido diseñado específicamente para disminuir la expresión de esta enzima o por la administración de inhibidores farmacológicos (TDGA o ST1326). Se encontraron que tanto la inhibición genética o bioquímica de la actividad de CPT1 era suficiente para disminuir la ingesta de alimentos y la producción de glucosa endógena en los tejidos periféricos. Estos resultados indican que los cambios en la tasa de oxidación de lípidos en las neuronas selectivas señala la disponibilidad de nutrientes en el hipotálamo, que a su vez modula la conducta alimentaria.

No se puede descartar que los efectos sobre la conducta alimentaria sean mediados por el malonil-CoA en lugar de ser por la actividad CPT1 en sí misma o por los niveles de aciles-CoA. De hecho, cada vez hay más pruebas que implican al malonil-CoA como un posible mediador en la vía hipotalámica que indica el estado energético y media en el comportamiento alimenticio en roedores, por ejemplo se ha visto que:

1. **Inhibición de la FAS:** La prueba principal se deriva de la observación de que los potentes inhibidores farmacológicos de la FAS (C75 y cerulina) suprimen la ingesta de alimento que causa la pérdida sustancial de peso en la obesidad, así como en los ratones delgados. La reducción de la ingesta de alimentos es rápida (<2h) y dosis-dependiente. La inyección icv de C75 aumenta rápidamente la concentración de malonil-CoA en el hipotálamo. Junto con el aumento de malonil-CoA, las neuronas del núcleo arcuato se activan (Gao, S. 2003), seguido por la bajada en la regulación del péptido orexigénico y una subida en la regulación de los péptidos anorexigénicos en el hipotálamo (Hu, Z. 2003). Sin embargo, la inyección previa de un inhibidor de la ACC, que bloquea la formación de malonil-CoA, previene el aumento de C75 en el hipotálamo inducido por malonil-CoA y evita la supresión de la ingesta de alimentos (Hu, Z. 2003). Estos resultados sugieren que los niveles de malonil-CoA desempeñan un papel fundamental al actuar tanto como un sustrato de la FAS y como un inhibidor de CPT1.

2. **La manipulación genética de MCD**: Otros estudios han demostrado que la sobre-expresión de MCD en el núcleo ventromedial del hipotálamo, aumenta la ingesta de alimentos y el peso corporal (Hu, Z. 2005).

3. **Los niveles fisiológicos de malonil-CoA en el hipotálamo**: También se ha observado que las perturbaciones fisiológicas y nutricionales también alteran notablemente la concentración de malonil-CoA y la ingesta de alimentos. En el estado de ayuno la concentración de malonil-CoA en el hipotálamo es baja (0.1-0.2 µM), mientras que en la realimentación después de un ayuno (que produce saciedad) causa un aumento en los niveles de malonil-CoA, de 1-1.4 µM (Hu, Z. 2003).

Todos estos datos evidencian la participación de la CPT1 hipotalámica en el control de la ingesta y la homeostasis energética.

8.1.1.2 Una nueva isoforma expresada en cerebro: CPT1C

Se ha demostrado que CPT1C se expresa en todas las áreas cerebrales, mientras que CPT1A se limita a algunas áreas y CPT1B no se expresa en él. Al parecer, el origen de CPT1C se debe a una duplicación génica, ya que sólo se ha encontrado en mamíferos (Price, N. 2002).

El análisis de similitud de secuencias de aminoácidos y el porcentaje de identidad entre las distintas isoformas, reveló que CPT1C es más similar a CPT1A que a CPT1B (Tabla 2) (Wolfgang, M.J. 2006). A diferencia de las otras isoformas, CPT1C presenta una cola adicional (de aproximadamente 30 aa) en el extremo C-terminal de la proteína que las otras isoformas no lo contienen (Figura 5).

La estructura 3-D de CPT1C ha sido construida gracias al modelaje por homología con el modelo actual de CPT1A (Tesis de Esther Gratacòs). En el modelo propuesto en la figura 6, se muestra los sitios putativos para la carnitina (blanco) y el palmitoil-CoA (magenta). Gracias a un estudio de alineamiento de secuencia de aminoácidos de las diferentes isoformas de CPT1 de humano, de ratón y de rata, se observó que CPT1C contiene todos los residuos implicados en la unión a la carnitina bien conservados. Los residuos implicados en la unión al palmitoil-CoA, también están conservados en su mayoría, aunque con algunos cambios que no parecen influir en la actividad de esta isoenzima. Es importante tener en cuenta que los residuos que participan en la catálisis de la reacción en CPT1A, también se conservan en la secuencia de CPT1C y que los residuos que forman el canal hidrofóbico donde los substratos se unen, tienen la misma distribución espacial que en el modelo de CPT1A (Figura 7). Los datos obtenidos por este modelo 3-D de CPT1C sugieren que esta enzima sería capaz de catalizar la conversión de palmitoil-CoA en palmitoilcarnitina.

CPT1C se localiza exclusivamente en el sistema nervioso central, con una distribución homogénea en todas las áreas del cerebro (el hipocampo, el cerebelo, la corteza, el hipotálamo, y otros) (Figura 8) (Price, N. 2002). También se conoce que CPT1C se expresa principalmente en el retículo endoplásmico de las neuronas (Figura 10 y 11) (Sierra, A.Y. 2008).

A pesar de que la estructura y los dominios son similares a CPT1A y CPT1B, cuando se realizaron ensayos radiométricos de actividad CPT1, no se le encontró actividad catalítica (Figura 12) (Price, N. 2002, Wolfgang, M.J. 2006). También se ha demostrado que CPT1C tiene la habilidad de unirse al malonil-CoA a una Kd similar a la de CPT1A y se sugiere que CPT1C estaría regulando la disponibilidad de malonil-CoA en el cerebro (Price, N. 2002; Wolfgang, M.J. 2006).

8.1.1.2.1 Función fisiológica de CPT1C

Con el fin de elucidar el papel de esta isoenzima *in vivo*, dos grupos desarrollaron ratones deficientes en CPT1C (CPT1C-KO) (Price, N. 2002, Gao, X.F. 2009). El primer modelo de ratón CPT1C-KO fue desarrollado por el grupo del Dr. Lane y sus colegas (Price, N. 2002), y vieron que los ratones CPT1C-KO no mostraban anomalías ni en el desarrollo o tamaño de los órganos, ni tampoco en la temperatura corporal en comparación con los ratones salvajes. Cuando estos ratones fueron alimentados con una comida estándar de laboratorio (SC), los ratones CPT1C-KO mostraron una reducción en el peso corporal total de aproximadamente el 15% y una disminución en la ingesta de alimentos de un 25% (Figura 13). Cuando a estos ratones se les sometió a una dieta rica en grasa (HFD, 45% grasas), éstos eran más susceptibles a la obesidad, aumentando la ganancia de peso a pesar de reducir la ingesta, (Figura 14), llegando a ser resistentes a la insulina y teniendo un gasto energético periférico menor (Price, N. 2002).

El otro modelo de ratón CPT1C-KO fue desarrollado por el Dr. Wu y sus colegas (Gao, X.F. 2009) y presenta un fenotipo metabólico similar al modelo anterior. Los ratones CPT1C-KO desarrollaron un fenotipo de resistencia a la insulina más grave que los ratones salvajes cuando éstos eran alimentados con una dieta rica en grasa (HFD). Además, en el hígado y en el músculo, la expresión de genes que

promueven la oxidación de ácidos grasos como CPT1A, CPT1B, PdK4, Acadm, estaban notablemente reducidos en los ratones CPT1C-KO (Figura 15). Contrario a los resultados anteriores, la sobre-expresión de CPT1C en el hipotálamo protege a los ratones salvajes de la ganancia de peso cuando estos son alimentados con una dieta rica en grasas (Dai, Y. 2007). En conjunto, estos resultados sugieren que CPT1C es necesaria para la regulación de la homeostasis energética.

Recientemente, nuevos datos demuestran que ratas a las que se le ha sobre-expresado CPT1C en el núcleo arcuato del hipotálamo consumen más alimentos que los ratones control (Gao, S. 2011). Además, la sobre-expresión de CPT1C en el núcleo arcuato del hipotálamo también induce el aumento de los niveles del péptido orexigénico, el neuropéptido Y (NPY). Además, los efectos anteriores son bloqueados cuando a los ratones se les inyecta miriocina (un inhibidor de la síntesis *de novo* de ceramidas). La miriocina bloquea el aumento producido por el efecto de CPT1C en los niveles de ceramida, la ingesta de alimentos y los niveles de NPY. Estos resultados sugieren que los efectos de CPT1C sobre el control de la ingesta de alimentos están mediados por la regulación de la síntesis *de novo* de ceramidas (Figura 16 y 17).

Otro grupo, el del Dr. Wolfgang, ha desarrollado un ratón transgénico que sobreexpresa CPT1C en el cerebro (Reamy, A.A. 2011). Los ratones que sobrexpresan CPT1C presentan un retraso del crecimiento y una profunda microcefalia. Por otra parte, cuando los ratones transgénicos fueron alimentados con una dieta baja en grasas, los ácidos grasos de larga cadena se agotaron en el cerebro. Al contrario, estos cuando los ratones fueron alimentados con una dieta rica en grasas, el metabolismo periférico fue mayor, siendo resistentes a la obesidad. Estos resultados confirman el papel de CPT1C en la homeostasis energética.

Finalmente, otro artículo reciente demuestra que CPT1C se expresa con frecuencia en tumores humanos de pulmón y su función es proteger a las células cancerosas de la muerte inducida por la deprivación de glucosa o hipoxia (Zaugg, L. 2011). Por lo tanto, la deficiencia en CPT1C suprime el crecimiento del tumor, lo que sugiere a CPT1C como una nueva diana potencial en el tratamiento de tumores hipóxicos.

8.1.2 Esfingolípidos

Los esfingolípidos son una clase de lípidos complejos que contienen un ácido graso amida vinculado a una base de cadena larga (esfingoide). Estos compuestos tienen numerosas funciones, como por ejemplo en la vía de regulación de la transducción de señales, etc. (Degroote, S. 2004; Marchesini, N. 2007). Durante la última década, metabolitos como la ceramida (Cer), la esfingosina (SPH), la esfingosina 1-fosfato (S1P) y la ceramida 1-fosfato (C1P) se han convertido en lípidos bioactivos, siendo una nueva clase de lípidos biomoduladores de las funciones celulares, como la proliferación, el crecimiento, la migración, la diferenciación, la senescencia y la apoptosis. (Cuvillier, O. 2001; Hannun, Y.A. 2000; Kolesnick, RN 1998; Kolesnick, R. 2002; Luberto, C. 2002; Malisan, F. 2002; Pettus, B.J. 2002; Spiegel, S. 1998; Spiegel, S. 2003; Tettamanti, G. 1994). También se sugiere que los esfingolípidos son mediadores esenciales del crecimiento celular y de respuesta a estrés en el sistema nervioso.

Las diferentes combinaciones de bases esfingoides de cadena larga, de ácidos grasos y de grupos de la cabeza, permiten la formación de un gran número de esfingolípidos y glucoesfingolípidos.

La esfingosina y sus bases esfingoides relacionadas, tienen un papel en la regulación del citoesqueleto de actina, la endocitosis, el ciclo celular y la apoptosis. (Smith, E.R. 2000). Aún más énfasis se ha puesto en la C1P y en la S1P las cuales se ha visto que median la regulación de la apoptosis (Obeid, LM 1993), la senescencia celular (Venable, M.E. 1995), la supervivencia celular, la migración celular, la inflamación (Hla, T. 2004) y el tráfico vesicular (Chalfant, C.E. 2005; Mitsutake, S. 2004; Hinkovska Galcheva, V. 2005). La ceramida es el núcleo central en el metabolismo de los esfingolípidos y está también

involucrada en la regulación de los procesos de transducción de señales, la detención del ciclo celular inducido y promueve la apoptosis, una forma de muerte celular programada. Además, la ceramida juega un papel importante en la regulación de la autofagia, la diferenciación celular, la supervivencia, la vejez, la diabetes, la resistencia a la insulina, en trastornos neurodegenerativos, en la aterosclerosis y en la respuesta inflamatoria (Hannun, Y.A. 1996).

8.1.2.1 Síntesis de esfingolípidos

Las vías metabólicas de los esfingolípidos simples y complejos se muestran en las figuras 18 y 19. Los metabolitos son interconvertibles, y esto hace complejo determinar el papel específico de cada uno. La ceramida es considerada como la estructura central en el metabolismo de los esfingolípidos y puede ser sintetizada a través de varios pasos, como por ejemplo a través de la vía de síntesis *de novo*. Esta ruta se inicia con la condensación del aminoácido serina y del palmitoil-CoA para formar 3-cetodihidroesfingosina, una reacción catalizada por la serina palmitoiltransferasa (SPT). Esto se reduce a la forma de dihidroesfingosina (esfinganina), la cual es acilada por la dihidroceramida sintasa. Este proceso se inicia en el retículo endoplasmático y continúa en el aparato de Golgi.

Además, la ceramida también puede ser producida por la hidrólisis de la esfingomielina por acción de la esfingomielinasa (SMasa). Hay tres tipos de esfingomielinasas: la ácida, la alcalina y la neutra. La esfingomielinasa ácida se encuentra en los lisosomas, mientras que la esfingomielinasa neutra se encuentra tanto en el citosol como en la membrana plasmática (Hannun, Y.A. 1994). Además, la ceramida puede ser a su vez fosforilada por la ceramida quinasa (CK) para dar la ceramida 1-fosfato (C1P), o puede ser utilizada para la síntesis de esfingomielina o glicoesfingolípidos. Esta vía ofrece un rápido aumento de los niveles de ceramida celulares en respuesta a diversos estímulos. (Goni, F.M. 2002; Levade, T. 1999; Marchesini, N. 2004).

La ceramida también puede ser degradada por ceramidasas (CDase) para dar esfingosina, y algunas ceramidasas pueden catalizar la reacción inversa, y funcionar como una ceramida sintasa, para dar la ceramida-1-fosfato y la esfingosina (SPH) también se puede convertir en esfingosina 1-fosfato (S1P) por una familia de esfingosinas quinasas (SPhKs) (figura 19).

8.1.3 Sinaptogénesis

La sinaptogénesis es un proceso complejo en el que los sitios especializados de comunicación entre neuronas, llamados sinapsis funcionales, se forman. La formación de las sinapsis en los vertebrados se produce durante un período prolongado del desarrollo, empezando en el embrión hasta la vida postnatal temprana, aunque también se produce en el organismo adulto, donde se cree que contribuye a la formación de la memoria y el aprendizaje.

En los vertebrados, la mayoría de las sinapsis son químicas, en las que las señales eléctricas del axón son traducidas en señales químicas en forma de neurotransmisores, los cuales son liberados por vesículas en la terminal presináptica. Los neurotransmisores difunden a través de la hendidura sináptica activando así, canales iónicos situados en la zona post-sináptica y convirtiendo la señal química en un nuevo impulso eléctrico. En el sistema nervioso se encuentran dos categorías de sinapsis, las inhibitorias y las excitatorias. Se les llama así, debido a su efecto sobre el potencial de membrana postsináptico, a su estructura y a su organización molecular.

Las sinapsis glutamatérgicas usan el glutamato como neurotransmisor, el cual actúa sobre los receptores AMPA y NMDA expresados en la región post-sináptica. Las propiedades funcionales de una

sinapsis cambian cuando el organismo se desarrolla, debido a modificaciones pre-sinápticas y post-sinápticas. Durante el desarrollo, la mayoría de las sinapsis poseen inicialmente receptores NMDA funcionales y son carentes de receptores AMPA. La primera actividad de los receptores NMDA es importante para la formación del contacto durante el desarrollo. Una vez que el contacto sináptico se ha establecido, la actividad de los receptores NMDA puede inducir a la inserción de los receptores AMPA, que conducen a la plena sinapsis funcional (Constantine-Paton, M. 1998). Además, como era de esperar, la composición de las subunidades de los receptores AMPA cambia durante la maduración y la actividad, como se describirá más en detalle en la próxima sección.

8.1.3.1 Espinas dendríticas

Las espinas dendríticas fueron observadas por primera vez hace más de 100 años, por el neurocientífico español Santiago Ramón y Cajal (Ramón y Cajal, 1981) utilizando la tinción de Golgi. Él fue el primero en describir a las espinas como pequeñas protuberancias que salían de las proyecciones ramificadas de una neurona, es decir, las dendritas, y sugirió que éstas son en realidad sitios de contacto entre neuronas. Las espinas dendríticas se definen como estructuras pequeñas (0,5-2 µm de longitud) que emergen de las dendritas a través de un cuello delgado, o eje, que termina en una ampliación de bulbo, la cabeza de la espina (el volumen va de 0,01 a 0,8 μm^3), y sirve como sitio de contacto sináptico.

Las espinas se han dividido en varios tipos, como delgadas, gruesas, de copa, o en forma de hongo (Lippman, J. 2005). Sin embargo, la clasificación arbitraria de las espinas en estas cuatro categorías, sobreestima la gran heterogeneidad de la morfología de las espinas dendríticas, ya que son estructuras dinámicas, capaces de cambiar su tamaño, forma y figura en una escala de tiempo de minutos (Dunaevsky et al, 1999; Parnass et al, 2000) (figura 21).

Las espinas dendritas se encuentran en una densidad lineal de 1-10 por µm de longitud dendrítica en neuronas maduras. La mayoría de las sinapsis excitatorias en el cerebro de mamíferos adultos se producen en las espinas, y una espina madura tiene una sola sinapsis la cual se encuentra en la cabeza. Por lo tanto, las espinas dendríticas representan el compartimento principal para la entrada unitaria de postsinápticos excitatorios (Tsay, D. 2004), y se sabe que es el tamaño de la cabeza de la espina la que se correlaciona con la fuerza sináptica (Schikorki, T.1997; Matsuzaki, M. 2001).

El sitio de contacto entre la espina dendrítica y una terminal presináptica está marcado por la densidad postsináptica (PSD), un engrosamiento de la densidad electrónica de la membrana postsináptica. El PSD contiene la maquinaria molecular que vincula la transmisión sináptica a varias cascadas de señalización y los componentes del citoesqueleto. A diferencia del eje dendrítico, la cabeza de la espina dendrítica es altamente enriquecida en filamentos de actina (Fifkova, E. 1982; Matus, A. 1982), los cuales median los cambios en la forma y en la motilidad de la espina dendrítica (Fischer, M. 1998).

8.1.3.1.1 De filopodios a espinas dendríticas

Por definición, los filopodios son delgadas y largas (>2µm) protuberancias, muy móviles y con una esperanza de vida corta. En general, las neuronas jóvenes tienen más filopodios, mientras que las maduras contienen espinas dendríticas maduras (Dailey, M.E. 1996). Aunque hay varias hipótesis, la formación de las espinas dendríticas no está clara, parece ser que los filopodios tienen la función de facilitar el encuentro casual entre un axón y una dendrita. Una vez realizado el contacto, ya sea físico, a través de adhesiones célula-célula o químico, a través de señales, se puede iniciar una sinapsis y proceder a través de las medidas adecuadas a su maduración. Varias familias de moléculas, incluyendo

receptores, proteínas de anclaje, y proteínas reguladoras del citoesqueleto, se ha demostrado que pueden regular el número y la forma de las espinas dendríticas.

8.1.3.2 Receptores AMPA

Los receptores AMPA son una subclase de receptores de glutamato ionotrópicos que median en la transmisión neuronal excitatoria rápida en el sistema nervioso central de mamíferos (SNC). Los otros dos miembros dentro de este grupo incluyen los receptores NMDA, que son cruciales para la inducción de determinadas formas de plasticidad como potenciación a largo plazo (LTP) y depresión a largo plazo (LTD) (Bear, M.F. 1994), y los receptores de kainato que juegan un papel importante en la modulación y la plasticidad de la respuesta sináptica (Lerma, J. 2006).

Los receptores AMPA son hetero-tetrámeros, compuestos por diferentes combinaciones de subunidades: GluR1, GluR2, GluR3 o GluR4, aunque la subunidad más destacada es GluR2 (Nakanishi, S. 1992). Estas subunidades se combinan en diferentes estequiometrias para formar canales iónicos con distintas propiedades funcionales (Hollmann, M. 1994).

Cada subunidad posee un gran dominio N-terminal extracelular, tres dominios transmembrana (TM1, TM3 y TM4), una horquilla que contribuye al poro (M2) y un dominio C-terminal citoplasmático. Las cuatro subunidades tienen dominios extracelulares y transmembrana muy similares, pero difieren en su cola citoplasmática, la cual ofrece la interacción específica con proteínas de anclaje que se unen a proteínas de señalización (por ejemplo, quinasas, fosfatasas), así como a proteínas del citoesqueleto (por ejemplo, la actina) (Collingridge, G.L. 2004; Kim, E. 2004; Nicoll, R.A. 2006). La composición de las subunidades de los receptores AMPA cambia durante el desarrollo y la actividad neuronal.

En el hipocampo, la mayoría de receptores AMPA se componen de subunidades GluR1-GluR2 o GluR2 GluR3-, mientras que GluR4 se produce principalmente durante las primeras etapas después del parto (Wenthold, R.J. 1996; Zhu, J.J. 2000). En la actividad neuronal y la activación de los receptores NMDA, la subunidad GluR1 (GluR1-GluR2 heterómeros) se añade a la superficie sináptica aumentando así la transmisión sináptica. En contraste, los receptores que contienen GluR2, incluyendo GluR2-GluR3 heterómeros y homómeros GluR2, están en ciclo de forma continua entre las zonas sinápticas y no sinápticas, independientemente de la actividad neuronal (Hayashi, Y. 2000). La comprensión de la regulación del tráfico de los receptores AMPA, es de gran importancia en procesos de plasticidad sináptica.

Se han encontrado una gran variedad de moléculas, que asociadas con los receptores AMPA, controlando su tráfico. Además de controlar el tráfico, estas moléculas intracelulares también regulan su estabilidad y sus propiedades electrofisiológicas. Estos procesos parecen estar, en gran medida, controlados a través de las interacciones entre el extremo carboxilo intracelular de los receptores AMPA y las proteínas efectoras (Dong, H. 1997; Xia, J. 1999).

8.2 OBJECTIVOS

Objetivo general*:* Determinar la función molecular y fisiológica de la enzima CPT1C.

Objetivos específicos*:*

1. Identificar la actividad de CPT1C y caracterizar sus parámetros cinéticos en cultivos de células de mamífero.
2. Determinar si CPT1C está involucrada en la síntesis *de novo* de ceramidas.
3. Estudiar la expresión de CPT1C a lo largo del desarrollo del ratón y en el sistema nervioso periférico.

4. Caracterizar la implicación de CPT1C en el comportamiento motor y cognitivo.
5. Estudiar la función de CPT1C en la morfología de las espinas dendríticas y en el tráfico de los receptores AMPA en la membrana plasmática de neuronas de hipocampo.

8.3 RESULTADOS

8.3.1 Caracterización enzimática de la enzima CPT1C

La familia de las enzimas carnitina palmitoiltransferasas (CPT1) se localizan principalmente en la mitocondria, pero la isoforma CPT1C, se localiza en el retículo endoplasmático de las neuronas. Resultados preliminares de nuestro grupo, han demostrado que el palmitoil-CoA es el sustrato utilizado por CPT1C, aunque hasta la fecha no se le ha podido detectar actividad CPT1. Nuestros objetivos en los siguientes experimentos serán: la identificación de la actividad CPT1C y la caracterización de sus parámetros cinéticos.

8.3.1.1 Actividad CPT1C en células de mamífero

La actividad CPT1C fue medida en células PC12 y HEK293T transfectadas con el vector pIRES-CPT1C, que sobre-expresaba CPT1C, o con el vector vacío, pIRES (como control de la actividad endógena) utilizando el reactivo Metafectene para la transfección. Tras 48 horas de transfección y una eficiencia de la misma del 80% (figura 30), las células fueron lisadas y los niveles de palmitoil-carnitina fueron medidos en 20 µg de la fracción microsomal por el método de análisis HPLC-MS/MS. Mediante la técnica de western blot, la sobre-expresión de la enzima fue comprobada. 40 µg de microsomas o mitocondrias aisladas de células transfectadas con pIRES vacío (Ø), pIRES-CPT1C (C) o pIRES-CPT1A (A) (usado como control mitocondrial) fueron corridas en un gel al 10% SDS-acrilamida. Como se muestra en la figura 30, la proteína CPT1C se sobreexpresa en la fracción microsomal de las células transfectadas con pIRES-CPT1C. La misma membrana fue des-hibridada y re-incubada con el anticuerpo anti-CPT1A, utilizado como control de la fracción mitocondrial para determinar la correcta separación entre microsomas y mitocondrias. Como se demuestra en la figura 31, no se observaron niveles de proteína de CPT1A en la fracción microsomal, con lo cual, el protocolo utilizado para el fraccionamiento celular nos permitió observar la actividad específica de CPT1C en microsomas aislados.

Posteriormente, la actividad CPT1 fue medida en 20 µg de microsomas aislados de células PC12 y HEK293 transfectadas con el vector pIRES-CPT1C o pIRES vacío (utilizado como control para medir la actividad CPT1 endógena). Los niveles de palmitoil-carnitina fueron medidos por el método de análisis de HPLC-MS/MS. La Figura 32 muestra que la actividad CPT1 aumenta en valores absolutos un 0.57 o un 0.13 nmoles de palmitoil-carnitina/mg proteína/min en los microsomas de las células PC12 y HEK293 que sobreexpresaban CPT1C. Este resultado nos indica que la enzima CPT1C tiene una actividad CPT1 baja ya que, aunque CPT1C esté sobre-expresada, tan sólo se observa un 50% de aumento en la actividad CPT1 en la fracción celular enriquecida en microsomas. Por el contrario, la sobre-expresión de CPT1A aumenta de 4 -5 veces la actividad CPT1.

8.3.1.2 Caracterización de los parámetros enzimáticos de CPT1C

El siguiente paso fue medir los parámetros cinéticos de CPT1C: Km y Vmax. Para este ensayo, las células fueron transfectadas con el vector pIRES-CPT1C. A las 48h, 20 µg de microsomas aislados de células que sobre-expresaban CPT1C fueron ensayados durante 5 minutos a 30ºC, con concentraciones crecientes

de palmitoil-CoA (de 5 a 300 µM, con la concentración constante de carnitina) y de carnitina (de 20 a 500 µM, con la concentración constante de palmitoil-CoA).

La figura 33A muestra los datos representativos de cuatro experimentos independientes de la actividad CPT1 (nmoles de palmitoil-carnitina / mg de proteína • min). Los parámetros cinéticos de la enzima se calcularon restando a CPT1C la actividad del plásmido vacío (como control de la actividad endógena de microsomas). Los resultados (Figura 33B) muestran que CPT1C tiene una afinidad similar a CPT1A por sus sustratos: la carnitina y el palmitoil-CoA. Los valores de Vmax para el palmitoil-CoA y para la carnitina eran 70 veces inferiores para CPT1C que para CPT1A y en consecuencia, la eficiencia catalítica (Vmax/Km) de CPT1C para el palmitoil-CoA y para la carnitina fueron 320 y 25 veces inferiores a los de CPT1A, respectivamente. Los resultados indican que CPT1C tiene una actividad CPT1 baja y una eficiencia catalítica reducida en comparación con la de CPT1A.

8.3.1.3 La actividad CPT1C en el cerebro

El siguiente paso fue medir la actividad CPT1 en microsomas aislados de corteza cerebral de ratones WT y CPT1C-KO ayunados. 20 µg de microsomas aislados fueron utilizados para el ensayo de actividad CPT1. El producto de la reacción, el palmitoil-carnitina, fue medido por HPLC-MS/MS. Como se muestra en la figura 34, no se observaron diferencias significativas entre ambos genotipos en la actividad CPT1 de microsomas aislados de cerebro.

8.3.1.4 Niveles de aciles-carnitina en diferentes áreas del cerebro

Debido a que no se encontraron diferencias significativas en la actividad CPT1 entre los ratones CPT1C-KO y los WT, realizamos otra aproximación para ver si la enzima CPT1C era activa. Para ello, medimos los niveles de aciles carnitina de cadena larga como por ejemplo: el palmitoil-, estearoil- y oleoil-carnitina en ratones CPT1C-KO y WT en condiciones de alimento y ayuno.

Como se representa en la tabla 3, los ratones CPT1C-KO ayunados muestran una disminución en los niveles de aciles-carnitina en comparación con los ratones WT, siendo estadísticamente significativo en hipocampo, hipotálamo y cerebelo. En animales alimentados no se detectaron diferencias significativas entre los grupos, sugiriendo que la actividad CPT1C es mayor en el estado de ayuno.

Estos resultados indican que la enzima CPT1C no es activa en microsomas aislados pero si lo es *in vivo*. CPT1C es capaz de convertir los aciles-CoA en aciles-carnitina en condiciones que requieren un incremento en la oxidación de ácidos grasos tales como el ayuno.

8.3.1.5 Niveles de ARNm de CPT1A y B en diferentes áreas del cerebro

Con el fin de elucidar si la disminución observada en los niveles de aciles-carnitina en los ratones CPT1C-KO eran producidos por la ausencia de CPT1C o por una alteración en la expresión de las otras isoformas CPT1, los niveles de ARNm de CPT1A y B fueron medidos en diferentes áreas del cerebro de ratones alimentados y ayunados.

Como se muestra en la tabla 4, no se observaron diferencias en la expresión ni de CPT1A ni de CPT1B entre ambos genotipos, ya fuese en condiciones de ayuno o *ad libitum*. Este resultado sugiere que la reducción de aciles-carnitina observada en los ratones CPT1C-KO es debida a una actividad nula de CPT1C, más que una consecuencia indirecta de la regulación a la baja de CPT1A o CPT1B.

8.3.2 Estudio de la implicación de CPT1C en la vía de síntesis de ceramida

Recientemente hemos descrito en la literatura que CPT1C regula la ingesta a través de la modulación de los niveles de ceramida en el hipotálamo (Gao, S. 2011). Por lo tanto, decidimos medir los niveles de ceramidas en diferentes áreas del cerebro como por ejemplo: cerebelo, hipocampo, estriado y corteza motora en ratones CPT1C-KO y WT, alimentados y ayunados.

Los resultados demuestran que los ratones CPT1C-KO tienen una reducción en los niveles de ceramidas en todas las regiones del cerebro analizadas respecto a los WT (figura 35). En cerebelo y estriado, los niveles de ceramidas en ayuno aumentaron en los ratones WT, pero no en los ratones CPT1C-KO, lo que resultó en una gran diferencia en la concentración de ceramida entre los genotipos durante el ayuno. Por el contrario, en el hipocampo y corteza motora, los niveles de ceramidas en ratones WT no fueron modificados por el ayuno, pero si se redujeron en los ratones CPT1C-KO respecto a los WT.

En resumen, los ratones CPT1C-KO tienen una disminución en los niveles de ceramidas en ayunas en comparación con los del WT, principalmente en las ceramidas de cadena larga (C16:0 C18:0 y C18:1) pero no en los de cadena muy larga (C24:1). Este resultado sugiere que CPT1C debe estar modulando los niveles de ceramidas de cadena larga en el cerebro.

8.3.2.1 Participación de CPT1C en la síntesis de novo de la ceramida

Los datos anteriores sugieren que CPT1C participa en la síntesis de ceramidas, pero éstas pueden ser producidas por dos mecanismos diferentes: en primer lugar las ceramidas pueden generarse a través de la vía *de novo* o en segundo lugar, por la acción de las esfingomielinasas (SMases), que hidrolizan la esfingomielina (SM), para dar ceramida y fosforilcolina.

Teniendo en cuenta que CPT1C se encuentra localizada en el retículo endoplasmático y es allí donde la síntesis *de novo* de ceramida es realizada, nos pareció interesante verificar si CPT1C estaba regulando esta vía.

Para comprobar esta hipótesis, sobre-expresamos CPT1C en neuronas de hipocampo con virus adenoasociados (AAV1-CPT1C) y mediante la técnica de Western blot se comprobó la sobre-expresión de CPT1C. Como se muestra en la figura 36, los niveles de proteína de CPT1C fueron cuatro veces más elevados en las células transducidas con los virus AAV1-CPT1C que en las células control (AAV1-GFP).

Después de comprobar que la sobreexpresión con los virus funcionaba, el siguiente paso fue transducir neuronas de hipocampo en 7DIV con AAV1-CPT1C y AAV1-GFP. Las células en 14DIV fueron lisadas y los niveles de ceramidas fueron medidos por LC-ESI-MS/MS System (API3000 PE Sciex). Los niveles de ceramidas fueron normalizados mediante el control de células transducidas con AAV1-GFP, dándole el valor del 100%. Como se observa en la figura 37, la sobre-expresión de CPT1C provoca un aumento del doble en los niveles de ceramidas de casi todos los tipos de ceramidas analizados en comparación con las células control.

Posteriormente, para verificar que este incremento en los niveles de ceramidas eran producidos a través de la síntesis *de novo*, las células fueron transducidas con los virus AAV1-CPT1C o AAV1-GFP en neuronas en 7DIV. En la 14DIV fueron tratadas con miriocina (inhibidor específico de la serina-palmitoil transferasa, la primera enzima en la síntesis *de novo* de ceramidas) a 10 µM durante 8 horas. Tras la incubación, las células fueron recogidas y las ceramidas fueron extraídas.

En la figura 38 se representa el porcentaje de los niveles de ceramida, en las células transducidas con AAV1-CPT1C respecto a las células control (AAV1-GFP), con o sin tratamiento con miriocina. En el gráfico se muestra que el aumento en los niveles de ceramidas inducidos por la sobre-expresión de CPT1C,

fueron bloqueados por el efecto de la miriocina, lo que sugiere que CPT1C regula o facilita la síntesis *de novo* de ceramidas.

8.3.3 Expresión de CPT1C

CPT1C se expresa en el SNC, por lo que en esta sección nos planteamos dos preguntas, la primera fue si esta enzima se expresaba únicamente en la fase adulta del ratón o por el contrario, su expresión aumentaba durante el desarrollo del ratón. La segunda pregunta era si CPT1C podría estar localizada en el sistema nervioso periférico.

8.3.3.1 Expresión de CPT1C a lo largo del desarrollo del ratón

Los niveles de ARNm y de expresión proteica de CPT1C fueron medidos en ratones de diferentes edades por PCR a tiempo real y por Western Blot. En la figura 39A están representados los niveles de ARNm de CPT1C y se muestra un aumento en la expresión de CPT1C a lo largo del desarrollo del ratón, siendo esta más abundante en la fase adulta. El mismo resultado se observó en los niveles de proteína (Figura 39B). Por lo tanto, la proteína CPT1C se expresa a lo largo del desarrollo del ratón alcanzando el pico máximo de expresión a la edad adulta.

8.3.3.2 Expresión de CPT1C en el sistema nervioso periférico (SNP)

El siguiente objetivo era determinar si CPT1C se expresaba en el sistema nervioso periférico (SNP), además de en cerebro.

Para ello se utilizaron dos tejidos periféricos diferentes: el asta ventral de la médula espinal (compuesto principalmente por neuronas motoras) y los ganglios sensoriales (principalmente formados por neuronas sensoriales), ambas muestras fueron proporcionadas por el Dr. Xavier Navarro de la Universidad Autónoma de Barcelona.

Los niveles de expresión de la proteína CPT1C fueron analizados por la técnica de Western blot. Como se muestra en la figura 40, CPT1C se expresa en ambas regiones, tanto en el ganglio sensorial como en el asta ventral de la médula espinal, lo que indica que CPT1C se expresa en el sistema nervioso periférico, aunque a niveles más bajos que en cerebro. Además, parece que CPT1C se expresa en mayor cantidad en las neuronas motoras que en las neuronas sensoriales.

8.3.4 Caracterización del fenotipo motor y cognitivo de los ratones CPT1C-KO

La mayoría de los grupos que estudian CPT1C están interesados en el papel de CPT1C en el hipotálamo, donde su función es la de regular la ingesta de alimento y la homeostasis energética. Nuestro grupo estaba interesado en conocer el papel de CPT1C en otras regiones del cerebro además de en el hipotálamo, por esta razón, una batería de pruebas conductuales fueron realizadas en ratones WT y CPT1C-KO.

8.3.4.1 Estudio metabólico: ingesta de alimento y metabolismo periférico

El primer paso fue comprobar que los ratones CPT1C-KO que habíamos desarrollado, tuviesen el mismo

fenotipo metabólico que los descritos en la literatura. Para ello, varios parámetros como la ingesta, el peso y la temperatura corporal fueron medidos.

Tal y como muestra en la tabla 5, los ratones CPT1C-KO comen un 10% menos que los animales WT a pesar de que tienen el mismo peso corporal a la edad adulta. Este resultado sugiere que los ratones CPT1C-KO tienen alterada la regulación de la homeostasis energética ya que pesan igual pero comen menos.

Debido a que no se observaron diferencias en el peso corporal entre los genotipos a la edad adulta, se decidió mirar el peso corporal de los ratones a lo largo de su desarrollo postnatal, desde la primera semana hasta la semana 16. Como se muestra en la figura 41, no se observaron diferencias entre los genotipos en el peso corporal durante el desarrollo postnatal. Es importante destacar que nuestro modelo de ratón CPT1C-KO muestra un fenotipo metabólico similar al descrito en la literatura (Wolfgang, M.J. 2006; Gao, X.F. 2009), confirmando así, el papel de CPT1C en la ingesta de alimentos y en la regulación de la homeostasis energética.

Posteriormente se decidió analizar si CPT1C estaba regulando el metabolismo de los tejidos periféricos. Para ello se midió la actividad CPT1 en muestras de hígado y músculo de animales CPT1C-KO y WT ayunados. Se observó que los ratones CPT1C-KO tenían disminuida la actividad CPT1 en el músculo y en el hígado en un 20% y 40% respecto a los ratones WT (figura 42). Para ver si la disminución en la oxidación periférica observada en el experimento anterior, era debida a una baja regulación de la expresión de las isoformas CPT1A y CPT1B, los niveles de expresión de ARNm de los genes CPT1A y B y del gen pdk4 (utilizado como control de la β-oxidación de ácidos grasos) fueron medidos. Como se muestra en la figura 43, la expresión de ARNm de los genes CPT1A, CPT1B y pdk4 estaba reducida notablemente en los ratones CPT1C-KO en condiciones de ayuno. Este resultado indica que la oxidación periférica de ácidos grasos en ratones CPT1C-KO no responde a las señales centrales producidas por el hipotálamo.

8.3.4.2 Histología

Con el propósito de ver si la deficiencia en CPT1C en el cerebro producía alteraciones en la estructura morfológica de algunas áreas cerebrales importantes para los posteriores estudios de conducta, se realizó un examen histológico de las regiones del cerebelo, hipocampo y corteza cerebral.

Los ratones CPT1C-KO no presentaron ninguna alteración en la morfología de ninguna de las estructuras estudiadas (Figura 44).

8.3.4.3 Estudios de comportamiento en ratones CPT1C-KO

CPT1C se expresa en todas las regiones del cerebro, no sólo en el hipotálamo, por lo tanto decidimos hacer una batería de pruebas conductuales para ver el posible papel de CPT1C en otras áreas cerebrales.

8.3.4.3.1 Prueba del SHIRPA

La primera prueba fue el test de SHIRPA. Consiste en un protocolo semi-cuantitativo con pruebas de rutina para identificar y caracterizar alteraciones en el fenotipo del ratón.

No se observaron diferencias significativas entre los genotipos en todas las pruebas realizadas, excepto la que reveló que los ratones CPT1C-KO presentaban hipoactividad y una reducida respuesta de escape en la prueba de escape por contacto (Tabla 7).

A consecuencia de las alteraciones motoras detectadas en los ratones CPT1C-KO en la prueba de SHIRPA, se propuso realizar una serie de pruebas motoras específicas para medir la actividad, la fuerza o

la coordinación motora de estos ratones.

8.3.4.3.2 Pruebas motoras

Posteriormente, se realizaron una serie de pruebas motoras para ver si los ratones CPT1C-KO tenían afectaciones motoras.

La primera prueba fue el test de actimetría. Esta prueba consistía en medir la actividad motora circadiana del ratón. Los ratones CPT1C-KO mostraron una actividad locomotora muy reducida durante todo el período circadiano (24h), siendo la diferencia más relevante durante la actividad espontánea en el período de oscuridad, cuando el animal suele ser más activo (figura 45). Por otra parte, esta hipoactividad también se vio afectada durante las primeras dos horas de estancia en la jaula, esta actividad se llama "actividad exploratoria" y los animales la suelen tener aumentada debido a que quieren reconocer el nuevo lugar. En resumen, la actividad locomotora total en los ratones CPT1C-KO estaba reducida en un 70% (WT: 51,6 ± 6,4 $x10^3$; KO: 35,9 ± 2,1 $x10^3$, $p < 0,05$).

El siguiente paso fue medir la coordinación motora. Para ello se llevaron a cabo dos pruebas: la de andar sobre la rueda (*rotarod*) y la de medir la distancia entre las huellas de las patas. La prueba de andar sobre la rueda consiste en medir la latencia (tiempo) de permanencia sobre la rueda a velocidades que van desde 4 a 34 rpm. Es una medida de equilibrio, coordinación motora y condición física. Los resultados de esta prueba mostraron que no había diferencias significativas entre los ratones CPT1C-KO y WT cuando la prueba se realizaba a velocidades bajas. Sin embargo, a velocidades más altas, los ratones CPT1C-KO tuvieron latencias significativamente menores que los WT (Figura 46). Por otra parte, cuando los ratones fueron sometidos a la prueba de la rueda de aceleración, donde se aumentó la velocidad de rotación de 4 a 40 rpm durante una única sesión de 1 minuto, el rendimiento de los ratones CPT1C-KO fue menor que la de los ratones WT, corroborando así la disfunción en la coordinación motora observada en la prueba del rotarod (Figura 47). La siguiente prueba fue medir la distancia entre las huellas de los animales, examinando así el patrón de la marcha. Los ratones CPT1C-KO mostraron una reducción significativa en comparación con los ratones WT en la longitud de la zancada (distancia entre cada paso) en una distancia máxima de 20 cm (figura 48). Los resultados observados revelaron que los ratones CPT1C-KO tenían alterada la coordinación motora, ya que mostraban una disminución en la distancia entre las huellas y una menor latencia de caída en la prueba de la rueda en comparación con los ratones WT.

La fuerza muscular del ratón fue medida a través de la fuerza de agarre de las patas delanteras y a través de la prueba de colgarse de la barra. Tras medir la fuerza de agarre de las patas delanteras, los ratones CPT1C-KO mostraron una reducción en la fuerza de agarre en comparación con los controles (figura 49). En la prueba de colgarse de la barra, el ratón se tenía que agarrar a ella con las patas delanteras y la latencia de caída y la latencia de usar las patas traseras para subir a la barra fueron medidas con un tiempo máximo de 60 segundos (s). La tabla 7 muestra diferencias significativas entre los genotipos. La latencia de caída fue mayor en los ratones CPT1C-KO en comparación con los WT, 41,83 y 60 segundos, respectivamente. Además el 66,7% de los ratones CPT1C-KO se cayeron durante la prueba mientras que ninguno de los ratones WT lo hizo. Por otra parte, el 100% de los ratones WT utilizaron sus patas traseras para subir a la barra, mientras que sólo el 66,7% de los ratones CPT1C-KO lo hicieron, y además, los que fueron capaces de hacerlo, tardaron mucho más tiempo que los ratones WT, 42,58 segundos en lugar de 6,33 segundos.

En su conjunto todos estos resultados demuestran que los ratones CPT1C-KO son hipoactivos y muestran claras deficiencias en la función motora, especialmente en las habilidades de coordinación y fuerza.

Posteriormente, analizamos si las alteraciones observadas en la reducción de la ingesta de alimentos en

los ratones CPT1C-KO eran debidas a una alteración en la homeostasis energética o si era un problema motor para conseguir la comida en la jaula. Para ello, el alimento fue colocado en el interior de la jaula y el consumo de comida fue medido durante 4 días. Como se muestra en la figura 50, los ratones CPT1C-KO consumieron significativamente menos comida que los ratones WT. Este resultado sugiere que los ratones CPT1C-KO tienen alteraciones en la ingesta de alimentos, las cuales no son causadas por la disfunción motora sino, por alteraciones en la señalización hipotalámica.

8.3.4.3.3 Prueba de memoria y aprendizaje: prueba del laberinto acuático de Morris

La memoria y el aprendizaje de los ratones CPT1C-KO fueron evaluados mediante la prueba del laberinto acuático de Morris (MWM), test dependiente del hipocampo. El laberinto de agua consta de una piscina circular, en la que los ratones tienen que encontrar una plataforma escondida en un tiempo máximo de 60s. Para ello los ratones son ayudados de unas señales colocadas alrededor de la piscina para que se puedan orientar durante la búsqueda.

Durante la primera parte del laberinto acuático de Morris, los ratones tenían que aprender a nadar. Posteriormente, en la prueba de capacitación, los ratones tenían que aprender que debían subir a la plataforma para poder salir de ella.

Posteriormente, los ratones procedieron con la prueba de adquisición. Esta prueba consiste en medir el tiempo que el ratón tarda en encontrar la plataforma a lo largo de 10 sesiones (días). En esta parte de la prueba, la plataforma se localiza al noroeste (NE) de la piscina y el animal debe aprender a utilizar las señales distales de navegación para trazar una ruta directa a la plataforma. Los ratones CPT1C-KO mostraron latencias superiores en aprender donde estaba localizada la plataforma, mostrando una curva de aprendizaje significativamente diferente a la de los ratones WT, lo que indica que los ratones CPT1C-KO tienen alterado el aprendizaje espacial (Figura 51A, B).

Debido a que los ratones CPT1C-KO tenían disminuidas las habilidades motoras y de coordinación, se comprobó si las alteraciones en el aprendizaje en los ratones CPT1C-KO eran consecuencia de las alteraciones motoras. Para ello, la velocidad de nado y la flotación fueron medidas. Como se observa en la figura 52, no hay diferencias entre los grupos ni en la velocidad de nado ni en la flotación, lo que sugiere que los ratones CPT1C-KO tenían alteraciones en el aprendizaje, las cuales no estaban asociadas con la discapacidad motora.

La siguiente parte de la prueba fue la sesión con pistas, donde el objetivo era encontrar una plataforma visible que contenía una bandera negra en la parte superior. Esta prueba se repitió durante dos días. La latencia de escape de los ratones CPT1C-KO fue similar a la de los ratones WT (Figura 53) lo que indica que los ratones CPT1C-KO tienen las mismas habilidades básicas ((la vista intacta, la capacidad motora (natación) y la misma motivación (escapar del agua)) que los ratones WT.

Para evaluar la memoria visual-espacial, se realizó la prueba de la eliminación. En esta prueba, la plataforma fue retirada de la piscina y se midió el tiempo empleado en el cuadrante donde solía estar localizada la plataforma. Como se observa en la figura 54, no hubo diferencias significativas entre los grupos en referencia a la preferencia por el cuadrante, lo que indica que una vez la posición de la plataforma fue aprendida, se retuvo igual en los ratones CPT1C-KO que en los ratones WT. Este resultado sugiere que el déficit de CPT1C se limita a la fase de aprendizaje.

La memoria y el aprendizaje también se midieron en la prueba de inversión *(reversal)*, donde la plataforma se colocó en el lado opuesto de la piscina. Los animales tenían que aprender una nueva localización y olvidar la anterior (flexibilidad cognitiva). Como se observa figura 55 no se detectaron diferencias significativas entre los genotipos en el porcentaje de tiempo dedicado a la búsqueda de la plataforma en el antiguo cuadrante (NE). Sin embargo, cuando se midió el tiempo empleado en la búsqueda de la nueva localización de la plataforma (SW), los ratones CPT1C-KO pasaron mucho menos

tiempo en el nuevo cuadrante (SW), por lo tanto refuerza el concepto de que los ratones CPT1C-KO tienen alterado el aprendizaje dependiente del hipocampo.

En su conjunto, todos estos resultados demuestran que la deficiencia en CPT1C afecta al aprendizaje espacial sin afectar a la memoria o la flexibilidad cognitiva.

8.3.5 Estudio de la función de CPT1C en neuronas del hipocampo

8.3.5.1 CPT1C está localizada en el RE de las espinas dendríticas

Con el fin de determinar la localización exacta de la proteína CPT1C en neuronas de hipocampo, se realizaron estudios de inmunofluorescencia en secciones de cerebro. Las secciones de hipocampo fueron incubadas con anti-CPT1C y anti-GFAP (proteína fibrilar glial, un marcador de astrocitos). Como se observa en la figura 56, CPT1C (en verde) se expresa en las neuronas piramidales del hipocampo.

El siguiente experimento fue el análisis de la localización de CPT1C en las neuronas de hipocampo. Para ello se transfectaron cultivos neuronales de hipocampo con el plásmido CPT1C-EGFP, un plásmido que codifica para la proteína CPT1C fusionada a la región N-terminal de EGFP. Como muestra la figura 57A, CPT1C se encuentra a lo largo de la neurona, tanto en el cuerpo neuronal como en las dendritas. Por último quisimos confirmar la localización subcelular de CPT1C en el RE y para ello transfectamos las neuronas con el plásmido pDS-ER-RED el cual tiñe el RE de rojo y CPT1C fue detectada con anti-CPT1C (verde). Tal y como muestra la figura 57B, CPT1C se encuentra en el RE de las neuronas de hipocampo.

8.3.5.2 Densidad y morfología de las espinas dendríticas.

La morfología de las espinas dendríticas y la formación de sinapsis son muy importantes en los procesos de memoria y aprendizaje. Tal y como se observó en el experimento anterior, donde se vio que los ratones CPT1C-KO tenían alterado el aprendizaje, se decidió estudiar la densidad y la morfología de las protusiones (espinas dendríticas) en neuronas de hipocampo.

Para visualizar las protusiones (espinas dendríticas), neuronas hipocampales de ratones CPT1C-KO y WT fueron transfectadas a los 13 días in vitro (DIV) con la proteína verde fluorescente (EGFP). Posteriormente, las células a la 15DIV fueron fijadas y las protuberancias dendríticas fueron analizadas. Tal y como se describe en la literatura, la maduración de las espinas dendríticas en los cultivos primarios de neuronas de hipocampo se produce en la 14DIV en función de la densidad celular del cultivo. Es en ese momento, en el que la morfología de las espinas dendríticas se caracteriza por una disminución en su longitud y por la formación de espinas en forma de hongo (Ethell y Yamaguchi, 1999).

Como se muestra en la figura 58, la densidad media de protusiones es igual entre los ratones CPT1C-KO y los WT, con una media de 6,0 ± 0,2 y 6,6 ± 0,26 protusiones por 10 µm de dendrita, respectivamente (Figura 58A). Respecto a la morfología de la espina dendrítica, las neuronas de los ratones CPT1C-KO y la de los ratones WT mostraron un patrón claramente diferente respecto a la longitud de la protusión (Figura 58B, C). La longitud de las protuberancias en las neuronas CPT1C-KO fue aproximadamente de un 20% más largas que en los ratones WT. Por otra parte, un 56,79% ± 2,97 de las dendritas eran más cortas de una micra en las neuronas CPT1C-KO en comparación con el 87,05% ± 1,69 en las neuronas control (WT). Las neuronas de los ratones CPT1C-KO mostraron notablemente más filopodios que las células control (WT) (Figura 58D).

Está descrito en la literatura, que la formación de la cabeza de la espina dendrítica es considerada como

un indicador de madurez. El número de espinas maduras (setas y bultos) por cada 10 µm de dendrita fue menor en las neuronas CPT1C-KO que en la de los WT (Figura 58E, F). También hemos encontrado que las neuronas CPT1C-KO tienen menos espinas maduras (hongos y bultos), 56.79% ± 2.97 en comparación con las células WT, 87.05% ± 1.69. Por otra parte, el área de la cabeza fue similar en ambos casos: 0,23 μm^2 ± 0,005 y 0,22 ± 0,006 μm^2, en CPT1C-KO y WT, respectivamente. Este resultado significa que las neuronas CPT1C-KO tienen más neuronas inmaduras que los WT, pero las que son maduras, son igual de maduras que las del ratón WT. En conjunto, estos resultados demuestran claramente el papel de CPT1C en la maduración de la espina dendrítica.

8.3.5.2.1 Rescate de la morfología dendrítica de las neuronas CPT1C-KO añadiendo C6-ceramida

Los resultados anteriores muestran que CPT1C promueve la maduración de las espinas dendríticas. Por otra parte, CPT1C también participa en la síntesis de ceramidas. Se ha descrito previamente que la disminución de esfingolípidos y colesterol resultó en una pérdida de espinas dendríticas y en el alargamiento de las restantes (Hering, H. 2003). Por lo tanto, quisimos comprobar si la ceramida era capaz de rescatar la morfología de la espina dendrítica observada en los ratones CPT1C-KO.

La primera aproximación que hicimos fue sobre-expresar CPT1C en cultivos de neuronas CPT1C-KO para ver si revertíamos la morfología de las espinas. Para ello, transfectamos las neuronas CPT1C-KO a la 10DIV con el vector pIRES-CPT1C-EGFP, vector que expresa las dos proteínas, la CPT1C y la GFP. Los resultados demostraron que la sobre-expresión de CPT1C en las neuronas deficientes para la enzima, reducía la densidad de filopodios y aumentaba el porcentaje de espinas maduras a valores similares a los del WT (figura 59B, C).

El siguiente paso fue revertir el fenotipo tratando a las neuronas CPT1C-KO con C6-ceramida exógena. Para ello, las neuronas CPT1C-KO y WT fueron tratadas con 1,5 µM C6-ceramida a la 5DIV. Está descrito en la literatura que la ceramida promueve la supervivencia celular en los estadios inmaduros de las neuronas del hipocampo, por el contrario, en neuronas maduras, el tratamiento produce la muerte celular, incluso a esta baja concentración de ceramida exógena (Mitoma, J. 1998). Por esta razón, el tratamiento se realizó en neuronas de hipocampo inmaduras (5DIV). Posteriormente, las células fueron transfectadas con el vector EGFP en 13DIV y dos días después, las células fueron fijadas (15DIV) y las espinas dendríticas fueron analizadas.

Como se observa en la figura 59A, el promedio de la longitud de las protusiones se redujo de 1,43 µm ± 0,03 a 1,17 µm ± 0,03, en las células CPT1C-KO tratadas con la C6-ceramida exógena. En consecuencia, la proporción de filopodios se redujo de 2,3 µm ± 0,18 a 0,45 µm ± 0,07 en las células CPT1C-KO tratadas con C6-ceramida, mientras que el porcentaje de espinas maduras aumento casi un 40% en las neuronas CPT1C-KO tratadas (Figura 59A). Por lo tanto, la ceramida exógena revirtió el fenotipo de las neuronas CPT1C-KO disminuyendo los filopodios inmaduros y restaurando la densidad de las espinas maduras hasta alcanzar niveles casi normales.

8.3.5.3 Marcadores sinápticos

Experimentos anteriores sugieren que la deficiencia en CPT1C afecta a la maduración de las espinas dendríticas. Por lo tanto, nuestra pregunta fue, que estaba pasando a nivel de sinapsis.

Para analizar la formación de sinapsis, se analizó la distribución de las proteínas pre-y post-sinápticas, como la sinapsina 1 y PSD-95, respectivamente, mediante la tinción de inmunofluorescencia en cultivos neuronales de hipocampo de ratones CPT1C-KO y WT en 15DIV. La densidad de sinapsis se determinó contando el número de grupos PSD-95 o sinapsina 1 positivos a lo largo de la dendrita. Los números se normalizaron respecto a un tramo de la dendrita de 100 µm.

Los resultados no mostraron cambios significativos en el número ni de PSD-95 ni de sinapsina 1 entre los genotipos. Este resultado sugiere que la falta de CPT1C no afecta al número de marcadores sinápticos en los cultivos de neuronas maduras (15DIV) de hipocampo (figura 60).

8.3.5.4 Niveles de los receptores AMPA en cultivos neuronales de hipocampo

Las espinas dendríticas suelen recibir la mayoría de las sinapsis excitatorias en las neuronas del hipocampo. Para determinar si una reducción de espinas maduras en el ratón CPT1C-KO refleja una pérdida en la formación de sinapsis excitadoras, la cantidad de receptores AMPA y el tráfico del mismo fueron examinados.

Distintos protocolos experimentales se realizaron para el estudio de los receptores AMPA y su tráfico. Se estudió la subunidad GluR2 del receptor AMPA porque es una de las subunidades más abundante y se expresa de manera constitutiva en la sinapsis.

Los niveles totales de la subunidad GluR2 del receptor AMPA fueron medidos mediante la técnica del western blot. Los resultados mostraron que los ratones CPT1C-KO tenían reducidos los niveles totales de la subunidad (figura 61).

Posteriormente estudiamos los niveles de GluR2 en la superficie neuronal. Para ello se realizó un ensayo de inmunofluorescencia contra el dominio extracelular de la proteína GluR2 en las neuronas hipocampales de ratones WT y CPT1C-KO en 14DIV. La intensidad de fluorescencia a lo largo de la dendrita y la intensidad de fluorescencia de cada punto de la superficie fueron determinadas. Se encontró que los ratones CPT1C-KO tenían un número significativamente menor de receptores GluR2 a lo largo de la superficie de la dendrita y que el tamaño de los puntos era menor. Estos resultados sugieren que las neuronas de los ratones CPT1C-KO expresan niveles más bajos de receptores AMPA en la superficie de las neuronas que los ratones WT (Figura 62).

El siguiente paso fue saber si CPT1C interfería en el tráfico de los receptores AMPA. Para ello se utilizó una técnica de inmunofluorescencia. Se incubaron las neuronas con el anticuerpo primario GluR2 extracelular. Posteriormente, las células fueron estimuladas con AMPA a 100 µM durante 10 minutos para producir la internalización del receptor, seguido de una fijación con paraformaldehido al 4%. Los receptores AMPA retenidos en la superficie celular se detectaron con un anticuerpo secundario verde, Alexa Fluor 488. Después las células fueron permeabilizadas y un anticuerpo secundario rojo, Cy3 fue utilizado para detectar a los receptores internalizados. Los niveles de internalización fueron cuantificados como porcentaje de internalización de GluR2 versus el total de GluR2. Los resultados mostraron que en condiciones basales no había diferencias en la internalización de los receptores AMPA, pero tras la estimulación con AMPA, los ratones CPT1C-KO mostraron un aumento en la internalización del receptor GluR2 respecto a los WT (Figura 63). Este resultado muestra una clara alteración en el tráfico de receptores AMPA en los ratones CPT1C-KO, lo que sugiere que CPT1C tiene un papel en la regulación del tráfico de los receptores AMPA.

8.4 DISCUSIÓN

CPT1C es una enzima que se expresa en el retículo endoplasmático de todas las neuronas (Dai, Y. 2007; Sierra, AY 2008), pero hasta ahora, sólo se ha encontrado su participación en la ingesta y en el control de la homeostasis energética. Por lo tanto, su ubicación y su intrigante función desconocida, hace su estudio atractivo.

El presente trabajo muestra que CPT1C tiene una función completamente diferente a CPT1A y B, mostrando un papel anabólico en lugar de catabólico, regulando así, la síntesis de novo de ceramidas. A nivel fisiológico, CPT1C está involucrada en el aprendizaje espacial y en la función motora. Por otra parte, hemos demostrado que la falta de CPT1C produce una alteración en la maduración de las espinas dendríticas, que es revertida por el tratamiento con ceramidas.

8.4.1 CPT1C tiene baja actividad CPT1

Existe una alta similitud de secuencia entre CPT1C y las otras isoformas CPT1. La información obtenida por el modelo tridimensional muestra que CPT1C puede catalizar la misma reacción que CPT1A y B, pero hasta el momento ningún grupo ha sido capaz de medir su actividad.

Nosotros hemos sido capaces de medir la actividad específica de CPT1C. Los resultados mostraron que la actividad catalítica de CPT1C es muy baja, 100 veces menor que la isoforma CPT1A, aunque muestra una afinidad por los sustratos, palmitoil-CoA y carnitina similar a la isoforma CPT1A.

El hecho de que los otros grupos no encontraran actividad CPT1C, podría deberse al hecho de que midieron la actividad CPT1C en las mitocondrias. No fue hasta el año 2008, donde nuestro grupo demostró que CPT1C se encontraba en el retículo endoplasmático y no en las mitocondrias. Además, el método que se utilizó para determinar la actividad de CPT1C fue un método radiométrico. Tal vez, este método no es lo suficientemente sensible para detectar la baja actividad de CPT1C. Nuestro grupo desarrolló un método más sensible para determinar la actividad catalítica de la enzima en microsomas (Jauregui, O. 2007). Este método se basa en el HPLC-MS/MS y es 100 veces más sensible que el radiométrico, la cual cosa nos permitió medir la baja actividad de CPT1C.

El hecho de que la enzima tenga una baja actividad CPT1, puede deberse a varias hipótesis entre las cuales: Una hipótesis sería que CPT1C necesita unirse a alguna proteína estructural para tener actividad y el hecho de trabajar con microsomas aislados haría que estuviésemos eliminando alguna molécula necesaria para que CPT1C sea activa. La otra hipótesis sería que CPT1C no sea activa y que actúe simplemente como un sensor de malonil-CoA y/o aciles-CoA, y que bajo ciertas condiciones, como ausencia de malonil-CoA o presencia de aciles-CoA como durante el ayuno, podría cambiar su conformación y mediante la interacción con otras proteínas, activar alguna vía metabólica.

8.4.2 CPT1C está involucrado en la síntesis *de novo* de la ceramida

Aunque la función exacta de CPT1C no se ha descubierto en el presente estudio, nuestros datos demuestran que CPT1C regula el metabolismo de ceramidas. Hemos visto una reducción en los niveles de ceramidas en todas las áreas del cerebro analizadas respeto a los ratones WT. Se ha descrito en la literatura que los niveles de ceramidas en ayuno o condiciones de alimentación están regulados de manera diferente dependiendo de la zona analizada. Estos resultados están en concordancia con los nuestros, en los que parece que las diferentes áreas cerebrales estén reguladas de manera diferente y además, se ha demostrado que un aumento en los niveles de ceramida en el cerebro produce un deterioro cognitivo y motor (de la Monte, S.M. 2010). Por lo tanto, la reducción en los niveles de ceramidas observados en los ratones CPT1C-KO podría estar produciendo las alteraciones en el

aprendizaje y en la función motora que hemos observado en los ratones deficientes en CPT1C.

Una de las aportaciones relevantes de esta Tesis es la confirmación de que CPT1C facilita la síntesis *de novo* de ceramidas. Previamente habíamos descrito esta participación en el núcleo arcuato del hipotálamo (Gao, S. 2011), y ahora lo demostramos en cultivos neuronales de hipocampo. No sabemos el mecanismo molecular por el cual CPT1C regula los niveles de ceramidas, pero en base a nuestros datos, proponemos dos posibles hipótesis: En primer lugar, debido a que CPT1C se localiza en el RE, donde SPT y la ceramida sintasa (CerS) se localizan y debido a que CPT1C tiene una baja actividad, es posible que CPT1C esté interaccionando físicamente con SPT o CerS modulando así su actividad. Entonces, bajo condiciones de ayuno o por una reducción de los niveles de malonil-CoA, CPT1C podría cambiar su conformación y activar a estas enzimas y, en consecuencia, aumentar la síntesis *de novo* de ceramidas (figura 64). La segunda hipótesis es que CPT1C podría facilitar la entrada de aciles-CoA a la luz del retículo endoplasmático (RE), evitando así que sean utilizados en otras vías metabólicas en el citosol y puedan ser utilizados para la síntesis *de novo* de ceramidas. En apoyo a esta hipótesis, se ha descrito en la literatura la existencia de transportadores de aciles-CoA dependientes de carnitina a través de la membrana del RE (Arduini, A. 1994; Abo-Hashema, K.A. 1999; Gooding, J.M. 2004), por lo que sugerimos que CPT1C podría ser ese transportador (figura 65). Sin embargo, la posibilidad de que CPT1C entre aciles-CoA al interior del RE es poco probable debido a que las enzimas SPT y CerS tienen sus sitios activos en el región del citosol y no en el lumen del RE.

8.4.3 Funciones fisiológicas de la enzima CPT1C

8.4.3.1 CPT1C regula la ingesta de alimentos y el metabolismo periférico

CPT1C se expresa ampliamente en todo el sistema nervioso central y periférico, lo que indica que tiene un amplio papel en el neurometabolismo (Wolfgang, M.J. 2006).

Nuestros resultados demuestran que los ratones CPT1C-KO no responden metabólicamente a las señales de ayuno, lo que les lleva a no poder aumentar la oxidación periférica de ácidos grasos en condiciones donde se necesita un aporte de energía, como también se está descrito en la literatura (Wolfgang, M.J. 2006). Además, cuando estos ratones CPT1C-KO son alimentados con una dieta rica en grasa, son más sensibles a la obesidad y a la diabetes (Gao, X.F. 2009), por el contrario, la sobre-expresión de CPT1C protege a los ratones de la obesidad (Dai, Y. 2007). Parece ser que los ratones CPT1C-KO pierden la capacidad de detectar en el hipotálamo, el aumento de ácidos grasos no esterificados circulantes (NEFA) causados por una dieta rica en grasa o por el ayuno (CNOP, M. 2008; Finn, P.F. 2006), y por lo tanto, no son capaces de enviar la información a los tejidos periféricos.

Además, durante el ayuno, los niveles de malonil-CoA son rápidamente enviados al músculo esquelético y al hígado, para que los ácidos grasos sean β-oxidados. Esta señal parece ser transmitida por el sistema nervioso simpático (SNS). El hecho de que CPT1C se encuentre en el SNP y que la deficiencia de CPT1C produzca una reducción en la β-oxidación en el músculo y en el hígado, sugiere que CPT1C podría estar regulando la respuesta a los nutrientes en el eje entre el SNC y el SNP.

Por otra parte, se ha demostrado una correlación de causa-efecto entre la actividad CPT1C y la expresión de neuropéptidos orexigénicos o anorexígenos, donde la sobre-expresión de CPT1C en el hipotálamo aumenta la ingesta de los ratones (Gao, S. 2011). Nosotros también hemos demostrado el papel de CPT1C en el control de la ingesta, aunque otros experimentos deben ser realizados para aclarar la participación CPT1C en el control del apetito. Sin embargo, numerosos estudios sugieren que es CPT1A la principal isoforma implicada en la regulación de la ingesta de alimentos. En el año 2003, el

grupo de Rossetti demostró que la inhibición genética de CPT1A en el hipotálamo resultó en una disminución de los niveles de la proteína AgRP y neuropéptido Y (Obici, S. 2003). Teniendo en cuenta que CPT1C tiene una actividad 100 veces menor que CPT1A, y que ésta no participa en la oxidación mitocondrial debido a su ubicación en el RE, sugiere que CPT1C no participa directamente en el control del apetito, sino que podría estar involucrada en el secuestro de malonil-CoA. La capacidad de CPT1C de unirse a malonil-CoA ha sido demostrado (Wolfgang, M.J. 2006). Por lo tanto, nuestra hipótesis sería que la CPT1C hipotalámica se uniría al malonil-CoA reduciendo así, la disponibilidad intracelular del mismo, para poder unirse a CPT1A. Por lo tanto, la deficiencia en CPT1C permitiría una mayor disponibilidad del malonil-CoA, lo que provocaría una disminución de la actividad CPT1A y, en consecuencia, una reducción en la ingesta de alimentos (figura 66).

8.4.3.2 Los ratones CPT1C-KO tienen alteraciones motoras y en el aprendizaje

Nuestro trabajo demuestra que CPT1C tiene otras funciones aparte de la regulación de la ingesta de alimentos y la homeostasis energética. Los ratones deficientes en CPT1C presentan déficits en la coordinación motora, desequilibrio y debilidad muscular. Además, los ratones CPT1C-KO tienen niveles bajos de ceramidas y de aciles-carnitina en el cerebelo, cuerpo estriado y corteza motora, zonas implicados en la función motora. Además, el hallazgo de que CPT1C se exprese también en el sistema nervioso periférico, define nuevos lugares donde la deficiencia de CPT1C puede ser la responsable del deterioro motor. Por otro lado, la reducción en la oxidación de ácidos grasos presente en el músculo esquelético de los ratones CPT1C-KO, podría generar la debilidad muscular y ser la causa de la alteración en las pruebas de fuerza ya que se ha visto que la miopatía, hipotonía y debilidad muscular son características típicas de los defectos en la oxidación de ácidos grasos, los cuales se manifiestan con mayor frecuencia en condiciones de ayuno (van Adel, B.A. 2009).

En relación con la cognición, los ratones deficientes en CPT1C presentan problemas en el aprendizaje espacial ya que éstos tardan más tiempo en aprender donde está localizada la plataforma. Es importante destacar que las deficiencias motoras no afectan al test. Por otro lado, la memoria y la flexibilidad cognitiva no están alteradas en los ratones CPT1C-KO. Este resultado indicaría que la deficiencia en CPT1C afecta al proceso de consolidación de la información, pero no a la retención o a la extinción de ésta. Este fenotipo podría estar directamente relacionado con la maduración de las espinas dendríticas, las cuales están afectadas en los ratones CPT1C-KO ya que se ha visto que en pacientes y modelos de animales con retraso mental, muestran unas espinas dendríticas inmaduras.

El deterioro espacial en los ratones CPT1C-KO, sugiere que el hipocampo está afectado, cómo lo confirma la disminución en los niveles de palmitoil-carnitina encontrados en esta región. La flexibilidad cognitiva, la cual no se encuentra altera en los ratones CPT1C-KO, depende del correcto funcionamiento de la corteza prefrontal, una región donde no se encontraron alterados los niveles de aciles-carnitina.

Hay algunos documentos que relacionan el hipotálamo con las tareas del hipocampo. Por ejemplo, la leptina, la hormona de la saciedad, está descrito que su administración induce la mejora de la memoria y el aprendizaje (Harvey, J. 2007). El mismo papel juega la grelina, la hormona del hambre, la cual en el hipocampo, está implicada en la morfología de las espinas dendríticas y en la locomoción. Animales deficientes para esta hormona, tienen un menor número de espinas dendríticas y sinapsis (Carlini, V.P. 2002; Diano, S. 2006). Además, datos publicados de nuestro grupo sugieren que los ratones CPT1C-KO no responden a la vía de la leptina (Gao, S. 2011), lo que podría estar relacionado con las alteraciones en la morfología de las espinas dendríticas y con los problemas motores y de aprendizaje observados en los ratones CPT1C-KO. A nivel de comportamiento, estos resultados demuestran por primera vez la participación de CPT1C en la función motora y la cognición, lo que abre la puerta a la posibilidad de que

mutaciones en CPT1C, podrían ser la causa de algunas discapacidades motoras y de aprendizaje de causa desconocida en humanos.

8.4.3.3 CPT1C está implicada en la maduración de la espina dendrítica

Se piensa que los filopodios son los precursores de las espinas dendríticas durante el desarrollo neuronal (Dailey, M.E. 1996; Ziv, N.E. 1996; Dunaevsky, A. 1999; Marrs, G.S. 2001). Los filopodios son remplazados por espinas cortas, con cabeza y cuello corto, que forman la espina madura. Sin embargo, las moléculas que regulan la extensión de filopodios y su maduración a espinas, siguen siendo desconocidas.

Nuestros resultados implican a CPT1C en la maduración de las espinas dendríticas. Las neuronas deficientes en CPT1C tienen un aumento en el número de filopodios, dándoles un aspecto peludo, sin alterar la densidad total de las protuberancias dendríticas, lo que indica que CPT1C no es necesaria para la formación de la protuberancia, pero si es necesaria para la conversión de los filopodios en espinas maduras.

Se ha descrito que algunas patologías tienen alteraciones en la conversión de filopodios a espinas dendríticas maduras. Por lo tanto, alteraciones en la forma de la espina dendrítica podrían verse manifestadas en los cambios de comportamiento. La formación de la espina dendrítica, la estabilización y / o la eliminación, son los componentes claves en la plasticidad sináptica y sirven como base para el aprendizaje y la memoria. Por otra parte, el área de la cabeza de la espina indica la maduración de ésta. Nuestros resultados demuestran que no hay diferencias entre los genotipos en referencia al área de la espina, con lo cual, este resultado nos explicaría porqué los ratones CPT1C-KO tienen alterado el aprendizaje, pero no la memoria.

Por otro lado, la síntesis de esfingolípidos tiene lugar en la cara citosólica de la membrana del RE. Los esfingolípidos son una parte importante de la membrana plasmática, y en las neuronas, su síntesis aumenta durante el crecimiento de las neuritas (Araki, W. 1997). La composición de los esfingolípidos también determina la fluidez de membrana y la forma de la espina. La implicación de CPT1C en la síntesis de ceramidas, precursor de los esfingolípidos, sugeriría que la alteración en la morfología de las espinas dendríticas podría estar causada por la alteración en la síntesis de ceramidas en los ratones CPT1C-KO, la cual cosa fue confirmada por la reversión de la morfología de las espinas en los ratones deficientes en CPT1C, tras el tratamiento con ceramida exógena.

Estudios recientes demuestran la importancia de las ceramidas en la formación de las espinas dendríticas, en el proceso de aprendizaje y memoria y en la fuerza sináptica. Un artículo reciente describe la presencia de una nueva isoenzima, una sintetasa de aciles-CoA de cadena larga (ACSL4) que se localiza específicamente en el RE de las neuronas. Su deficiencia aumenta el porcentaje de filopodios y reduce el porcentaje de espinas maduras (Meloni, I. 2009). Esto pone de relieve la importancia de los ácidos grasos en el metabolismo de la espinogénesis e indica que ACSL podría proporcionar el sustrato necesario para la síntesis de ceramidas en el RE de las neuronas. Otro estudio que correlaciona las ceramidas con la formación de espinas dendríticas es Hering, H. 2003. Los autores muestran que la inhibición de colesterol unido a la síntesis de ceramidas, provoca alteraciones en la densidad y la morfología de las espinas dendríticas. El mecanismo por el cual se regula la maduración de las espinas a través de las ceramidas se desconoce. Sin embargo, las ceramidas se unen y regulan la actividad de algunas enzimas y proteínas de señalización, como quinasas, fosfatasas o receptores de membrana (Breslow, D.K. 2010). Un ejemplo es la proteína fosfatasa 1 (PP1), la cual es activada por ceramidas (Chalfant, C.E. 1999) y ha sido implicada en la conversión de los filopodios en espinas maduras (Terry-Lorenzo, R.T. 2005). Además, la ceramida es la base de todos los esfingolípidos celulares que, junto con el colesterol, son componentes esenciales en la composición de las balsas lipídicas (lipid rafts). Todos

estos fenómenos son necesarios para la estabilidad y la maduración de la sinapsis en las espinas dendríticas.

8.4.3.4 CPT1C participa en la estabilización de los receptores AMPA en la superficie celular de la espina

La transmisión sináptica de las neuronas excitatorias en el cerebro de los mamíferos es mediada en gran parte por los receptores AMPA que están situados en la superficie de las espinas dendríticas. La cantidad de receptores postsinápticos AMPA se correlaciona con el tamaño de la sinapsis y con la dimensión de la cabeza de la espina dendrítica (Matsuzaki, M. 2001). Hay una relación directa entre los receptores AMPA y la formación de las espinas dendríticas, aunque el mecanismo molecular aún se desconoce.

En el hipocampo, la mayoría de los receptores AMPA se componen de subunidades GluR1-GluR2 o GluR2-GluR3, los homómeros de GluR2 son raros. Uno de los factores cruciales para la plasticidad sináptica es el número de receptores AMPA activos en la superficie de la membrana plasmática y su tráfico. De acuerdo con esto, nuestro ensayo de inmunofluorescencia demostró que el receptor AMPA de superficie (GluR2) es menos abundante en ratones CPT1C-KO, aunque sus niveles de internalización son mayores que los de los ratones WT. Es probable que CPT1C esté participando en la estabilización de los receptores AMPA en la superficie celular de las neuronas, lo que contribuye a la regulación del tráfico de los receptores AMPA, y ésto lo podría hacer a través de las balsas lipídicas.

Por otra parte, las ceramidas también pueden ser generadas por la acción de una familia de enzimas que catabolizan la esfingomielina, son las esfingomielinasas. Hay tres clases de esfingomielinasas, que en base a su pH óptimo se clasifican en esfingomielinasa neutra, ácida y alcalina. Tres esfingomielinasas neutras (nSMase) han sido identificados, pero es la nSMase2 la que está altamente expresada en las neuronas del hipocampo y es importante para la regulación de actividades relacionadas con la memoria sináptica (Wheeler, D. 2009). Ratones a los cuales se les ha administrado GW4869, un inhibidor específico de SMasa2, muestran dificultades para aprender donde estaba localizada la plataforma durante la fase de adquisión en el test del laberinto de la piscina, pero no mostraban alteraciones en los episodios de memoria como los que son necesarios para la tareas de inversión o eliminación (Tabatadze, N. 2010). Este resultado está en concordancia con nuestros resultados, donde la falta de CPT1C produce una reducción en los niveles de ceramidas, afectando así a la tarea del aprendizaje.

En base a nuestros datos, en los que hemos visto que CPT1C participa en la maduración de las espinas dendríticas a través de la síntesis de ceramidas, se propone otra posible función para la enzima CPT1C. Nuestra hipótesis es que CPT1C podría estar regulando la síntesis o el pool de esfingolípidos necesarios para la formación de las balsas lipídicas. Las balsas lipídicas son microdominios lípidos ricos en esfingolípidos y colesterol (Tsui-Pierchala, B.A. 2002). Un gran número de receptores de señalización, complejos y canales iónicos han sido propuestos como supuestos componentes de las balsas lipídicas, los cuales contribuyen a la morfología de la espinas dendrítica y a la transmisión sináptica (Hering, H. 2003). Varios receptores de glutamato (NMDA y AMPA) y proteínas postsináptica de anclaje, incluyendo la proteína de densidad postsináptica (PSD-95), canales iónicos, proteínas de adhesión y los elementos del complejo SNARE, se localizan también en estas balsas lipídicas (Hering, H. 2003). Las balsas lipídicas también están involucradas en el tráfico de membrana, y juegan un papel en la endocitosis de las proteínas de la superficie celular y en la clasificación intracelular (Nichols, B.J. 2001).

La falta de CPT1C podría causar una reducción en los niveles de ceramidas, los cuales conducirían a una alteración en la formación de las balsas lipídicas y ésto se traduciría en una inestabilidad de los

receptores AMPA de superficie, en la pérdida de la maduración de las espinas dendríticas y en la disfunción motora y cognitiva.

8.4.4 CONCLUSIONES Y PERSPECTIVAS FUTURAS

Los diferentes enfoques propuestos en este trabajo se han centrado en elucidar el posible papel de CPT1C en las neuronas, en concreto en la transmisión sináptica. Su ubicación en el RE, su baja actividad y su papel en la síntesis de ceramidas sugiere que CPT1C podría desempeñar un papel diferente al de las otras isoformas CPT1. La amplitud de las deficiencias observadas debidas a la falta de CPT1C en los ratones CPT1C-KO indica que CPT1C debe participar en una función general e importante en las neuronas.

Los resultados de este trabajo muestran que CPT1C tiene otras funciones fisiológicas además de la regulación de la ingesta de alimentos y la homeostasis energética. Se demuestra que la función molecular de CPT1C es la regulación de la síntesis *de novo* de ceramidas en las neuronas, las cuales son necesarias para la maduración de las espinas dendríticas durante el desarrollo cerebral. A nivel de comportamiento, se demuestra por primera vez la participación de CPT1C en el aprendizaje y en las habilidades motoras.

Por lo tanto, en el futuro, más estudios deben ser realizados para explicar la relación entre CPT1C y la síntesis *de novo* de ceramidas: si CPT1C aumenta la entrada de aciles-CoA al RE o si es un simple sensor de malonil-CoA que activa a proteínas implicadas en la síntesis *de novo* de ceramidas y ver también si las ceramidas sintetizadas por CPT1C tienen funciones señalizadoras o estructurales.

Finalmente, nosotros proponemos el siguiente esquema en el cual se describe hipotéticamente el papel de CPT1C en el retículo endoplásmico de la neurona. Nosotros sugerimos que CPT1C, por un mecanismo todavía desconocido, aumenta la síntesis *de novo* de ceramidas. Entonces, quizás a través de los lípidos señalizadores o a través de las balsas lipídicas, participa en la morfología de las espinas, y en el anclaje de los receptores AMPA a la membrana plasmática. Por lo tanto, una alteración de esta vía produciría las alteraciones motoras y cognitivas observadas en el ratón CPT1C-KO.

8.5 CONCLUSIONES

1. La enzima CPT1C tiene una actividad carnitina palmitoiltransferasa 1 inferior a CPT1A, mostrando una menor eficiencia catalítica por la carnitina y el palmitoil-CoA.
2. Los ratones CPT1C-KO muestran niveles bajos de aciles-carnitinas y ceramidas respecto a los ratones salvajes, indicando que los ratones CPT1C-KO tienen alterado el metabolismo lipídico.
3. CPT1C facilita la síntesis *de novo* de ceramidas en cultivos primarios de neuronas de hipocampo.
4. La expresión de la proteína CPT1C aumenta durante el desarrollo del ratón, alcanzando el pico máximo de expresión a la edad adulta.
5. CPT1C, además de estar expresada en el sistema nervioso central, también se expresa en el sistema nervioso periférico, aunque parece ser que a niveles más bajos.
6. La carencia de CPT1C no produce alteraciones en la morfología de la estructura del córtex, hipocampo o cerebelo.
7. La deficiencia en CPT1C produce un deterioro en el aprendizaje espacial, sin afectar a la memoria o a la flexibilidad cognitiva.

8. Los ratones CPT1C-KO son hipoactivos y muestran claras deficiencias en la función motora, especialmente en las habilidades de coordinación y fuerza.
9. La carencia de CPT1C produce una alteración en la maduración de las espinas dendríticas, aumentando la densidad de filopodios y reduciendo la densidad de espinas en forma de setas y bultos, sin afectar a la densidad de las protusiones ni al número de sinapsis.
10. Los niveles de ceramidas regulados por CPT1C controlan la maduración de las espinas dendríticas en cultivos neuronales de hipocampo.
11. A nivel post-sináptico, CPT1C está involucrada en el tráfico de los receptores AMPA ya que la deficiencia en CPT1C reduce en el número de receptores AMPA (subunidad GluR2) en la superficie celular y aumenta la internalización del receptor AMPA.

REFERENCES

CHAPTER 9 : REFERENCES

Abo-Hashema, K. A., Cake, M. H., Lukas, M. A., & Knudsen, J. (1999). Evaluation of the affinity and turnover number of both hepatic mitochondrial and microsomal carnitine acyltransferases: Relevance to intracellular partitioning of acyl-CoAs. *Biochemistry, 38*(48), 15840-15847.

Abulrob, A., Tauskela, J. S., Mealing, G., Brunette, E., Faid, K., & Stanimirovic, D. (2005). Protection by cholesterol-extracting cyclodextrins: A role for N-methyl-D-aspartate receptor redistribution. *Journal of Neurochemistry, 92*(6), 1477-1486. doi:10.1111/j.1471-4159.2005.03001.x

Andrews, Z. B., Liu, Z. W., Walllingford, N., Erion, D. M., Borok, E., Friedman, J. M., . . . Diano, S. (2008). UCP2 mediates ghrelin's action on NPY/AgRP neurons by lowering free radicals. *Nature, 454*(7206), 846-851. doi:10.1038/nature07181

Ainscow, E. K., & Rutter, G. A. (2002). Glucose-stimulated oscillations in free cytosolic ATP concentration imaged in single islet beta-cells: Evidence for a Ca2+-dependent mechanism. *Diabetes, 51 Suppl 1*, S162-70.

Araki, W., & Wurtman, R. J. (1997). Control of membrane phosphatidylcholine biosynthesis by diacylglycerol levels in neuronal cells undergoing neurite outgrowth. *Proceedings of the National Academy of Sciences of the United States of America, 94*(22), 11946-11950.

Arana, L., Gangoiti, P., Ouro, A., Trueba, M., & Gomez-Munoz, A. (2010). Ceramide and ceramide 1-phosphate in health and disease. *Lipids in Health and Disease, 9*, 15. doi:10.1186/1476-511X-9-15

Arduini, A., Denisova, N., Virmani, A., Avrova, N., Federici, G., & Arrigoni-Martelli, E. (1994). Evidence for the involvement of carnitine-dependent long-chain acyltransferases in neuronal triglyceride and phospholipid fatty acid turnover. *Journal of Neurochemistry, 62*(4), 1530-1538.

Arstikaitis, P., Gauthier-Campbell, C., Carolina Gutierrez Herrera, R., Huang, K., Levinson, J. N., Murphy, T. H., . . . El-Husseini, A. (2008). Paralemmin-1, a modulator of filopodia induction is required for spine maturation. *Molecular Biology of the Cell, 19*(5), 2026-2038. doi:10.1091/mbc.E07-08-0802

Bajjalieh, S. M., Martin, T. F., & Floor, E. (1989). Synaptic vesicle ceramide kinase. A calcium-stimulated lipid kinase that co-purifies with brain synaptic vesicles. *The Journal of Biological Chemistry, 264*(24), 14354-14360.

Bear, M. F., & Malenka, R. C. (1994). Synaptic plasticity: LTP and LTD. *Current Opinion in Neurobiology, 4*(3), 389-399.

Ben Gedalya, T., Loeb, V., Israeli, E., Altschuler, Y., Selkoe, D. J., & Sharon, R. (2009). Alpha-synuclein and polyunsaturated fatty acids promote clathrin-mediated endocytosis and synaptic vesicle recycling. *Traffic (Copenhagen, Denmark), 10*(2), 218-234. doi:10.1111/j.1600-0854.2008.00853.x

Bieber, L. L. (1988). Carnitine. *Annual Review of Biochemistry, 57*, 261-283. doi:10.1146/annurev.bi.57.070188.001401

Blochl, A., & Thoenen, H. (1996). Localization of cellular storage compartments and sites of constitutive and activity-dependent release of nerve growth factor (NGF) in primary cultures of hippocampal neurons. *Molecular and Cellular Neurosciences, 7*(3), 173-190. doi:10.1006/mcne.1996.0014

Brann, A. B., Scott, R., Neuberger, Y., Abulafia, D., Boldin, S., Fainzilber, M., & Futerman, A. H. (1999). Ceramide signaling downstream of the p75 neurotrophin receptor mediates the effects of nerve growth factor on outgrowth of cultured hippocampal neurons. *The Journal of Neuroscience : The Official Journal of the Society for Neuroscience, 19*(19), 8199-8206.

Breslow, D. K., & Weissman, J. S. (2010). Membranes in balance: Mechanisms of sphingolipid homeostasis. *Molecular Cell, 40*(2), 267-279. doi:10.1016/j.molcel.2010.10.005

Buccoliero, R., & Futerman, A. H. (2003). The roles of ceramide and complex sphingolipids in neuronal cell function. *Pharmacological Research : The Official Journal of the Italian Pharmacological Society, 47*(5), 409-419.

Burnashev, N., Monyer, H., Seeburg, P. H., & Sakmann, B. (1992). Divalent ion permeability of AMPA receptor channels is dominated by the edited form of a single subunit. *Neuron, 8*(1), 189-198.

Calabrese, B., Wilson, M. S., & Halpain, S. (2006). Development and regulation of dendritic spine synapses. *Physiology (Bethesda, Md.), 21*, 38-47. doi:10.1152/physiol.00042.2005

Carlini, V. P., Monzon, M. E., Varas, M. M., Cragnolini, A. B., Schioth, H. B., Scimonelli, T. N., & de Barioglio, S. R. (2002). Ghrelin increases anxiety-like behavior and memory retention in rats. *Biochemical and Biophysical Research Communications, 299*(5), 739-743.

Carling, D. (2004). The AMP-activated protein kinase cascade--a unifying system for energy control. *Trends in Biochemical Sciences, 29*(1), 18-24.

Chalfant, C. E., & Spiegel, S. (2005). Sphingosine 1-phosphate and ceramide 1-phosphate: Expanding

roles in cell signaling. *Journal of Cell Science, 118*(Pt 20), 4605-4612. doi:10.1242/jcs.02637

Chalfant, C. E., Kishikawa, K., Mumby, M. C., Kamibayashi, C., Bielawska, A., & Hannun, Y. A. (1999). Long chain ceramides activate protein phosphatase-1 and protein phosphatase-2A. activation is stereospecific and regulated by phosphatidic acid. *The Journal of Biological Chemistry, 274*(29), 20313-20317.

Chung, H. J., Xia, J., Scannevin, R. H., Zhang, X., & Huganir, R. L. (2000). Phosphorylation of the AMPA receptor subunit GluR2 differentially regulates its interaction with PDZ domain-containing proteins. *The Journal of Neuroscience : The Official Journal of the Society for Neuroscience, 20*(19), 7258-7267.

Cnop, M. (2008). Fatty acids and glucolipotoxicity in the pathogenesis of type 2 diabetes. *Biochemical Society Transactions, 36*(Pt 3), 348-352. doi:10.1042/BST0360348

Cohen, I., Guillerault, F., Girard, J., & Prip-Buus, C. (2001). The N-terminal domain of rat liver carnitine palmitoyltransferase 1 contains an internal mitochondrial import signal and residues essential for folding of its C-terminal catalytic domain. *The Journal of Biological Chemistry, 276*(7), 5403-5411. doi:10.1074/jbc.M009555200

Cohen, I., Kohl, C., McGarry, J. D., Girard, J., & Prip-Buus, C. (1998). The N-terminal domain of rat liver carnitine palmitoyltransferase 1 mediates import into the outer mitochondrial membrane and is essential for activity and malonyl-CoA sensitivity. *The Journal of Biological Chemistry, 273*(45), 29896-29904.

Colledge, M., Snyder, E. M., Crozier, R. A., Soderling, J. A., Jin, Y., Langeberg, L. K., . . . Scott, J. D. (2003). Ubiquitination regulates PSD-95 degradation and AMPA receptor surface expression. *Neuron, 40*(3), 595-607.

Collingridge, G. L., Isaac, J. T., & Wang, Y. T. (2004). Receptor trafficking and synaptic plasticity. *Nature Reviews.Neuroscience, 5*(12), 952-962. doi:10.1038/nrn1556

Constantine-Paton, M., & Cline, H. T. (1998). LTP and activity-dependent synaptogenesis: The more alike they are, the more different they become. *Current Opinion in Neurobiology, 8*(1), 139-148.

Coogan, A. N., O'Neill, L. A., & O'Connor, J. J. (1999). The P38 mitogen-activated protein kinase inhibitor SB203580 antagonizes the inhibitory effects of interleukin-1beta on long-term potentiation in the rat dentate gyrus in vitro. *Neuroscience, 93*(1), 57-69.

Cota, D., Proulx, K., Smith, K. A., Kozma, S. C., Thomas, G., Woods, S. C., et al. (2006). Hypothalamic mTOR signaling regulates food intake. *Science (New York, N.Y.), 312*(5775), 927-930. doi:10.1126/science.1124147

Cuvillier, O., & Levade, T. (2001). Sphingosine 1-phosphate antagonizes apoptosis of human leukemia cells by inhibiting release of cytochrome c and Smac/DIABLO from mitochondria. *Blood, 98*(9), 2828-2836.

Dai, Y., Wolfgang, M. J., Cha, S. H., & Lane, M. D. (2007). Localization and effect of ectopic expression of CPT1c in CNS feeding centers. *Biochemical and Biophysical Research Communications, 359*(3), 469-474. doi:10.1016/j.bbrc.2007.05.161

Dailey, M. E., & Smith, S. J. (1996). The dynamics of dendritic structure in developing hippocampal slices. *The Journal of Neuroscience : The Official Journal of the Society for Neuroscience, 16*(9), 2983-2994.

Dalva, M. B. (2009). Neuronal activity moves protein palmitoylation into the synapse. *The Journal of Cell Biology, 186*(1), 7-9. doi:10.1083/jcb.200906101

Darios, F., & Davletov, B. (2006). Omega-3 and omega-6 fatty acids stimulate cell membrane expansion by acting on syntaxin 3. *Nature, 440*(7085), 813-817. doi:10.1038/nature04598

Darios, F., Wasser, C., Shakirzyanova, A., Giniatullin, A., Goodman, K., Munoz-Bravo, J. L., . . . Davletov, B. (2009). Sphingosine facilitates SNARE complex assembly and activates synaptic vesicle exocytosis. *Neuron, 62*(5), 683-694. doi:10.1016/j.neuron.2009.04.024

Day, C. A., & Kenworthy, A. K. (2009). Tracking microdomain dynamics in cell membranes. *Biochimica Et Biophysica Acta, 1788*(1), 245-253. doi:10.1016/j.bbamem.2008.10.024

de la Monte, S. M., Tong, M., Nguyen, V., Setshedi, M., Longato, L., & Wands, J. R. (2010). Ceramide-mediated insulin resistance and impairment of cognitive-motor functions. *Journal of Alzheimer's Disease : JAD, 21*(3), 967-984. doi:10.3233/JAD-2010-091726

Degroote, S., Wolthoorn, J., & van Meer, G. (2004). The cell biology of glycosphingolipids. *Seminars in Cell & Developmental Biology, 15*(4), 375-387. doi:10.1016/j.semcdb.2004.03.007

Demaugre, F., Bonnefont, J. P., Cepanec, C., Scholte, J., Saudubray, J. M., & Leroux, J. P. (1990). Immunoquantitative analysis of human carnitine palmitoyltransferase I and II defects. *Pediatric Research, 27*(5), 497-500.

Diano, S., Farr, S. A., Benoit, S. C., McNay, E. C., da Silva, I., Horvath, B., . . . Horvath, T. L. (2006). Ghrelin controls hippocampal spine synapse density and memory performance. *Nature Neuroscience, 9*(3), 381-388. doi:10.1038/nn1656

Dong, H., O'Brien, R. J., Fung, E. T., Lanahan, A. A., Worley, P. F., & Huganir, R. L. (1997). GRIP: A synaptic PDZ domain-containing protein that interacts with AMPA receptors. *Nature, 386*(6622), 279-284. doi:10.1038/386279a0

Dunaevsky, A., Tashiro, A., Majewska, A., Mason, C., & Yuste, R. (1999). Developmental regulation of spine motility in the mammalian central nervous system. *Proceedings of the National Academy of Sciences of the United States of America, 96*(23), 13438-13443.

Ehlers, M. D. (2000). Reinsertion or degradation of AMPA receptors determined by activity-dependent endocytic sorting. *Neuron, 28*(2), 511-525.

el Bawab, S., Mao, C., Obeid, L. M., & Hannun, Y. A. (2002). Ceramidases in the regulation of ceramide levels and function. *Sub-Cellular Biochemistry, 36*, 187-205.

El-Husseini, A. E., Schnell, E., Chetkovich, D. M., Nicoll, R. A., & Bredt, D. S. (2000). PSD-95 involvement in maturation of excitatory synapses. *Science (New York, N.Y.), 290*(5495), 1364-1368.

Engert, F., & Bonhoeffer, T. (1999). Dendritic spine changes associated with hippocampal long-term synaptic plasticity. *Nature, 399*(6731), 66-70. doi:10.1038/19978

Esser, V., Brown, N. F., Cowan, A. T., Foster, D. W., & McGarry, J. D. (1996). Expression of a cDNA isolated from rat brown adipose tissue and heart identifies the product as the muscle isoform of carnitine palmitoyltransferase I (M-CPT I). M-CPT I is the predominant CPT I isoform expressed in both white (epididymal) and brown adipocytes. *The Journal of Biological Chemistry, 271*(12), 6972-6977.

Essmann, C. L., Martinez, E., Geiger, J. C., Zimmer, M., Traut, M. H., Stein, V., . . . Acker-Palmer, A. (2008). Serine phosphorylation of ephrinB2 regulates trafficking of synaptic AMPA receptors. *Nature Neuroscience, 11*(9), 1035-1043. doi:10.1038/nn.2171

Farr, S. A., Yamada, K. A., Butterfield, D. A., Abdul, H. M., Xu, L., Miller, N. E., . . . Morley, J. E. (2008). Obesity and hypertriglyceridemia produce cognitive impairment. *Endocrinology, 149*(5), 2628-2636. doi:10.1210/en.2007-1722

Fasano, C., Miolan, J. P., & Niel, J. P. (2003). Modulation by C2 ceramide of the nicotinic transmission within the coeliac ganglion in the rabbit. *Neuroscience, 116*(3), 753-759.

Fath, T., Ke, Y. D., Gunning, P., Gotz, J., & Ittner, L. M. (2009). Primary support cultures of hippocampal and substantia nigra neurons. *Nature Protocols, 4*(1), 78-85. doi:10.1038/nprot.2008.199

Ferdinandusse, S., Mulders, J., IJlst, L., Denis, S., Dacremont, G., Waterham, H. R., & Wanders, R. J. (1999). Molecular cloning and expression of human carnitine octanoyltransferase: Evidence for its role in the peroxisomal beta-oxidation of branched-chain fatty acids. *Biochemical and Biophysical Research Communications, 263*(1), 213-218. doi:10.1006/bbrc.1999.1340

Fiala, J. C., Feinberg, M., Popov, V., & Harris, K. M. (1998). Synaptogenesis via dendritic filopodia in developing hippocampal area CA1. *The Journal of Neuroscience : The Official Journal of the Society for Neuroscience, 18*(21), 8900-8911.

Fifkova, E., & Delay, R. J. (1982). Cytoplasmic actin in neuronal processes as a possible mediator of synaptic plasticity. *The Journal of Cell Biology, 95*(1), 345-350.

Finn, P. F., & Dice, J. F. (2006). Proteolytic and lipolytic responses to starvation. *Nutrition (Burbank, Los Angeles County, Calif.), 22*(7-8), 830-844. doi:10.1016/j.nut.2006.04.008

Fischer, M., Kaech, S., Knutti, D., & Matus, A. (1998). Rapid actin-based plasticity in dendritic spines. *Neuron, 20*(5), 847-854.

Frank, C., Giammarioli, A. M., Pepponi, R., Fiorentini, C., & Rufini, S. (2004). Cholesterol perturbing agents inhibit NMDA-dependent calcium influx in rat hippocampal primary culture. *FEBS Letters, 566*(1-3), 25-29. doi:10.1016/j.febslet.2004.03.113

Fraser, F., Corstorphine, C. G., & Zammit, V. A. (1997). Topology of carnitine palmitoyltransferase I in the mitochondrial outer membrane. *The Biochemical Journal, 323 (Pt 3)*(Pt 3), 711-718.

Furukawa, K., & Mattson, M. P. (1998). The transcription factor NF-kappaB mediates increases in calcium currents and decreases in NMDA- and AMPA/kainate-induced currents induced by tumor necrosis factor-alpha in hippocampal neurons. *Journal of Neurochemistry, 70*(5), 1876-1886.

Furuya, S., Mitoma, J., Makino, A., & Hirabayashi, Y. (1998). Ceramide and its interconvertible metabolite sphingosine function as indispensable lipid factors involved in survival and dendritic differentiation of cerebellar purkinje cells. *Journal of Neurochemistry, 71*(1), 366-377.

Futerman, A. H., Stieger, B., Hubbard, A. L., & Pagano, R. E. (1990). Sphingomyelin synthesis in rat liver occurs predominantly at the cis and medial cisternae of the golgi apparatus. *The Journal of Biological Chemistry, 265*(15), 8650-8657.

Gao, S., & Lane, M. D. (2003). Effect of the anorectic fatty acid synthase inhibitor C75 on neuronal activity in the hypothalamus and brainstem. *Proceedings of the National Academy of Sciences of the United States of America, 100*(10), 5628-5633. doi:10.1073/pnas.1031698100

Gao, S., Kinzig, K. P., Aja, S., Scott, K. A., Keung, W., Kelly, S., . . . Moran, T. H. (2007). Leptin activates hypothalamic acetyl-CoA carboxylase to inhibit food intake. *Proceedings of the National Academy of Sciences of the United States of America, 104*(44), 17358-17363. doi:10.1073/pnas.0708385104

Gao, S., Zhu, G., Gao, X., Wu, D., Carrasco, P., Casals, N., . . . Lopaschuk, G. D. (2011). Important roles of brain-specific carnitine palmitoyltransferase and ceramide metabolism in leptin hypothalamic control of feeding. *Proceedings of the National Academy of Sciences of the United States of America, 108*(23), 9691-9696. doi:10.1073/pnas.1103267108

Gao, X. F., Chen, W., Kong, X. P., Xu, A. M., Wang, Z. G., Sweeney, G., & Wu, D. (2009). Enhanced susceptibility of Cpt1c knockout mice to glucose intolerance induced by a high-fat diet involves elevated hepatic gluconeogenesis and decreased skeletal muscle glucose uptake. *Diabetologia, 52*(5), 912-920. doi:10.1007/s00125-009-1284-0

Gerlai, R., Henderson, J. T., Roder, J. C., & Jia, Z. (1998). Multiple behavioral anomalies in GluR2 mutant mice exhibiting enhanced LTP. *Behavioural Brain Research, 95*(1), 37-45.

Gerrow, K., Romorini, S., Nabi, S. M., Colicos, M. A., Sala, C., & El-Husseini, A. (2006). A preformed complex of postsynaptic proteins is involved in excitatory synapse development. *Neuron, 49*(4), 547-562. doi:10.1016/j.neuron.2006.01.015

Ghidoni, R., Sala, G., & Giuliani, A. (1999). Use of sphingolipid analogs: Benefits and risks. *Biochimica Et Biophysica Acta, 1439*(1), 17-39.

Goni, F. M., & Alonso, A. (2002). Sphingomyelinases: Enzymology and membrane activity. *FEBS Letters, 531*(1), 38-46.

Gooding, J. M., Shayeghi, M., & Saggerson, E. D. (2004). Membrane transport of fatty acylcarnitine and free L-carnitine by rat liver microsomes. *European Journal of Biochemistry / FEBS, 271*(5), 954-961.

Goodman, Y., & Mattson, M. P. (1996). Ceramide protects hippocampal neurons against excitotoxic and oxidative insults, and amyloid beta-peptide toxicity. *Journal of Neurochemistry, 66*(2), 869-872.

GRAY, E. G., & GUILLERY, R. W. (1963). A note on the dendritic spine apparatus. *Journal of Anatomy, 97*, 389-392.

Greger, I. H., Khatri, L., Kong, X., & Ziff, E. B. (2003). AMPA receptor tetramerization is mediated by Q/R editing. *Neuron, 40*(4), 763-774.

Grutzendler, J., Kasthuri, N., & Gan, W. B. (2002). Long-term dendritic spine stability in the adult cortex. *Nature, 420*(6917), 812-816. doi:10.1038/nature01276

Hanley, J. G. (2008). PICK1: A multi-talented modulator of AMPA receptor trafficking. *Pharmacology & Therapeutics, 118*(1), 152-160. doi:10.1016/j.pharmthera.2008.02.002

Hanley, J. G., & Henley, J. M. (2005). PICK1 is a calcium-sensor for NMDA-induced AMPA receptor trafficking. *The EMBO Journal, 24*(18), 3266-3278. doi:10.1038/sj.emboj.7600801

Hanley, J. G., Khatri, L., Hanson, P. I., & Ziff, E. B. (2002). NSF ATPase and alpha-/beta-SNAPs disassemble the AMPA receptor-PICK1 complex. *Neuron, 34*(1), 53-67.

Hannun, Y. A. (1994). The sphingomyelin cycle and the second messenger function of ceramide. *The Journal of Biological Chemistry, 269*(5), 3125-3128.

Hannun, Y. A. (1996). Functions of ceramide in coordinating cellular responses to stress. *Science (New York, N.Y.), 274*(5294), 1855-1859.

Hannun, Y. A., & Luberto, C. (2000). Ceramide in the eukaryotic stress response. *Trends in Cell Biology, 10*(2), 73-80.

Hannun, Y. A., & Obeid, L. M. (2008). Principles of bioactive lipid signalling: Lessons from sphingolipids. *Nature Reviews.Molecular Cell Biology, 9*(2), 139-150. doi:10.1038/nrm2329

Harms, K. J., & Dunaevsky, A. (2007). Dendritic spine plasticity: Looking beyond development. *Brain Research, 1184*, 65-71. doi:10.1016/j.brainres.2006.02.094

Harvey, J. (2007). Leptin regulation of neuronal excitability and cognitive function. *Current Opinion in Pharmacology, 7*(6), 643-647. doi:10.1016/j.coph.2007.10.006

Hayashi, Y., Shi, S. H., Esteban, J. A., Piccini, A., Poncer, J. C., & Malinow, R. (2000). Driving AMPA receptors into synapses by LTP and CaMKII: Requirement for GluR1 and PDZ domain interaction. *Science (New York, N.Y.), 287*(5461), 2262-2267.

Hering, H., & Sheng, M. (2001). Dendritic spines: Structure, dynamics and regulation. *Nature Reviews.Neuroscience, 2*(12), 880-888. doi:10.1038/35104061

Hering, H., Lin, C. C., & Sheng, M. (2003). Lipid rafts in the maintenance of synapses, dendritic spines, and surface AMPA receptor stability. *The Journal of Neuroscience : The Official Journal of the Society for Neuroscience, 23*(8), 3262-3271.

Hinkovska-Galcheva, V., Boxer, L. A., Kindzelskii, A., Hiraoka, M., Abe, A., Goparju, S., . . . Shayman, J. A. (2005). Ceramide 1-phosphate, a mediator of phagocytosis. *The Journal of Biological Chemistry, 280*(28), 26612-26621. doi:10.1074/jbc.M501359200

Hirokawa, N., & Takemura, R. (2005). Molecular motors and mechanisms of directional transport in neurons. *Nature Reviews.Neuroscience, 6*(3), 201-214. doi:10.1038/nrn1624

Hla, T. (2004). Physiological and pathological actions of sphingosine 1-phosphate. *Seminars in Cell & Developmental Biology, 15*(5), 513-520. doi:10.1016/j.semcdb.2004.05.002

Hollmann, M., & Heinemann, S. (1994). Cloned glutamate receptors. *Annual Review of Neuroscience, 17*, 31-108. doi:10.1146/annurev.ne.17.030194.000335

Hollmann, M., Hartley, M., & Heinemann, S. (1991). Ca2+ permeability of KA-AMPA--gated glutamate receptor channels depends on subunit composition. *Science (New York, N.Y.), 252*(5007), 851-853.

Holtmaat, A., Wilbrecht, L., Knott, G. W., Welker, E., & Svoboda, K. (2006). Experience-dependent and cell-type-specific spine growth in the neocortex. *Nature, 441*(7096), 979-983. doi:10.1038/nature04783.

Horvath, T. L., Andrews, Z. B., & Diano, S. (2009). Fuel utilization by hypothalamic neurons: Roles for ROS. *Trends in Endocrinology and Metabolism: TEM, 20*(2), 78-87. doi:10.1016/j.tem.2008.10.003

Huang, K., & El-Husseini, A. (2005). Modulation of neuronal protein trafficking and function by palmitoylation. *Current Opinion in Neurobiology, 15*(5), 527-535. doi:10.1016/j.conb.2005.08.001

Hu, Z., Cha, S. H., Chohnan, S., & Lane, M. D. (2003). Hypothalamic malonyl-CoA as a mediator of feeding behaviour. *Proceedings of the National Academy of Sciences of the United States of America, 100*(22), 12624-12629. doi:10.1073/pnas.1834402100

Ito, A., & Horigome, K. (1995). Ceramide prevents neuronal programmed cell death induced by nerve growth factor deprivation. *Journal of Neurochemistry, 65*(1), 463-466.

Jauregui, O., Sierra, A. Y., Carrasco, P., Gratacos, E., Hegardt, F. G., & Casals, N. (2007). A new LC-ESI-MS/MS method to measure long-chain acylcarnitine levels in cultured cells. *Analytica Chimica Acta, 599*(1), 1-6. doi:10.1016/j.aca.2007.07.066

Jeon, H. J., Lee, D. H., Kang, M. S., Lee, M. O., Jung, K. M., Jung, S. Y., & Kim, D. K. (2005). Dopamine release in PC12 cells is mediated by ca(2+)-dependent production of ceramide via sphingomyelin pathway. *Journal of Neurochemistry, 95*(3), 811-820. doi:10.1111/j.1471-4159.2005.03403.x

Jia, Z., Agopyan, N., Miu, P., Xiong, Z., Henderson, J., Gerlai, R., . . . Roder, J. (1996). Enhanced LTP in mice deficient in the AMPA receptor GluR2. *Neuron, 17*(5), 945-956.

Kajimoto, T., Okada, T., Yu, H., Goparaju, S. K., Jahangeer, S., & Nakamura, S. (2007). Involvement of sphingosine-1-phosphate in glutamate secretion in hippocampal neurons. *Molecular and Cellular Biology, 27*(9), 3429-3440. doi:10.1128/MCB.01465-06

Kahn, B. B., Alquier, T., Carling, D., & Hardie, D. G. (2005). AMP-activated protein kinase: Ancient energy gauge provides clues to modern understanding of metabolism. *Cell Metabolism, 1*(1), 15-25. doi:10.1016/j.cmet.2004.12.003

Kasai, H., Fukuda, M., Watanabe, S., Hayashi-Takagi, A., & Noguchi, J. (2010). Structural dynamics of dendritic spines in memory and cognition. *Trends in Neurosciences, 33*(3), 121-129. doi:10.1016/j.tins.2010.01.001

Kim, E., & Sheng, M. (2004). PDZ domain proteins of synapses. *Nature Reviews.Neuroscience, 5*(10), 771-781. doi:10.1038/nrn1517

Knott, G. W., Holtmaat, A., Wilbrecht, L., Welker, E., & Svoboda, K. (2006). Spine growth precedes synapse formation in the adult neocortex in vivo. *Nature Neuroscience, 9*(9), 1117-1124. doi:10.1038/nn1747

Kolesnick, R. (2002). The therapeutic potential of modulating the ceramide/sphingomyelin pathway. *The Journal of Clinical Investigation, 110*(1), 3-8. doi:10.1172/JCI16127

Kolesnick, R. N., & Kronke, M. (1998). Regulation of ceramide production and apoptosis. *Annual Review of Physiology, 60*, 643-665. doi:10.1146/annurev.physiol.60.1.643

Lavrentyev, E. N., Matta, S. G., & Cook, G. A. (2004). Expression of three carnitine palmitoyltransferase-I isoforms in 10 regions of the rat brain during feeding, fasting, and diabetes. *Biochemical and Biophysical Research Communications, 315*(1), 174-178. doi:10.1016/j.bbrc.2004.01.040.

Lahiri, S., & Futerman, A. H. (2005). LASS5 is a bona fide dihydroceramide synthase that selectively utilizes palmitoyl-CoA as acyl donor. *The Journal of Biological Chemistry, 280*(40), 33735-33738. doi:10.1074/jbc.M506485200.

Lee, S. H., Simonetta, A., & Sheng, M. (2004). Subunit rules governing the sorting of internalized AMPA receptors in hippocampal neurons. *Neuron, 43*(2), 221-236. doi:10.1016/j.neuron.2004.06.015

Leonard, A. S., Davare, M. A., Horne, M. C., Garner, C. C., & Hell, J. W. (1998). SAP97 is associated with the alpha-amino-3-hydroxy-5-methylisoxazole-4-propionic acid receptor GluR1 subunit. *The Journal of Biological Chemistry, 273*(31), 19518-19524.

Lerma, J. (2006). Kainate receptor physiology. *Current Opinion in Pharmacology, 6*(1), 89-97. doi:10.1016/j.coph.2005.08.004

Levade, T., & Jaffrezou, J. P. (1999). Signalling sphingomyelinases: Which, where, how and why? *Biochimica Et Biophysica Acta, 1438*(1), 1-17.

Lindqvist, A., Mohapel, P., Bouter, B., Frielingsdorf, H., Pizzo, D., Brundin, P., & Erlanson-Albertsson, C. (2006). High-fat diet impairs hippocampal neurogenesis in male rats. *European Journal of Neurology : The Official Journal of the European Federation of Neurological Societies, 13*(12), 1385-1388. doi:10.1111/j.1468-1331.2006.01500.x

Lippman, J., & Dunaevsky, A. (2005). Dendritic spine morphogenesis and plasticity. *Journal of Neurobiology, 64*(1), 47-57. doi:10.1002/neu.20149

Lohse, I., Reilly, P., & Zaugg, K. (2011). The CPT1C 5'UTR contains a repressing upstream open reading frame that is regulated by cellular energy availability and AMPK. *PloS One, 6*(9), e21486. doi:10.1371/journal.pone.0021486

Lopez, M., Lage, R., Saha, A. K., Perez-Tilve, D., Vazquez, M. J., Varela, L., . . . Vidal-Puig, A. (2008). Hypothalamic fatty acid metabolism mediates the orexigenic action of ghrelin. *Cell Metabolism, 7*(5), 389-399. doi:10.1016/j.cmet.2008.03.006

Lopez, M., Lelliott, C. J., & Vidal-Puig, A. (2007). Hypothalamic fatty acid metabolism: A housekeeping pathway that regulates food intake. *BioEssays : News and Reviews in Molecular, Cellular and Developmental Biology, 29*(3), 248-261. doi:10.1002/bies.20539

Lopez-Vinas, E., Bentebibel, A., Gurunathan, C., Morillas, M., de Arriaga, D., Serra, D., . . . Gomez-Puertas, P. (2007). Definition by functional and structural analysis of two malonyl-CoA sites in carnitine palmitoyltransferase 1A. *The Journal of Biological Chemistry, 282*(25), 18212-18224. doi:10.1074/jbc.M700885200

Luberto, C., Kraveka, J. M., & Hannun, Y. A. (2002). Ceramide regulation of apoptosis versus differentiation: A walk on a fine line. lessons from neurobiology. *Neurochemical Research, 27*(7-8), 609-617.

Mainen, Z. F., Jia, Z., Roder, J., & Malinow, R. (1998). Use-dependent AMPA receptor block in mice lacking GluR2 suggests postsynaptic site for LTP expression. *Nature Neuroscience, 1*(7), 579-586. doi:10.1038/2812

Majewska, A. K., Newton, J. R., & Sur, M. (2006). Remodeling of synaptic structure in sensory cortical areas in vivo. *The Journal of Neuroscience : The Official Journal of the Society for Neuroscience, 26*(11), 3021-3029. doi:10.1523/JNEUROSCI.4454-05.2006

Malisan, F., & Testi, R. (2002). GD3 ganglioside and apoptosis. *Biochimica Et Biophysica Acta, 1585*(2-3), 179-187.

Marchesini, N., & Hannun, Y. A. (2004). Acid and neutral sphingomyelinases: Roles and mechanisms of regulation. *Biochemistry and Cell Biology = Biochimie Et Biologie Cellulaire, 82*(1), 27-44. doi:10.1139/o03-091

Marchesini, N., Jones, J. A., & Hannun, Y. A. (2007). Confluence induced threonine41/serine45 phospho-beta-catenin dephosphorylation via ceramide-mediated activation of PP1cgamma. *Biochimica Et Biophysica Acta, 1771*(12), 1418-1428. doi:10.1016/j.bbalip.2007.10.003

Marin-Padilla, M. (1972). Structural abnormalities of the cerebral cortex in human chromosomal aberrations: A golgi study. *Brain Research, 44*(2), 625-629.

Marrs, G. S., Green, S. H., & Dailey, M. E. (2001). Rapid formation and remodeling of postsynaptic densities in developing dendrites. *Nature Neuroscience, 4*(10), 1006-1013. doi:10.1038/nn717

Marza, E., & Lesa, G. M. (2006). Polyunsaturated fatty acids and neurotransmission in caenorhabditis elegans. *Biochemical Society Transactions, 34*(Pt 1), 77-80. doi:10.1042/BST0340077

Matsuda, S., Mikawa, S., & Hirai, H. (1999). Phosphorylation of serine-880 in GluR2 by protein kinase C prevents its C terminus from binding with glutamate receptor-interacting protein. *Journal of Neurochemistry, 73*(4), 1765-1768.

Matsuzaki, M., Ellis-Davies, G. C., Nemoto, T., Miyashita, Y., Iino, M., & Kasai, H. (2001). Dendritic spine geometry is critical for AMPA receptor expression in hippocampal CA1 pyramidal neurons. *Nature Neuroscience, 4*(11), 1086-1092. doi:10.1038/nn736

Matus, A., Ackermann, M., Pehling, G., Byers, H. R., & Fujiwara, K. (1982). High actin concentrations in brain dendritic spines and postsynaptic densities. *Proceedings of the National Academy of Sciences of the United States of America, 79*(23), 7590-7594.

McGarry, J. D., & Brown, N. F. (1997). The mitochondrial carnitine palmitoyltransferase system. from concept to molecular analysis. *European Journal of Biochemistry / FEBS, 244*(1), 1-14.

McGarry, J. D., & Foster, D. W. (1980). Regulation of hepatic fatty acid oxidation and ketone body production. *Annual Review of Biochemistry, 49*, 395-420. doi:10.1146/annurev.bi.49.070180.002143

McGarry, J. D., Mills, S. E., Long, C. S., & Foster, D. W. (1983). Observations on the affinity for carnitine, and malonyl-CoA sensitivity, of carnitine palmitoyltransferase I in animal and human tissues. demonstration of the presence of malonyl-CoA in non-hepatic tissues of the rat. *The Biochemical Journal, 214*(1), 21-28.

McGarry, J. D., Woeltje, K. F., Kuwajima, M., & Foster, D. W. (1989). Regulation of ketogenesis and the renaissance of carnitine palmitoyltransferase. *Diabetes/metabolism Reviews, 5*(3), 271-284.

Meloni, I., Parri, V., De Filippis, R., Ariani, F., Artuso, R., Bruttini, M., . . . Renieri, A. (2009). The XLMR gene ACSL4 plays a role in dendritic spine architecture. *Neuroscience, 159*(2), 657-669. doi:10.1016/j.neuroscience.2008.11.056

Meng, Y., Zhang, Y., & Jia, Z. (2003). Synaptic transmission and plasticity in the absence of AMPA glutamate receptor GluR2 and GluR3. *Neuron, 39*(1), 163-176.

Mitoma, J., Ito, M., Furuya, S., & Hirabayashi, Y. (1998). Bipotential roles of ceramide in the growth of hippocampal neurons: Promotion of cell survival and dendritic outgrowth in dose- and developmental stage-dependent manners. *Journal of Neuroscience Research, 51*(6), 712-722.

Mitsutake, S., Kim, T. J., Inagaki, Y., Kato, M., Yamashita, T., & Igarashi, Y. (2004). Ceramide kinase is a mediator of calcium-dependent degranulation in mast cells. *The Journal of Biological Chemistry, 279*(17), 17570-17577. doi:10.1074/jbc.M312885200

Mizutani, Y., Kihara, A., & Igarashi, Y. (2005). Mammalian Lass6 and its related family members regulate synthesis of specific ceramides. *The Biochemical Journal, 390*(Pt 1), 263-271. doi:10.1042/BJ20050291

Mizutani, Y., Kihara, A., & Igarashi, Y. (2006). LASS3 (longevity assurance homologue 3) is a mainly testis-specific (dihydro)ceramide synthase with relatively broad substrate specificity. *The Biochemical Journal, 398*(3), 531-538. doi:10.1042/BJ20060379

Monyer, H., Burnashev, N., Laurie, D. J., Sakmann, B., & Seeburg, P. H. (1994). Developmental and regional expression in the rat brain and functional properties of four NMDA receptors. *Neuron, 12*(3), 529-540.

Morillas, M., Gomez-Puertas, P., Roca, R., Serra, D., Asins, G., Valencia, A., & Hegardt, F. G. (2001). Structural model of the catalytic core of carnitine palmitoyltransferase I and carnitine octanoyltransferase (COT): Mutation of CPT I histidine 473 and alanine 381 and COT alanine 238 impairs the catalytic activity. *The Journal of Biological Chemistry, 276*(48), 45001-45008. doi:10.1074/jbc.M106920200

Morrison, C. D., Xi, X., White, C. L., Ye, J., & Martin, R. J. (2007). Amino acids inhibit agrp gene expression via an mTOR-dependent mechanism. *American Journal of Physiology.Endocrinology and Metabolism, 293*(1), E165-71. doi:10.1152/ajpendo.00675.2006

Mousavi, S. A., Malerod, L., Berg, T., & Kjeken, R. (2004). Clathrin-dependent endocytosis. *The Biochemical Journal, 377*(Pt 1), 1-16. doi:10.1042/BJ20031000

Nakanishi, S. (1992). Molecular diversity of glutamate receptors and implications for brain function. *Science (New York, N.Y.), 258*(5082), 597-603.

Nichols, B. J., Kenworthy, A. K., Polishchuk, R. S., Lodge, R., Roberts, T. H., Hirschberg, K., . . . Lippincott-Schwartz, J. (2001). Rapid cycling of lipid raft markers between the cell surface and golgi complex. *The Journal of Cell Biology, 153*(3), 529-541.

Nicoll, R. A., Tomita, S., & Bredt, D. S. (2006). Auxiliary subunits assist AMPA-type glutamate receptors. *Science (New York, N.Y.), 311*(5765), 1253-1256. doi:10.1126/science.1123339

Nishimune, A., Isaac, J. T., Molnar, E., Noel, J., Nash, S. R., Tagaya, M., . . . Henley, J. M. (1998). NSF binding to GluR2 regulates synaptic transmission. *Neuron, 21*(1), 87-97.

Numakawa, T., Nakayama, H., Suzuki, S., Kubo, T., Nara, F., Numakawa, Y., . . . Taguchi, T. (2003). Nerve growth factor-induced glutamate release is via p75 receptor, ceramide, and ca(2+) from ryanodine receptor in developing cerebellar neurons. *The Journal of Biological Chemistry, 278*(42), 41259-41269. doi:10.1074/jbc.M304409200

Obeid, L. M., Linardic, C. M., Karolak, L. A., & Hannun, Y. A. (1993). Programmed cell death induced by ceramide. *Science (New York, N.Y.), 259*(5102), 1769-1771.

Obici, S., Feng, Z., Arduini, A., Conti, R., & Rossetti, L. (2003). Inhibition of hypothalamic carnitine palmitoyltransferase-1 decreases food intake and glucose production. *Nature Medicine, 9*(6), 756-761. doi:10.1038/nm873

Ogretmen, B., Pettus, B. J., Rossi, M. J., Wood, R., Usta, J., Szulc, Z., . . . Hannun, Y. A. (2002). Biochemical mechanisms of the generation of endogenous long chain ceramide in response to exogenous short chain ceramide in the A549 human lung adenocarcinoma cell line. role for endogenous ceramide in mediating the action of exogenous ceramide. *The Journal of Biological Chemistry, 277*(15), 12960-12969. doi:10.1074/jbc.M110699200

Okabe, S., Miwa, A., & Okado, H. (2001). Spine formation and correlated assembly of presynaptic and postsynaptic molecules. *The Journal of Neuroscience : The Official Journal of the Society for Neuroscience, 21*(16), 6105-6114.

Okamoto, P. M., Gamby, C., Wells, D., Fallon, J., & Vallee, R. B. (2001). Dynamin isoform-specific interaction with the shank/ProSAP scaffolding proteins of the postsynaptic density and actin cytoskeleton. *The Journal of Biological Chemistry, 276*(51), 48458-48465. doi:10.1074/jbc.M104927200

Obici, S., Feng, Z., Arduini, A., Conti, R., & Rossetti, L. (2003). Inhibition of hypothalamic carnitine palmitoyltransferase-1 decreases food intake and glucose production. *Nature Medicine, 9*(6), 756-761. doi:10.1038/nm873

Osten, P., Khatri, L., Perez, J. L., Kohr, G., Giese, G., Daly, C., . . . Ziff, E. B. (2000). Mutagenesis reveals a role for ABP/GRIP binding to GluR2 in synaptic surface accumulation of the AMPA receptor. *Neuron, 27*(2), 313-325.

Ostroff, L. E., Fiala, J. C., Allwardt, B., & Harris, K. M. (2002). Polyribosomes redistribute from dendritic shafts into spines with enlarged synapses during LTP in developing rat hippocampal slices. *Neuron, 35*(3), 535-545.

Owen, D. M., Williamson, D., Rentero, C., & Gaus, K. (2009). Quantitative microscopy: Protein dynamics and membrane organisation. *Traffic (Copenhagen, Denmark), 10*(8), 962-971. doi:10.1111/j.1600-0854.2009.00908.x

Park, M., Penick, E. C., Edwards, J. G., Kauer, J. A., & Ehlers, M. D. (2004). Recycling endosomes supply AMPA receptors for LTP. *Science (New York, N.Y.), 305*(5692), 1972-1975. doi:10.1126/science.1102026

Park, M., Salgado, J. M., Ostroff, L., Helton, T. D., Robinson, C. G., Harris, K. M., & Ehlers, M. D. (2006). Plasticity-induced growth of dendritic spines by exocytic trafficking from recycling endosomes. *Neuron, 52*(5), 817-830. doi:10.1016/j.neuron.2006.09.040

Parnass, Z., Tashiro, A., & Yuste, R. (2000). Analysis of spine morphological plasticity in developing hippocampal pyramidal neurons. *Hippocampus, 10*(5), 561-568. doi:2-X

Patrick, G. N., Bingol, B., Weld, H. A., & Schuman, E. M. (2003). Ubiquitin-mediated proteasome activity is required for agonist-induced endocytosis of GluRs. *Current Biology : CB, 13*(23), 2073-2081.

Perestenko, P. V., & Henley, J. M. (2003). Characterization of the intracellular transport of GluR1 and GluR2 alpha-amino-3-hydroxy-5-methyl-4-isoxazole propionic acid receptor subunits in hippocampal neurons. *The Journal of Biological Chemistry, 278*(44), 43525-43532. doi:10.1074/jbc.M306206200

Petralia, R. S., Wang, Y. X., Sans, N., Worley, P. F., Hammer, J. A.,3rd, & Wenthold, R. J. (2001). Glutamate receptor targeting in the postsynaptic spine involves mechanisms that are independent of myosin va. *The European Journal of Neuroscience, 13*(9), 1722-1732.

Pettus, B. J., Chalfant, C. E., & Hannun, Y. A. (2002). Ceramide in apoptosis: An overview and current perspectives. *Biochimica Et Biophysica Acta, 1585*(2-3), 114-125.

Ping, S. E., & Barrett, G. L. (1998). Ceramide can induce cell death in sensory neurons, whereas ceramide analogues and sphingosine promote survival. *Journal of Neuroscience Research, 54*(2), 206-213.

Prange, O., & Murphy, T. H. (2001). Modular transport of postsynaptic density-95 clusters and association with stable spine precursors during early development of cortical neurons. *The Journal of Neuroscience : The Official Journal of the Society for Neuroscience, 21*(23), 9325-9333.

Price, N., van der Leij, F., Jackson, V., Corstorphine, C., Thomson, R., Sorensen, A., & Zammit, V. (2002). A novel brain-expressed protein related to carnitine palmitoyltransferase I. *Genomics, 80*(4), 433-442.

Ramon y Cajal, S. (1981). Procedures in current practice. the classic: On the writing of scientific papers. *Clinical Orthopaedics and Related Research, (155)*(155), 1-6.

Reamy, A. A., & Wolfgang, M. J. (2011). Carnitine palmitoyltransferase-1c gain-of-function in the brain results in postnatal microencephaly. *Journal of Neurochemistry, 118*(3), 388-398. doi:10.1111/j.1471-4159.2011.07312.x; 10.1111/j.1471-4159.2011.07312.x

Riboni, L., Prinetti, A., Bassi, R., Caminiti, A., & Tettamanti, G. (1995). A mediator role of ceramide in the regulation of neuroblastoma Neuro2a cell differentiation. *The Journal of Biological Chemistry, 270*(45), 26868-26875.

Riebeling, C., Allegood, J. C., Wang, E., Merrill, A. H.,Jr, & Futerman, A. H. (2003). Two mammalian longevity assurance gene (LAG1) family members, trh1 and trh4, regulate dihydroceramide synthesis using different fatty acyl-CoA donors. *The Journal of Biological Chemistry, 278*(44), 43452-43459. doi:10.1074/jbc.M307104200

Rohrbough, J., Rushton, E., Palanker, L., Woodruff, E., Matthies, H. J., Acharya, U., . . . Broadie, K. (2004). Ceramidase regulates synaptic vesicle exocytosis and trafficking. *The Journal of Neuroscience : The Official Journal of the Society for Neuroscience, 24*(36), 7789-7803. doi:10.1523/JNEUROSCI.1146-04.2004

Rufer, A. C., Thoma, R., & Hennig, M. (2009). Structural insight into function and regulation of carnitine palmitoyltransferase. *Cellular and Molecular Life Sciences : CMLS, 66*(15), 2489-2501. doi:10.1007/s00018-009-0035-1

Salaun, C., Greaves, J., & Chamberlain, L. H. (2010). The intracellular dynamic of protein palmitoylation. *The Journal of Cell Biology, 191*(7), 1229-1238. doi:10.1083/jcb.201008160

Sans, N., Racca, C., Petralia, R. S., Wang, Y. X., McCallum, J., & Wenthold, R. J. (2001). Synapse-associated protein 97 selectively associates with a subset of AMPA receptors early in their biosynthetic pathway. *The Journal of Neuroscience : The Official Journal of the Society for Neuroscience, 21*(19), 7506-7516.

Schikorski, T., & Stevens, C. F. (1997). Quantitative ultrastructural analysis of hippocampal excitatory synapses. *The Journal of Neuroscience : The Official Journal of the Society for Neuroscience, 17*(15), 5858-5867.

Shen, L., Liang, F., Walensky, L. D., & Huganir, R. L. (2000). Regulation of AMPA receptor GluR1 subunit surface expression by a 4. 1N-linked actin cytoskeletal association. *The Journal of Neuroscience : The Official Journal of the Society for Neuroscience, 20*(21), 7932-7940.

Sierra, A. Y., Gratacos, E., Carrasco, P., Clotet, J., Urena, J., Serra, D., . . . Casals, N. (2008). CPT1c is localized in endoplasmic reticulum of neurons and has carnitine palmitoyltransferase activity. *The Journal of*

Biological Chemistry, 283(11), 6878-6885. doi:10.1074/jbc.M707965200

Smith, E. R., Merrill, A. H., Obeid, L. M., & Hannun, Y. A. (2000). Effects of sphingosine and other sphingolipids on protein kinase C. *Methods in Enzymology, 312*, 361-373.

Sommer, B., Keinanen, K., Verdoorn, T. A., Wisden, W., Burnashev, N., Herb, A., . . . Seeburg, P. H. (1990). Flip and flop: A cell-specific functional switch in glutamate-operated channels of the CNS. *Science (New York, N.Y.), 249*(4976), 1580-1585.

Song, I., & Huganir, R. L. (2002). Regulation of AMPA receptors during synaptic plasticity. *Trends in Neurosciences, 25*(11), 578-588.

Sorensen, A., Travers, M. T., Vernon, R. G., Price, N. T., & Barber, M. C. (2002). Localization of messenger RNAs encoding enzymes associated with malonyl-CoA metabolism in mouse brain. *Brain Research.Gene Expression Patterns, 1*(3-4), 167-173.

Spiegel, S., & Milstien, S. (2003). Sphingosine-1-phosphate: An enigmatic signalling lipid. *Nature Reviews.Molecular Cell Biology, 4*(5), 397-407. doi:10.1038/nrm1103

Spiegel, S., Cuvillier, O., Edsall, L. C., Kohama, T., Menzeleev, R., Olah, Z., . . . Wang, F. (1998). Sphingosine-1-phosphate in cell growth and cell death. *Annals of the New York Academy of Sciences, 845*, 11-18.

Stahelin, R. V. (2009). Lipid binding domains: More than simple lipid effectors. *Journal of Lipid Research, 50 Suppl*, S299-304. doi:10.1194/jlr.R800078-JLR200

Swartz, K. J. (2008). Sensing voltage across lipid membranes. *Nature, 456*(7224), 891-897. doi:10.1038/nature07620

Tabatadze, N., Savonenko, A., Song, H., Bandaru, V. V., Chu, M., & Haughey, N. J. (2010). Inhibition of neutral sphingomyelinase-2 perturbs brain sphingolipid balance and spatial memory in mice. *Journal of Neuroscience Research, 88*(13), 2940-2951. doi:10.1002/jnr.22438

Takeda, S., Mitsutake, S., Tsuji, K., & Igarashi, Y. (2006). Apoptosis occurs via the ceramide recycling pathway in human HaCaT keratinocytes. *Journal of Biochemistry, 139*(2), 255-262. doi:10.1093/jb/mvj026

Terry-Lorenzo, R. T., Roadcap, D. W., Otsuka, T., Blanpied, T. A., Zamorano, P. L., Garner, C. C., . . . Ehlers, M. D. (2005). Neurabin/protein phosphatase-1 complex regulates dendritic spine morphogenesis and maturation. *Molecular Biology of the Cell, 16*(5), 2349-2362. doi:10.1091/mbc.E04-12-1054

Tettamanti, G., & Riboni, L. (1994). Gangliosides turnover and neural cells function: A new perspective. *Progress in Brain Research, 101*, 77-100.

Toman, R. E., Spiegel, S., & Faden, A. I. (2000). Role of ceramide in neuronal cell death and differentiation. *Journal of Neurotrauma, 17*(10), 891-898.

Tomita, S., Adesnik, H., Sekiguchi, M., Zhang, W., Wada, K., Howe, J. R., . . . Bredt, D. S. (2005). Stargazin modulates AMPA receptor gating and trafficking by distinct domains. *Nature, 435*(7045), 1052-1058. doi:10.1038/nature03624

Tomita, S., Chen, L., Kawasaki, Y., Petralia, R. S., Wenthold, R. J., Nicoll, R. A., & Bredt, D. S. (2003). Functional studies and distribution define a family of transmembrane AMPA receptor regulatory proteins. *The Journal of Cell Biology, 161*(4), 805-816. doi:10.1083/jcb.200212116

Tsay, D., & Yuste, R. (2004). On the electrical function of dendritic spines. *Trends in Neurosciences, 27*(2), 77-83. doi:10.1016/j.tins.2003.11.008

Tsui-Pierchala, B. A., Encinas, M., Milbrandt, J., & Johnson, E. M.,Jr. (2002). Lipid rafts in neuronal signaling and function. *Trends in Neurosciences, 25*(8), 412-417.

Venable, M. E., Lee, J. Y., Smyth, M. J., Bielawska, A., & Obeid, L. M. (1995). Role of ceramide in cellular senescence. *The Journal of Biological Chemistry, 270*(51), 30701-30708.

Washbourne, P., Bennett, J. E., & McAllister, A. K. (2002). Rapid recruitment of NMDA receptor transport packets to nascent synapses. *Nature Neuroscience, 5*(8), 751-759. doi:10.1038/nn883

Wenthold, R. J., Petralia, R. S., Blahos, J.,II, & Niedzielski, A. S. (1996). Evidence for multiple AMPA receptor complexes in hippocampal CA1/CA2 neurons. *The Journal of Neuroscience : The Official Journal of the Society for Neuroscience, 16*(6), 1982-1989.

Wheeler, D., Knapp, E., Bandaru, V. V., Wang, Y., Knorr, D., Poirier, C., . . . Haughey, N. J. (2009). Tumor necrosis factor-alpha-induced neutral sphingomyelinase-2 modulates synaptic plasticity by controlling the membrane insertion of NMDA receptors. *Journal of Neurochemistry, 109*(5), 1237-1249. doi:10.1111/j.1471-4159.2009.06038.x

Wolfgang, M. J., Kurama, T., Dai, Y., Suwa, A., Asaumi, M., Matsumoto, S., . . . Lane, M. D. (2006). The brain-specific carnitine palmitoyltransferase-1c regulates energy homeostasis. *Proceedings of the National Academy of Sciences of the United States of America, 103*(19), 7282-7287. doi:10.1073/pnas.0602205103

Xia, J., Zhang, X., Staudinger, J., & Huganir, R. L. (1999). Clustering of AMPA receptors by the synaptic PDZ domain-containing protein PICK1. *Neuron, 22*(1), 179-187.

Yamazaki, N., Shinohara, Y., Shima, A., & Terada, H. (1995). High expression of a novel carnitine palmitoyltransferase I like protein in rat brown adipose tissue and heart: Isolation and

characterization of its cDNA clone. *FEBS Letters, 363*(1-2), 41-45.

Yang, S. N. (2000). Ceramide-induced sustained depression of synaptic currents mediated by ionotropic glutamate receptors in the hippocampus: An essential role of postsynaptic protein phosphatases. *Neuroscience, 96*(2), 253-258.

Zammit, V. A. (1999). The malonyl-CoA-long-chain acyl-CoA axis in the maintenance of mammalian cell function. *The Biochemical Journal, 343 Pt 3*, 505-515.

Zammit, V. A. (2008). Carnitine palmitoyltransferase 1: Central to cell function. *IUBMB Life, 60*(5), 347-354. doi:10.1002/iub.78

Zaugg, K., Yao, Y., Reilly, P. T., Kannan, K., Kiarash, R., Mason, J., . . . Mak, T. W. (2011). Carnitine palmitoyltransferase 1C promotes cell survival and tumor growth under conditions of metabolic stress. *Genes & Development, 25*(10), 1041-1051. doi:10.1101/gad.1987211

Zhu, J. J., Esteban, J. A., Hayashi, Y., & Malinow, R. (2000). Postnatal synaptic potentiation: Delivery of GluR4-containing AMPA receptors by spontaneous activity. *Nature Neuroscience, 3*(11), 1098-1106. doi:10.1038/80614

Ziff, E. B. (2007). TARPs and the AMPA receptor trafficking paradox. *Neuron, 53*(5), 627-633. doi:10.1016/j.neuron.2007.02.006

Ziv, N. E., & Smith, S. J. (1996). Evidence for a role of dendritic filopodia in synaptogenesis and spine formation. *Neuron, 17*(1), 91-102.

Zoghbi, H. Y. (2003). Postnatal neurodevelopmental disorders: Meeting at the synapse? *Science (New York, N.Y.), 302*(5646), 826-830. doi:10.1126/science.1089071

Zuo, Y., Lin, A., Chang, P., & Gan, W. B. (2005). Development of long-term dendritic spine stability in diverse regions of cerebral cortex. *Neuron, 46*(2), 181-189. doi:10.1016/j.neuron.2005.04.001

PUBLICATIONS

NEW LC-ESI-MS/MS METHOD TO MEASURE LONG-CHAIN ACYLCARNITINE LEVELS IN CULTURED CELLS.

Jauregui, O., Sierra, A. Y., **Carrasco, P**., Gratacos, E., Hegardt, F. G., & Casals, N. (2007).

Analytica Chimica Acta, 599(1), 1-6.

Available online at www.sciencedirect.com
ScienceDirect
Analytica Chimica Acta 599 (2007) 1–6
ANALYTICA CHIMICA ACTA
www.elsevier.com/locate/aca

Review

A new LC–ESI-MS/MS method to measure long-chain acylcarnitine levels in cultured cells

Olga Jáuregui [a], Adriana Y. Sierra [b], Patricia Carrasco [b], Esther Gratacós [b], Fausto G. Hegardt [c], Núria Casals [b,*]

[a] *Scientific & Technical Services, University of Barcelona, Spain*
[b] *Molecular and Cellular Unit, School of Health Sciences, International University of Catalonia, Spain*
[c] *Department of Biochemistry and Molecular Biology, University of Barcelona, School of Pharmacy, Spain*

Received 12 June 2007; received in revised form 27 July 2007; accepted 30 July 2007
Available online 3 August 2007

Abstract

The quantitative evaluation of long-chain acylcarnitines in lipid extracts from cultured cells or tissues is a prerequisite to study carnitine palmitoyltransferase (CPT) activity. There is thus a need for the accurate measurement of the concentration of long-chain acylcarnitines at the lowest concentration present in lipid extracts. Here we report a fast and reliable quantitative method based on the use of weak acid extraction and liquid chromatography–electrospray ionization tandem mass spectrometry (LC–ESI-MS/MS) to quantify acylcarnitines through hydrophilic interaction chromatography. The method was validated using isotopic dilution and the results allow the analysis of a large number of samples at low concentration levels (down to 0.35 nmol L^{-1} for palmitoylcarnitine) with good inter- and intra-day precision. The method was used for the quantitative study of changes in concentration of palmitoylcarnitine and other acylcarnitines in PC-12 cells over-expressing *CPT1a* gene. It was also used to measure CPT1 activity in mitochondria isolated from transfected cells, giving similar results to the more common radiometric method, but with higher sensitivity.

Keywords: Acylcarnitines; Carnitine palmitoyltransferase activity; Liquid chromatography–electrospray ionization tandem mass spectrometry; Hydrophilic interaction chromatography

Contents

* Corresponding author at: Facultat de Ciències de la Salut, Universitat Internacional de Catalunya, C/Josep Trueta s/n. E-08190 Sant Cugat del Valles, Barcelona, Spain.
E-mail address: ncasals@csc.uic.es (N. Casals).

0003-2670/$ – see front matter © 2007 Elsevier B.V. All rights reserved.
doi:10.1016/j.aca.2007.07.066

1. Introduction

Long-chain fatty acids enter the mitochondrial matrix, where they undergo beta-oxidation and the generated reduction equivalents were transferred to the mitochondrial respiratory chain to form ATP. The activated forms of fatty acids, acyl-CoAs, are transported across the mitochondrial membrane to the matrix by the CPT1/CACT/CPT2 system. Carnitine palmitoyl transferase 1 (CPT1) is localized in the outer mitochondrial membrane and facilitates the *trans*-esterification of activated long-chain acyl-CoAs and carnitine to give acylcarnitines. This is subsequently transported across mitochondrial inner membrane by the carnitine acylcarnitine transporter (CACT), and then reconverted to (the corresponding) CoA-esters by carnitine palmitoyl transferase 2 (CPT2) in the mitochondrial matrix [1]. The analysis of long-chain acylcarntines in lipid cell extracts provides a powerful selective tool with which to study the activity and function of the CPT1/CACT/CPT2 system in cells.

Various approaches have been proposed for the analysis of acylcarnitines in biological samples. Among these, HPLC-based methods with UV absorbance or fluorescence detection need derivatization steps. Thus, the classic procedure used in many newbornscreening centers is based on the formation of butyl ester derivatives and direct MS/MS analysis [2–6]. Pentafluorophenacyl esters of acylcarnitines separated by ion-exchange/reversed-phase HPLC [7] and 2-(2,3-naphthalimino)ethyl trifluoromethanesulfonate esters separated by HPLC with fluorescence detection [8] are other approaches for the analysis of acylcarnitines in biological samples. A further method is the use of ion-pairing reagents in the LC mobile phase such as heptafluorobutyric acid (HFBA) [9] in order to allow acylcarnitines to be retained in reversed-phase LC columns. In this case, good separation of the acylcarnitines was obtained, and detection limits of 1 nmol L^{-1} were achieved in MS/MS analysis. Nevertheless, the use of ion-pairing reagents such as HFBA is not recommended because putative contamination of the LC–MS system prevents the analysis in negative-ion mode. Ion exchange solid phase extraction, derivatization and GC-MS have also been applied [10].

Stevens et al. [11] analyzed acylcarnitines in human plasma by isotope-dilution tandem mass spectrometry, and an innovative procedure for the analysis of plasma acylcarnitines using on-line SPE-LC–ESI-MS/MS has recently been presented. The procedure operates without derivatization and uses a mobile phase containing ammonium acetate at pH 7.6 and methanol, and a valve-switching system. Protein precipitation with acetonitrile, centrifugation and extraction/cleaning via the on-line SPE system has also been applied [12,13].

Among the various MS and MS/MS approaches, that most frequently used is direct sample injection, and the precursor-ion scan of m/z 85 (the major fragment produced by collision-induced dissociation of all butylated acylcarnitines) produces a profile of all acylcarnitines present in the sample [3–6,13,14]. Given that endogenous materials in biological samples can cause ion suppression, thus introducing error in the results, liquid chromatography is frequently coupled to mass spectrometry in small molecule-metabolism laboratories. This is primarily due to the high sensitivity and selectivity of this combined technique and its ability to separate, detect, and identify metabolites in the presence of endogenous materials.

Here we describe an easy and sensitive method to analyze the changes in long-chain acylcarnitine levels in cells as a consequence of transient over-expression of *CPT1a* (the gene that encodes the liver CPT1 enzyme). A new LC procedure allows acylcarnitines to be separated in 12 min with an ammonium formate/acetonitrile mobile phase at low concentrations, without the need for derivatization, and obviating ion-pairing reagents in the mobile phase. The method also takes advantage of a simple extraction procedure.

2. Experimental methods

2.1. Materials

Standards palmitoylcarnitine, myristoylcarnitine and arachidonoylcarnitine were from Sigma–Aldrich. Palmitoylcarnitine-d_3 (Cambridge Isotope Laboratories, USA) was used as internal standard. Acetonitrile HPLC-grade (Sigma–Aldrich, St. Louis, MO, USA), ammonium formate (Panreac, Montcada i Reixac, Spain) and ultrapure water (MilliQ) from Millipore System (Bedford, USA) were used in HPLC analysis.

2.2. Culture and transfection of PC-12 cells

Clonal neural PC-12 cells were grown at 37 °C in the presence of 5% CO_2 in DMEM with high glucose containing 2 mM glutamine, 5% foetal calf serum, 10% horse serum, penicillin (100 units mL^{-1}) and streptomycin (100 μg mL^{-1}).

Cells cultured in 10 cm plates were transfected with 20 μg of plasmid DNA (purified with the Qiagen Maxi Prep Kit, Quiagen, UK) using Lipofectamine Plus reagent (Roche Applied Science, USA) according to the manufacturer's protocol. Cells were collected 48 h after transfection. Transfection efficiency as assessed by FACS analysis was about 50%.

2.3. Plasmid contructions

The coding region of rat CPT1a gene was cloned in vector pIRES2-EGFP (Clontech, BD Biosciences, Europe), to give pIRES2-EGFP-CPT1a, which permits both CPT1a and EGFP (green fluorescent protein) to be translated from a single bicistronic mRNA. Cells were transfected with empty vector pIRES2-EGFP (control cells) or with pIRES2-EGFP-CPT1a (CPT1 over-expressing cells).

2.4. Cell lipid extraction

Cells were washed in cold PBS buffer and gently collected with a pipette. They were then centrifuged at 700 × *g* max for 5 min at 4 °C and washed in PBS. Aliquots of 20 μL were taken for Bradford protein assay. After that, 200 μL of 0.2 M NaCl was added to the pellet and the mixture was immediately frozen in liquid N_2. To separate aqueous and lipid phases, 750 μL of Folch reagent (chloroform:methanol, 2:1) and 50 μL of 0.1 M KOH were added and, after vigorous mixing using a Vortex mixer, the phases were separated by 15 min centrifugation at 2000 × *g* at 4 °C. The top aqueous phase was removed and the lipid phase was washed in 200 μL of methanol/water/chloroform (48:47:3). After vortex-mixing, it was again centrifuged at 700 × *g* for 5 min at 4 °C and the lower phase (lipid extract) was dried.

2.5. Mitochondria isolation

Cells were recovered by centrifugation at 1200 × *g* for 5 min at 4 °C, washed in 1.5 mL PBS, and re-suspended in 2 mL of lysis buffer (250 mM sucrose, 10 mM Tris pH 7.4, 1 mM EDTA, supplemented with 1 mM PMSF, 0.5 mM benzamidine, 10 ng mL^{-1} leupeptin and 100 ng mL^{-1} pepstatin). Cells were disrupted by Douncer homogenization (30 pulses with loose pestle and 30 pulses with tight pestle). Homogenates were centrifuged at 2000 × *g* max for 3 min at 4 °C to remove cell debris. This crude extracted was further centrifuged at 10,000 × *g* for 30 min at 4 °C to give the mitochondrial pellet. The supernatant was discarded and pellet was immediately used for the carnitine palmitoyltransferase activity assay.

2.6. CPT1 activity

The substrates were palmitoyl-CoA and carnitine. In the radiometric assay L-(methyl-3H) carnitine (Amersham Bioscience, USA) was used. Enzyme activity was assayed for 4 min at 30 °C in a total volume of 200 μL. The protein sample, 40 μL (20–40 μg), was pre-incubated for 1 min, and 160 μL of the reaction mixture was then added. The final concentrations were 105 mM Tris–HCl (pH 7.2), 2 mM KCN, 15 mM KCl, 4 mM $MgCl_2$, 4 mM ATP, 250 μM reduced glutathione, 50 μM palmitoyl-CoA, 400 μM carnitine or L-(methyl-3H) carnitine (0.3 μCi), and 0.1% defatted bovine albumin. Reactions were arrested by the addition of 200 μL HCl 1.2N. The internal standard pamitoylcarnitine-d_3 was added at that moment. Acylcarnitine products formed in the assay reaction were extracted with water-saturated *n*-butanol and analyzed by HPLC–MS/MS or by a Coulter counter (radiometric method). Values were given as means of three independent experiments performed. All protein concentrations were determined using the Bradford protein assay (Bio-Rad, USA) with bovine serum albumin as standard.

2.7. LC–MS/MS conditions

The HPLC system used was a Perkin-Elmer Series 200 (Norwalk, CT, USA) quaternary pump equipped with an autosampler. For the analysis of the extracts, an Atlantis HILIC Silica (Waters, Milford, USA) column (150 mm × 2.1 mm, 3.0 μm) was used. Isocratic separation was done with 200 mmol L^{-1} ammonium formate pH 3, acetonitrile and water at the proportions 5:86:9 (v/v) and a constant flow-rate of 200 μL min^{-1}. To reduce the residual matrix effect reaching the mass spectrometer, a divert valve (Valco, Houston, USA) drained off the LC eluent. MS and MS/MS experiments were performed on an API 3000 triple quadrupole mass spectrometer (PE Sciex, Concord, Ont., Canada). All the analyses were performed using the Turbo Ionspray source in positive ion mode with the following settings: capillary voltage +4500 V, nebulizer gas (N_2) 10 a.u., curtain gas (N_2) 12 a.u., collision gas (N_2) 4 a.u. The drying gas (N_2) was heated to 400 °C and introduced at a flow-rate of 5000 cm^3 min^{-1}.

All the MS and MS/MS parameters were optimized by infusion experiments: individual standard solutions of acylcarnitines (1 ng μL^{-1}) were infused into the mass spectrometer at a constant flow-rate of 5 μL min^{-1} using a Model 11 syringe pump (Harvard Apparatus, Holliston, MA, USA). Full scan data acquisition was performed by scanning from *m/z* 50 to 500 in a profile mode and using a cycle time of 2 s with a step size of 0.1 u and a pause between each scan of 2 ms. In product ion-scan experiments MS/MS product ions were produced by collision-activated dissociation (CAD) of selected precursor ions in the collision cell of the triple quadrupole mass spectrometer, and mass was analyzed using the second analyzer of the instrument. However, in precursor ion-scan experiments, Q1 gives information on all the possible precursors of the selected ion in Q3 of the triple quadrupole. Additional experimental conditions for MS/MS included collision energy (depending on the compound), CAD gas (N_2) at 6 (arbitrary) units, and scan range, as necessary for the precursor selected. Precursor ion scan experiments were performed by scanning Q1 between 150 and 700 u. In all the experiments both quadrupoles Q1 and Q3 operated at unit resolution.

MRM (multiple reaction monitoring) acquisition was done monitoring one transition for each compound (see Table 1) with a dwell time of 700 ms. The MRM mode was required because many compounds could present the same nominal molecular mass, and the combination of the parent mass and unique fragment ions was used to selectively monitor acylcarnitines. Internal standard palmitoylcarnitine-d_3 (4 μL of a solution of 20 μg mL^{-1}) was added to samples before extraction to give a final concentration of 0.2 μg mL^{-1}. The same concentration was present in the standards used for quantification. A graph plotting area of palmitoylcarnitine/palmitoylcarnitine-d_3 ratios against concentration of palmitoylcarnitine/palmitoylcarnitine-d_3 ratios

Table 1
MS/MS data for the compounds studied

Compound	Full scan (m/z)	Product ion scan	MRM transition	DP	CE
Myristoylcarnitine	372.3	313.3, 211.1, 85.2	372.3/85.2	40	30
Arachidonoylcarnitine	456.4	397.4, 85.2	456.4/85.2	40	40
Palmitoylcarnitine	400.4	341.4, 239.5, 144.3, 85.2	400.4/85.2[a]	40	35
			400.4/341.4[b]		
Palmitoylcarnitine-d_3	403.4	341.1, 239.5, 85.2	403.4/85.2	40	35

[a] MRM transition used for quantification purposes.
[b] MRM transition used for confirmation purposes.

was used for quantification. The MRM transitions used for this purpose were 400.4/85.2 for palmitoylcarnitine and 403.4/85.2 for palmitoylcarnitine-d_3.

3. Results and discussion

3.1. LC separation

The HILIC column uses hydrophilic interaction chromatography to retain and separate polar compounds. It was used successfully to separate acylcarnitines, thus avoiding ion-pairing reagents, with good resolution, reproducible retention times and good peak shapes. Fig. 1A shows the chromatogram for a standard solution containing all the standards of acylcarnitines at individual concentrations of 200 ng mL^{-1}. Fig. 1B shows the chromatogram for a lipid cell extract. Elution occurred in the order of increasing hydrophilicity. This approach has the advantage of using an MS-friendly mobile phase (acetonitrile/water/ammonium formate) with a high content of organic modifier (86%), which improves ESI signal. In addition, since polar compounds eluted later than the hydrophobic compounds, ion

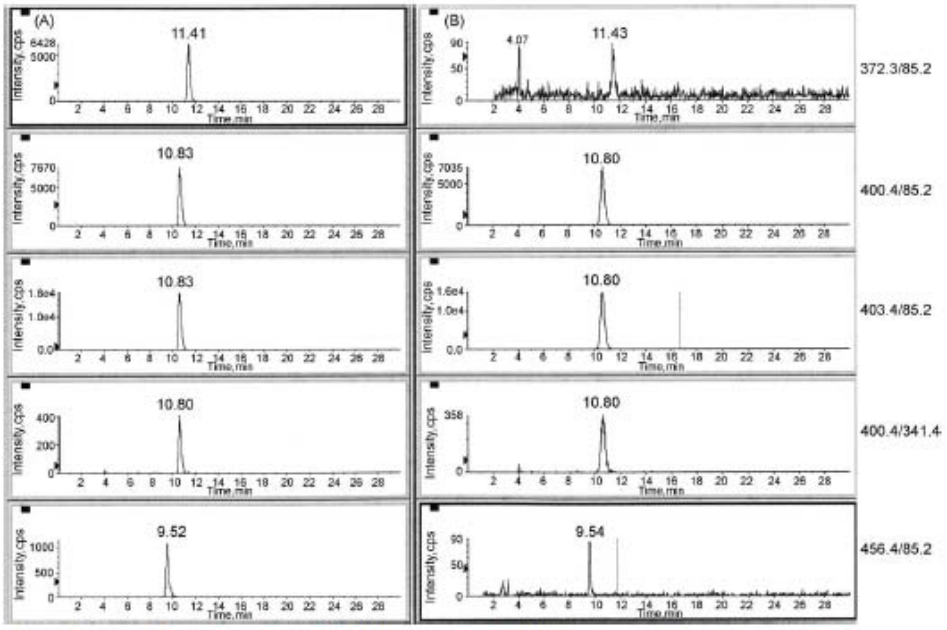

Fig. 1. Trace chromatogram of acylcarnitines using the LC–ESI-MS/MS conditions (MRM mode) described in the text: x-axis = time (min); y-axis = intensity (cps). Peaks: 456.4/85.2 arachidonoylcarnitine, 400.4/85.2 palmitoylcarnitine (identification and quantification), 400.4/341.4 palmitoylcarnitine (confirmation), 403.4/85.2 palmitoylcarnitine-d_3 (internal standard), 372.3/85.2 miristoylcarnitine. (A) Standard solution, 200 ng mL^{-1} for each compound. (B) Lipid extract from CPT1a over-expressing cells.

suppression at the beginning of the chromatograms was minimized.

3.2. Mass spectrometry

Analyses were carried out in positive-ion mode since sensitivity was higher than in negative-ion mode. Moreover, only in this mode there was a common *m/z* 85 product ion for all acylcarnitines. In positive mode, the spectrum for acylcarnitines gave the positively charged molecule $[M+H]^+$ in full scan mode. The carboxylic group of acylcarnitines is protonated under acidic conditions, resulting in the production of positively charged quaternary amines. Product ion-scan spectra were studied for each compound and similar behaviour was observed: loss of the $N(CH_3)_3$-fragment gave the $[M-59]^+$ ion. In the same way, all compounds showed the loss of 102 u. Finally, *m/z* 144 and *m/z* 85 were common fragment ions for all the acylcarnitines studied. Collision energy was optimized for each transition in infusion experiments. Optimum values are presented in Table 1. Fragmentation involves the loss of the fatty acid and trimethylamine, resulting in the generation of a stable fragment ion with *m/z* 85.

The chromatogram of blank sample was examined and no interference was found.

Isotope dilution mass spectrometry is the technique of choice for most clinical analyses, since it does not depend on sample recovery, and it also generates results with high precision. Although MS/MS can be considered a selective technique, this selectivity may be overestimated owing to the complexity of biological samples. This technique can produce false-positive results, especially when low resolution MS detection is used. In order to minimize this risk, appropriate confirmation was performed in low-resolution instruments (e.g. triple quadrupole instruments) by acquiring two transitions and measuring the ratio between them. In our case three transitions were monitored for the determination of palmitoylcarnitine in a lipid environment: 400.4/85.2 for quantitation purposes, 400.4/341.4 for confirmation purposes and 403.4/85.2 for the labelled internal standard. The ratio between the two transitions for palmitoylcarnitine was also calculated for each sample in order to avoid false positives. All the samples gave an ion ratio that was within the ion ratio for the standards, ±20%. It should be pointed out that the ion ratio criterion was only applicable for concentrations above 0.6 ng mL^{-1} owing to the lower intensity of the 400.4/341.4 as compared to the 400.4/85 transition.

3.3. Performance characteristics

Linearity. Calibration curves were prepared in the LC mobile phase and injected into the LC–ESI-MS/MS system. The peak areas were plotted against the corresponding concentration to obtain the calibration curve. The method was linear over the range from 2 to 2000 ng mL^{-1}. The residuals analysis for this concentration range was (mean (S.D.)): 96.8% (±8.8) using $1/x^2$ weighting [15]. As mentioned above, the internal standard approach using labelled compounds is the most valid method for quantitation purposes in LC–MS. In our case, palmitoylcarnitine-d_3 was used. Five calibration curves were plotted on five separate days in order to establish the robustness of the method. Low relative standard deviation (2.95%) was obtained in the measured slope of the calibration curves on 5 different days.

Sensitivity. The limit of detection (LoD) and the limit of quantification (LoQ) were calculated by repeated injections of diluted standard solutions. The LoD was estimated as the concentration of palmitoylcarnitine that generated a peak with a signal-to-noise ratio of 3. LoQ was calculated at a signal-to-noise ratio of 10. The LoD and LoQ were 0.14 ng mL^{-1} (0.35 nmol L^{-1}) and 0.48 ng mL^{-1} (1.2 nmol L^{-1}). respectively (in standard solutions), similar to the limits of 1 nmol L^{-1}, as published by other authors [9].

Precision. To assess the precision, 10 repetitive injections of three standard solutions of 10, 100 and 800 ng mL^{-1} were done in one day (intra-day precision) and on three different days (inter-day precision). The results expressed as coefficient of variation (%) are satisfactory in terms of concentration for run-to-run (9.1, 10.1 and 4.5% for 10, 100 and 800 ng mL^{-1}, respectively) and for day-to-day precision (12.1, 11.3 and 6.2% for 10, 100 and 800 ng mL^{-1}, respectively). The precision in terms of retention time also showed acceptable values (0.24% and 2.74% for run-to-run and for day-to-day precision, respectively).

3.4. Quantification of palmitoyl carnitine in lipid fraction of cell extracts

To determine whether this method could be used to study long-chain acylcarnitine levels in cell extracts, we altered the proportions of CPT1/CACT/CPT2 in PC-12 cultured cells by over-expressing CPT1a gene, and we measured the alteration of acylcarnitine profiles in lipid cell extracts. Samples were first analyzed in full-scan mode and then in precursor ion-scan mode of *m/z* 85. Cells over-expressing CPT1a were expected to have increased levels of palmitoylcarnitine in the lipid fraction. Major differences between control and CPT1a over-expressing cells were found in chromatographic peak areas corresponding to palmitoylcarnitine levels (Fig. 2). There was also a strong

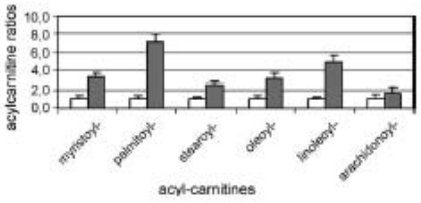

Fig. 2. Levels of different acylcarnitines in PC12 cells over-expressing CPT1a. Control PC-12 cells were transfected with empty plres vector (white columns) and CPT1a over-expressing cells were transfected by plres-CPT1a plasmid (grey columns). Forty eight hours after transfection, lipid cell extracts were obtained and acylcarnitines were determined by LC–ESI-MS/MS in precursor ion scan mode of *m/z* 85. Palmitoylcarnitine ratios = area below the chromatographic peak respect to control cells. These values represent the mean of three independent experiments.

Table 2
CPT1 activity (nmol mg^{-1} min^{-1}) in mitochondria of PC-12 cells

PC-12 cells	HPLC–MS/MS method	Radiometric method
Control cells	2.91 ± 0.43	3.12 ± 0.56
CPT1a over-expressing cells	7.13 ± 0.51	8.03 ± 0.41

Mitochondria were isolated from PC-12 cells 48 h after transfection. CPT1 activity was assayed in 40 μg of mitochondria using both methods: the HPLC–MS/MS method and the radiometric assay. Three separate experiments were performed. Control cells are PC-12 cells transfected with the empty expression vector.

increase in other acylcarnitines that may have been produced by CPT1a enzyme, like stearoylcarnitine and oleoylcarnitine. Levels of palmitoylcarnitine were also measured using MRM mode, with palmitoylcarnitine-d_3 as internal standard. About 1.59 and 8.84 ng mL^{-1} ($n = 3$) of palmitoylcarnitine were present in lipid extracts of control and CPT1a over-expressing cells. There was a 5–6-fold increase in palmitoylcarnitine levels as a consequence of the increase of CPT1 activity. The LC–ESI-MS/MS method described allows the simple measurement of differences in acylcarnitine levels in cells, with great accuracy.

3.5. CPT1 activity in isolated mitochondria of cells

CPT1 activity in cell extracts has traditionally been measured by a radiometric assay [16], using palmitoyl-CoA and L-(methyl-3H) carnitine as substrates. Recently, van Vlies et al. [17] described an improved enzyme assay for CPT1 activity in fibroblasts using tandem mass spectrometry, but propylation of the sample was required. We decided to use our HPLC–MS/MS method to measure CPT1 activity in mitochondria isolated from PC-12 cells. About 40 μg of mitochondria was incubated with palmitoyl-CoA and carnitine for 4 min, and levels of palmitoyl-carnitine were determined in MRM mode, with palmitoylcarnitine-d_3 as internal standard (Table 2). CPT1 activity in PC-12 cells measured by the HPLC–MS/MS method gave similar values to those returned by the radiometric assay.

The LC–ESI-MS/MS technique was more sensitive than the radiometric method. The limit of sensitivity of the LC–ESI-MS/MS method described here was 0.48 ng mL^{-1}, which corresponds to a CPT1 activity of 0.001 nmol (min mg)$^{-1}$ in our assay conditions (40 μg of protein, 4 min of assay time. To establish the limit of sensitivity of the radiometric assay we calculated the standard deviation of ten blank points (the assay mix solution without cell sample), in cpm values. The standard deviation of the blank was 27 cpm, with a coefficient of variation of 2%. The limit of sensitivity (a signal-to-noise ratio of 3) was 81 cpm, which corresponds to a CPT1 activity of 0.401 nmol mg^{-1} min^{-1}, about 400 times less sensitive than the LC–ESI-MS/MS described herein.

The method presented here constitutes an optimal procedure not only to measure acylcarnitine levels in cells, but also to measure CPT1 activity that is below the detection limit of the radiometric assay.

4. Conclusions

The use of quantitative LC–ESI-MS/MS has been shown to be highly sensitive and specific for the analysis of long-chain acylcarnitines in metabolic studies. The use of the HILIC column affords the ability to analyse acylcarnitines without prior derivatization. Analysis of underivatized acylcarnitines simplifies sample preparation and offers the added advantage of removing any potential errors caused by the derivatization procedure itself. Using three identification points (retention time and when possible, two MRM transitions), LoQ values of 1.2 nmol L^{-1} were obtained. In addition, a high confidence level was attained through the isotope ratio of two ions monitored within 20% of the theoretical isotopic ratio, even in complex samples such as lipid cell extracts. LC–ESI-MS/MS can also be used to measure CPT1 activity in cells with much higher sensitivity than the radiometric method.

Acknowledgments

The editorial help of Robin Rycroft is gratefully acknowledged. This study was supported by grants SAF2004-06843-C03 and SAF2007-61926 from the *Ministerio de Educación y Ciencia*, Spain, by CIBER Institute of Fisiopatologia, Obesidad y Nutrición (CB06/03), Instituto de Salud Carlos III, Spain, by the *Ajut de Suport als Grups de Recerca de Catalunya* (2005SGR-00733), and by grant from *Fundació La Marató de TV3* (2007), Catalunya. AYS and PC are recipients of fellowships from Universitat Internacional de Catalunya.

References

[1] J.D. McGarry, N.F. Brown, Eur. J. Biochem. 244 (1997) 1–14.
[2] C.T. Cavedon, P. Bourdoux, K. Mertens, H.V. Van Thi, N. Herremans, C. de Laet, P. Goyens, Clin. Chem. 51 (2005) 745–752.
[3] A. Liu, M. Pasquali, J. Chromatogr. B: Analyt. Technol. Biomed. Life Sci. 827 (2005) 193–198.
[4] D.H. Chace, S.L. Hillman, J.L. Van Hove, E.W. Naylor, Clin. Chem. 43 (1997) 2106–2113.
[5] P. Mueller, A. Schulze, I. Schindler, T. Ethofer, P. Buehrdel, U. Ceglarek, Clin. Chim. Acta 327 (2003) 47–57.
[6] Y. Hasegawa, M. Iga, M. Kimura, Y. Shigematsu, S. Yamaguchi, J. Chromatogr. B: Analyt. Technol. Biomed. Life Sci. 823 (2005) 13–17.
[7] P.E. Minkler, S.T. Ingalls, C.L. Hoppel, Anal. Chem. 77 (2005) 1448–1457.
[8] P.E. Minkler, J. Kerner, K.N. North, C.L. Hoppel, Clin. Chim. Acta 352 (2005) 81–92.
[9] S.H. Cho, J. Lee, W.Y. Lee, B.C. Chung, Rapid Commun. Mass Spectrom. 20 (2006) 1741–1746.
[10] J.F. Van Bocxlaer, A.P. De Leenheer, Clin. Chem. 39 (1993) 1911–1917.
[11] R.D. Stevens, S.L. Hillman, S. Worthy, D. Sanders, D.S. Millington, Clin. Chem. 46 (2000) 727–729.
[12] A.K. Ghoshal, T. Guo, N. Soukhova, S.J. Soldin, Clin. Chim. Acta 358 (2005) 104–112.
[13] A.K. Ghoshal, J. Balay, S.J. Soldin, Clin. Chim. Acta 365 (2006) 352–353.
[14] D.H. Chace, J.C. DiPerna, B.L. Mitchell, B. Sgroi, L.F. Hofman, E.W. Naylor, Clin. Chem. 47 (2001) 1166–1182.
[15] M.M. Kiser, J.W. Dolan, LC–GC Eur. 17 (2004) 138–143.
[16] M. Morillas, P. Gomez-Puertas, A. Bentebibel, E. Selles, N. Casals, A. Valencia, F.G. Hegardt, G. Asins, D. Serra, J. Biol. Chem. 278 (2003) 9058–9063.
[17] N. van Vlies, J.P. Ruiter, M. Doolaard, R.J. Wanders, F.M. Vaz, Mol. Genet. Metab. 90 (2007) 24–29.

CPT1C IS LOCALIZED IN ENDOPLASMIC RETICULUM OF NEURONS AND HAS CARNITINE PALMITOYLTRANSFERASE ACTIVITY.

Sierra, A. Y., Gratacos, E., **Carrasco, P**., Clotet, J., Urena, J., Serra, D., et al. (2008).

The Journal of Biological Chemistry, 283(11), 6878-6885.

THE JOURNAL OF BIOLOGICAL CHEMISTRY VOL. 283, NO. 11, pp. 6878–6885, March 14, 2008

CPT1c Is Localized in Endoplasmic Reticulum of Neurons and Has Carnitine Palmitoyltransferase Activity*

Received for publication, September 24, 2007, and in revised form, December 13, 2007 Published, JBC Papers in Press, January 11, 2008, DOI 10.1074/jbc.M707965200

Adriana Y. Sierra[‡1,2], Esther Gratacós[‡1], Patricia Carrasco[‡2], Josep Clotet[‡], Jesús Ureña[§], Dolors Serra[¶‖], Guillermina Asins[¶‖], Fausto G. Hegardt[¶‖], and Núria Casals[‡‖3]

From the [‡]Molecular and Cellular Unit, School of Health Sciences, Universitat Internacional de Catalunya, Josep Trueta s/n, Sant Cugat del Vallés, Barcelona 08195, the [§]Department of Cell Biology, Faculty of Biology, University of Barcelona, Diagonal 645, and Institute de Recerca Biomédica de Barcelona, Josep Samitier 1–5, 08028 Barcelona, the [¶]Department of Biochemistry and Molecular Biology, University of Barcelona, School of Pharmacy, 08028 Barcelona, and the [‖]Centro de Investigación Biomédica en Red (CIBER) Institute of Fisiopatología de la Obesidad y Nutrición (CB06/03), Instituto de Salud Carlos III, 28029 Madrid, Spain

CPT1c is a carnitine palmitoyltransferase 1 (CPT1) isoform that is expressed only in the brain. The enzyme has recently been localized in neuron mitochondria. Although it has high sequence identity with the other two CPT1 isoenzymes (a and b), no CPT activity has been detected to date. Our results indicate that CPT1c is expressed in neurons but not in astrocytes of mouse brain sections. Overexpression of CPT1c fused to the green fluorescent protein in cultured cells demonstrates that CPT1c is localized in the endoplasmic reticulum rather than mitochondria and that the N-terminal region of CPT1c is responsible for endoplasmic reticulum protein localization. Western blot experiments with cell fractions from adult mouse brain corroborate these results. In addition, overexpression studies demonstrate that CPT1c does not participate in mitochondrial fatty acid oxidation, as would be expected from its subcellular localization. To identify the substrate of CPT1c enzyme, rat cDNA was overexpressed in neuronal PC-12 cells, and the levels of acylcarnitines were measured by high-performance liquid chromatography-mass spectrometry. Palmitoylcarnitine was the only acylcarnitine to increase in transfected cells, which indicates that palmitoyl-CoA is the enzyme substrate and that CPT1c has CPT1 activity. Microsomal fractions of PC-12 and HEK293T cells overexpressing CPT1c protein showed a significant increase in CPT1 activity of 0.57 and 0.13 nmol·mg^{-1}·min^{-1}, respectively, which is ~50% higher than endogenous CPT1 activity. Kinetic studies demonstrate that CPT1c has similar affinity to CPT1a for both substrates but 20–300 times lower catalytic efficiency.

Carnitine palmitoyltransferase 1 (CPT1)[4] catalyzes the conversion of long chain fatty acyl-CoAs into acylcarnitines, the first step in the transport of long chain fatty acids from the cytoplasm to the mitochondrial matrix, where they undergo β-oxidation. This reaction is not only central to the control of fatty acid oxidation, but it also determines the availability of long chain acyl-CoA for other processes, notably the synthesis of complex lipids.

There are three different CPT1 isozymes: CPT1a (also called L-CPT1) encoded by *CPT1a*, CPT1b (also called M-CPT1) encoded by *CPT1b*, and the recently described CPT1c (also called CPT1-C) encoded by *CPT1c*. *CPT1a* and *CPT1b* have been extensively studied since they were cloned for the first time, in 1993 and 1995, respectively (1, 2). CPT1a is the most ubiquitous expressed isoform and is found not only in liver but also in pancreas, kidney, brain, blood, and embryonic tissues. CPT1b is expressed only in brown adipose tissue, muscle, and heart. Both isozymes present significantly different kinetic and regulatory properties: CPT1a displays higher affinity for its substrate carnitine and a lower affinity for the physiological inhibitor malonyl-CoA than the muscle isoform (3). In addition, the amino acid residues that are critical for catalytic activity or malonyl-CoA sensitivity have been identified for both enzymes, and three-dimensional structures have been predicted based on the carnitine acetyl transferase, carnitine octanoyl transferase, and carnitine palmitoyltransferase II crystals (4). CPT1a and CPT1b are localized in the outer mitochondrial membrane with the N and C termini facing to the cytosolic side. Western blotting and activity characterization suggested that CPT1a is also localized in microsomes, but expression studies with EGFP fused to the C terminus of CPT1a showed that CPT1a is targeted only to mitochondria and that previous detection of CPT1a in microsomes was probably derived from membrane contact sites between ER and mitochondria (5). CPT1a and CPT1b have a critical role in the heart, liver, and pancreatic β-cells and are potential targets for the treatment of metabolic disorders, including diabetes and coronary heart disease.

Less is known about CPT1c. Although the protein sequence is highly similar to that of the other two isozymes, CPT1c expressed in yeast or HEK293T cells displays no catalytic activity with common acyl-CoA esters as substrates (6, 7). One

* This work was supported in part by the Ministerio de Educación y Ciencia, Spain (Grants SAF2004-06843-C03 and SAF2007-61926), by Ajut de Suport als Grups de Recerca de Catalunya (Grant 2005SGR-00733), and by the Fundació La Marató de TV3 (2007), Catalunya. The costs of publication of this article were defrayed in part by the payment of page charges. This article must therefore be hereby marked "*advertisement*" in accordance with 18 U.S.C. Section 1734 solely to indicate this fact.

[1] Both authors contributed equally to this work.

[2] Recipients of fellowships from the Universitat Internacional de Catalunya.

[3] To whom correspondence should be addressed. Tel.: 93-50-42005; Fax: 93-50-42001; E-mail: ncasals@csc.uic.es.

[4] The abbreviations used are: CPT1, carnitine palmitoyltransferase 1; EGFP, enhanced green fluorescent protein; ER, endoplasmic reticulum; PBS, phosphate-buffered saline; BSA, bovine serum albumin; HPLC, high-performance liquid chromatography; LC, liquid chromatography; ESI, electrospray ionization; MS/MS, tandem mass spectrometry.

explanation is that palmitoyl-CoA is not a substrate for CPT1c and that another brain-specific acyl-CoA might be its natural substrate. Expression studies indicate that CPT1c is localized exclusively in the central nervous system, with homogeneous distribution in all areas (hippocampus, cortex, hypothalamus, and others). The pattern resembles that of FAS, acetyl-CoA carboxylase-α (enzymes related to biosynthesis) rather than CPT1a or ACC-β (enzymes related to oxidation) (6, 8). The capacity of CPT1c to bind malonyl-CoA has been demonstrated, and it has been suggested that CPT1c regulates malonyl-CoA availability in the brain cell.

It has recently been reported that knock-out mice for CPT1c ingest less food and have a lower body weight when fed a standard diet. When these animals are fed high fat chow, body weight increases more than control animals, and they become resistant to insulin, suggesting that CPT1c is involved in energy homeostasis and control of body weight (7). Moreover, ectopic overexpression of CPT1c by stereotactic hypothalamic injection of a CPT1c adenoviral vector protects mice from adverse weight gain caused by high fat diet (9).

Herein we report that CPT1c is localized in neurons but not in astrocytes of adult brain. We also demonstrate that CPT1c is localized in the ER of the cells and not in mitochondria, and that CPT1c shows carnitine palmitoyltransferase activity.

EXPERIMENTAL PROCEDURES

Culture of PC-12, SHSY5Y, Fibroblasts, and HEK293T Cells

The human neuroblastoma cell line, SHSY5Y, the human embryonic kidney-derived cell line, HEK293T, and human fibroblasts cells were grown at 37 °C in the presence of 5% CO_2 in Dulbecco's modified Eagle's medium with high glucose containing 2 mM glutamine, 10% fetal calf serum, penicillin (100 units/ml), and streptomycin (100 μg/ml). Medium for PC-12 cells was Dulbecco's modified Eagle's medium with high glucose containing 2 mM glutamine, sodium pyruvate, 5% fetal calf serum, 10% horse serum, penicillin (100 units/ml), and streptomycin (100 μg/ml).

Cells cultured in 24-wells plates were transfected with 0.8 μg of plasmid (purified with the Qiagen Maxi Prep Kit) using Lipofectamine Plus reagent (Invitrogen) according to the manufacturer's protocol. Transfection efficiency was ~30–50%.

Plasmid Constructions

For pCPT1c-EGFP and pCPT1a-EGFP, rat CPT1c cDNA was obtained by reverse transcription-PCR performed with 2 μg of total rat brain RNA. The 2700-bp fragment amplified was cloned in pBluescript and sequenced. pEGFP-N3 vector (from Clontech, BD Biosciences) was used to clone the coding region of *CPT1c* or *CPT1a*, to create pCPT1c-EGFP and pCPT1a-EGFP, respectively. pCPT1c-EGFP and pCPT1a-EGFP plasmids encode CPT1c and CPT1a proteins fused to the N-terminal region of EGFP, respectively.

Chimera Constructions

pCPT1ac-EGFP—460 bp of the 5′ coding sequence of rat *CPT1a* gene was PCR-amplified with primers that created an HindIII site and an HpaI site at the ends of the amplified fragment. This PCR product was cloned into a pCPT1c-EGFP plasmid previously digested by HindIII and HpaI (which deleted the 460 bp of the 5′ terminus of *CPT1c* coding sequence). The resulting plasmid encodes a fused protein constituted by the N terminus and the two transmembrane domains of CPT1a, the catalytic domain of CPT1c, and EGFP.

pCPTca-EGFP—A segment of the first 462 bp of rat *CPT1c* gene was PCR-amplified with two primers that created a HindIII site a PpuMI site at the ends of the amplified fragment. This PCR product was digested and cloned into a pCPT1a-EGFP plasmid, previously digested by HindIII and PpuMI (which deleted the 460 bp of the 5′ terminus of *CPT1c* coding sequence). The resulting vector contained the N terminus, the two transmembrane domains of CPT1c, and the catalytic domain of CPT1a fused to EGFP.

pIRES-CPT1a and pIRES-CPT1c—The coding regions of rat *CPT1a* and *CPT1c* were cloned in vector pIRES2-EGFP (Clontech, BD Biosciences), which permits both the gene of interest and the EGFP gene to be translated from a single bicistronic mRNA.

Co-localization Studies in Brain Sections

For co-localization studies we performed combined *in situ* hybridization/immunocytochemistry or double immunofluorescence, using standard protocols.

For combined *in situ* hybridization, coronal sections (30 μm) from adult mouse forebrains were used. Processed sections were hybridized overnight at 56 °C, with *cpt1c* Riboprobes (full rat cDNA) labeled with digoxigenin-d-UTP (Roche Applied Science) at a concentration of 500 ng/ml. After stringent washing, sections were incubated at 4 °C overnight with an anti-DIG antibody (1/2000) conjugated to alkaline phosphatase (Roche Applied Science) and developed with 5-bromo-4-chloro-3-indolyl phosphate/nitro blue tetrazolium substrate (Invitrogen). Tissue sections were mounted on gelatinized slides with Mowiol. Those sections that were hybridized with control sense Riboprobes did not give any hybridization signal.

After *in situ* hybridization, some slices were collected and processed by immunofluorescence. The primary antibody was mouse anti-NeuN (1:75, Chemicon). The secondary antibody was biotinylated (Vector Laboratories, Inc., Burlingame, CA). The streptavidin-horseradish peroxidase complex was from Amersham Biosciences. Sections were developed with 0.03% diaminobenzidine and 0.003% hydrogen peroxide, mounted onto slides, and dehydrated, and coverslips were added with synthetic resin.

In double immunofluorescence experiments, sections obtained as indicated above were incubated with primary antibodies against glial fibrillary acidic protein (1/500, Chemicon MAB360) and CPT1c (1/100) overnight at 4 °C in the same blocking solution. The sections were washed three times in PBS (0.1 M) and incubated for 2 h with secondary antibodies coupled to fluorochromes Alexa 488 (for green fluorescence) and Alexa 568 (for red fluorescence) at a dilution of 1/500. Sections were mounted with Mowiol and observed using a confocal Leica TCS SP2 microscope (Leica Lasertechnik GmbH, Mannheim, Germany). Images were saved in TIFF format and analyzed using Adobe Photoshop 3.0.

CPT1c Location and Activity

Co-localization Studies in Culture Cells

Cultured cells were grown on lysine-treated coverslips in 24-well plates. Co-localization studies were performed 48 h after transfection with plasmids containing *CPT1c* or *CPT1a* fused to the 5′-end of EGFP. To visualize the ER, cells were washed twice in PBS (10 mM), fixed with 3% paraformaldehyde in 100 mM phosphate buffer and 60 mM sucrose for 15 min at room temperature, and then washed twice in PBS. Cells were permeabilized with 1% (w/v) of Triton X-100 in PBS and 20 mM glycine for 10 min at room temperature and then washed twice in PBS. Nonspecific binding of antibody was blocked by incubation with 1% (w/v) BSA in PBS with glycine 20 mM at room temperature for 30 min. Cells were then incubated with mouse anti-calnexin polyclonal antibody (BD Biosciences, 1:50 in 1% (w/v) BSA/PBS/20 mM glycine/0.2% Triton X-100) for 1 h at 37 °C. After washing twice in PBS/20 mM glycine, cells were incubated with goat anti-mouse Alexafluor 546 (Molecular Probes, 1:500 in 1% (w/v) BSA/PBS/20 mM glycine/0.2% Triton X-100) for 1 h at 37 °C, and then washed twice in PBS. Coverslips were mounted on glass slides with Mowiol. Mitochondria were visualized by incubating cells with 500 nM MitoTracker Orange CM-H2TMRos (Molecular Probes) in complete medium for 30 min, followed by 30 min in complete medium without MitoTracker, after which they were fixed as mentioned above.

Fluorescent staining patterns were visualized by using a fluorescence microscope (Leica). The captured images were processed using Adobe Photoshop 5.0.

RNA Extraction and Real-time PCR Conditions

RNA was extracted from cells by the TRIzol method (Invitrogen) and quantified spectrophotometrically. 2 μg of total RNA was incubated with DNase and reverse transcribed by Superscript III (Invitrogen) following the manufacturer's conditions. 2 μl of reaction was used in the real-time PCR amplification with TaqMan and primers designed by Applied Biosystems, following the manufacturer's conditions. An 18 S expression assay was used to normalize the samples.

Lipid Extraction

Cells were washed in cold PBS buffer and gently collected with a pipette. They were then centrifuged at 700 × *g* for 5 min at 4 °C and washed in PBS. 20 μl of samples was taken for Bradford protein assay. After that, 200 μl of 0.2 M NaCl was added to the pellet, and the mixture was immediately frozen in liquid N_2. To separate aqueous and lipid phases, 750 μl of Folch reagent (chloroform:methanol, 2:1) and 50 μl of 0.1 M KOH were added, and, after vigorous vortex mixing, the phases were separated by 15-min centrifugation at 2000 × *g* at 4 °C. The top aqueous phase was removed, and the lipid phase was washed in 200 μl of methanol/water/chloroform (48:47:3). After vortex mixing, centrifugation was performed at 700 × *g* for 5 min at 4 °C, and the lower phase (lipid extract) was dried.

Quantification of Acylcarnitines by HPLC

Acylcarnitines were analyzed via an LC-ESI-MS/MS System (API 3000 PE Sciex) in positive ionization mode as described in a previous study (10). Quantification was done through multiple reaction monitoring experiments using the isotope dilution method with deuterated palmitoylcarnitine as internal standard (200 ng·ml^{-1}). 10 μl of sample was injected in the LC-ESI-MS/MS system. Multiple reaction monitoring transitions were as follows: 400.4/85.2 for quantification of palmitoylcarnitine, 4001.4/341.4 for confirmation of palmitoylcarnitine, and 403.4/85.2 for quantification of d_3-palmitoylcarnitine. The method was linear over the range from 2 to 2000 ng·ml^{-1}. The limit of detection and the limit of quantification were 0.14 ng·ml^{-1} (0.35 nmol·liter^{-1}) and 0.48 ng·ml^{-1} (1.2 nmol·liter^{-1}), respectively (in standard solutions).

Microsome Purification

Cells were recovered by centrifugation at 1200 × *g* for 5 min at 4 °C, washed in 1.5 ml of PBS, and re-suspended in 2 ml of lysis buffer (250 mM sucrose, 10 mM Tris, pH 7.4, 1 mM EDTA, supplemented with 1 mM phenylmethylsulfonyl fluoride, 0.5 mM benzamidine, 10 ng/ml leupeptin, and 100 ng/ml pepstatin). Cells were disrupted by Dounce homogenization (30 pulses with loose pestle and 30 pulses with tight pestle). Homogenates were centrifuged at 2,000 × *g* for 3 min at 4 °C to remove cell debris. This crude extracted was further centrifuged at 10,000 × *g* for 30 min at 4 °C to remove the mitochondrial fraction. Supernatant was centrifuged at 10,000 × *g* for 1 h at 4 °C to sediment the microsomal fraction. Pellets were immediately used in the carnitine palmitoyltransferase activity assay.

CPT1 Activity

Radiometric Method—Carnitine acyltransferase activity was determined by the radiometric method as previously described (11). The substrates were palmitoyl-CoA and L-[*methyl*-^{3}H]carnitine. Enzyme activity was assayed for 4 min at 30 °C in a total volume of 200 μl. The protein sample, 40 μl (20 μg), was preincubated for 1 min, and then 160 μl of the reaction mixture was added. The final concentrations were 105 mM Tris-HCl (pH 7.2), 2 mM KCN, 15 mM KCl, 4 mM $MgCl_2$, 4 mM ATP, 250 μM reduced glutathione, 50 μM palmitoyl-CoA, 400 μM L-[*methyl*-^{3}H]carnitine (0.3 μCi), and 0.1% defatted bovine albumin. Reactions were stopped by the addition of 200 μl of HCl 1.2 N, and the product acyl-L-[*methyl*-^{3}H]carnitine was extracted with water-saturated *n*-butanol. Values were estimated by analyzing the data from three experiments performed in triplicate. All protein concentrations were determined using the Bio-Rad protein assay with bovine albumin as standard.

Chromatographic Method—The same procedure used previously (11) was followed except that all carnitine used was cold (not radioactive). In addition, acylcarnitines extracted with water-saturated *n*-butanol were analyzed by an LC-ESI-MS/MS system, as described above.

Western Blot Experiments

A polyclonal rabbit antibody against the last 15 residues (796–810) of mouse CPT1c was developed following the indications in a previous study (7), by Sigma-Genosys. The specificity of the antibody was determined by enzyme-linked immunosorbent assay and Western blot experiments. For CPT1a detection, a polyclonal antibody against amino acids 317–430

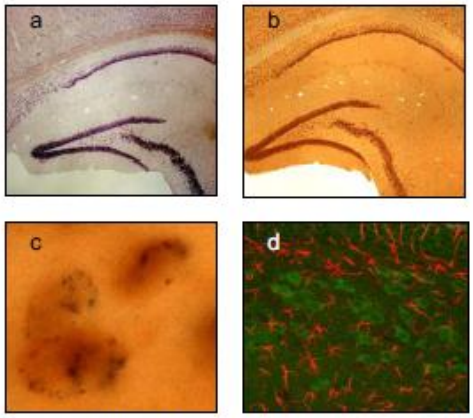

FIGURE 1. **Co-localization studies of CPT1c mRNA with NeuN and glial fibrillary acidic protein proteins in brain sections.** Brain sections were processed using *in situ* hybridization with *CPT1c* antisense Riboprobe (*a*) or immunocytochemistry with NeuN primary antibodies and biotinylated secondary antibodies (*b*) or both methods (*c*). Mouse adult brain sections were processed by double immunocytochemistry with CPT1c antibodies (*green* stain) and glial fibrillary acidic protein (molecular marker of astrocytes, *red* stain) (*d*).

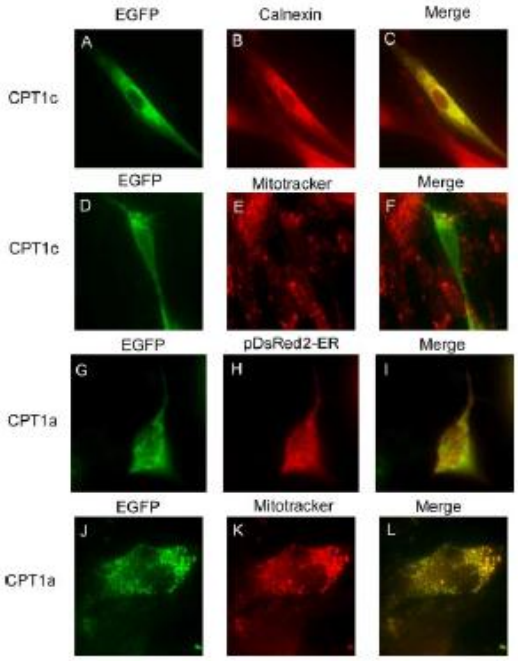

FIGURE 2. **Co-localization studies of CPT1c in mitochondria and ER.** Fibroblasts were transfected with pCPT1c-EGFP (*A–F*) or pCPT1a-EGFP (*G–L*) and incubated with anti-calnexin as primary antibody (*B*) or stained by MitoTracker (*E* and *K*) or co-transfected with pDsRed2-ER (*H*). Images were taken by confocal microscopy with a filter to see *green* emission, *red* emission, or the *merged image* (*C*, *F*, *I*, and *L*).

of rat-CPT1a (12) was used. Generally, 60 μg of protein extracts was subjected to SDS-PAGE. A 1:2000 dilution of anti-CPT1c was used as primary antibody. The secondary antibody was used at 1:5000 dilution. The blots were developed with the ECL Western blotting system from Amersham Biosciences.

Palmitate Oxidation

Palmitate oxidation to CO_2 and acid-soluble products were measured in PC-12 cells 48 h after transfection. On the day of the assay, cells were washed in Krebs-Ringer bicarbonate/Hepes buffer (KRBH)/0.1% BSA, preincubated at 37 °C for 30 min in KRBH/1% BSA, and washed again. Cells were incubated for 2 h at 37 °C with fresh KRBH containing 2.5 mM glucose, 0.8 mM carnitine, 0.25 mM palmitate, and 1 μCi/ml [1-^{14}C]palmitate bound to 1% BSA. Oxidation measurements were performed as previously described (13).

RESULTS

CPT1c Cell Type Localization

To identify the types of brain cell in which *CPT1c* is expressed, co-localization studies with NeuN (a nuclear neuronal marker), or glial fibrillary acidic protein (an astrocyte marker), antibodies were performed in adult mouse brain sections. Fig. 1 shows co-labeling of *CPT1c* mRNA, as revealed by *in situ* hybridization studies, with NeuN. This pattern confirms that *CPT1c* is expressed mainly in neurons. In addition, no co-localization was detected between CPT1c and glial fibrillary acidic protein (double immunohistochemistry) (Fig. 1*d*), indicating that CPT1c is not present in brain astrocytes.

CPT1c Subcellular Localization

CPT1c Is Localized in ER of Cultured Cells—To study the intracellular localization of CPT1c, fibroblasts were transiently transfected with pCPT1a-EGFP or pCPT1c-EGFP, which encode CPT1a or CPT1c proteins, respectively, fused at their C-terminal end to EGFP. 48–52 h after transfection, the fluorescence pattern shown by CPT1a-EGFP (which was expressed in a punctuate manner) was different from that of CPT1c-EGFP (which was expressed in a reticular manner). Co-localization studies were performed with MitoTracker, a potential-sensitive dye that accumulates in mitochondria, and with anti-calnexin, an ER integral protein. In some experiments cells were co-transfected with pDsRed2-ER (Clontech, Takara BioEurope, SAS), a subcellular localization vector that stains the ER red. Fig. 2 clearly shows that CPT1c is localized in the ER membrane, but not in mitochondria. In contrast, CPT1a is localized in mitochondria, as previously described in other cells (5). The slight co-localization of CPT1a with the product of pDsRed2-ER may be due to the contacts between the ER membrane and the mitochondrial outer membrane, labeled as mitochondrial-associated membranes. To assess whether either isoform is localized in peroxisomes, other organelles implicated in fatty acid oxidation, co-localization studies were performed with anti-PMP70, a peroxisomal membrane protein. No major co-localization was observed between PMP70 and CPT1c or CPT1a. The slight co-localization of CPT1c with PM70 may be due to a residual localization of this protein in peroxisomes (Fig. 3). The same experiments were performed with SH-SY5Y cells, PC-12 cells, and HEK293T cells with same results.

CPT1c Is Localized in Microsomal Fraction of Adult Mouse Brain—To eliminate the possibility that overexpression experiments in cultured cells could modify the subcellular localization of CPT1c, we performed Western blot experiments with different cellular fractions of some adult mouse tissues. CPT1c was only present in brain tissue and absent in any other tissues analyzed (Fig. 4). In addition, CPT1c was localized in the microsomal fraction of brain (Fig. 4). Only some levels of CPT1c protein were present in brain mitochondria, probably by residual contamination from microsomes. The same membranes, once de-hybridized, were used with CPT1a antibodies, as a positive control for mitochondria. CPT1a was present at high levels in mitochondria from liver and kidney, and some residual levels were found in the microsomal fraction of all tissues examined.

The N-terminal Region of the Protein Is Responsible for CPT1c-specific Subcellular Localization—We aimed to test whether the N-terminal end of CPT1c was responsible for the ER localization. We made new chimeric plasmid constructions in which 460 bp of the 5′ end of *CPT1a* gene (which encodes the two trans-membrane domains) and the mitochondrial import signal described by the Prip-Buus group (14) was replaced by the 5′ end of *CPT1c*, and *vice versa* (see *scheme* in Fig. 5). The recombinant plasmids were called pCPT1ca-EGFP and pCPT1ac-EGFP, respectively. SY-SHSY cells transiently transfected with those constructions showed that CPT1ca-EGFP was localized in ER, and that CPT1ac-EGFP was localized in mitochondria, indicating that exchange of N-terminal ends between the two CPT1 isoforms swapped the intracellular localization of recombinant chimeric proteins (Fig. 5). These results demonstrate that the N-terminal end of CPT1c lacks the mitochondrial import signal present in CPT1a and contains a putative microsomal targeting signal responsible for ER localization.

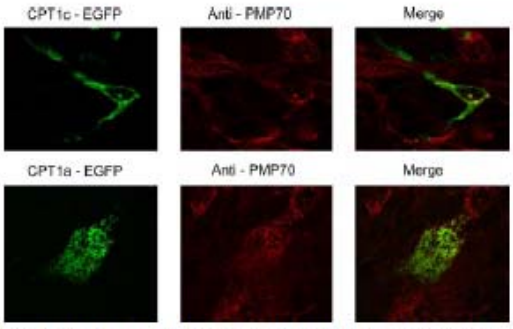

FIGURE 3. **Co-localization studies of CPT1c in perixosomes.** HEK293T cells transfected by pCPT1c-EGFP or pCPT1a-EGFP were incubated with anti-PMP70 as primary antibody. Images were taken by confocal microscopy with a filter to see *green* emission, *red* emission, or the *merged image*.

CPT1c Does Not Participate in Fatty Acid Oxidation—To examine whether CPT1c participates in mitochondrial fatty acid oxidation, we measured increases in CO_2 in PC-12 cells overexpressing CPT1c. As expected by its subcellular localization, CPT1c did not increase fatty acid oxidation, whereas CPT1a did (Table 1).

CPT1c Substrate Identification

To identify the substrate of CPT1c, we overexpressed the enzyme in PC-12 cells and attempted to identify any increased acylcarnitine species present in the lipid cell extract, 48 h after transient transfection. PC-12 cells were easily transfected with Lipofectamine (Invitrogen) or Metafecten (Biontex, Germany) with transfection efficiencies of ~40–70% of total PC-12 cells, as measured by the fluorescence in a cell-counter FACS Scan. PC-12 cells were transfected with pIRES-CPT1c, pIRES-CPT1a, or empty pIRES. Western blot experiments showed a 5- to 10-fold increase in CPT1c and CPT1a levels in transfected cells. The lipid fraction of transfected cells was extracted, and the levels of acylcarnitines were measured. To quantify acylcarnitines, we used a new HPLC-MS/MS method where no derivatization or ionic-pair chromatography is needed (10). Precursor ion scan of m/z 85 experiment allows the identification of all acylcarnitines present in the sample. Areas below chromatographic peaks (chromatograms acquired in multiple reaction monitoring mode) were measured for all acylcarnitines detected. Fig. 6 shows relative areas from chromatographic peaks present in overexpressing cells compared with control (cells transfected with empty expression vector). Cells transfected with pIRES-CPT1c showed an increase of >2-fold in palmitoylcarnitine levels (Fig. 6). No other acylcarnitine was significantly increased. Cells transfected with pIRES-CPT1a (positive control) showed a 5-fold increase in palmitoylcarnitine levels and a 2- to 3-fold increase in other long chain acylcarnitines. The Wilcoxon statistic test (a non-parametric test for two paired samples) between CPT1c-transfected cells and control cells indicated that only palmitoylcarnitine levels increased significantly in CPT1c-transfected cells. These results indicate that CPT1c has carnitine palmitoyltransferase activity and that palmitoyl-CoA is a substrate for the CPT1c isoenzyme.

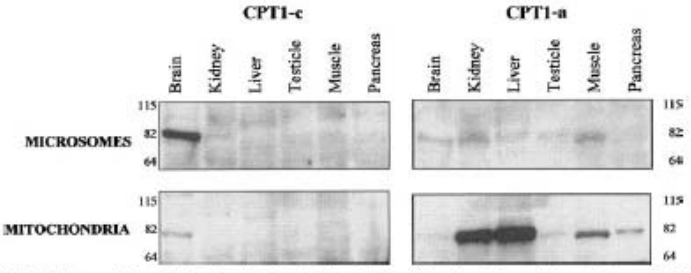

FIGURE 4. **Western blot of CPT1c in mitochondrial and ER cell fractions from different tissues of adult mouse.** 60 μg of protein cell fraction was run in each line. The same membranes were incubated with anti-CPT1c and anti-CPT1a antibodies.

CPT1c Activity

Once palmitoyl-CoA had been identified as a CPT1c substrate, we compared CPT1 activity in isolated microsomal fractions of PC-12 and

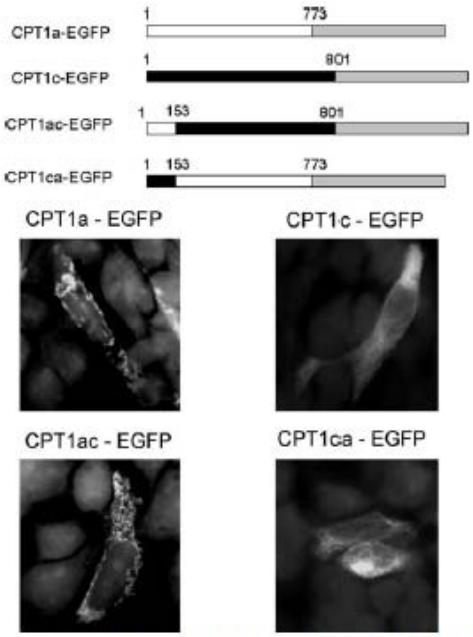

FIGURE 5. **Subcellular localization of fused proteins CPT1a-EGFP, CPT1c-EGFP, CPT1ca-EGFP, and CPT1ac-EGFP in cultured cells.** *Top*, schematic representation of fusion proteins. *CPT1a* coding region is represented in *white*, *CPT1c* coding region in *black*, and *EGFP* coding region in *gray*. *Bottom*, SH-SY5Y human neuroblastoma cells were transfected with recombinant plasmids. 48 h after transfection, cells were visualized in a fluorescence microscope using a 100× objective. CPT1a-EGFP and CPT1ac-EGPF have mitochondrial localization (punctuate pattern). CPT1c-EGFP and CPT1ca-EGFP present a ER localization (reticular pattern).

TABLE 1

Palmitate oxidation in PC-12 cells overexpressing CPT1c

48 h after transfection of cultured cells with pIRES-CPT1c, pIRES-CPT1a, or empty pIRES, cells were incubated for 2 h with [1-^{14}C]palmitate. Palmitate oxidation to CO_2 was determined. Data are presented as the mean ± S.E. of three independent experiments. Data for CPT1a are significantly different from control cells ($p < 0.05$).

	[^{14}C]CO_2 production
	nmol/mg/h
Empty pIRES	6.1 ± 0.9
pIRES-CPT1c	5.7 ± 0.7
pIRES-CPT1a	9.2 ± 2.1

HEK293T cells transfected with pIRES-CPT1c with the activity in fractions transfected with empty pIRES vector. CPT1c was overexpressed >10-fold, and the protein was found mainly in the microsomal fraction (Fig. 7*A*). Western blot membrane was reprobed with mouse anti-CPT1a antibodies to determine the residual CPT1a protein present in the microsomal fraction of PC-12 cells (Fig. 7*B*), which is responsible for the endogenous activity in microsomes of control cells. The same antibodies could not be used in HEK293T cells, because they do not recognize the human CPT1a protein. Palmitoylcarnitine formed in the CPT1 assay was measured by the same HPLC-MS/MS method used to identify the substrate (10). Microsomes from CPT1c-transfected cells showed a 50% increase in CPT1 activity compared with control cells (endogenous activity) (Table 2). K_m and V_{max} values for both substrates were calculated (Fig. 8 and Table 3). K_m values were similar to those of CPT1a (25), whereas V_{max} values were 66 times lower than those of CPT1a (25). For example, CPT1c catalytic efficiencies for palmitoyl-CoA and carnitine were 320 and 25 times lower, respectively, than those of CPT1a. CPT1 sensitivity to malonyl-CoA was not measured in cultured transfected cells, because CPT1c activity was too low and the microsomal fraction always retained residual CPT1a activity that masked any inhibitory effect of malonyl-CoA.

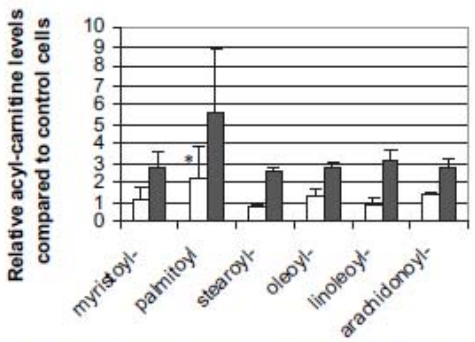

FIGURE 6. **Relative levels of different acyl-carnitines in PC12 cells.** PC-12 cells were transfected with empty pIRES vector (control cells), or pIRES-CPT1c (*white columns*), or pIRES-CPT1a (*black columns*). 48 h after transfection lipid extracts were obtained, and acylcarnitines were determined by HPLC-mass spectrum chromatography. The *y*-axis represents the area below the chromatographic peak compared with control cells. These values represent the mean of three independent experiments except for palmitoylcarnitine, which represents the mean of six independent experiments. *, $p < 0.05$ *versus* control cells. The amounts of palmitoylcarnitine, myristoylcarnitine, and arachidonoylcarnitine in control cells were 0.5 ± 0.2, 0.2 ± 0.1, and 0.02 ± 0.01 nmol/mg, respectively. For oleoylcarnitine and linoleoylcarnitine, only the chromatographic peak was measured.

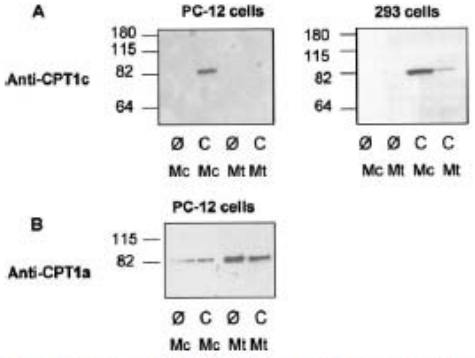

FIGURE 7. **Western blot of transfected PC-12 and HEK293T cells.** Cells were transfected with pIRES-CPT1c (*C*), or empty pIRES (*Ø*). 40 μg of microsomes (*mc*) or mitochondria (*mt*) were run in each lane of SDS-acrylamide gel. *A*, anti-ratCPT1c antibody; *B*, anti-rat-CPT1a antibody.

DISCUSSION

The presence of a third CPT1 isoform, CPT1c, in the mammalian brain is intriguing. It might show specific expression

TABLE 2

Carnitine palmitoyl transferase activity in PC-12 and HEK293T cells

Cells were transfected with pIRES-CPT1c or empty vector pIRES (control cells). 48 h after transfection, cells were collected and 40 mg of microsomal fraction was assayed for CPT1 activity. The palmitoylcarnitine formed in the assay was determined by HPLC-mass chromatography. Activity is presented as the mean ± S.E. Wilcoxon test for non-parametric paired samples was used. n = number of experiments. Absolute and percent increases in CPT1c activity are compared to control cells.

Cells	Plasmid transfection	n	Activity	p	Absolute increase	Percent increase
			nmol palmitoylcarnitine/mg/min			%
PC12	Control	7	1.37 ± 0.81	<0.05		
	CPT1c	7	1.94 ± 0.96	<0.05	0.57	41.6
293	Control	9	0.22 ± 0.11	<0.05		
	CPT1c	9	0.35 ± 0.18	<0.05	0.13	59

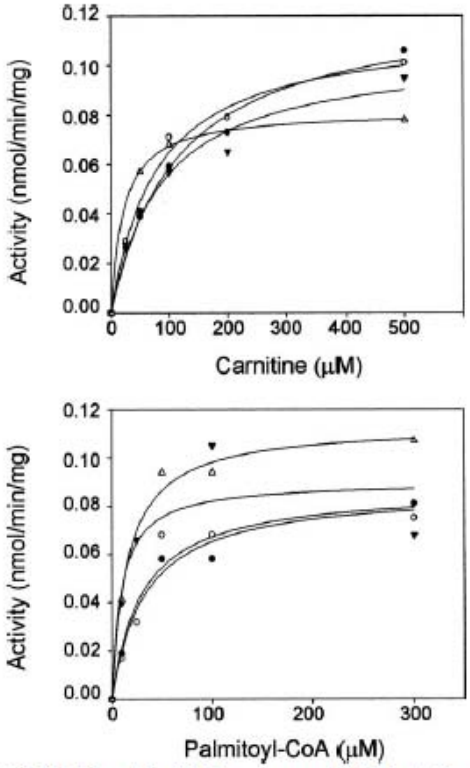

FIGURE 8. **Kinetic analysis of CPT1c overexpressed in PC-12 cells.** 20 μg of microsomes was incubated at increasing concentrations of carnitine (*upper*) and palmitoyl-CoA (*lower*), and CPT1 activity was measured.

patterns, cellular localization, or biochemical properties that would make it different enough from the other two isoforms to explain its occurrence. The data we report here on the peculiarities of CPT1c may provide clues to its cellular function.

CPT1c is expressed only in the mammalian brain. The other CPT1 isoforms are expressed in other tissues and are present in other organisms like birds, fishes, reptiles, amphibians, or insects. This suggests that CPT1c has a specific function in more evolved brains. Price *et al.* (6) showed that CPT1c is expressed in all regions of brain, in a similar pattern to that shown by neurons. Dai *et al.*, have recently demonstrated that CPT1c is localized to neurons of the central nervous system (9). Our results confirm these findings and demonstrate that CPT1c is not expressed in astrocytes, suggesting that CPT1c function is specific to neurons.

TABLE 3

Kinetic parameters of CPT1c overexpressed in PC-12 cells

Microsomes of PC-12 cells overexpressing CPT1c were assayed for activity with different palmitoyl-CoA and carnitine concentrations to calculate K_m and V_{max} values for both substrates. The results are the mean ± S.D. of three experiments. CPT1a kinetic parameters were obtained from a previous study (25).

Parameter	Isoform	
	CPT1c	CPT1a
K_m palmitoyl-CoA (mM)	25.35 ± 7.77	4.9 ± 0.3
V_{max} palmitoyl-CoA (nmol/min/mg)	0.095 ± 0.012	6.3 ± 0.4
Catalytic efficiency palmitoyl-CoA (V_{max}/K_m)	0.004	1.28
K_m carnitine (mM)	58.53 ± 21.31	127.0 ± 4.5
V_{max} carnitine (nmol/min/mg)	0.090 ± 0.010	6.6 ± 0.8
Catalytic efficiency carnitine (V_{max}/K_m)	0.002	0.05

The notion that CPT1c is localized in mitochondria stems from an observation of CPT1c protein in mitochondrial fraction of cells (6) and from co-localization studies with MitoTracker in GT1–7 hypothalamic cells (9). In the first study (6), CPT1c was also found in the microsomal fraction, as revealed by Western blot experiments, although the authors attributed this to contamination problems in cellular fractioning process. In the second study (9) the authors conclude that CPT1c co-localizes with MitoTracker, although the images did not show perfect matching and co-localization studies were not performed with any ER marker. In contrast, subcellular localization studies performed by our group in cultured cells and also in adult brain clearly demonstrate that CPT1c is localized in the ER, not in mitochondria. These results indicate that CPT1c has a different metabolic function than CPT1a or CPT1b, which is other than facilitating the import of long chain fatty acid into mitochondria or peroxisomes to undergo β-oxidation, as demonstrated in palmitate oxidation experiments. Localization of CPT1c in the ER implicates it in a biosynthetic rather than a catabolic pathway.

Intracellular localization experiments with chimeric proteins indicate that the N-terminal region of CPT1c, which includes the two transmembrane domains, is responsible for ER-specific localization. These results complement previous studies in CPT1a protein (14). Prip-Buus and colleagues demonstrate that a region just downstream of the second transmembrane domain (residues 123–147) is important for mitochondrial transport of CPT1a. Amino acid sequence comparison between CPT1a and CPT1c demonstrates that the putative mitochondrial transport sequence is partially altered in CPT1c, with fewer positively charged amino acids (one charged residue *versus* four). In addition, the second transmembrane domain is longer in CPT1c than in the other two isoforms, which may enable it to sort proteins to the ER rather than to mitochondrial outer membrane (15).

Previous studies (6, 7) had shown that CPT1c had no enzyme activity in yeast or HEK293T cells with palmitoyl-CoA or other acyl-CoA molecules as substrate. This indicated that the CPT1c

substrate could be a rare acyl-CoA specific to the brain. We thus attempted to measure variations in all acylcarnitine levels in neural cells overexpressing CPT1c. We found that palmitoylcarnitine was the only product that was increased, indicating that palmitoyl-CoA is the preferred acyl-CoA substrate for CPT1c. Activity measurements in microsomal fractions from PC-12 and HKE293T cells confirmed that CPT1c has carnitine palmitoyltransferase activity. The failure of other authors (6, 7) to detect CPT1c activity has two possible explanations: 1) they used mitochondrial fractions instead of microsomal and 2) they used a radiometric assay instead of a chromatographic method. The HPLC-MS/MS method produces reliable and accurate measurements of palmitoylcarnitine concentrations in biological samples with a sensitivity limit of 0.48 ng/ml, which corresponds to a specific activity of 0.0045 nmol·mg^{-1}·min^{-1} in our CPT1 assay conditions (10). The limit of sensitivity of the radiometric assay, calculated as the standard deviation of ten blank points with a signal-to-noise ratio of 3, corresponds to specific activity of 0.4 nmol·mg^{-1}·min^{-1}. This indicates that the chromatographic method is 100 times more sensitive than the radiometric, as described elsewhere (10). Recently, other authors have also measured CPT1 activity by a tandem mass spectrometry method because of its accuracy and sensitivity (16).

CPT1c has 100 times lower specific activity than CPT1a and CPT1b. One explanation is that CPT1c participates in a biosynthetic pathway, facilitating the constant transport of palmitate across the ER membrane, rather than in a highly active catabolic pathway such as fatty acid oxidation. Another explanation is that CPT1c acts as a metabolic sensor. CPT1c may have low activity in standard or optimal conditions (assay conditions), but its activity increases in certain situations (stress, presence of signal molecules, and others).

Lane and co-workers (7) conclude that hypothalamic CPT1c has a role in energy homeostasis and the control of food ingestion. In addition to this localized function, the wide distribution of the protein in the brain suggests a more general, ubiquitous function, perhaps related with the equilibrium between acyl-CoA pools in the cytosol and the ER lumen. Although it is not known whether CPT2 is present in ER of neurons, we hypothesize that CPT1c facilitates the entry of palmitoyl-CoA to the ER lumen. It is been reported that palmitoyl-CoA cannot cross the ER membrane, although palmitoylcarnitine can (17–20). CPT1a or CPT1b, probably localized in mitochondria-endoplasmic reticulum connections (mitochondrial-associated membrane) (21) may facilitate the entry of palmitoyl-CoA to the reticulum. In the brain, however, fatty acids are not usually oxidized, and levels of CPT1a or CPT1b are low or nonexistent. Thus the occurrence of a specific CPT1c localized in the ER membrane may ensure the entry of palmitoyl-CoA to the lumen of ER. Another possibility is that CPT1c modulates the palmitoyl-CoA pool associated with the ER, thus regulating the synthesis of ceramide and sphingolipids, which are important for signal transduction, modification of neuronal membranes, and brain plasticity (22–24).

Acknowledgments—The editorial help of Robin Rycroft is gratefully acknowledged. We also thank Prof. M. D. Lane for the gift of anti-CPT1c antibodies for use in the initial experiments.

REFERENCES

1. Esser, V., Britton, C. H., Weis, B. C., Foster, D. W., and McGarry, J. D. (1993) *J. Biol. Chem.* **268**, 5817–5822
2. Yamazaki, N., Shinohara, Y., Shima, A., and Terada, H. (1995) *FEBS Lett.* **363**, 41–45
3. McGarry, J. D., and Brown, N. F. (1997) *Eur. J. Biochem.* **244**, 1–14
4. Lopez-Viñas, E., Bentebibel, A., Gurunathan, C., Morillas, M., de Arriaga, D., Serra, D., Asins, G., Hegardt, F. G., and Gomez-Puertas, P. (2007) *J. Biol. Chem.* **282**, 18212–18224
5. Broadway, N. M., Pease, R. J., Birdsey, G., Shayeghi, M., Turner, N. A., and David Saggerson, E. (2003) *Biochem. J.* **370**, 223–231
6. Price, N., van der Leij, F., Jackson, V., Corstorphine, C., Thomson, R., Sorensen, A., and Zammit, V. (2002) *Genomics* **80**, 433–442
7. Wolfgang, M. J., Kurama, T., Dai, Y., Suwa, A., Asaumi, M., Matsumoto, S., Cha, S. H., Shimokawa, T., and Lane, M. D. (2006) *Proc. Natl. Acad. Sci. U. S. A.* **103**, 7282–7287
8. Sorensen, A., Travers, M. T., Vernon, R. G., Price, N. T., and Barber, M. C. (2002) *Brain Res. Gene Expr. Patterns* **1**, 167–173
9. Dai, Y., Wolfgang, M. J., Cha, S. H., and Lane, M. D. (2007) *Biochem. Biophys. Res. Commun.* **359**, 469–474
10. Jáuregui, O., Sierra, A. Y., Carrasco, P., Gratacós, E., Hegardt, F. G., and Casals, N. (2007) *Anal. Chim. Acta* **599**, 1–6
11. Morillas, M., Gomez-Puertas, P., Roca, R., Serra, D., Asins, G., Valencia, A., and Hegardt, F. G. (2001) *J. Biol. Chem.* **276**, 45001–45008
12. Prip-Buus, C., Cohen, I., Kohl, C., Esser, V., McGarry, J. D., and Girard, J. (1998) *FEBS Lett.* **429**, 173–178
13. Herrero, L., Rubi, B., Sebastian, D., Serra, D., Asins, G., Maechler, P., Prentki, M., and Hegardt, F. G. (2005) *Diabetes* **54**, 462–471
14. Cohen, I., Guillerault, F., Girard, J., and Prip-Buus, C. (2001) *J. Biol. Chem.* **276**, 5403–5411
15. Horie, C., Suzuki, H., Sakaguchi, M., and Mihara, K. (2002) *Mol. Biol. Cell* **13**, 1615–1625
16. van Vlies, N., Ruiter, J. P., Doolaard, M., Wanders, R. J., and Vaz, F. M. (2007) *Mol. Genet. Metab.* **90**, 24–29
17. Washington, L., Cook, G. A., and Mansbach, C. M., 2nd. (2003) *J. Lipid Res.* **44**, 1395–1403
18. Abo-Hashema, K. A., Cake, M. H., Power, G. W., and Clarke, D. (1999) *J. Biol. Chem.* **274**, 35577–35582
19. Gooding, J. M., Shayeghi, M., and Saggerson, E. D. (2004) *Eur. J. Biochem.* **271**, 954–961
20. Arduini, A., Denisova, N., Virmani, A., Avrova, N., Federici, G., and Arrigoni-Martelli, E. (1994) *J. Neurochem.* **62**, 1530–1538
21. Rusinol, A. E., Cui, Z., Chen, M. H., and Vance, J. E. (1994) *J. Biol. Chem.* **269**, 27494–27502
22. Buccoliero, R., and Futerman, A. H. (2003) *Pharmacol. Res.* **47**, 409–419
23. Ohanian, J., and Ohanian, V. (2001) *Cell Mol. Life Sci.* **58**, 2053–2068
24. van Echten-Deckert, G., and Herget, T. (2006) *Biochim. Biophys. Acta* **1758**, 1978–1994
25. Morillas, M., Gómez-Puertas, P., Bentebibel, A., Sellés, E., Casals, N., Valencia, A., Hegardt, F. G., Asins, G., and Serra, D. (2003) *J. Biol. Chem.* **278**, 9058–9063

ADDITIONS AND CORRECTIONS

This paper is available online at www.jbc.org

THE JOURNAL OF BIOLOGICAL CHEMISTRY VOL. 283, NO. 18, p. 12680, May 2, 2008

VOLUME 283 (2008) PAGES 7733–7744

Amyloidogenic processing but not amyloid precursor protein (APP) intracellular C-terminal domain production requires a precisely oriented APP dimer assembled by transmembrane G*XXX*G motifs.

Pascal Kienlen-Campard, Bernadette Tasiaux, Joanne Van Hees, Mingli Li, Sandra Huysseune, Takeshi Sato, Jeffrey Z. Fei, Saburo Aimoto, Pierre J. Courtoy, Steven O. Smith, Stefan N. Constantinescu, and Jean-Noël Octave

On Page 7743, the "Acknowledgments" should read as follows. "We thank T. C. Südhof for the generous gift of APPGal4 constructs, L. Mercken for help with sαAPP and sβAPP quantification, N. Sergeant and A. Delacourte for antibodies directed against the APP C terminus, and F. N'Kuli for excellent technical assistance. The mass spectrometric analysis of immunoprecipitated Aβ samples shown in Supplemental Fig. 1 was performed at the Freie University Berlin in the Mass Spectrometry Core Facility of the Institute for Chemistry and Biochemistry (Prof. Gerd Multhaup) by Lisa Münter and Chris Weise."

VOLUME 283 (2008) PAGES 6878–6885

CPT1c is localized in endoplasmic reticulum of neurons and has carnitine palmitoyltransferase activity.

Adriana Y. Sierra, Esther Gratacós, Patricia Carrasco, Josep Clotet, Jesús Ureña, Dolors Serra, Guillermina Asins, Fausto G. Hegardt, and Núria Casals

On Page 6878, right column, line 8 from the bottom, the following sentence should be added after "contact sites between ER and mitochondria (5)": Price *et al.* (6) demonstrated that when rat CPT1c was expressed heterologously in *Pichia pastoris*, it was targeted exclusively to the microsomes. In addition, these authors found CPT1c in the endoplasmic reticular and mitochondrial fractions of homogenized rat brain, although they indicated that the mutual contamination of the two cell membrane fractions was very substantial.

IMPORTANT ROLES OF BRAIN-SPECIFIC CARNITINE PALMITOYLTRANSFERASE AND CERAMIDE METABOLISM IN LEPTIN HYPOTHALAMIC CONTROL OF FEEDING.

Gao, S., Zhu, G., Gao, X., Wu, D., **Carrasco, P**., Casals, N., et al. (2011).

Proceedings of the National Academy of Sciences of the United States of America, 108(23), 9691-9696

Important roles of brain-specific carnitine palmitoyltransferase and ceramide metabolism in leptin hypothalamic control of feeding

Su Gao[a], Guangjing Zhu[b], Xuefei Gao[c], Donghai Wu[c], Patricia Carrasco[d], Núria Casals[d], Fausto G. Hegardt[e], Timothy H. Moran[b], and Gary D. Lopaschuk[a,1]

[a]Department of Pediatrics, Mazankowski Alberta Heart Institute, University of Alberta, Edmonton, AB, Canada T6G 2S2; [b]Department of Psychiatry and Behavioral Sciences, The Johns Hopkins University School of Medicine, Baltimore, MD 21205; [c]Key Laboratory of Regenerative Biology, Guangzhou Institute of Biomedicine and Health, Chinese Academy of Sciences, Guangzhou 510530, China; [d]Basic Sciences Department and Centro de Investigación Biomédica en Red de la Fisiopatología de la Obesidad y Nutrición, School of Medicine and Health Sciences, Universitat Internacional de Catalunya, Barcelona 08195, Spain; and [e]Department of Biochemistry and Molecular Biology and Centro de Investigación Biomédica en Red de la Fisiopatología de la Obesidad y Nutrición, Facultat de Farmàcia, Universitat de Barcelona, E-08028 Barcelona, Spain

Edited* by Solomon H. Snyder, The Johns Hopkins University School of Medicine, Baltimore, MD, and approved April 21, 2011 (received for review March 1, 2011)

Brain-specific carnitine palmitoyltransferase-1 (CPT-1c) is implicated in CNS control of food intake. In this article, we explore the role of hypothalamic CPT-1c in leptin's anorexigenic actions. We first show that adenoviral overexpression of CPT-1c in hypothalamic arcuate nucleus of rats increases food intake and concomitantly up-regulates orexigenic neuropeptide Y (NPY) and Bsx (a transcription factor of NPY). Then, we demonstrate that this overexpression antagonizes the anorectic actions induced by central leptin or compound cerulenin (an inhibitor of fatty acid synthase). The overexpression of CPT-1c also blocks leptin-induced down-regulations of NPY and Bsx. Furthermore, the anorectic actions of central leptin or cerulenin are impaired in mice with brain CPT-1c deleted. Both anorectic effects require elevated levels of hypothalamic arcuate nucleus (Arc) malonyl-CoA, a fatty acid-metabolism intermediate that has emerged as a mediator in hypothalamic control of food intake. Thus, these data suggest that CPT-1c is implicated in malonyl-CoA action in leptin's hypothalamic anorectic signaling pathways. Moreover, ceramide metabolism appears to play a role in leptin's central control of feeding. Leptin treatment decreases Arc ceramide levels, with the decrease being important in leptin-induced anorectic actions and down-regulations of NPY and Bsx. Of interest, our data indicate that leptin impacts ceramide metabolism through malonyl-CoA and CPT-1c, and ceramide de novo biosynthesis acts downstream of both malonyl-CoA and CPT-1c in mediating their effects on feeding and expressions of NPY and Bsx. In summary, we provide insights into the important roles of malonyl-CoA, CPT-1c, and ceramide metabolism in leptin's hypothalamic signaling pathways.

Obesity is a major cause of insulin-resistance and diabetes. An imbalance between food intake and energy expenditure contributes to the development of obesity. The CNS regulates energy homeostasis with the hypothalamus playing a critical role (1, 2). Mounting evidence now shows that fatty acid metabolism in the hypothalamus plays important roles in the central regulation of energy homeostasis (3–17). In this regard, malonyl-CoA, an intermediate in fatty acid de novo biosynthesis, is emerging as a player in the hypothalamus (3, 5, 6, 8–13).

Hypothalamic malonyl-CoA metabolism has been implicated in leptin-induced anorectic actions (9, 12, 13). Leptin, an important physiological regulator of food intake and body weight, exerts its anorectic effects partly by inducing an increase in malonyl-CoA level in the hypothalamic arcuate nucleus (Arc) (12). In addition to fatty acid biosynthesis, recent data also suggest a role for carnitine palmitoyltransferase-1 (CPT-1), a key enzyme in mitochondrial fatty acid β-oxidation (7, 18), in hypothalamic regulation of energy balance. Fatty acid biosynthesis and β-oxidation are linked by malonyl-CoA–mediated inhibition of CPT-1 acyltransferase activity (12). In the hypothalamus, the CPT-1 liver isoform (CPT-1a) is the predominant type possessing the prototypical acyltransferase activity (7). Our previous results have demonstrated that leptin treatment does not alter the levels of substrates of CPT-1a, long-chain fatty acyl-CoAs (12). Furthermore, upon leptin treatment, the levels of products of CPT-1a, long-chain acylcarnitines, were also not altered (19). Together, these results show that leptin treatment may not affect CPT-1a activity, although it raises the level of malonyl-CoA (an inhibitor of CPT-1a). It should be noted that the activity of CPT-1–mediated fatty acid β-oxidation is very low in the brain compared with the peripheral tissues (20, 21). As a result, the CPT-1a activity in the hypothalamus may be resistant to further inhibition exerted by malonyl-CoA. This possibility may underlie the difficulties in detecting the expected inhibition of CPT-1a in these experiments. Alternatively, because of the inherently low basal activity, CPT-1a may not be in a position that is subject to the regulation of malonyl-CoA, particularly under the condition that increases malonyl-CoA level. In our subsequent studies (19), we artificially increased the CPT-1a activity in the Arc and were able to detect a leptin-induced inhibition of CPT-1a. However, our data reveal that this CPT-1a inhibition is not implicated in leptin's anorectic actions (19). Thus, despite a significant role of malonyl-CoA, CPT-1a does not seem to be an important player in leptin's hypothalamic control of food intake (12). This dissociation promotes us to identify alternative downstream targets of malonyl-CoA action in leptin's feeding pathways.

The brain-specific isoform of CPT-1 (CPT-1c), with the sequence similar to the other CPT-1 isozymes (1a and 1b), is expressed in the hypothalamus (22, 23). The molecular function of CPT-1c has not been well defined and the initial studies suggested that CPT-1c did not have the prototypical acyltransferase activity (22, 23). A later study using a more sensitive activity assay identified a very weak acyltransferase activity (20–300 times lower than CPT-1a and -1b) (24). This activity of CPT-1c is atypical as it preferentially uses palmitoyl-CoA as substrate (24). Of interest, CPT-1c is expressed in Arc neurons (25) and CPT-1c knockout animals manifest reduced food intake and weight gain (23). These findings demonstrate that null function of CPT-1c is associated with the anorectic effect, an action in the same direction as the feeding effect produced by exogenous leptin. We further predict that inhibition of CPT-1c functions is a step in leptin's anorectic signaling pathways. Moreover, it has recently been shown that a

Author contributions: S.G., G.Z., X.G., D.W., N.C., F.G.H., T.H.M., and G.D.L. designed research; S.G., G.Z., X.G., P.C., and N.C. performed research; D.W., N.C., F.G.H., T.H.M., and G.D.L. contributed new reagents/analytic tools; S.G., G.Z., X.G., D.W., P.C., N.C., F.G.H., T.H.M., and G.D.L. analyzed data; and S.G., N.C., F.G.H., T.H.M., and G.D.L. wrote the paper.

The authors declare no conflict of interest.

*This Direct Submission article had a prearranged editor.

[1]To whom correspondence should be addressed. E-mail: gary.lopaschuk@ualberta.ca.

This article contains supporting information online at www.pnas.org/lookup/suppl/doi:10.1073/pnas.1103267108/-/DCSupplemental.

significant portion of CPT-1c is localized in the endoplasmic reticulum (ER) (24), suggesting that CPT-1c is involved in ER functions. Taken together, these data lead to our hypothesis that CPT-1c acts to modulate leptin's anorectic actions by impacting certain ER functions. In this article, we examined the roles of CPT-1c in leptin's Arc signaling pathways. We further explored how CPT-1c interacts with one of the many functions of the ER, ceramide metabolism (24), to impact leptin's hypothalamic control of food intake.

Results

CPT-1c Modulates the Anorectic Actions of Leptin and Cerulenin. CPT-1c is widely distributed in CNS neurons (25). To address the arcuate-specific role of CPT-1c, we delivered a recombinant adenoviral vector encoding wild-type human CPT-1c into the arcuate nucleus of rats using stereotaxic surgery. Arc delivery of the virus resulted in an increased Arc level of CPT-1c without altering the level of CPT-1a or CPT-2 (Fig. 1*A*). The levels of long-chain acylcarnitines, products and a reliable indicator of CPT-1 acyltransferase activity (24, 26), were not changed following the overexpression (Fig. 1*A*), which is consistent with the prediction that CPT-1c has a very low CPT-1 activity in vivo (21). However, this lack of change of acylcarnitine levels indicates that CPT-1c overexpression did not interfere with CPT-1a activity. Consistent with a previous report (25), Arc overexpression of CPT-1c did not produce significant changes of daily food consumption or body weight gain under ad libitum-fed condition (Fig. S1). However, following an overnight fast, the rats with Arc overexpression of CPT-1c consumed more food than the null rats (Fig. 1*B*). This overexpression also induced an increase in the

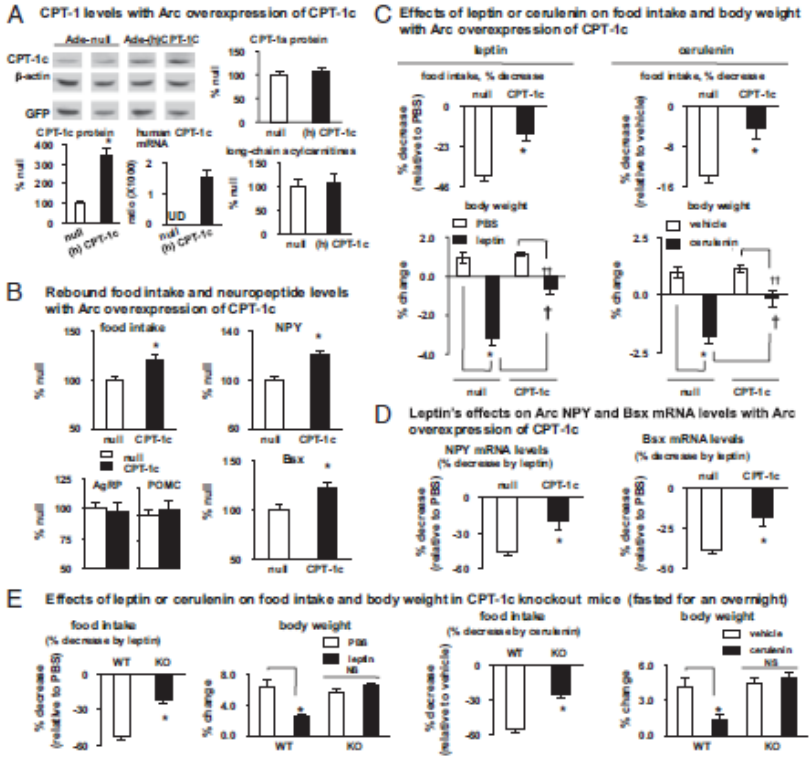

Fig. 1. CPT-1c modulates the anorectic actions of leptin and cerulenin. The adenovirus that encodes human CPT-1c and coexpresses GFP (Ade-CPT-1c) was delivered into the Arc of rats. The adenoviral vector expressing GFP alone was used as the null control (Ade-null). After 4 d following the delivery of the viruses, the rats were killed. (*A*) CPT-1c and CPT-1a protein levels in the Arc were quantitated ($n = 10$). Two representative blots of CPT-1c, GFP and actin from each treated group are shown. The Arc mRNA levels of human (h)-CPT-1c ($n = 12$), rat-CPT-1a ($n = 4–5$), and CPT-2 ($n = 6$) were quantitated and the mRNA levels of (h)-CPT-1c are shown. Rat-CPT-1a: Ade-null, 100 ± 4.4%, Ade-(h)-CPT-1c, 94 ± 4.9%; $P > 0.05$. CPT-2: Ade-null, 100 ± 6.8%, Ade-(h)-CPT-1c, 96 ± 12%; $P > 0.05$. Arc levels of long-chain acylcarnitines (palmitoylcarnitine, stearoylcarnitine, and oleoylcarnitine) were measured ($n = 5$). (*B*) After 4 d following the delivery of the viruses, the rats were fasted over a dark cycle (12 h). Then, some rats were provided with food and the food intakes at 24 h following food presentation are shown ($n = 9–13$). The other rats were killed after the fast. The mRNA levels of NPY, AgRP, POMC, and Bsx were measured (NPY: $n = 12$; AgRP and POMC: $n = 10$; Bsx: $n = 4–6$). (*C*) After 4 d following the delivery of the viruses, the rats received an intra-Arc infusion of leptin (1 μg) or cerulenin (40 μg) at 2 h before the onset of the dark cycle and food intakes and body weights were monitored ($n = 5$). The percent inhibitions of food intake at 24 h following the treatments are shown. The changes in 24-h body weight are also presented. (*D*) The rats with Arc overexpression of CPT-1c received an Arc infusion of leptin as described in *C* and were killed after the dark cycle (12 h). The mRNA levels of NPY and Bsx mRNA were quantitated. The percent decreases in NPY or Bsx mRNA level by leptin (relative to PBS) are shown (NPY: $n = 12$; Bsx: $n = 11–12$). (*E*) The mice with brain CPT-1c deleted (CPT-1c knockout) or their wild-type littermates were fasted over a dark cycle (12 h). Then, the mice received an intracerebroventricular injection of leptin (4 μg in PBS) or cerulenin (125 μg in 25% DMSO). For both treatments (leptin, $n = 4–5$; cerulenin, $n = 4–5$), the percent inhibitions (relative to the vehicle) of food intake at 24 h following the injections are shown. The changes in 24-h body weight are also shown. WT, wild-type; KO, CPT-1c knockout.

level of the Arc orexigenic neuropeptide Y (NPY) (Fig. 1*B*), an important mediator in central control of feeding (1). In addition, the brain-specific homeobox factor (Bsx), a transcription factor of NPY expression (27), was up-regulated following the overexpression of CPT-1c (Fig. 1*B*). The levels of other Arc neuropeptides involved in food intake, such as agouti-related peptide (AgRP) and preopiomelanocortin (POMC), were not altered (Fig. 1*B*). Next, we assessed the role for CPT-1c in leptin's action on food intake by infusing leptin directly into the Arc overexpressing CPT-1c. In these rats, leptin-induced anorectic effects (under ad libitum conditions) were significantly attenuated compared with the null condition (Fig. 1*C*). To evaluate the role of CPT-1c in the specific context of Arc malonyl-CoA feeding mechanisms, we disrupted the activity of fatty acid synthase (FAS) by infusing cerulenin, a FAS inhibitor (3, 6), into the Arc overexpressing CPT-1c. FAS uses malonyl-CoA as a substrate and central cerulenin treatment exerts anorectic actions by increasing hypothalamic malonyl-CoA level (3, 6). Similar to our findings with leptin, the anorectic actions by cerulenin were antagonized by Arc overexpression of CPT-1c (Fig. 1*C*). Leptin reduces feeding and body weight partly through down-regulating NPY and Bsx levels (1, 12). Our data showed that these leptin-

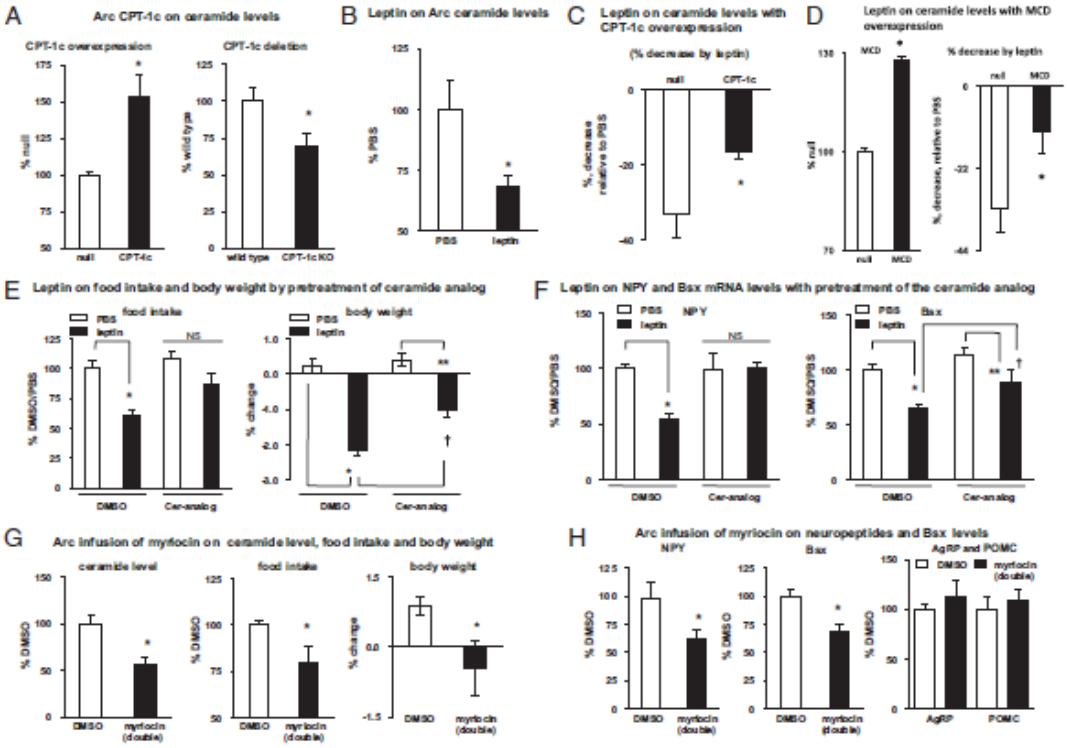

Fig. 2. Arc ceramide metabolism is required in leptin's anorectic actions. (*A*) CPT-1c overexpression: the Ade-CPT-1c or Ade-GFP (null) was delivered into the Arc of rats. The rats were killed following 8-h food deprivation and ceramide levels in the Arc were measured ($n = 7$). CPT-1c deletion: The CPT-1c knockout mice and their wild-type littermates were killed under ad libitum-fed conditions. The ceramide levels in the mediobasal hypothalamus encompassing the Arc were measured ($n = 5–6$). (*B*) Before the dark cycle, leptin (1 μg in PBS) was infused into the Arc of rats. Ceramide levels (at 8 h following the infusion) were measured ($n = 8–12$). (*C*) The rats with Arc overexpression of CPT-1c or GFP (null), under ad libitum-fed conditions, received an intra-Arc infusion of leptin (1 μg in PBS) before the dark cycle. Arc ceramide levels (at 8 h following the infusion) in these rats were measured. The percent decreases in ceramide level by leptin (relative to PBS) are shown ($n = 8–9$) (note: the CPT-1c overexpression per se under ad libitum-fed conditions has no significant effect on the ceramide level.). (*D*) The Ade-MCD or Ade-GFP (null) was delivered into the Arc of rats. After 4 d following the delivery of the viruses, some rats were killed after a period (8 h) of food deprivation. Arc ceramide levels in these rats were measured ($n = 5$). The other rats, under ad libitum-fed conditions, received an intra-Arc infusion of leptin (1 μg in PBS) before the dark cycle. Arc ceramide levels (at 8 h following the infusion) were measured. The percent decreases in ceramide level by leptin (relative to PBS) are shown ($n = 8–9$) (note: the MCD overexpression of per se under ad libitum-fed conditions has no significant effect on the ceramide level). (*E* and *F*) At 4 h before the dark onset, *N*-Hexanoyl-D-sphingosine (2.5 μg in DMSO), a cell-permeable analog of natural ceramide (Cer-analog), was infused into the Arc. Two hours later (i.e., 2 h before the dark onset), the rats received an intra-Arc infusion of leptin (1 μg in PBS). (*E*) Some rats received food at the onset of the dark cycle and the food intakes and body weights at 24 h following leptin infusion are shown ($n = 6$). (*F*) The other rats were fasted over the dark cycle (12 h) and were then killed. The mRNA levels of NPY and Bsx in these rats were quantitated ($n = 5–6$). (*G*) Food was removed before onset of the dark cycle and the rats received one intra-Arc infusion of myriocin (4 μg in DMSO). Six hours later, these rats received the other intra-Arc infusion of myriocin (4 μg in DMSO). After another 2-h period for recovery, some rats were killed for ceramide assay ($n = 5$) (note: to this end, these rats had been fasted for 8 h). The other rats were presented with food. The food intakes and body weights at 24 h after the first injection are shown ($n = 12–13$). (*H*) The rats received the double myriocin treatment as described in *G*. After 12 h following the first infusion, the rats were killed. The mRNA levels of Arc neuropeptides ($n = 6–9$) and Bsx ($n = 6–8$) in these rats were measured.

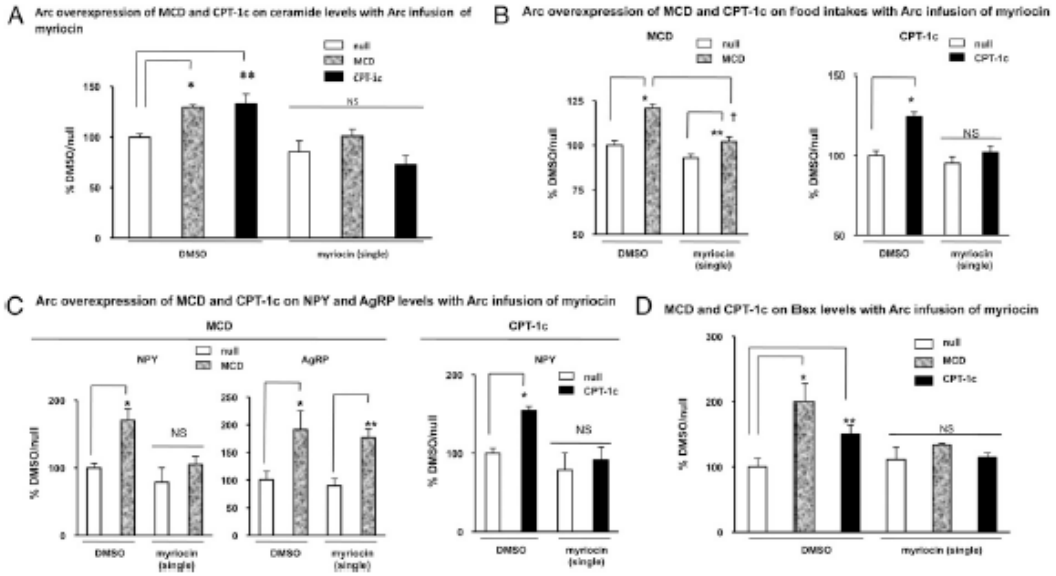

Fig. 3. Ceramide de novo biosynthesis mediates malonyl-CoA and CPT-1c actions on food intake and body weight. (*A* and *B*) The rats with Arc overexpression of MCD ($n = 8$), CPT-1c ($n = 12$), or GFP (null, $n = 16$) received a single intra-Arc infusion of myriocin (4 μg in DMSO) before the dark cycle and food was removed. Eight hours later, (*A*) some rats were killed and were then used for ceramide assay; (*B*) the other rats were provided with food and the food intakes at 24 h following the infusion are shown. (MCD: $n = 5$–6; CPT-1c: $n = 7$–10). (*C* and *D*) The rats with Arc overexpression of MCD, CPT-1c, or GFP (null) received myriocin treatment as described above. The rats were killed after the dark cycle (12 h) during which period no food was present. The mRNA levels of NPY, AgRP (*C*) ($n = 5$–7) and Bsx (*D*) ($n = 5$–6) in these rats were quantitated.

induced changes were attenuated in the animals with Arc overexpression of CPT-1c (Fig. 1*D*). We previously reported that leptin treatment in the similar experimental setting did not affect the level of AgRP or POMC (by both real-time PCR and in situ hybridization) (12), so their responses to leptin were not examined in the current study.

We have shown that ectopical expression of CPT-1c modulates leptin's anorectic actions. The immediate question is whether this effect has physiological relevance in leptin's central feeding mechanisms. To address the issue, we injected leptin to mice with brain CPT-1c deleted and then monitored food intake and body weight. As expected, leptin-induced inhibitions of food intake and weight gain seen in wild-type mice were blocked in the knockout mice (Fig. 1*E*). To evaluate the role of CPT-1c specifically in the action of malonyl-CoA, we centrally injected cerulenin into these mice and found CPT-1c deletion blocked the anorectic actions of cerulenin (Fig. 1*E*). Taken together, these data show that CPT-1c may be a necessary component in the malonyl-CoA action in leptin's intracellular signaling pathways.

Arc Ceramide Metabolism Is Required for Leptin's Anorectic Actions. A significant portion of CPT-1c resides in the ER and CPT-1c preferentially binds palmitoyl-CoA (24). These findings drove us to hypothesize that CPT-1c plays a role in the ceramide metabolism that starts in the ER and uses palmitoyl-CoA as a substrate (24). In support, we found Arc overexpressing CPT-1c (under fasting condition) had an increased ceramide level, and the Arc with CPT-1c deleted had a decreased level (Fig. 2*A*). Leptin treatment is expected to alter hypothalamic ceramide level because CPT-1c is involved in leptin's hypothalamic actions. Indeed, we found that leptin reduced the ceramide level in the Arc (Fig. 2*B*), and this reduction was attenuated by CPT-1c overexpression (Fig. 2*C*). As the increase in Arc malonyl-CoA level is required in leptin's central anorectic effects (12), we also assessed the role of malonyl-CoA in ceramide metabolism. Malonyl-CoA decarboxylase (MCD), an enzyme degrading malonyl-CoA (12), was overexpressed in the Arc and ceramide levels were then measured. Previous results demonstrated that MCD overexpression in the Arc reduces malonyl-CoA level, increases food intake, and blocks leptin-mediated inhibition of feeding (9, 19). Here we showed that MCD overexpression up-regulated ceramide level and blocked leptin-induced down-regulation of Arc ceramide level (Fig. 2*D*). Together, these data suggest that leptin induces the decrease in Arc ceramide level through the actions of malonyl-CoA and CPT-1c. Next, we evaluated the relevance of ceramide metabolism in leptin's anorectic signaling actions. We found that Arc pretreatment with *N*-hexanoyl-D-sphingosine, a cell-penetrating analog of natural ceramides (28), blocked leptin-induced anorectic actions (Fig. 2*E*). In parallel, the ceramide analog blocked or attenuated leptin-mediated down-regulation of NPY and Bsx (Fig. 2*F*). To determine the specificity of the observed feeding effects of the compounds, we centrally infused ciliary neurotrophic factor (CNTF) into the rats that had received the pretreatment with the ceramide analog or had CPT-1c overexpressed in the Arc. Previous evidence has demonstrated that CNTF produces anorectic actions without affecting the hypothalamic acetyl-CoA carboxylase and malonyl-CoA metabolic pathway.* In our studies, the overexpression of CPT-1c or pretreatment with the ceramide analog did not block CNTF-mediated anorectic actions (Fig. S2). Thus, the effects of both CPT-1c and ceramide appear to be specific for the malonyl-CoA anorectic action.

*Wood, et al. The Endocrine Society's 91st Annual Meeting, ENDO 09, June 10–13, 2009, Washington, DC.

Finally, we examined the independent effects of Arc ceramide on food intake and body weight. The compound myriocin, an inhibitor of ceramide biosynthesis, was used to reduce the ceramide level. Myriocin does so by inhibiting serine palmitoyltransferase (SPT), the key rate-limiting enzyme of ceramide de novo biosynthesis (29, 30). The brain expresses SPT (30) and we found a significant mRNA level of SPT in the Arc (comparable to the levels of AgRP and POMC). We infused myriocin into the Arc and monitored feeding and body weight. We found that Arc administration (two injections separated by 6 h), which effectively reduced ceramide level in the Arc, lowered food intake and weight gain (Fig. 2*G*). Along with these changes, NPY and Bsx levels were decreased (Fig. 2*H*). As was the case with CPT-1c, myriocin treatment did not affect the mRNA level of AgRP or POMC (Fig. 2*H*). We then tested the feeding effect of elevated ceramide level in the Arc. The dosage of the ceramide analog used in the wild-type animals reached a limit beyond which nonspecific or toxic effects will appear. As a result, we infused the compound with the same dosage into the rats with Arc overexpression of CPT-1c (that can be induced to show an increased level of Arc ceramide). As expected, under ad libitum-fed conditions, the compound increased food intake (24 h after the infusion: DMSO: 100 ± 2.9%; the ceramide analog: 110 ± 4.0%; $P < 0.05$).

Ceramide de Novo Synthesis Mediates Arc Malonyl-CoA and CPT-1c Actions on Food Intake. We have shown that both malonyl-CoA and CPT-1c affect leptin's actions on ceramide level and food intake. We further hypothesized that ceramide de novo synthesis mediates these effects. In support of the hypothesis, we found that myriocin infusion (single dosage) prevented the increase in ceramide level induced by MCD or CPT-1c (Fig. 3*A*). These data demonstrate that de novo synthesis of ceramide contributes to the effects of malonyl-CoA and CPT-1c on ceramide metabolism. Next, we evaluated the relevance of ceramide de novo synthesis in the actions of malonyl-CoA and CPT-1c on feeding. We subjected the rats to a period of food deprivation and infused myriocin at the onset of the fast. Arc overexpression of MCD (lowering malonyl-CoA) or CPT-1c increased rebound feeding, and myriocin treatments stopped the developments of the increase in food intake (Fig. 3*B*). It should be noted that we injected myriocin as a single dosage in this particular experiment, so that myriocin treatment alone did not affect feeding (Fig. 3*B*). Along with the blockade of food intake, we found that MCD- and CPT-1c–mediated up-regulations of NPY (9) were also blocked by central myriocin (Fig. 3*C*). The up-regulation of AgRP level by MCD (9) was not affected by myriocin treatment (Fig. 3*C*), suggesting a NPY-specific effect in the central actions of de novo biosynthesis of ceramide. The MCD or CPT-1c–induced up-regulation of Bsx was also blocked by myriocin treatment (Fig. 3*D*).

Finally, we assessed the physiological relevance of the changes of Arc ceramide levels (Fig. S3). We showed that fasting increased the Arc ceramide levels and refeeding reduced the elevated levels. We also demonstrated that the up-regulation of Arc ceramide levels by fasting is CPT-1c–dependent, as the change is negated in the mice with Arc deletion of CPT-1c (Fig. S3).

Discussion

Previous results have challenged the role of CPT-1a in leptin's Arc anorectic signaling pathways (12, 19). Our current studies identify CPT-1c as a potential mediator in leptin's hypothalamic anorectic actions. CPT-1c also appears to be a necessary component in the anorectic actions induced by central cerulenin. Because the anorectic actions of both leptin and cerulenin require the increase in Arc malonyl-CoA level, CPT-1c is likely implicated in the malonyl-CoA signaling action in leptin's Arc intracellular pathways.

Although the exact biochemical functions of CPT-1c have not been uncovered in the present study, our data suggest that CPT-1c regulates ceramide metabolism. Importantly, ceramide metabolism appears to play a role in CPT-1c's effect on food intake. In particular, we provide evidence supporting a role of ceramide de novo biosynthesis in mediating CPT-1c action on feeding. Based on these data, we propose that CPT-1c would act to intervene with ER ceramide de novo biosynthesis. There are several potential mechanisms underlying this proposal. First, because CPT-1c is localized in the ER (24) where SPT resides, it is possible that CPT-1c physically interacts with SPT to modulate the activity of ceramide de novo biosynthesis. Second, as it has a preferential affinity for palmitoyl-CoA (24), CPT-1c may increase the local availability of palmitoyl-CoA for use by SPT to synthesize ceramide. Finally, CPT-1c may act as a transporter for shuttling palmitoyl-CoA into the ER for use in ceramide synthesis. This potential mechanism is effective in interpreting the observed changes in ceramide levels when malonyl-CoA levels alter concomitantly (e.g., MCD overexpression). By the inhibitory effect on mitochondrial CPT-1a, malonyl-CoA can affect the availability of palmitoyl-CoA to SPT, and thus the subsequent ceramide de novo biosynthesis. However, once palmitoyl-CoA is shuttled into the ER, ceramide biosynthesis will be free of the intervention by malonyl-CoA–mediated inhibition of CPT-1a. This scenario sets an ideal subcellular environment for the de novo biosynthetic pathway of ceramide to exert a regulatory signaling role. The potential interaction of CPT-1c with ceramide metabolism appears to have physiological relevance as our data also suggest that CPT-1c is required in fasting-induced increase in ceramide levels.

Ceramide metabolism plays roles in the signaling mechanisms underlying a variety of physiological functions, such as apoptosis, cell growth, and cell differentiation (29). Of relevance, elevated ceramide biosynthesis in the periphery has been implicated in the pathogenesis of obesity and type-2 diabetes (29). Our data suggest a role for ceramide metabolism in the hypothalamic controls of feeding and body weight. Of interest in leptin's signaling actions, we show that leptin reduces ceramide level in the Arc, which is a significant step in leptin-mediated anorectic effects and down-regulations of NPY and Bsx. In leptin's action on ceramide metabolism, it seems that both malonyl-CoA and CPT-1c are involved. Our data indicate that, in addition to CPT-1c, malonyl-CoA action can also impact Arc ceramide metabolism. Moreover, similar to CPT-1c, the downstream signaling actions of malonyl-CoA's effect on feeding also involve ceramide de novo synthesis. Because malonyl-CoA and CPT-1c play roles in leptin's actions on feeding, ceramide de novo synthesis may be a component in leptin's hypothalamic anorectic signaling pathways. Taking these data together, we propose a model that leptin reduces ceramide level and food intake via increasing malonyl-CoA and inducing CPT-1c inhibition, resulting in the decreased ceramide de novo synthesis (Fig. S4). Because CPT-1c can bind malonyl-CoA, malonyl-CoA might directly inhibit CPT-1c functions (Fig. S4, pathway-1). Our data are indeed consistent with this proposed pathway. Reduced malonyl-CoA level (under either fasting or MCD overexpression), which is anticipated to activate CPT-1c, is associated with the increases in ceramide levels and food intake. However, it should be particularly noted that malonyl-CoA may also interact with other yet-to-be identified mediators to modulate ceramide metabolism and food intake (Fig. S4, pathway-2). In this case, malonyl-CoA and CPT-1c can act in parallel, as they converge on ceramide de novo synthesis, to control food intake. A definitive answer would depend on identifying the range of the molecular functions of CPT-1c, which is fully warranted. In this model, our results identify NPY, among the major Arc neuropeptides, as a common effector in the actions of malonyl-CoA, CPT-1c, and ceramide metabolism on food intake. These data may suggest that the CPT-1c/ceramide pathway has greater effects on the expression of NPY than the other neuropeptides, such as AgRP and POMC. In addition, CPT-1c might regulate ceramide metabolism in the neurons that specifically express NPY.

Increased ceramide level might activate the ER stress cascade (31) and hypothalamic ER stress can impair leptin receptor signaling (32, 33). In our studies, we did not find any evidence to

suggest the involvement of ER stress in CPT-1c and ceramide actions (Fig. S5). Moreover, CPT-1c and ceramide metabolism seem to act independent of several other mediators of leptin's intracellular signaling pathways, such as signal transducer and activator of transcription 3 (STAT3), forkhead box protein O1 (FoxO1), and mammalian target of rapamycin (mTOR) (Fig. S6). Notably, our results suggest that the activation of STAT3 by leptin is not affected by either CPT-1c overexpression or ceramide treatment. However, impaired STAT3 signaling plays a critical role in ER stress-induced disruption of leptin signaling (32). Taken together, CPT-1c and ceramide appear to antagonize leptin's anorectic actions through ER stress-independent processes. In addition, the responses of the pathway of AMP-kinase (AMPK)/acetyl-CoA carboxylase (ACC) to leptin are also not affected by CPT-1c and ceramide actions (Fig. S6), which is consistent with the proposed downstream positions of CPT-1 and ceramide metabolism in leptin's malonyl-CoA signaling pathway. Our results suggest that Bsx and NPY lie downstream in the pathway by which CPT-1c and ceramide metabolism mediate leptin anorectic signaling actions (Fig. S4). Consistent with this argument, it has been reported that ceramide can increase glutamate release via enhancing exocytosis (34) and glutamate can up-regulate NPY mRNA levels in CNS neurons (35). A number of the downstream metabolites of ceramide, such as sphingosine and sphigosine-1 phosphate, are implicated in signaling transduction pathways (29), so these metabolites might play roles in ceramide-mediated control of food intake and energy balance.

Finally, we address the specificity of the pharmacological approaches used in our studies. In the anorectic effects of cerulenin, the specific CPT-1c deletion would not block cerulenin-mediated feeding actions if cerulenin used nonspecific targets to reduce food intake. In the ceramide experiments, myriocin and the compound of ceramide analog produced the opposing feeding effects, which is most likely because of their opposing molecular actions on ceramide metabolism rather than other nonspecific effects.

In summary, we provide strong evidence in support of an important role for CPT-1c in leptin's Arc anorectic signaling pathways. CPT-1c may mediate malonyl-CoA's signaling aspect in leptin feeding actions by regulating ceramide de novo synthesis. Targeting CPT-1c and ceramide metabolism in the Arc may offer effective approaches to prevent overweight and development of obesity.

Methods

Following central infusions of the adenoviruses or different compounds, food intake and body weight were monitored. At designated time points, the animals were killed and brains were dissected; then, different biochemical assays were run. Detailed methods are described in the *SI Methods*.

ACKNOWLEDGMENTS. We thank Prof. Jens Bruening and Dr. Dolors Serra for their critical advice and generous assistance in revising our manuscript, and Dr. Wendy Keung, Ms. Amy Barr, Mr. Ken Strynadka, and Mr. Thomas Panakkezhum for their critical technical assistance. These studies are funded mainly by a grant from the Canadian Diabetes Association and a fellowship of the Heart and Stroke Foundation of Canada (to S.G.). X.G. and D.W. acknowledge grants from the National Basic Research Program of China (973 Program 2011CB504004 and 2010CB945500); F.G.H., N.C., and P.C. acknowledge grants from Ministry of Education and Science, Spain (Grant SAF2007-61926 to F.G.H.), and from Instituto de Salud Carlos III (Grant CIBERobn CB06/03/0026 to F.G.H. and research contract to P.C.); T.H.M. acknowledges National Institutes of Health Grant DK19302; G.D.L. is a scientist of the Alberta Heritage Foundation for Medical Research; technical support was from the Cardiovascular Research Center (CVRC) and ABACUS Research Center in the University of Alberta.

1. Schwartz MW, Woods SC, Porte D, Jr., Seeley RJ, Baskin DG (2000) Central nervous system control of food intake. *Nature* 404:661–671.
2. Moran TH, Gao S (2006) Looking for food in all the right places? *Cell Metab* 3: 233–234.
3. Loftus TM, et al. (2000) Reduced food intake and body weight in mice treated with fatty acid synthase inhibitors. *Science* 288:2379–2381.
4. Obici S, et al. (2002) Central administration of oleic acid inhibits glucose production and food intake. *Diabetes* 51:271–275.
5. Gao S, Lane MD (2003) Effect of the anorectic fatty acid synthase inhibitor C75 on neuronal activity in the hypothalamus and brainstem. *Proc Natl Acad Sci USA* 100: 5628–5633.
6. Hu Z, Cha SH, Chohnan S, Lane MD (2003) Hypothalamic malonyl-CoA as a mediator of feeding behavior. *Proc Natl Acad Sci USA* 100:12624–12629.
7. Obici S, Feng Z, Arduini A, Conti R, Rossetti L (2003) Inhibition of hypothalamic carnitine palmitoyltransferase-1 decreases food intake and glucose production. *Nat Med* 9:756–761.
8. Hu Z, Dai Y, Prentki M, Chohnan S, Lane MD (2005) A role for hypothalamic malonyl-CoA in the control of food intake. *J Biol Chem* 280:39681–39683.
9. He W, Lam TK, Obici S, Rossetti L (2006) Molecular disruption of hypothalamic nutrient sensing induces obesity. *Nat Neurosci* 9:227–233.
10. López M, et al. (2006) Tamoxifen-induced anorexia is associated with fatty acid synthase inhibition in the ventromedial nucleus of the hypothalamus and accumulation of malonyl-CoA. *Diabetes* 55:1327–1336.
11. Chakravarthy MV, et al. (2007) Brain fatty acid synthase activates PPARalpha to maintain energy homeostasis. *J Clin Invest* 117:2539–2552.
12. Gao S, et al. (2007) Leptin activates hypothalamic acetyl-CoA carboxylase to inhibit food intake. *Proc Natl Acad Sci USA* 104:17358–17363.
13. Wolfgang MJ, et al. (2007) Regulation of hypothalamic malonyl-CoA by central glucose and leptin. *Proc Natl Acad Sci USA* 104:19285–19290.
14. Aja S, et al. (2008) Pharmacological stimulation of brain carnitine palmitoyltransferase-1 decreases food intake and body weight. *Am J Physiol Regul Integr Comp Physiol* 294:R352–R361.
15. Andrews ZB, et al. (2008) UCP2 mediates ghrelin's action on NPY/AgRP neurons by lowering free radicals. *Nature* 454:846–851.
16. López M, et al. (2008) Hypothalamic fatty acid metabolism mediates the orexigenic action of ghrelin. *Cell Metab* 7:389–399.
17. Mera P, et al. (2009) C75 is converted to C75-CoA in the hypothalamus, where it inhibits carnitine palmitoyltransferase 1 and decreases food intake and body weight. *Biochem Pharmacol* 77:1084–1095.
18. Pocai A, et al. (2006) Restoration of hypothalamic lipid sensing normalizes energy and glucose homeostasis in overfed rats. *J Clin Invest* 116:1081–1091.
19. Gao S, et al. (2011) Malonyl-CoA mediates leptin hypothalamic control of feeding independent of inhibition of CPT-1a. *Am J Physiol Regul Integr Comp Physiol*, 10.1152/ajpregu.00092.2011.
20. Lopaschuk GD, Ussher JR, Jaswal JS (2010) Targeting intermediary metabolism in the hypothalamus as a mechanism to regulate appetite. *Pharmacol Rev* 62:237–264.
21. Wolfgang MJ, Lane MD (2011) Hypothalamic malonyl-CoA and CPT1c in the treatment of obesity. *FEBS J* 278:552–558.
22. Price N, et al. (2002) A novel brain-expressed protein related to carnitine palmitoyltransferase I. *Genomics* 80:433–442.
23. Wolfgang MJ, et al. (2006) The brain-specific carnitine palmitoyltransferase-1c regulates energy homeostasis. *Proc Natl Acad Sci USA* 103:7282–7287.
24. Sierra AY, et al. (2008) CPT1c is localized in endoplasmic reticulum of neurons and has carnitine palmitoyltransferase activity. *J Biol Chem* 283:6878–6885.
25. Dai Y, Wolfgang MJ, Cha SH, Lane MD (2007) Localization and effect of ectopic expression of CPT1c in CNS feeding centers. *Biochem Biophys Res Commun* 359: 469–474.
26. Jáuregui O, et al. (2007) A new LC-ESI-MS/MS method to measure long-chain acylcarnitine levels in cultured cells. *Anal Chim Acta* 599(1):1–6.
27. Lage R, et al. (2010) Ghrelin effects on neuropeptides in the rat hypothalamus depend on fatty acid metabolism actions on BSX but not on gender. *FASEB J* 24: 2670–2679.
28. Fillet M, et al. (2003) Mechanisms involved in exogenous C2- and C6-ceramide-induced cancer cell toxicity. *Biochem Pharmacol* 65:1633–1642.
29. Yang G, et al. (2009) Central role of ceramide biosynthesis in body weight regulation, energy metabolism, and the metabolic syndrome. *Am J Physiol Endocrinol Metab* 297: E211–E224.
30. Hojjati MR, et al. (2005) Effect of myriocin on plasma sphingolipid metabolism and atherosclerosis in apoE-deficient mice. *J Biol Chem* 280:10284–10289.
31. Chen CL, et al. (2008) Ceramide induces p38 MAPK and JNK activation through a mechanism involving a thioredoxin-interacting protein-mediated pathway. *Blood* 111:4365–4374.
32. Ozcan L, et al. (2009) Endoplasmic reticulum stress plays a central role in development of leptin resistance. *Cell Metab* 9(1):35–51.
33. Won JC, et al. (2009) Central administration of an endoplasmic reticulum stress inducer inhibits the anorexigenic effects of leptin and insulin. *Obesity (Silver Spring)* 17:1861–1865.
34. Tang N, Ong WY, Zhang EM, Chen P, Yeo JF (2007) Differential effects of ceramide species on exocytosis in rat PC12 cells. *Exp Brain Res* 183:241–247.
35. Schwarzer C, Sperk G (1998) Glutamate-stimulated neuropeptide Y mRNA expression in the rat dentate gyrus: a prominent role of metabotropic glutamate receptors. *Hippocampus* 8:274–288.

MALONYL-COA MEDIATES LEPTIN HYPOTHALAMIC CONTROL OF FEEDING INDEPENDENT OF INHIBITION OF CPT1A.

Gao, S., Keung, W., Serra, D., Wang, W., **Carrasco, P**., Casals, N., et al. (2011).

American Journal of Physiology.Regulatory, Integrative and Comparative Physiology, 301(1), R209-17.

Am J Physiol Regul Integr Comp Physiol 301: R209–R217, 2011.
First published April 20, 2011; doi:10.1152/ajpregu.00092.2011.

Malonyl-CoA mediates leptin hypothalamic control of feeding independent of inhibition of CPT-1a

Su Gao,[1] Wendy Keung,[1] Dolors Serra,[3] Wei Wang,[1] Patricia Carrasco,[2] Nuria Casals,[2] Fausto G. Hegardt,[3] Timothy H. Moran,[4] and Gary D. Lopaschuk[1]

[1]*Department of Pediatrics, Mazankowski Alberta Heart Institute, University of Alberta, Edmonton, Alberta, Canada;* [2]*Basic Sciences Department and Centro de Investigación Biomedica en Red Fisiopatología de la Obesidad y Nutrición (CIBERObn), School of Medicine and Health Sciences, Universitat Internacional de Catalunya, Josep Trueta s/n, Barcelona, Spain;* [3]*Department of Biochemistry and Molecular Biology and Institute of Biomedicine, Facultat de Farmàcia, University of Barcelona, and CIBERObn, Catalonia, Spain;* [4]*Department of Psychiatry and Behavioral Sciences, The Johns Hopkins University School of Medicine, Baltimore, Maryland*

Submitted 22 February 2011; accepted in final form 14 April 2011

Gao S, Keung W, Serra D, Wang W, Carrasco P, Casals N, Hegardt FG, Moran TH, Lopaschuk GD. Malonyl-CoA mediates leptin hypothalamic control of feeding independent of inhibition of CPT-1a. *Am J Physiol Regul Integr Comp Physiol* 301: R209–R217, 2011. First published April 20, 2011; doi:10.1152/ajpregu.00092.2011.—Hypothalamic fatty acid metabolism is involved in central nervous system controls of feeding and energy balance. Malonyl-CoA, an intermediate of fatty acid biosynthesis, is emerging as a significant player in these processes. Notably, hypothalamic malonyl-CoA has been implicated in leptin's feeding effect. Leptin treatment increases malonyl-CoA level in the hypothalamic arcuate nucleus (Arc), and this increase is required for leptin-induced decrease in food intake. However, the intracellular downstream mediators of malonyl-CoA's feeding effect have not been identified. A primary biochemical action of malonyl-CoA is the inhibition of the acyltransferase activity of carnitine palmitoyltransferase-1 (CPT-1). In the hypothalamus, the predominant isoform of CPT-1 that possesses the acyltransferase activity is CPT-1 liver type (CPT-1a). To address the role of CPT-1a in malonyl-CoA's anorectic action, we used a recombinant adenovirus expressing a mutant CPT-1a that is insensitive to malonyl-CoA inhibition. We show that Arc overexpression of the mutant CPT-1a blocked the malonyl-CoA-mediated inhibition of CPT-1 activity. However, the overexpression of this mutant did not affect the anorectic actions of leptin or central cerulenin for which an increase in Arc malonyl-CoA level is also required. Thus, CPT-1a does not appear to be involved in the malonyl-CoA's anorectic actions induced by leptin. Furthermore, long-chain fatty acyl-CoAs, substrates of CPT-1a, dissociate from malonyl-CoA's actions in the Arc under different feeding states. Together, our results suggest that Arc intracellular mechanisms of malonyl-CoA's anorectic actions induced by leptin are independent of CPT-1a. The data suggest that target(s), rather than CPT-1a, mediates malonyl-CoA action on feeding.

carnitine palmitoyltransferase; food intake; hypothalamus

OBESITY IS A MAJOR HEALTH problem and a major cause of insulin-resistance and diabetes. An imbalance between energy intake and energy expenditure can lead to overweight and contribute to the development of obesity and the metabolic syndrome. The hypothalamus plays a critical role in the central nervous system (CNS) control of feeding and energy balance (21, 28). A large body of evidence now shows that fatty acid metabolism participates in this action of the hypothalamus (1, 3, 5–7, 9, 11, 12, 15, 17, 18, 20, 23, 24). In this regard, malonyl-CoA, an intermediate in fatty acid biosynthesis, is emerging as a significant player in the hypothalamic control of feeding and body energy balance (5–7, 9, 11, 12, 15, 18). Recent data have linked malonyl-CoA signaling action to the hypothalamic intracellular pathways of leptin in the central regulation of energy balance (6, 9). In the hypothalamus, leptin treatment increases malonyl-CoA level via inhibiting AMP-activated protein kinase (AMPK) and activating acetyl-CoA carboxylase (ACC) (2, 6). Notably, the increase of hypothalamic malonyl-CoA induced by leptin takes place specifically in the arcuate nucleus (Arc) (6), a critical site in mediating leptin's central actions on feeding and energy balance (28). Despite these findings, the intracellular mechanisms by which malonyl-CoA impacts feeding remain unclear. It is known that malonyl-CoA inhibits the acyltransferase activity of carnitine palmitoyltransferase-1 (CPT-1) that converts long-chain fatty acyl-CoA (LCFA-CoA) to long-chain acylcarnitine (9, 23). CPT-1 has liver- and muscle-isoforms, with the hypothalamus mainly expressing the liver isoform (CPT-1a) (23). Pharmacological studies have demonstrated that intracerebroventricular administration of compound ST-1326, a specific CPT-1a inhibitor, inhibits Arc CPT-1a activity, increases cellular LCFA-CoA levels, and reduces food intake (23). Accumulation of hypothalamic LCFA-CoAs has been suggested to have anorectic effects as intracerebroventricular oleic acid (which can form LCFA-CoAs in cells) was shown to reduce food intake (24). Given that malonyl-CoA is a physiological inhibitor of CPT-1, inhibition of Arc CPT-1a and the ensuing increase of LCFA-CoAs have been proposed to mediate malonyl-CoA's anorectic signaling actions. However, a growing body of evidence now strongly challenges this hypothesis (16). For example, we previously demonstrated that exogenous leptin upregulates the malonyl-CoA level without affecting the level of LCFA-CoAs in the Arc (6). The result thus casts doubt on the role of CPT-1a as a mediator of malonyl-CoA's action in leptin feeding pathways. To clarify the role of CPT-1a in the Arc, we used a recombinant adenovirus expressing a mutant CPT-1a that is insensitive to malonyl-CoA inhibition (10). Using this mutant, we examined the feeding responses of the animals with a disruption of malonyl-CoA-mediated inhibition on CPT-1a acyltransferase activity.

Address for reprint requests and other correspondence: G. D. Lopaschuk, 423 Heritage Medical Research Bldg., Univ. of Alberta, Edmonton, Alberta T6G 2S2, Canada (e-mail: gary.lopaschuk@ualberta.ca).

MATERIALS AND METHODS

Animal preparations for feeding experiments. Animal experiments were performed in accordance with the guidelines of the Canadian Council for Animal Care, and were approved by the University of Alberta Animal Policy and Welfare Committee. Male Sprague-Dawley rats (225–300 g) were purchased from Charles River Laboratories. The rats were housed in a controlled (12:12-h light-dark) environment, and were allowed ad libitum access to standard laboratory chow and water, unless otherwise noted. Before the feeding experiments were started, the rats were handled daily and subjected to mock injections to minimize the stress from the experimental manipulation. In the leptin study, leptin or vehicle was administered at 1 h before the dark onset. Food intakes at 3 h and 23 h (overnight) after the dark onset, were monitored. Overnight body weight changes (24 h after the injection) were also monitored. In the cerulenin study, at 5 h before the dark onset, food was removed. Then, cerulenin or vehicle was administered, and food was not provided until the dark onset. Food intakes were monitored at 3 h and 19 h (overnight) after dark onset. Overnight body weight changes (24 h after the injection) were also monitored.

Brain sample preparations. At the designated time points, rats were euthanized by decapitation. Brains were rapidly dissected (within 1 min) and coronal brain sections were prepared using a cryostat or a brain matrix (Roboz Surgical Instrument, Gaithersburg, MD). Individual hypothalamic nuclei including Arc, ventromedial nucleus (VMN), lateral hypothalamic area (LHA), and paraventricular nucleus (PVN) were dissected according to the established protocol (6). The accuracy of the dissection was verified by comparing the characteristic neuropeptide mRNA levels as detailed previously (6).

Recombinant adenoviruses. The adenoviruses were delivered into the Arc (1×10^7 pfu/μl; 0.4 μl per side) by bilateral stereotaxic injection (6). The coordinates were anterior-posterior: −2.8 mm; dorsal-ventral: −9.5 mm; and medial-lateral: ± 0.4 mm. The accuracy of the injections was confirmed by histological analysis as described previously (6). The adenovirus encoding malonyl-CoA decarboxylase (MCD) contains the full-length human MCD (hMCD) coding sequence (27). The adenovirus encoding the wild-type CPT-1a contains the nucleotide sequence (58-2700) including the entire coding region of rat CPT-1a, and the same sequence was used to generate the mutant CPT-1a with the 593-methionine residual mutated to serine residual (22). The feeding experiments with leptin and cerulenin were conducted in the second week following the initial delivery of the adenoviruses. Significantly high levels of protein expressions or enzyme activities were reliably detected after 1 wk and these high levels last until at least 14 days (2 wk) following the delivery of the viruses.

Cannulation surgery and intracerebroventricular injection. Cannulas were implanted into either the lateral or third ventricle based on the established protocol (6). The accuracy of placement was confirmed by angiotensin-2 drinking test or histological analysis as previously described (6). After surgery, daily food intake and body weight were monitored. After body weights returned to the levels before surgery and the rats were fully habituated to the experimental manipulations, bolus injections of the chemicals (leptin and cerulenin) were administered intracerebroventricularly.

Chemicals. Leptin was obtained from A. F. Parlow (National Hormone and Pituitary Program, National Institute of Diabetes and Digestive and Kidney Diseases). For intracerebroventricular injection, a dose of 15 μg of leptin dissolved in PBS was chosen based on our previous studies (6). Cerulenin was obtained from Sigma (St. Louis, MO) and 125 μg in 25% DMSO/75% PBS (vehicle) was used in intracerebroventricular injection as previously described (1).

Quantifications of malonyl-CoA, LCFA-CoAs, and long-chain acylcarnitines. The CoA recycling assay was performed to measure the malonyl-CoA level, and HPLC was used to measure the levels of long-chain acyl-CoAs (consisting of palmitoyl-CoA, oleoyl-CoA, and stearoyl-CoA) as detailed elsewhere (6). To measure the levels of the long-chain acylcarnitines (LC-ACs), brain tissues were extracted with acetonitrile and 2-propanol (6). The extracts were dried under streams of nitrogen and were reconstituted in 300 μl acetonitrile and n-butanol (1:1). The samples were then filtered and loaded into HPLC coupled with mass spectrometer (13). The levels of LC-ACs (consisting of palmitoylcarnitine, oleoylcarnitine, and stearoylcarnitine) were quantitated as detailed previously (13).

MCD activity assay. Adenovirus encoding hMCD or green fluorescent protein (null) was stereotaxically delivered into the Arc. Individual hypothalamic nuclei (Arc, VMN, LHA, and PVN) were dissected from coronal brain sections. The MCD activity assay was performed based on established protocol (6, 27).

Carnitine palmitoyltransferase-1 (CPT-1) activity assay. The brain was removed from the skull within 40 s and was immediately sectioned using the brain matrix. The mediobasal hypothalamic area (MBH), LHA, and PVN were quickly dissected on ice, and the tissues were immediately homogenized in the cold lysis buffer (0.25 M sucrose, 5 mM Tris-HCl, and 1 mM EGTA, pH 7.4). The crude homogenate was centrifuged at 800 *g* for 10 min at 4°C. The resulting pellet was washed by resuspension in two volumes of the lysis buffer and was then centrifuged at 800 *g*. This step was repeated twice to maximize the yield of the mitochondrial fraction. The combined supernatant was centrifuged at 6,000 *g* for 15 min at 4°C. The resulting pellet (crude mitochondrial fraction) was gently resuspended in the lysis buffer and was used in the activity assay using a radiometric method (20).

Antibodies and Western blot analysis. The CPT-1a antibody (Ab) was generated as described elsewhere (29). Actin (Santa Cruz Biotechnology, Santa Cruz, CA) was used as the loading control in the Western blot analyses. The procedures of protein electrophoresis, transfer, and Ab detection were performed based on standard Western blot analysis protocol (Invitrogen, California). Densitometry was performed using Scion Image software (Scion, Frederick, MD).

Statistical analysis. Data are reported as means ± SE. Data consisting of two groups were analyzed by Student's *t*-test. Data consisting of three groups were analyzed by one-way ANOVA. These one-way ANOVAs, when they yielded significant overall effects, were further analyzed by the Newman-Keuls multiple comparison test for group comparisons. Data consisting of four or six groups were analyzed by two-way ANOVA. These two-way ANOVAs, when they yielded significant overall effects, were further analyzed by Bonferroni post tests for group comparisons. For all tests, $P < 0.05$ indicated significance.

RESULTS

M593S CPT-1a mutant is insensitive to malonyl-CoA inhibition. In this study, we used a M593S CPT-1a mutant to address the role of CPT-1a in malonyl-CoA-mediated anorectic actions. The M593S mutation results in an impaired interaction between malonyl-CoA and the malonyl-CoA binding site in CPT-1a (22). We first verified malonyl-CoA insensitivity of this mutant using yeast cells that do not possess endogenous CPT-1 acyltransferase activity (22). We transfected yeast cells with the vector that expresses this mutant (CPT-1a mt) or the wild-type CPT-1a (CPT-1a wt), and then measured CPT-1 acyltransferase activity using the extracts from these cells. We found that malonyl-CoA inhibitory effect on the mutant was nearly abolished (Fig. 1*A*). Next, we evaluated CPT-1 acyltransferase activities in the hypothalamus. The adenovirus encoding the CPT-1a mt, the CPT-1a wt, or the null virus was delivered bilaterally into the Arc. Two weeks following delivering the viruses, rats were euthanized, and CPT-1a protein levels were quantified in individual hypothalamic nuclei (Arc,

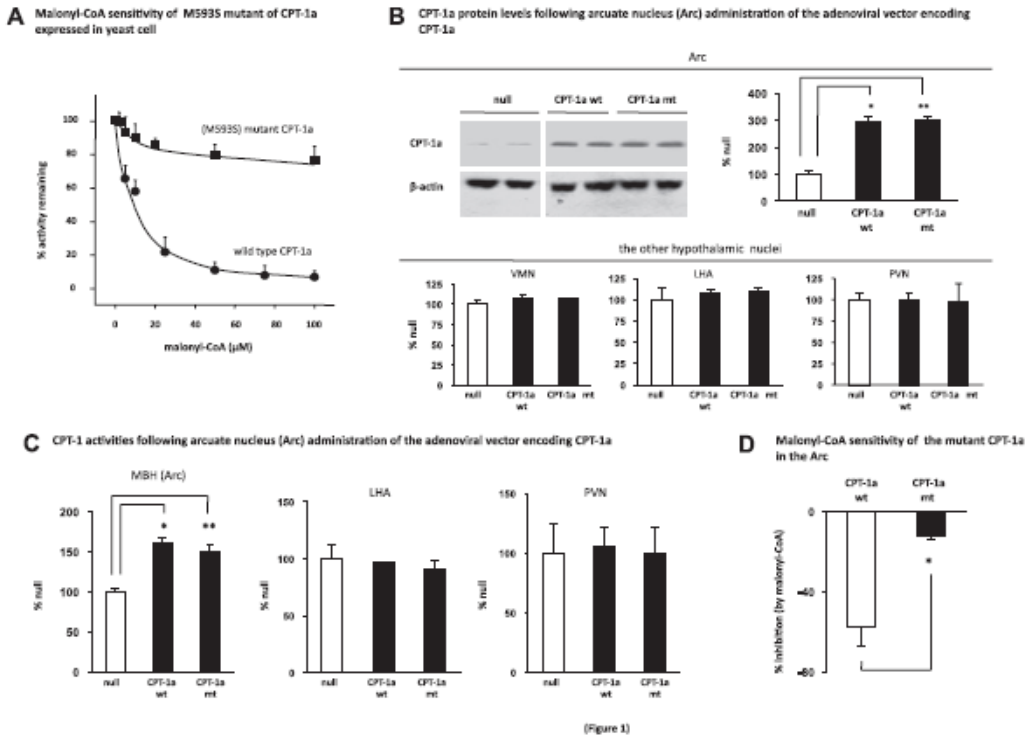

(Figure 1)

Fig. 1. M593S mutant of carnitine palmitoyltransferase liver type (CPT-1a) is insensitive to malonyl-CoA inhibition. *A*: yeast extract (10 μg of protein) of wild-type CPT-1a (CPT-1a wt) or M593S mutant CPT-1a (CPT-1a mt) was incubated with increasing concentrations of malonyl-CoA, and the CPT-1 activities in the extract were measured ($n = 4$–5). *B*: adenovirus (Ade) expressing the control (null, $n = 6$), CPT-1a wt ($n = 6$), or M593S CPT-1a mt ($n = 6$) was administered into the arcuate nucleus (Arc). Two weeks following the administration of the viruses, the rats were euthanized. The individual hypothalamic nuclei tissues [Arc, ventromedial nucleus (VMN), lateral hypothalmic area (LHA), and paraventricular nucleus (PVN)] were dissected from the brain sections, and the CPT-1a protein levels were examined by Western blot analysis. Two representative blots from the Arc of each group are shown, and the ratios of the band intensity of CPT-1a to that of β-actin were quantitated ($n = 6$; *, **vs. null, $P < 0.05$). *C*: 2 wk following Arc administration of the Ades encoding the null, CPT-1a wt, and CPT-1 mt ($n = 6$), the CPT acyltransferase activities in the mediobasal hypothalmic area (MBH) encompassing the entire Arc and some VMN, LHA, and the PVN were measured. The CPT-1a activities of individual VMN tissues were not measured (*, **vs. null, $P < 0.05$). *D*: 2 wk following the delivery of the viruses (encoding CPT-1a wt and CPT-1a mt), the rats were euthanized. The mediobasal hypothalamus (MBH) area containing the Arc was dissected, and the crude mitochondrial fraction was prepared. Exogenous malonyl-CoA (50 μM) was added to the mitochondrial preparation, and CPT-1 activity assay was conducted ($n = 8$). %Activity inhibition by malonyl-CoA (compared with the assay without the addition of exogenous malonyl-CoA) are presented (*vs. CPT-1a wt, $P < 0.05$).

VMN, LHA, and PVN). Compared with the rats injected with the null adenovirus, CPT-1a (wt or mt) adenoviral infections induced increases in CPT-1a protein levels in the Arc, while the CPT-1a protein levels were not altered in the VMN, LHA, or PVN (Fig. 1*B*). Concomitant with the increased protein levels, CPT-1 acyltransferase activities were also increased selectively in the MBH encompassing the Arc (Fig. 1*C*). Together, these data demonstrate Arc-specific overexpressions of CPT-1a as well as activations of CPT-1 following the stereotaxic Arc delivery of the viruses. We then evaluated the response of CPT-1a to exogenous malonyl-CoA. We prepared crude mitochondrial extract from the MBH region of the animals with Arc overexpressing the CPT-1a wt or the CPT-1a mt. Exogenous malonyl-CoA (50 μM) (20) was then added to the extracts, and the CPT-1 activity assay was conducted. As expected, we observed that the CPT-1a mt was resistant to the inhibitory effect of malonyl-CoA (Fig. 1*D*).

Increase in arc malonyl-CoA is required for leptin's anorectic actions. Before addressing the role of CPT-1a in leptin's malonyl-CoA signaling pathway, we confirmed the importance of malonyl-CoA in the central control of feeding and in leptin's anorectic actions. The adenovirus encoding MCD (Ade-MCD) (27), which lowers malonyl-CoA level (9), was administered into the Arc of rats. Consistent with the previous finding (9), Arc delivery of the Ade-MCD increased daily food intakes and body weight gains, compared with the rats treated with the null virus (Fig. 2*A*). Delivery of the Ade-MCD induced an increase in MCD activity in the Arc (Fig. 2*B*), while the MCD activity was not altered in the VMN (Fig. 2*B*) or in the LHA and PVN (LHA: MCD, 87 ± 4.7% vs. null, 100 ± 13%; PVN: MCD,

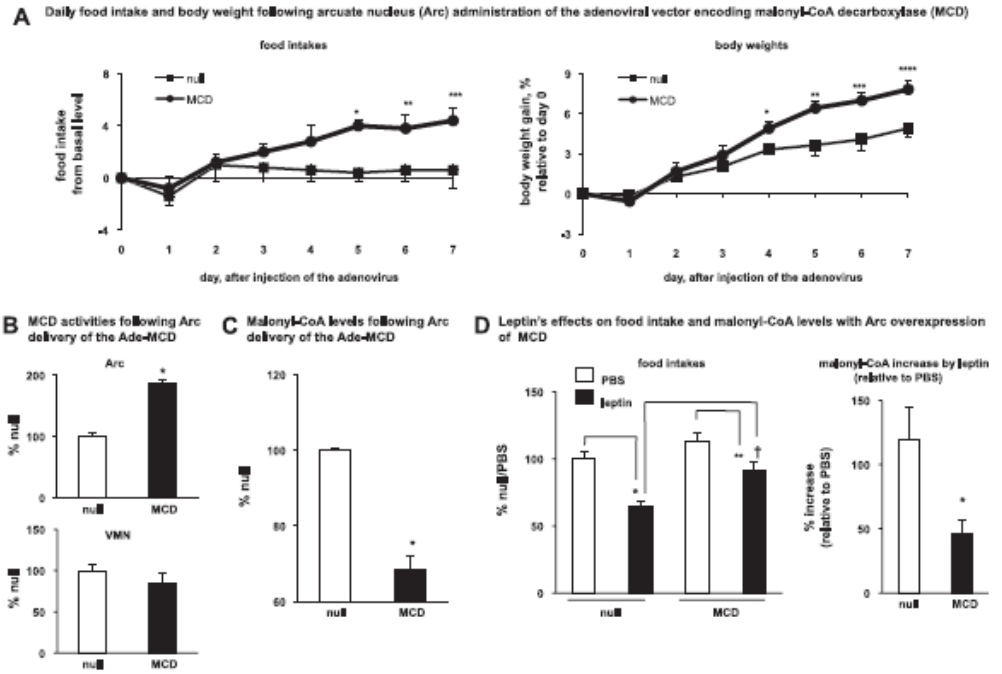

Fig. 2. Increase of Arc malonyl-CoA is required in leptin's anorectic actions. *A*: adenovirus encoding the malonyl-CoA decarboxylase (MCD: $n = 5$) or enhanced green fluorescent protein (null, $n = 5$) was administered into the Arc on *day 0*. Daily food intakes and daily body weights were monitored. The daily food intake before the virus injection was used as the baseline level. The differences between the daily food intake from *day 1* through *day 7* and the basal level are presented. The daily body weight from *day 1* through *day 7* was compared with *day 0* and the %body weight changes are presented. Food intakes: *, **vs. null, $P < 0.05$; ***vs. null, $P = 0.05$. Body weights: *, **, ***, ****vs. null, $P < 0.05$. *B*: after 1 wk following Arc delivery of the adenoviruses (MCD, $n = 5$; null, $n = 5$), the rats were euthanized. The MCD activities in individual hypothalamic nuclei (Arc, VMN, LHA, and PVN) were measured. The MCD activities from the Arc ($n = 5$) and the VMN ($n = 5$) are shown (*vs. null, $P < 0.05$). *C*: rats were subject to the similar procedures as described in *B*. Malonyl-CoA levels ($n = 3$–4) in the Arc were measured (*vs. null, $P < 0.05$). *D*: after 1 wk following the virus delivery, a bolus injection of leptin (15 μg, in PBS) was given intracerebroventricularly before the dark cycle. Then, the food intakes at 3 h after the dark onset were monitored ($n = 6$–9) (*vs. null/PBS, $P < 0.05$; **vs. MCD/PBS, $P < 0.05$; †vs. null/leptin, $P < 0.05$). Malonyl-CoA levels in the Arc were measured and %increases of malonyl-CoA level by leptin (as compared with PBS) are shown ($n = 6$–9; *$P < 0.05$, vs. null).

105 ± 1% vs. null, 100 ± 10%). In addition, following the delivery of the Ade-MCD, the malonyl-CoA level in the Arc was reduced (Fig. 2*C*). We then administered (intracerebroventricularly) leptin to the rats with Arc-specific activation of MCD. As we demonstrated in the previous study (6), leptin treatment increased the malonyl-CoA level in the Arc (leptin: 220%, PBS: 100%; $P < 0.05$). We further showed that the MCD overexpression attenuated the level of the increase in malonyl-CoA and antagonized the anorectic actions by leptin treatment (Fig. 2*D*). These results confirm that the increase in the Arc malonyl-CoA level is a significant contributor to leptin's anorectic effects.

Blocking malonyl-CoA inhibition of CPT-1 acyltransferase activity does not affect leptin's anorectic actions. We injected the adenovirus encoding CPT-1a wt (Ade-CPT-1a wt), the CPT-1a wt (Ade-CPT-1a mt) or the null (Ade-null) into the Arc of rats. Three to four days following the virus infections, daily food intakes and body weights returned to the preinjection levels. At least through the eighth day following the initial injection of the viruses, no significant body weight or feeding differences were found among these rats (data not shown). We then assessed the role of malonyl-CoA inhibition of CPT-1 in leptin's anorectic actions. During the second week following the initial delivery of the viruses (around the 11th day), leptin was injected to the rats. We found that Arc overexpression of CPT-1a mt (malonyl-CoA insensitive) did not affect leptin-induced feeding inhibition or weight loss (Fig. 3*A*). During this period (the 2nd week following the injection of the viruses), the adenoviral infections did not affect the daily (24 h) food intakes compared with the basal preinjection levels, and as in the first week described above, no significant differences of 24-h food intakes were found among all treated groups (basal level: 100 ± 3.2%, Ade-null: 103 ± 2.0%, Ade-CPT-1a wt: 97 ± 2.1%, Ade-CPT-1a mt: 95 ± 5.8%). Concomitant with producing similar anorectic effects, leptin induced similar increases in Arc malonyl-CoA levels in all treated groups (Fig. 3*B*). Since malonyl-CoA inhibition of CPT-1 acyltransferase activity is reversible (22), the CPT-1 activity assay using tissue

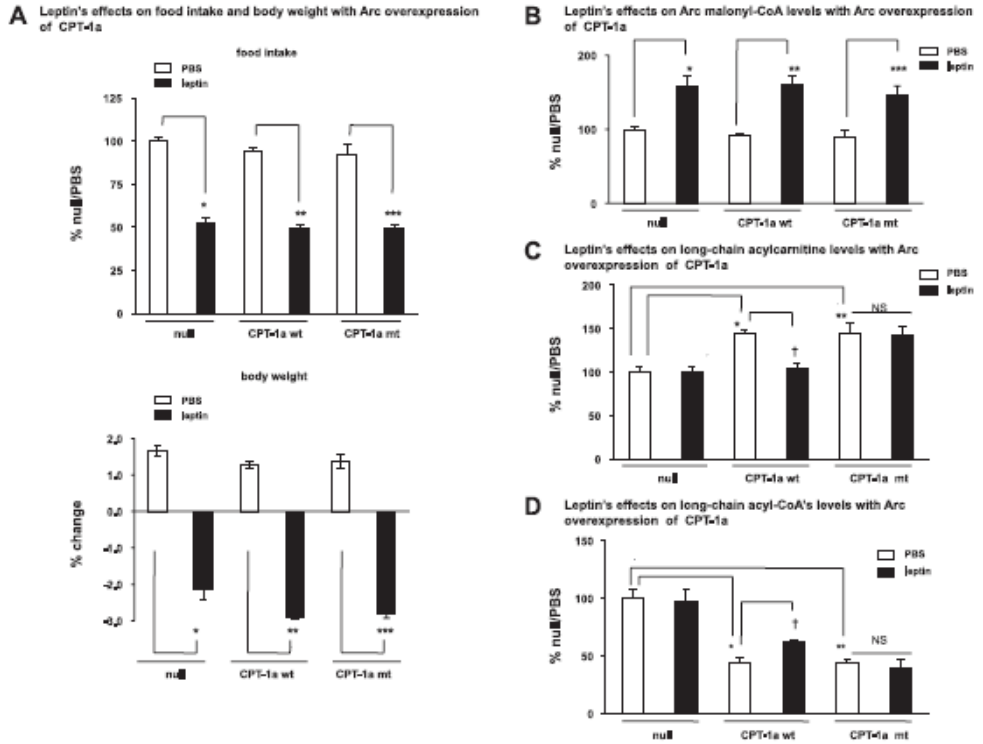

Fig. 3. Blocking malonyl-CoA inhibition of CPT-1 acyltransferase activity does not affect the anorectic action of leptin. *A*: during the 2nd wk following the Arc administration of Ade-CPT-1a wt, Ade-CPT-1a mt, or Ade-null, a bolus injection of leptin (15 μg in PBS) was given intracerebroventricularly to rats before the dark cycle. Overnight food intake and body weight were monitored ($n = 6$). Values from the rat having a targeted Arc overexpression of CPT-1a and an increase of CPT acyltransferase activity were included in the data analysis (*vs. null/PBS, $P < 0.05$; **vs. CPT-1a wt/PBS, $P < 0.05$; ***vs. CPT-1a mt/PBS, $P < 0.05$). *B–D*: after 1 wk following the Arc delivery of the adenoviruses (CPT-1a wt, CPT-1a mt, and null), a bolus injection of leptin (15 μg in PBS) was given intracerebroventricularly to the rats. The Arc levels (at 3 h after icv injection) of the malonyl-CoA (*B*, $n = 5–7$), long-chain acylcarnitines (*C*, $n = 5–6$), and the long-chain acyl-CoA's (*D*, $n = 5–8$) were measured. NS, differences between CPT-1a mt/PBS and CPT-1a mt/leptin are not significant. *B*: *vs. null/PBS, $P < 0.05$; **vs. CPT-1a wt/PBS, $P < 0.05$; ***vs. CPT-1a mt/PBS, $P < 0.05$. *C*: *CPT-1a wt/PBS vs. null/PBS, $P < 0.05$; **CPT-1a mt/PBS vs. null/PBS, $P < 0.05$; †CPT-1a wt/leptin vs. CPT-1a wt/PBS, $P < 0.05$; NS, CPT-1a mt/leptin vs. CPT-1a mt/PBS, not significant. *D*: *CPT-1a wt/PBS vs. null/PBS, $P < 0.05$; **CPT-1a mt/PBS vs. null/PBS, $P < 0.05$; †CPT-1a wt/leptin vs. CPT-1a wt/PBS, $P < 0.05$; NS, CPT-1a mt/leptin vs. CPT-1a mt/PBS, not significant.

extract is not informative in evaluating the in vivo effect of malonyl-CoA on CPT-1 activity. CPT-1 acyltransferase activity converts LCFA-CoAs to LC-ACs (13). We therefore assessed CPT-1a activity by measuring the levels of LC-ACs. As expected, activation of Arc CPT-1a increased LC-AC levels in the Arc (Fig. 3*C*). Leptin reduced LC-AC levels in the Arc that ectopically expresses the CPT-1a wt (Fig. 3*C*), indicating an inhibition of CPT-1 activity by leptin in these animals. In contrast, leptin did not affect LC-AC levels in the Arc overexpressing the CPT-1a mt (Fig. 3*C*), suggesting that leptin-induced accumulation of malonyl-CoA does not inhibit the CPT-1 activities in these animals. In parallel with the changes in the levels of LC-ACs, levels of total LCFA-CoAs (substrates for CPT-1a) were reduced by CPT-1a activation (Fig. 3*D*). Leptin induced the increase in LCFA-CoA levels in the Arc, ectopically expressing CPT-1a wt, while it did not affect LCFA-CoA levels in the Arc overexpressing the CPT-1a mt (Fig. 3*D*). It should be noted that these biochemical assays were performed at the time when the feeding experiment with leptin was conducted (i.e., in the 2nd week following viral injections). We also demonstrated (Fig. 1) that the effect of overexpressing the CPT-1a mt on antagonizing malonyl-CoA-mediated inhibition remained significant at a later time point (i.e., 2 wk following the viral injections). Thus, we demonstrated that during the period when the leptin-induced inhibition of CPT-1a were blocked, the leptin-induced feeding inhibition was not affected. Taken together, these data demonstrate that blocking malonyl-CoA inhibition of CPT-1a and the resulting increase in LCFA-CoA's level does not affect leptin's anorectic actions.

Blocking malonyl-CoA inhibition of CPT-1 acyltransferase activity does not affect the anorectic action of central cerulenin. To assess the role of CPT-1a in the specific context of malonyl-CoA signaling actions, we examined the feeding

CoA action in leptin's intracellular signaling pathways, the levels of LCFA-CoAs should also change in association with the level of malonyl-CoA. To assess this hypothesis, we examined the Arc levels of LCFA-CoAs and malonyl-CoA under fasting and refeeding conditions. Unexpectedly, we found that Arc LCFA-CoA levels were increased by fasting even though the malonyl-CoA level decreased (Fig. 5*A*), and these changes were reversed upon refeeding (Fig. 5*A*). Thus, in the Arc, the changes in LCFA-CoA levels appear to dissociate from those in malonyl-CoA's level under different feeding states. It is known that CPT-1-mediated fatty acid β-oxidation activity in the brain is trivial compared with the periphery (16). In determining the size of brain LCFA-CoA pool, other actions/pathways, such as exchange with the circulation, the action of acyl-CoA synthetase, and brain acyl-CoA hydrolase play more prominent roles (Fig. 5*B* and Ref. 16). Here, we showed that fasting elevated the fatty acid levels in the circulation, while refeeding brought down the elevated levels (Fig. 5*C*). Furthermore, the brain acyl-CoA hydrolase activity was lowered by fasting and elevated to prefasting level following refeeding (Fig. 5*D*). Although the physiological relevance of these changes is unclear, these metabolic events provide an interpretation for the observed dissociation of LCFA-CoAs from malonyl-CoA.

DISCUSSION

CPT-1a, a key enzyme in regulating mitochondrial fatty acid β-oxidation, has been proposed to be a candidate for mediating hypothalamic malonyl-CoA anorectic actions. In the CNS, as fatty acid β-oxidation activity is trivial, malonyl-CoA-mediated regulation of CPT-1 acyltransferase activity is not as significant in the brain as it is in the periphery (16). Indeed, in our present and previous studies (6), we found no change of the Arc levels of either LCFA-CoAs (substrates of CPT-1a) or LC-ACs (products of CPT-1a), upon leptin administration under normal conditions. These results suggest that leptin treatment does not affect CPT-1 acyltransferase activity in the Arc. Thus, Arc CPT-1a may not be implicated in leptin's central actions on feeding under normal conditions. In partic-

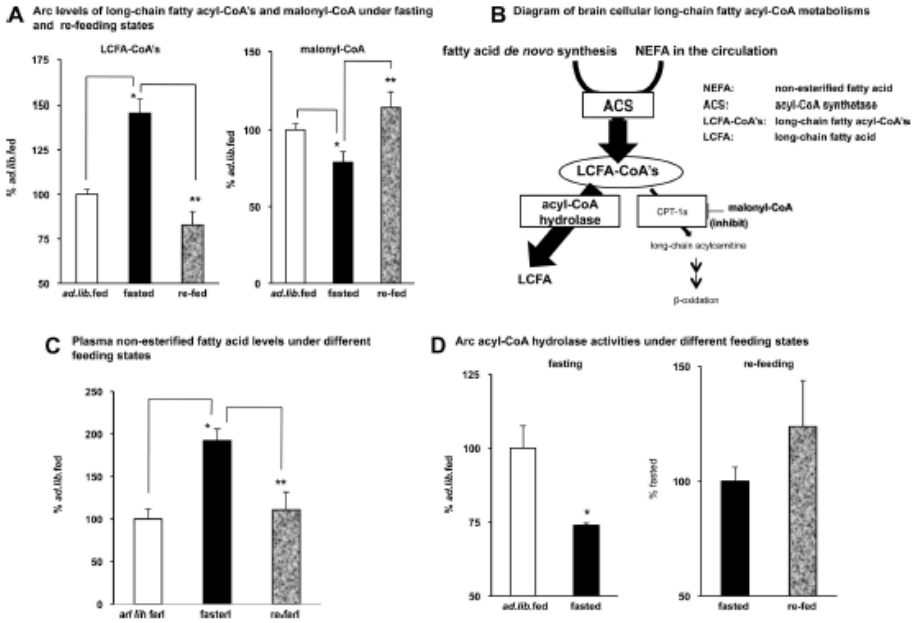

Fig. 5. Changes of long-chain fatty acyl-CoAs (LCFA-CoAs) levels in the Arc are dissociated from the changes of malonyl-CoA levels under fasting and refeeding conditions. *A*: some rats were fasted for 48 h (fasted, $n = 9$), and the other rats were refed for 3 h after being fasted for 48 h (refed, $n = 6$). Arc levels of LCFA-CoAs and malonyl-CoA were measured. Ad libitum fed ($n = 6$) was used as the control. *Fasted vs. ad libitum fed, $P < 0.05$; **refed vs. fasted, $P < 0.05$. *B*: schematic diagram of the metabolism of brain cellular LCFA-CoAs is shown. Intracellular LCFA either synthesized de novo or transported from the circulation is esterified by acyl-CoA synthetase (ACS) to form LCFA-CoAs. Hydrolysis by acyl-CoA hydrolase and the CPT-1a-mediated mitochondrial β-oxidation are 2 pathways that lower the cellular LCFA-CoA levels. In the brain, acyl-CoA hydrolase action plays a major role, while the mitochondrial β-oxidation is a minor pathway, in controlling the cellular LCFA-CoA's levels. *C*: rats were subjected to the fasting and refeeding procedure as described in *A*. Plasma levels of free fatty acid were measured ($n = 5$). Ad libitum fed was used as the control. *Fasted vs. ad libitum fed, $P < 0.05$; **refed vs. fasted, $P < 0.05$. *D*: some rats were fasted for 1 overnight (fasted, $n = 5$) and the other rats were refed for 3 h after being fasted for 2 overnights (refed, $n = 3$). Arc acyl-CoA hydrolase activities were measured. Note: the acyl-CoA hydrolase activity levels between 24 h fasting and 48 h fasting are comparable (*vs. ad libitum fed, $P < 0.05$).

ular, our data indicate that CPT-1a is not a critical component of malonyl-CoA signaling mechanisms in leptin's anorectic actions. Some potential mechanisms underlie this conclusion. First, due to the inherent heterogeneity of CNS cells (28), malonyl-CoA metabolism and CPT-1a expression might not take place in the same cells (31). Thus, the change of the malonyl-CoA level in response to leptin may occur in a population of cells that does not express CPT-1a. Second, malonyl-CoA produced by the two isoforms of ACC (ACC-1 and ACC-2) has different effects on CPT-1a activity. Compared with ACC2, the ACC-1-associated malonyl-CoA does not significantly affect CPT-1a-mediated fatty acid β-oxidation (19). It should be noted that we have demonstrated leptin specifically activates ACC-1 to increase the malonyl-CoA level (6). It follows that malonyl-CoA may not inhibit Arc CPT-1a in leptin's anorectic actions. Finally, due to the inherent nature of low activity, the CPT-1a in the Arc may not be subject to the regulation by malonyl-CoA, particularly when malonyl-CoA is increased. Under physiological conditions, the already low activity of CPT-1a in the Arc may be resistant to a further inhibition by malonyl-CoA. Under artificial conditions, such as when CPT-1a wt is ectopically overexpressed, leptin treatment does inhibit CPT-1a activity and increase LCFA-CoA's levels. However, the blockades of these changes fail to affect leptin's anorectic actions. Therefore, in the Arc, malonyl-CoA inhibition of CPT-1a seems unlikely to play a key role in mediating leptin's feeding actions. Our data also show that leptin's effect on body weight is independent of malonyl-CoA-mediated CPT-1a inhibition. Together with the results of food intake, we speculate that leptin's action on body energy expenditure would also be independent of malonyl-CoA's inhibitory effect on CPT-1a. However, a definitive conclusion requires direct measurement of energy expenditure in the experimental paradigm.

There have been increasing concerns (16) with the hypothesis that inhibiting Arc CPT-1a with the ensuing increases of LCFA-CoAs can produce anorectic effects (23, 24). Our results provide further evidence to support the notion that these biochemical events are not implicated in leptin's anorectic actions. In addition, particularly under acute experimental conditions (24), intracellular LCFA-CoA levels may not go up following the treatment with LCFAs (16, 24). Moreover, a growing body of evidence now shows that accumulation of hypothalamic LCFA-CoAs is indeed associated with increase in food intake, and increases in adiposity and body weight (3, 4, 25). Notably, ghrelin, an orexigenic factor that potently stimulates feeding, increases hypothalamic LCFA-CoA levels while inhibiting hypothalamic ACC, which reduces the malonyl-CoA level (3). Observed increases in LCFA-CoA levels suggest that the action of LCFA-CoAs, at least in ghrelin hypothalamic pathways, can dissociate from that of malonyl-CoA. In line with this prediction, we demonstrate a dissociation of the levels of LCFA-CoAs from that of malonyl-CoA under fasting and refeeding conditions. It is also worth pointing out that Arc overexpression of acyl-CoA synthetase raising LCFA-CoA levels does not induce the expected anorexigenic actions (personal communication with Dr. Jason Dyck, University of Alberta, Edmonton, AB, Canada). Together, these data strongly challenge the proposed anorectic role of Arc LCFA-CoA, and they also argue against the view that LCFA-CoAs can act as effectors of Arc malonyl-CoA-mediated anorectic actions.

Further challenge to a role of CPT-1a and LCFA-CoAs as mediators of malonyl-CoA feeding action comes from the study using compound C89b, a CPT-1 activator (1). It was expected that C89b treatment, by activating CPT-1a and thus reducing LCFA-CoA levels, would stimulate food intake. Surprisingly, the study demonstrated that C89b induced the same feeding response, i.e., an inhibition, as the increase in Arc malonyl-CoA level (1). These C89b data also directly contradict the previous finding that CPT-1a inhibition (with ST1326) reduces feeding. Because opposing actions on the same targets produce similar feeding effects, these data further suggest that CPT-1a and LCFA-CoAs are not implicated in the hypothalamic control of feeding. In support of this prediction, our results are also unfavorable for a significant role of Arc CPT-1a per se in the CNS control of feeding and body weight. In our studies, we were unable to detect significant changes of either food intake or body weight gain following Arc-specific activation of CPT-1a. Furthermore, we demonstrated that CPT-1a activity (by measuring the levels of LC-ACs) in the Arc was not significantly altered under either fasting or refeeding condition (ad libitum fed: 100 ± 17%, fasted: 104 ± 14%, refed: 112 ± 10%). Taking these findings together, Arc CPT-1a is unlikely to play a direct and key role in the central controls of feeding and energy balance.

The recent discovery of the brain-specific CPT-1 isoform, CPT-1c (26), may provide some insights into differential roles of CPT-1 isoforms in the central control of feeding and body energy balance. CPT-1c is structurally similar to CPT-1a and CPT-1b, but does not have an appreciable CPT acyltransferase activity (26, 30). Notably, CPT-1c has been implicated in the hypothalamic control of energy balance (30). Given that CPT-1c exhibits a high amino acid sequence similarity to the other CPT-1 members, those CPT-1a regulators (i.e., ST1326 and C89b) may have affected CPT-1c with the same pharmacological action, thus resulting in the same feeding effect. Furthermore, we anticipate that CPT-1c is an alternative downstream mediator in malonyl-CoA's anorectic signaling action. Indeed, our studies have provided evidence that CPT-1c is a downstream mediator of the malonyl-CoA action in leptin Arc anorectic signaling pathways (addressed in another manuscript).

Perspectives and Significance

Our data strongly suggest that the intracellular downstream pathways mediating Arc malonyl-CoA's anorectic effects induced by leptin are independent of CPT-1a. Our study thus leaves open the possibility of other target(s) as mediators of Arc malonyl-CoA anorectic signaling actions.

ACKNOWLEDGMENTS

We thank Amy Barr (University of Alberta, Alberta, Canada) for the preparation (amplification) of the recombinant adenoviruses. We thank Ken Strynadka and Thomas Panakkezhum (University of Alberta, Alberta, Canada) for the HPLC analysis of LCFA-CoAs.

GRANTS

These studies were funded by a grant from the Canadian Diabetes Association and a fellowship from Heart and Stroke Foundation of Canada (awarded to S. Gao). F. G. Hegardt, D. Serra, N. Casals, and P. Carrasco acknowledge grants from Ministry of Education and Science, Spain (Grant SAF2007-61926

to F. G. Hegardt), and from Instituto de Salud Carlos III (Grant CIBERobn CB06/03/0026 to F. G. Hegardt and research contract to P. Carrasco). G. D. Lopaschuk is a scientist of the Alberta Heritage Foundation for Medical Research.

DISCLOSURES

No conflicts of interest, financial or otherwise, are declared by the author(s).

REFERENCES

1. **Aja S, Landree LE, Kleman AM, Medghalchi SM, Vadlamudi A, McFadden JM, Aplasca A, Hyun J, Plummer E, Daniels K, Kemm M, Townsend CA, Thupari JN, Kuhajda FP, Moran TH, Ronnett GV.** Pharmacological stimulation of brain carnitine palmitoyl-transferase-1 decreases food intake and body weight. *Am J Physiol Regul Integr Comp Physiol* 294: R352–R361, 2008.
2. **Andersson U, Filipsson K, Abbott CR, Woods A, Smith K, Bloom SR, Carling D, Small CJ.** AMP-activated protein kinase plays a role in the control of food intake. *J Biol Chem* 279: 12005–12008, 2004.
3. **Andrews ZB, Liu ZW, Walllingford N, Erion DM, Borok E, Friedman JM, Tschop MH, Shanabrough M, Cline G, Shulman GI, Coppola A, Gao XB, Horvath TL, Diano S.** UCP2 mediates ghrelin's action on NPY/AgRP neurons by lowering free radicals. *Nature* 454: 846–851, 2008.
4. **Benoit SC, Kemp CJ, Elias CF, Abplanalp W, Herman JP, Migrenne S, Lefevre AL, Cruciani-Guglielmacci C, Magnan C, Yu F, Niswender K, Irani BG, Holland WL, Clegg DJ.** Palmitic acid mediates hypothalamic insulin resistance by altering PKC-θ subcellular localization in rodents. *J Clin Invest* 119: 2577–2589, 2009.
5. **Chakravarthy MV, Zhu Y, Lopez M, Yin L, Wozniak DF, Coleman T, Hu Z, Wolfgang M, Vidal-Puig A, Lane MD, Semenkovich CF.** Brain fatty acid synthase activates PPARα to maintain energy homeostasis. *J Clin Invest* 117: 2539–2552, 2007.
6. **Gao S, Kinzig KP, Aja S, Scott KA, Keung W, Kelly S, Strynadka K, Chohnan S, Smith WW, Tamashiro KL, Ladenheim EE, Ronnett GV, Tu Y, Birnbaum MJ, Lopaschuk GD, Moran TH.** Leptin activates hypothalamic acetyl-CoA carboxylase to inhibit food intake. *Proc Natl Acad Sci USA* 104: 17358–17363, 2007.
7. **Gao S, Lane MD.** Effect of the anorectic fatty acid synthase inhibitor C75 on neuronal activity in the hypothalamus and brainstem. *Proc Natl Acad Sci USA* 100: 5628–5633, 2003.
8. **Guzman-Ruiz R, Somoza B, Gil-Ortega M, Merino B, Cano V, Attane C, Castan-Laurell I, Valet P, Fernandez-Alfonso MS, Ruiz-Gayo M.** Sensitivity of cardiac carnitine palmitoyltransferase to malonyl-CoA is regulated by leptin: similarities with a model of endogenous hyperleptinemia. *Endocrinology* 151: 1010–1018.
9. **He W, Lam TK, Obici S, Rossetti L.** Molecular disruption of hypothalamic nutrient sensing induces obesity. *Nat Neurosci* 9: 227–233, 2006.
10. **Herrero L, Rubi B, Sebastian D, Serra D, Asins G, Maechler P, Prentki M, Hegardt FG.** Alteration of the malonyl-CoA/carnitine palmitoyltransferase I interaction in the beta-cell impairs glucose-induced insulin secretion. *Diabetes* 54: 462–471, 2005.
11. **Hu Z, Cha SH, Chohnan S, Lane MD.** Hypothalamic malonyl-CoA as a mediator of feeding behavior. *Proc Natl Acad Sci USA* 100: 12624–12629, 2003.
12. **Hu Z, Dai Y, Prentki M, Chohnan S, Lane MD.** A role for hypothalamic malonyl-CoA in the control of food intake. *J Biol Chem* 280: 39681–39683, 2005.
13. **Jauregui O, Sierra AY, Carrasco P, Gratacos E, Hegardt FG, Casals N.** A new LC-ESI-MS/MS method to measure long-chain acylcarnitine levels in cultured cells. *Anal Chim Acta* 599: 1–6, 2007.
14. **Lane MD, Hu Z, Cha SH, Dai Y, Wolfgang M, Sidhaye A.** Role of malonyl-CoA in the hypothalamic control of food intake and energy expenditure. *Biochem Soc Trans* 33: 1063–1067, 2005.
15. **Loftus TM, Jaworsky DE, Frehywot GL, Townsend CA, Ronnett GV, Lane MD, Kuhajda FP.** Reduced food intake and body weight in mice treated with fatty acid synthase inhibitors. *Science* 288: 2379–2381, 2000.
16. **Lopaschuk GD, Ussher JR, Jaswal JS.** Targeting intermediary metabolism in the hypothalamus as a mechanism to regulate appetite. *Pharmacol Rev* 62: 237–264, 2010.
17. **Lopez M, Lage R, Saha AK, Perez-Tilve D, Vazquez MJ, Varela L, Sangiao-Alvarellos S, Tovar S, Raghay K, Rodriguez-Cuenca S, Deoliveira RM, Castaneda T, Datta R, Dong JZ, Culler M, Sleeman MW, Alvarez CV, Gallego R, Lelliott CJ, Carling D, Tschop MH, Dieguez C, Vidal-Puig A.** Hypothalamic fatty acid metabolism mediates the orexigenic action of ghrelin. *Cell Metab* 7: 389–399, 2008.
18. **Lopez M, Lelliott CJ, Tovar S, Kimber W, Gallego R, Virtue S, Blount M, Vazquez MJ, Finer N, Powles TJ, O'Rahilly S, Saha AK, Dieguez C, Vidal-Puig AJ.** Tamoxifen-induced anorexia is associated with fatty acid synthase inhibition in the ventromedial nucleus of the hypothalamus and accumulation of malonyl-CoA. *Diabetes* 55: 1327–1336, 2006.
19. **Mao J, DeMayo FJ, Li H, Abu-Elheiga L, Gu Z, Shaikenov TE, Kordari P, Chirala SS, Heird WC, Wakil SJ.** Liver-specific deletion of acetyl-CoA carboxylase 1 reduces hepatic triglyceride accumulation without affecting glucose homeostasis. *Proc Natl Acad Sci USA* 103: 8552–8557, 2006.
20. **Mera P, Bentebibel A, Lopez-Vinas E, Cordente AG, Gurunathan C, Sebastian D, Vazquez I, Herrero L, Ariza X, Gomez-Puertas P, Asins G, Serra D, Garcia J, Hegardt FG.** C75 is converted to C75-CoA in the hypothalamus, where it inhibits carnitine palmitoyltransferase 1 and decreases food intake and body weight. *Biochem Pharmacol* 77: 1084–1095, 2009.
21. **Moran TH, Gao S.** Looking for food in all the right places? *Cell Metab* 3: 233–234, 2006.
22. **Morillas M, Gomez-Puertas P, Bentebibel A, Selles E, Casals N, Valencia A, Hegardt FG, Asins G, Serra D.** Identification of conserved amino acid residues in rat liver carnitine palmitoyltransferase I critical for malonyl-CoA inhibition. Mutation of methionine 593 abolishes malonyl-CoA inhibition. *J Biol Chem* 278: 9058–9063, 2003.
23. **Obici S, Feng Z, Arduini A, Conti R, Rossetti L.** Inhibition of hypothalamic carnitine palmitoyltransferase-1 decreases food intake and glucose production. *Nat Med* 9: 756–761, 2003.
24. **Obici S, Feng Z, Morgan K, Stein D, Karkanias G, Rossetti L.** Central administration of oleic acid inhibits glucose production and food intake. *Diabetes* 51: 271–275, 2002.
25. **Posey KA, Clegg DJ, Printz RL, Byun J, Morton GJ, Vivekanandan-Giri A, Pennathur S, Baskin DG, Heinecke JW, Woods SC, Schwartz MW, Niswender KD.** Hypothalamic proinflammatory lipid accumulation, inflammation, and insulin resistance in rats fed a high-fat diet. *Am J Physiol Endocrinol Metab* 296: E1003–E1012, 2009.
26. **Price N, van der Leij F, Jackson V, Corstorphine C, Thomson R, Sorensen A, Zammit V.** A novel brain-expressed protein related to carnitine palmitoyltransferase I. *Genomics* 80: 433–442, 2002.
27. **Sambandam N, Steinmetz M, Chu A, Altarejos JY, Dyck JR, Lopaschuk GD.** Malonyl-CoA decarboxylase (MCD) is differentially regulated in subcellular compartments by 5'AMP-activated protein kinase (AMPK). Studies using H9c2 cells overexpressing MCD and AMPK by adenoviral gene transfer technique. *Eur J Biochem* 271: 2831–2840, 2004.
28. **Schwartz MW, Woods SC, Porte D Jr, Seeley RJ, Baskin DG.** Central nervous system control of food intake. *Nature* 404: 661–671, 2000.
29. **Sebastian D, Herrero L, Serra D, Asins G, Hegardt FG.** CPT I overexpression protects L6E9 muscle cells from fatty acid-induced insulin resistance. *Am J Physiol Endocrinol Metab* 292: E677–E686, 2007.
30. **Wolfgang MJ, Kurama T, Dai Y, Suwa A, Asaumi M, Matsumoto S, Cha SH, Shimokawa T, Lane MD.** The brain-specific carnitine palmitoyltransferase-1c regulates energy homeostasis. *Proc Natl Acad Sci USA* 103: 7282–7287, 2006.
31. **Wolfgang MJ, Lane MD.** Hypothalamic malonyl-CoA and CPT1c in the treatment of obesity. *FEBS J* 278: 552–558, 2011.

CERAMIDE LEVELS REGULATED BY CPT1C CONTROL DENDRITIC SPINE MATURATION AND COGNITION

Patricia Carrasco, Ignasi Sahun, Jerome McDonald, Sara Ramirez, Jordi Jacas, Esther Gratacós, Adriana Y. Sierra, Dolors Serra, Laura Herrero, Amparo Acker-Palmer , Fausto G. Hegardt, Mara Dierssen and Núria Casals

In revision

CERAMIDE LEVELS REGULATED BY CPT1C CONTROL DENDRITIC SPINE MATURATION AND COGNITION

Patricia Carrasco[a,b], Ignasi Sahun[c], Jerome McDonald[c], Sara Ramirez[a,b], Jordi Jacas[a,b], Esther Gratacós, Adriana Y. Sierra[a], Dolors Serra[b,d], Laura Herrero[b,d], Amparo Acker-Palmer[e], Fausto G. Hegardt[b,d], Mara Dierssen[c,f] and Núria Casals[a,b]

[a]Department of Basic Sciences, Facultat de Medicina i Ciències de la Salut, Universitat Internacional de Catalunya (UIC), E-08195 Sant Cugat del Vallés, Spain.

[b]Centro de Investigación Biomédica en Red (CIBER) de Fisiopatología de la Obesidad y Nutrición (CIBERobn), Instituto de Salud Carlos III, E-28029 Madrid, Spain.

[c]Genes and Disease Program, Centre for Genomic Regulation (CRG), Parc de Recerca Biomèdica de Barcelona (PRBB), E-08003 Barcelona, Spain.

[d]Department of Biochemistry and Molecular Biology, School of Pharmacy, Universitat de Barcelona (UB), E-08028 Barcelona, Spain

[e]Institute of Cell Biology and Neuroscience and Frankfurt Institute for Molecular Life Sciences (FMLS), University of Frankfurt, Max-von-Laue-Str. 15, D-60438, Frankfurt am Main, Germany

[f]CIBER de Enfermedades RARAS (CIBERER), Instituto de Salud Carlos III, E-28029 Madrid, Spain.

Running head: CPT1C and spinogenesis

Address correspondence to: Núria Casals, Facultat de Medicina i Ciències de la Salut, Universitat Internacional de Catalunya, Josep Trueta s/n, E-08195 Sant Cugat del Valles, Spain. E-mail: ncasals@csc.uic.es

Keywords: endoplasmic reticulum, behavior, neuron, cognition, spinogenesis, sphingolipids

ABSTRACT

The brain specific isoform carnitine palmitoyl transferase 1C (CPT1C) has been implicated in the hypothalamic regulation of food intake and energy homeostasis. Nevertheless, its molecular function is not completely understood and its role in other brain areas is unknown. We demonstrate that CPT1C is expressed in pyramidal neurons of hippocampus and is located in ER throughout the neuron, even inside dendritic spines. We used molecular, cellular and behavioral approaches to determine CPT1C function. First, we analyzed the implication of CPT1C in ceramide metabolism. CPT1C over-expression in primary hippocampal cultured neurons increased ceramide levels, an effect that was blocked by treatment with myriocin, an inhibitor of the *de novo* synthesis of ceramide. Correspondingly, CPT1C knock-out (KO) mice showed reduced ceramide levels in hippocampus, mainly during fasting. At the cellular level, CPT1C deficiency altered dendritic spine morphology by increasing immature filopodia and reducing mature mushroom and stubby spines. Total protrusion density and spine head area in mature spines were unaffected. Treatment of cultured neurons with exogenous ceramide reverted the KO phenotype, as did ectopic over-expression of CPT1C, indicating that CPT1C regulation of spine maturation is mediated by ceramide. To study the repercussions of the KO phenotype on cognition, we performed the hippocampus-dependent Morris Water Maze (MWM) test on mice. Results show that CPT1C deficiency strongly impairs spatial learning. All these results demonstrate that CPT1C regulates the de novo synthesis of ceramide in ER of hippocampal neurons and this is a relevant mechanism for the correct maturation of dendritic spines and for proper spatial learning.

INTRODUCTION

Carnitine palmitoyl transferase 1 (CPT1) enzymes catalyze the conversion of long-chain acyl-CoA to acyl-carnitines, thus facilitating the transport of long-chain fatty acids across intracellular membranes. There are three isoforms: the liver isoform CPT1A (Esser,V. 1993), the muscle isoform CPT1B (Yamazaki,N. 1995) and the brain-specific isoform CPT1C (Price,N. 2002). CPT1A and CPT1B are localized in the outer mitochondrial membrane and are rate-limiting enzymes in fatty-acid beta-oxidation.

The main isoform in brain, CPT1C, highly differs from the two other isozymes. Its C-terminal region is longer than that of the other CPTs (Price,N. 2002). It is located in the endoplasmic reticulum (ER) of cells, rather than in mitochondria, and so it does not facilitate fatty acid oxidation (Sierra, A.Y. 2008). It has low CPT1 activity (Sierra, A.Y. 2008), but it binds the CPT1 physiological inhibitor malonyl-CoA with the same affinity as CPT1A (Wolfgang,M.J. 2006). Finally, CPT1C is only present in mammals and appears to stem from a relatively recent CPT1A gene duplication (Price,N. 2002). The other isozymes are expressed in such organisms as fish, reptiles, amphibians or insects. This suggests a specific role for CPT1C in more evolved brains.

At the physiological level, CPT1C contributes to the control of food intake and energy homeostasis (Wolfgang,M.J. 2006; Gao,X.F. 2009). Two independent groups developed a CPT1C KO mouse, and both lines showed decreased food intake respect to wild-type animals (WT). However, when

fed a high-fat diet, they were more susceptible to obesity and diabetes, presenting lower rates of peripheral fatty acid oxidation. All these effects were attributed to the hypothalamic function of CPT1C, since ectopic over-expression of CPT1C in hypothalamus protected mice from adverse weight gain caused by high-fat diet (Dai,Y. 2007). Moreover, the involvement of CPT1C in energy homeostasis has also been confirmed in transgenic animals over-expressing CPT1C specifically in brain (Reamy,A.A. 2011). At the molecular level, in collaboration with the group of Dr. Gary Lopaschuk, we showed that CPT1C is involved in the anorectic action of leptin, by modulating ceramide synthesis in the arcuate nucleus (ARC) of the hypothalamus (Gao,S. 2011).

Interestingly, recent findings in tumor cells showed a new, unexpected role of CPT1C in the metabolic transformations reported in tumor cell growth (Zaugg,K. 2011). The authors demonstrated that CPT1C is frequently expressed in human lung tumors and protects cancerous cells from death induced by glucose deprivation or hypoxia. The results suggest that CPT1C might provide unidentified fatty-acid derived products that would be beneficial for cell survival under metabolic stress.

However, despite these recent findings about CPT1C, little is known about its physiological role during brain development and function. The finding that CPT1C is highly expressed in hippocampus (Price,N. 2002) prompted us to look after other brain CPT1C functions beyond the control of energy homeostasis. Our results show that CPT1C is located in ER of hippocampal neurons and regulates the maturation of dendritic spines by activating the de novo synthesis of ceramide. At the behavioral level, we demonstrate for the first time that CPT1C is involved in spatial learning.

EXPERIMENTAL PROCEDURES

Construction of the targeting vector and generation of KO mice

A construct was generated using the pPNT vector (Tybulewicz,V.L. 1991). After correct recombination, this vector caused a 2.9 kb genomic deletion including exons 12 to 15. The targeting construct was electroporated into 129/SvEv embryonic stem cells (ESC) by *Centre de Biotecnologia Animal i Teràpia Gènica* (CBATEG) at the *Universitat Autonoma de Barcelona* (UAB). Two positive ESC clones were expanded and verified for correct recombination by PCR amplification and non-radioactive Southern blot analysis. CPT1C+/- cells were injected into C57BL/6J blastocyst. Chimeric mice displaying > 50% coat color chimerism were bred with C57BL/6J females to generate F1 offspring. The sixth backcrossed generation was used in all the experiments.

Animal housing

In behavioral studies, only males at 10-15 weeks of age were tested (n=12). All the behavioral testing was conducted by the same experimenters, blinded as to the genetic status of animals, in an isolated room and at the same time of day. All animal procedures met the guidelines of European Community Directive 86/609/EEC (EU directive n° 86/609, EU decree 2001-486) and Standards for Use of Laboratory Animals nº A5388-01 (NIH) and were approved by the Local Ethics Committee.

Morris water maze (MWM) Test

To test hippocampal-dependent spatial cognition, MWM was used, as described elsewhere (Arque,G. 2008). The water maze consisted of a circular pool (diameter, 1.20 m, height, 0.5 m). A white escape platform (15 cm diameter, height 24 cm) was located 1 cm below the water surface in a fixed position (NE quadrant, 22 cm away the wall). All the trials were recorded and traced with an image

tracking system (SMART, Panlab, Spain) connected to a video camera. Escape latencies, length of the swimming paths and swimming speed for each animal and trial were monitored and computed.

Cell cultures and plasmid transfection

Hippocampal cultured neurons were obtained and cultured as described elsewhere (Segura,I. 2007). For plasmid transfection, neurons were grown for 14 days *in vitro* (DIV), transfected using the Effecten kit (Quiagen), and analyzed at 15 DIV. After transfection, neurons were fixed with 4% paraformaldehyde and 4% sucrose in PBS. Samples were mounted using the Gel/Mount anti-fading medium (Biomeda).

Virus development and cell cultures infection

Two adeno-associated virus (AAV) vectors, serotype 1, AAV1-GFP, AAV1-CPT1C were constructed to drive cell expression of GFP and CPT1C respectively. Vector plasmids carried the transgene expression cassette including: the cytomegalovirus promoter; the cDNA sequence of GFP and the rat CPT1C (Price,N. 2002); the woodchuck posttranscriptional regulatory element (WPRE, acc #AY468 486) to enhance transcription (Grimm,D. 1998) ; and the bovine growth hormone polyadenosine transcription termination signal [bGH poly(A)] (bases 2326-2533 GenBank acc #M57764). The expression cassette was flanked by two inverted terminal repeats (ITRs) derived from AAV serotype 2. AAV1 vectors were produced in insect cells using baculovirus (Dentin,R. 2004). The vector preparations used in this study had titers of $1x10^{12}$ and $2.5x10^{12}$ genome copies (gc)/ml for AAV1-GFP and AAV1-CPT1C respectively.

AAV1-CPT1C virus infection was performed at 7DIV in cells cultured in six-well plates. Medium was removed and kept apart to be re-used later. 0.5 ml of neurobasal medium without B27 and containing 0.5 mM glutamine and AAV at a concentration of 100,000 virus per cell was added to each well and left to stand for 2 hours. Then, 1.5 ml of the pre-conditioned medium kept apart was added and left to stand for a further seven days. Then, cells were removed for analysis of CPT1C expression and ceramide levels. Myriocin (Sigma) treatment was performed eight hours before cells recollection.

Immunodetection in brain sections and cultured cells

Coronal sections (30µm) from adult mouse forebrains were incubated with primary antibodies against GFAP (1/500, Chemicon MAB360) and CPT1C (1/100) overnight at 4 ºC, washed three times in PBS 0.1 M and incubated for two hours with secondary antibodies coupled to fluorochromes Alexa 488 (for green fluorescence) and Alexa 568 (for red fluorescence) at a dilution 1/500. In cultured neurons, anti-calreticulin polyclonal antibody (BD Biosciences) was used at a dilution 1/50 for 1 hour at 37ºC, and for the red fluorescence, the secondary antibody goat anti-mouse Alexafluor 546 (Molecular Probes) (1/500) was used. Sections and coverslips were mounted with Mowiol and observed using a Confocal Leica TCS SP2 (Leica Lasertechnik GmbH, Mannheim Germany).

Image analysis and quantification of dendrite spine density

Images were acquired using a digital camera (SpotRT, Diagnostic Instruments) attached to an epifluorescence microscope (Zeiss) equipped with a 63x objective (Plan-Apochromat, Zeiss). All quantitative measurements were carried out using MetaMorph software (Molecular Devices). Approximately 100 dendrites from independent transfections were randomly selected for each construct to quantify number of protrusions in proximal 50-mm sections of dendrites. Lengths of protrusions were determined by measuring the distance between the tip and the base.

Western blot analysis

Rabbit antibodies against the *c-ter* region of mouse CPT1C were as described elsewhere (Sierra,A.Y. 2008). Generally, 60 μg protein extracts were subjected to SDS-PAGE. A 1:2000 dilution of anti-CPT1C primary antibodies and a 1:5000 dilution of secondary antibody were used. The blots were developed with the ECL Western blotting system (Amersham Biosciences).

Ceramide quantification

Ceramides were extracted and analyzed *via* an LC-ESI-MS/MS System (API 3000 PE Sciex) in positive ionization as described elsewhere (Merrill,A.H.,Jr 2005). Their concentrations were measured by MRM experiments using N-heptadecanoyl-D-*erytro*-sphingosine (C17-ceramide) as internal standard (50 $ng \cdot mL^{-1}$). The method was linear over the range from 2 to 600 $ng \cdot mL^{-1}$.

Statistics

Data are expressed as means ± SEM. Statistical significance was determined by Student's *t*-test for the difference between two groups, or one-way ANOVA with Bonferroni test for *post hoc* analysis for more than two groups. Performance in the rotarod and MWM tests were compared using repeated measures ANOVA. Values of $P<0.05$; $P<0.005$; $P<0.001$ were considered significant.

RESULTS

CPT1C is located throughout the ER of hippocampal neurons, even penetrating into dendritic spines.

It was previously described that CPT1C was highly expressed in hippocampus (Price,N. 2002). In order to determine the precise localization of the protein, we performed brain sections and incubated them with a anti-CPT1C antibody, kindly provided by Wolfgang laboratory and previously used in the literature (Dai,Y. 2007; Sierra,A.Y. 2008). Fig 1A clearly shows that CPT1C (in green) is expressed in pyramidal neurons of hippocampus. Astrocytes were identified by GFAP (glial fibrillary acidic protein, an astrocyte marker) antibody.

To analyze the detailed localization of CPT1C in hippocampal neurons, we performed neuronal primary cultures and transfected them with CPT1C-EGFP, a plasmid that encodes CPT1C fused to the N-terminal region of EGFP (green fluorescence protein) (Sierra,A.Y. 2008). Fig 1B shows that CPT1C is located throughout the neuron, in neuronal bodies and dendrites. Detailed photos of dendrites demonstrate that CPT1C is present mainly in shafts but also in spines (marked with arrows). The same cultures were transfected with pDS-Red (Clontech) that encondes the *Discosoma sp.* red fluorescent protein in the cytosol, to display the outline of the cell.

Finally, to confirm that sub-cellular localization of endogenous CPT1C was the ER, we transfected the cultured neurons with pDs-ER-Red2 (Clontech) that stains the ER red, and immunodetected endogenous CPT1C with anti-CPT1C antibody (in green). Fig 1C shows that CPT1C is localized in ER of cultured hippocampal neurons. We also performed double immunodetections with anti-CPT1C (in green) and anti-calreticulin (in red) antibodies. Fig 1D shows complet co-localization of these two proteins, confirming that CPT1C localizes to the ER membrane of neurons.

CPT1c facilitates the* de novo *synthesis of ceramide

Our group has recently reported that CPT1C regulates ceramide synthesis in arcuate nucleus of hypothalamus as part of the signal pathway of leptin (Gao,S. 2011). We wanted to examine whether CPT1C was also regulating ceramide levels in hippocampal neurons and determine the metabolic pathway implicated. We over-expressed CPT1C in primary hippocampal neurons using AAV1-CPT1C viruses. A four-fold increase in CPT1C protein levels (Fig 2A) resulted in a two-fold increase in ceramide levels with respect to control cells (cells infected with AAV1-GFP) (Fig 2B). CPT1C over-expression mainly increased saturated ceramides (C16:0, C18:0 and C20:0). Ceramides in Fig 2B are represented in percentage respect the control (cells transfected with AAV1-GFP), but ceramide C18:0 was the most abundant one in the hippocampal cultures (average concentration of 1 ng per µg of protein), being twenty times more concentrated than the rest.

As ceramide present in ER comes mainly from *de novo* synthesis, we examined whether CPT1C was regulating this pathway. We treated transduced cells with 10 µM myriocin for 8 hours. This is an inhibitor of serine palmitoyltransferase (SPT), the first enzyme in the *de novo* synthesis of ceramide. Fig 2C shows that treatment of cultured cells with myriocin blocked the increase in levels of C18:0 and C16:0 ceramides induced by CPT1C over-expression. As C18:0 is the predominant ceramide in these cells, we can conclude from the results that CPT1C facilitates the *de novo* synthesis of ceramide in hippocampal neurons.

CPT1C KO mice have reduced ceramide levels in hippocampus

To examine whether CPT1C is involved in the regulation of hippocampal ceramide synthesis in adult mice, we developed a CPT1C KO mouse (Fig S1) and measured ceramide levels in hippocampus from *ad libitum* and fasted mice. CPT1C KO mice showed lower ceramide levels in hippocampus than WT animals, mainly during fasting (Fig 3). In parallel to hippocampal cultures, the most abundant ceramide found in hippocampus was the C18:0 ceramide, being also about twenty times more abundant than the rest, which agrees with previous literature that says major ceramide in brain neurons is C18:0 (Ben-David,O. 2010). Importantly, C18:0 ceramide was reduced in KO mice during fasting, when it is known that malonyl-CoA concentration (the physiological inhibitor of CPT1 enzymes) is highly reduced (Tokutake 2010), suggesting that CPT1C activity is modulated by malonyl-CoA.

CPT1c deficiency increased filopodia density and reduced spine maturation in hippocampal neurons

To examine the effects of CPT1C deficiency on dendrite spine density and morphology, we performed primary hippocampal cultures from CPT1C KO and WT mice, transfected the neurons with green fluorescent protein (GFP) and examined dendritic spines at 15 DIV. Neurons from CPT1C KO mice had the same protrusion density but larger protrusion length than WT neurons (Fig 4A-C). Morphological analysis revealed that CPT1C KO mice had a strong increase in filopodia number and a marked reduction of mature (mushroom and stubby) spines (Fig 4D-G). However, the spine head area in mature spines was the same in both genotypes. Over-expression of CPT1C on KO cultures reduced filopodia density and increased the percentage of mature spines to values similar to WT cultures (Fig 5B,C), confirming the requirement of CPT1C for efficient spine maturation.

Ceramide treatment rescues CPT1C KO phenotype on spine morphology

To corroborate that the reduction in ceramide synthesis caused by CPT1C deletion is the cause of the spine phenotype we set up a rescue experiment in which CPT1C KO hippocampal cultures were

incubated with 1.5 μM of soluble C-6 ceramide for seven days (from 8 to 15DIV). The ceramide doses used (< 3μM) does not induce neuronal apoptosis in hippocampal cultures (Mitoma,J. 1998). Exogenous ceramide treatment reversed the CPT1C KO phenotype by decreasing immature filopodia and restoring mature spine density to normal levels (Fig 5A,C). These results indicate that CPT1C regulation of spine maturation is mediated by ceramide.

CPT1C KO mice had impaired spatial learning

To examine the spine maturation defects on cognition, we performed the Morris water maze (MWM) test. This test is usually used to measure hippocampus-dependent spatial navigation learning in mice. In the MWM, CPT1C KO showed significantly higher escape latency during (delayed learning) during the ten sessions of the acquisition phase (Fig 6A, B). The learning curves were significantly different from WT mice [repeated measures ANOVA $F(1.22)=6.726$, $p=0.017$] in the absence of swimming speed alteration, indicating pure learning impairment, with poorer performance not associated with motor deficits (Fig 6C). Moreover, in the cued session, where the platform is visible (black flag), the escape latency of CPT1C KO mice was similar to the WT (Fig 6A)

To test visuospatial memory, the platform was removed and the time spent in each quadrant was measured. No significant differences between genotypes were detected in the preference for the trained, quadrant indicating that once the platform position was learned, it was equally retained in CPT1C KO and WT mice (Fig 6D); the CPT1C KO deficits seem to be limited to the learning phase.

In the reversal test (Fig 6E), which evaluates the ability of the mice to learn a new platform position (cognitive flexibility), no significant differences were observed between genotypes in the percentage of time spent in the previously trained quadrant [(NE): repeated measures ANOVA, $F(1.22)=0.086$, $p=0.772$]. However, KO mice spent less time in the new goal quadrant [(SW): repeated measures ANOVA, $F(1.22)=8.676$, $p=0.007$], thus supporting the hypothesis of a hippocampal-dependent learning deficit in CPT1C KO mice.

DISCUSSION

Dendritic spine formation begins in the embryo and continues into early postnatal life, but also occurs in the adult organism, where it contributes significantly to learning and memory formation. We demonstrate that the brain isoform CPT1C is present in dendritic spines and regulates the *de novo* synthesis of ceramides in neurons, which is key to the transformation of dendritic filopodia into mature spines. This is the first time that CPT1C or ceramide synthesis has been directly involved in spine morphogenesis. At the physiological level, we show for the first time that CPT1C is involved in spatial learning.

CPT1C activates the* de novo *synthesis of ceramide

One of the relevant contributions of this study is the confirmation that CPT1C facilitates *de novo* synthesis of ceramide. We had previously described it in the ARC nucleus of hypothalamus (Gao,S. 2011), and we now demonstrate it in hippocampal cultured neurons. It may be a general phenomenon in neurons. We do not know the molecular mechanism by which CPT1C activates ceramide synthesis but two possible hypotheses can be discussed. The first is that CPT1C facilitates the entry of acyl-CoAs to the lumen of ER, preventing them from being used in other metabolic pathways in the cytosol, and enhancing the *de novo* synthesis of ceramides. In support of this hypothesis is the previously reported

canitine -dependent acyl-CoA transport across ER membrane (Arduini,A. 1994; Abo-Hashema,K.A. 1999; Gooding,J.M. 2004). Given that fatty acids are shared with multiple lipid metabolic processes, the localization of substrates and their shunting between competing pathways may have important roles in sphingolipid metabolism, as discussed elsewhere (Breslow,D.K. 2010). The second hypothesis is that CPT1C regulates, by protein-protein interaction, other enzymes from ceramide metabolism. Then, under fasting conditions or reduction of malonyl-CoA levels, CPT1C might change its conformation and activate other enzyme involved in the *de novo* synthesis of ceramide, like SPT or ceramide synthase (CerS). The fact that CPT1C has low catalytic activity *in vitro* (Sierra, A.Y. 2008; Wolfgang,M.J. 2006) is consistent with this second hypothesis.

CPT1C in dendritic spine maturation

Our results implicate CPT1C in dendritic spine maturation. In absolute numbers, in cultured hippocampal neurons from CPT1C KO mice, the increase in filopodia corresponds with the decline in mature spine number, without altering the overall density of dendritic protrusions, which indicates that CPT1C is not necessary for the formation of new protrusion. However, it is necessary for the conversion of filopodia into mature spines. In addition, results show that the effect of CPT1C on dendritic spines is mediated by ceramide. Ceramide addition to the cultured media at low concentration reversed the CPT1C KO phenotype and induced spine maturation. A recent study demonstrates the presence of a new long-chain acyl-CoA synthetase (ACSL4) isoenzyme that localizes specifically in ER of neurons. Its deficiency increases the percentage of filopodia and reduces the percentage of mature spines. (Meloni,I. 2009), correspondingly with our results. This highlights the importance of fatty-acid metabolism in spinogenesis and suggests that ACSL could provide the substrate necessary for ceramide synthesis in the ER of neurons.

There is only one study that correlates ceramide with the formation of dendritic spines (Hering,H. 2003). The authors report that coupled inhibition of cholesterol and ceramide synthesis causes alterations in the density and morphology of dendritic spines. Our work sheds light on the regulation of this process and identifies a role for CPT1C in the fine-tune modulation of ceramide synthesis, which is essential for the maturation of dendritic spines. The mechanism by which ceramides regulate spine maturation is unknown. However, ceramide binds to and regulates the activity of enzymes and signaling proteins such as kinases, phosphatases or membrane receptors (Breslow,D.K. 2010). One example is protein phosphatase 1 (PP1), which is activated by ceramide (Chalfant,C.E. 1999) and has been implicated in the conversion of filopodia into mature spines (Terry-Lorenzo,R.T. 2005). In addition, ceramide is the building block of all cellular sphingolipids which, in addition to cholesterol, are essential components of lipid rats. These membrane microdomains are needed for the correct trafficking, anchorage and activity of synaptic proteins and are preferred platforms for membrane-linked actin polymerization (Allen,J.A. 2007). All these phenomena are necessary for synapse stability and maturation of dendritic spines. So, the diminished ceramide levels found in CPT1C KO mice could alter the regulation of specific proteins or alter the formation of lipid rafts needed for synapse consolidation and spine maturation.

Physiologic relevance of CPT1C

CPT1C deficient mice present spatial learning impairment, with a clear delay in the acquisition phase, although they eventually learn and remember the location of the platform. It is important to emphasize that CPT1C deficiency does not affect swimming velocity or motivation, and that longer acquisition times correspond to learning deficiencies. On the other hand, memory and cognitive flexibility (ability to modify behavior in an increasingly demanding cognitive task) are not altered in

CPT1C KO mice. This indicates that CPT1C deficiency affects the process of consolidating new information, but not retention or extinction. This phenotype could be directly related with the impaired dendritic spine maturation found in CPT1C KO mice and with the intact spine head area of matures spines found in both genotypes**.** In cognitive sciences, it is accepted that spine-volume changes regulate new memory acquisition by enlarging and stabilizing smaller spines while the existing-memory persistence depends on changing volumes of larger spines (Kasai,H. 2010). In addition, in human patients and most animal models of mental retardation, dendritic spines tend to be abnormally small and immature.

Results from our work show that CPT1C has other physiological roles apart from the regulation of food intake and energy homeostasis. We demonstrate that the molecular function of CPT1C is the fine-tune regulation of the *de novo* synthesis of ceramide in neurons, which is need for spine maturation during brain development. At the behavioral level, we demonstrate for the first time the involvement of CPT1C in learning, which opens the possibility that CPT1C mutations might be the cause of some human cognition disabilities of unknown etiology.

AKNOWLEDGEMENTS

The editorial help of Robin Rycroft is gratefully acknowledged. The authors thank Josep Clotet for valuable discussions and Julia Geiger for technical support in cell cultures. This study was supported by grants SAF2007-61926 from the *Ministerio de Educación y Ciencia*, Spain; and by grant from *Fundació La Marató de TV3* (2007), Catalunya. A.Y.S. and P.C. were recipients of fellowships from Universitat Internacional de Catalunya. Present affiliation of A.Y.S. is: Ciencias de la Salud. Universidad Metropolitana, 50-576 Barranquilla, Colombia. CIBERobn and CIBERER are initiatives of ISCIII.

FIGURE LEGENDS

Figure 1: CPT1C location in hippocampal neurons. A. CPT1C is present in neurons of hippocampus, mainly pyramidal cells. Brain sections were double immunodetected with anti-CPT1C antibody (green) and anti-GFAP antibody (red). **B**. Hippocampal cultured neurons were double transfected with CPT1C-EGFP and pDS-Red at 11 DIV and visualized at 15 DIV. Images show that CPT1C is present in neuronal body, dendritic shaft and spines (marked with arrows). pDs-Red transfection was performed to display the outline of the neuron. **C**. Hippocampal cultured neurons were transfected with pDS-ER-Red to stain the ER. At 15 DIV, cells were immunodetected with anti-CPT1C antibodies (green). The merge image (yellow) demonstrates that CPT1C is localized to the ER membrane. **D**. Cultured neurons were double immunodetected with anti-CPT1C (green) and anti-calreticulin (red) antibodies. Nucleuses were stained with DAPI (blue). Yellow color in the merge image demonstrates that CPT1C co-localizes with calreticulin (ER marker).

Figure 2: Levels of ceramides in hippocampal neurons transduced with AAV-CPT1C. A. CPT1C expression was analyzed by Western blot with anti-CPT1C antibodies. Cell lysates from AAV-GFP and AAV-CPT1C transductions were analyzed. **B**: Levels of ceramides in hippocampal neurons transduced with AAV-GFP (as a control) and AVV-CPT1C at 7DIV. Cells were collected at 14DIV and analysed by HPLC-MS/MS. Data are represented as percentage respect to control cells (AAV-GFP). **C**. Levels of ceramides in hippocampal neurons transduced with AAV-GFP or AAV-CPT1C at 7DIV and treated with 10 μM of myriocin at 14DIV for 8 h. Then, cells were collected and analysed by HPLC-MS/MS. Data

represent the fold induction (in percentage) of ceramides levels in cells transduced with AVV-CPT1C and treated with or without myriocin respect the control cells (AAV-GFP transduced cells) treated with or without myriocin. Error bars are s.e.m.; * P<0.05. Student's *t* tests were used to assess statistical significance of the differences.

Figure 3: Ceramide levels in hippocampus from *ad libitum* and fasted CPT1C KO and WT mice. Fasted mice were deprived of food for 15 h. Different ceramide species were measured: ceramide C16:0, ceramide C18:0, ceramide C18:1, ceramide C20:0 and ceramide C24:1. Data are represented as percentage respect to fed WT mice. Error bars are s.e.m. N=6; * P<0.05, ** P<0.005, *** P<0.001, ANOVA test.

Figure 4. Dendritic spine density and morphology from CPT1C KO and WT hippocampal neurons. Hippocampal neurons were transfected (12DIV) with pEGFP to visualize the outline of the cell. Protrusions were analyzed two days after transfection. Protrusion density (**A**) and protrusion length (**B, C**) were measured. "A" indicates mature spines and "B" indicates filopodia. Spine morphology (**D-F**) was assayed by analysis of types of protrusions: filopodia (without head), mushroom (with head plus neck) and stubby (with only head). **G**. Percentage of mature spines (mushroom plus stubby) relative to the total number of protrusions was also measured. **H**. Spine head area was measured in mushroom and stubby spines. **I**. A representative image of dendritic spines from WT and CPT1C KO neurons. For the quantification of protrusion density, spine length and morphology approximately 100 dendrites from independent transfections were selected randomly. Student's *t* tests and ANOVA post hoc were used to assess statistical significance of the differences. (Error bars are s.e.m., * P<0.05; ** P<0.005; *** P<0.001).

Figure 5. Rescue of CPTC KO pheonotype on spine morphology by CPT1C expression or ceramide treatment. A. Hippocampal neurons were transfected with pIRES-CPT1C at 7 DIV and analyzed for spine morphology at 14 DIV. pIRES-CPT1C vector expresses both CPT1C and GFP proteins, which permit to visualize in green the cells over-expressing CPT1C. **B**. Hippocampal neurons treated with 1.5 µM C6-ceramide at 7DIV and transfected with GFP at 12DIV, fixed and analyzed for the morphology of dendritic protrusions at 14DIV. **C.** A representative image of dendritic spines from WT, KO, KO mice treated with C6-ceramide, and KO mice transfected with pIRES-CPT1C. For the quantification of spine morphology approximately 100 dendrites from independent transfections were selected randomly. Student's *t* tests and ANOVA post hoc were used to assess statistical significance of the differences. (Error bars are s.e.m., * P<0.05; *** P<0.001)..

Figure 6. : Spatial memory measured by MWM test. A. MWM performance of CPT1C KO and WT mice during the learning sessions as latency (s) to find the platform along the acquisition phase (A), removal (Rem) and cued sessions (Cue); Data are represented as mean $\pm$ s.e.m; * P<0.05, ANOVA; PT, pre-training. **B**. Visual pathway traced by all animals. White round platform is located in the northeast (NE) quadrant. **C**. Mean swimming speed along acquisition sessions. **D.** Percentage of time spent in the target quadrant (NE) during the removal session; discontinuous lines represent the chance level in this session. **E**: percentage of permanence in quadrants during the reversal (REV) session. Data are represented as mean $\pm$ s.e.m.; * P<0.05, ** P<0.01, *** P<0.001, ANOVA test.

Figure 1

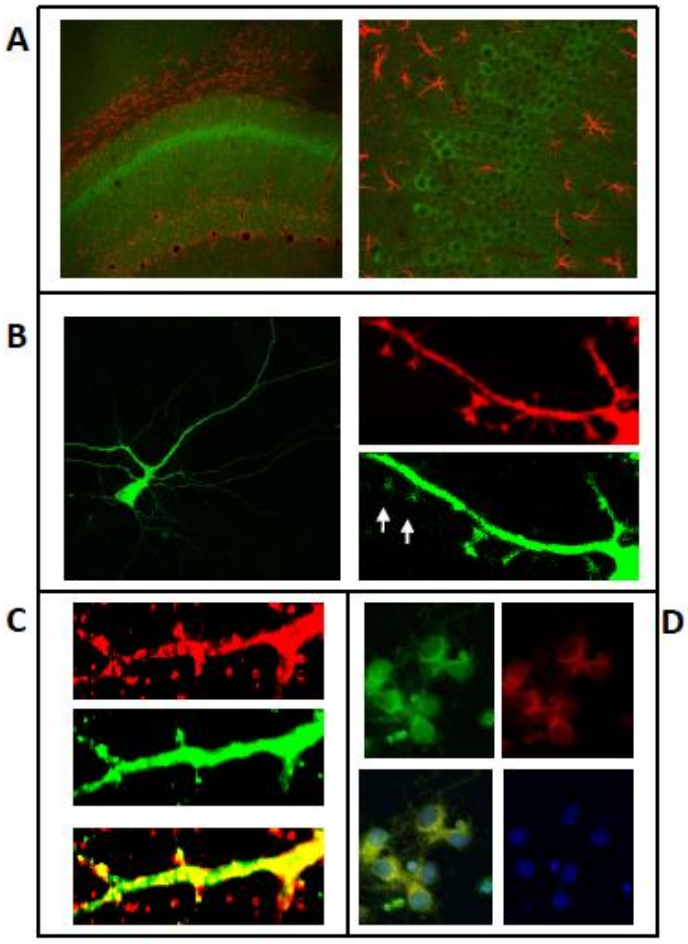

Figure 2

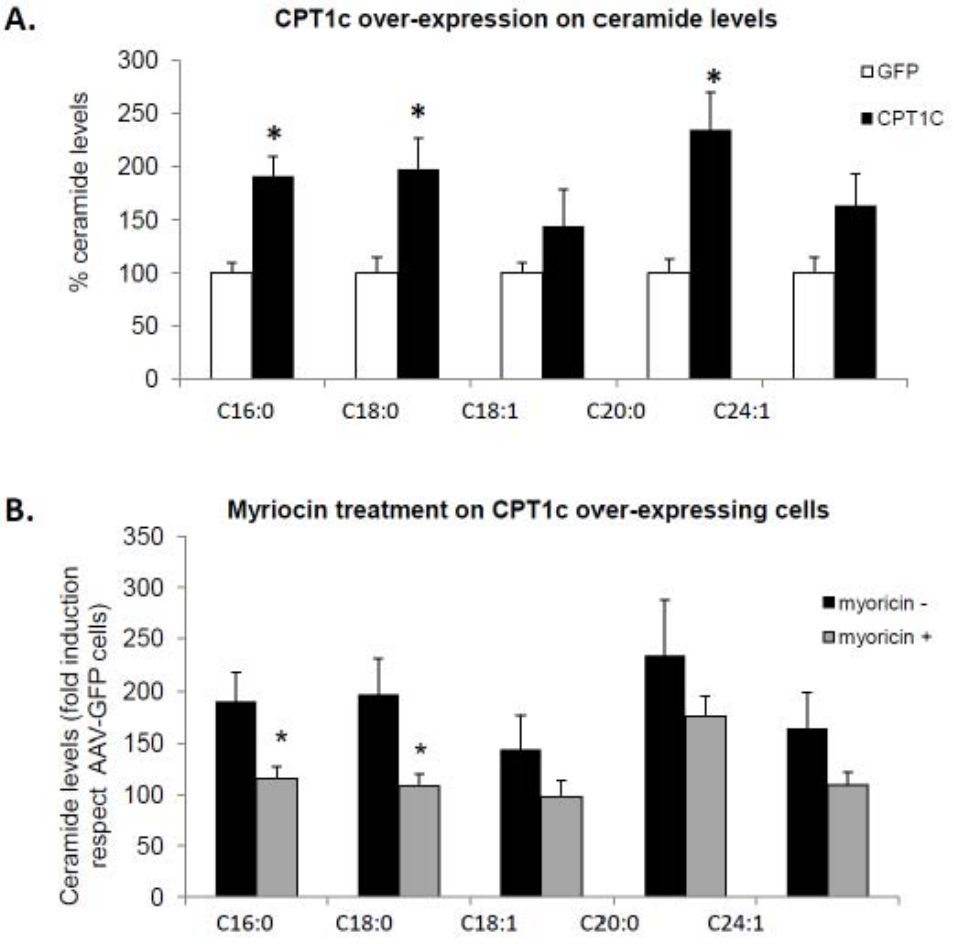
A.
CPT1c over-expression on ceramide levels
% ceramide levels
300
250
200
150
100
50
0
GFP
CPT1C
*
*
*
C16:0
C18:0
C18:1
C20:0
C24:1
B.
Myriocin treatment on CPT1c over-expressing cells
Ceramide levels (fold induction respect AAV-GFP cells)
350
300
250
200
150
100
50
0
myoricin -
myoricin +
*
*
C16:0
C18:0
C18:1
C20:0
C24:1

Figure 3

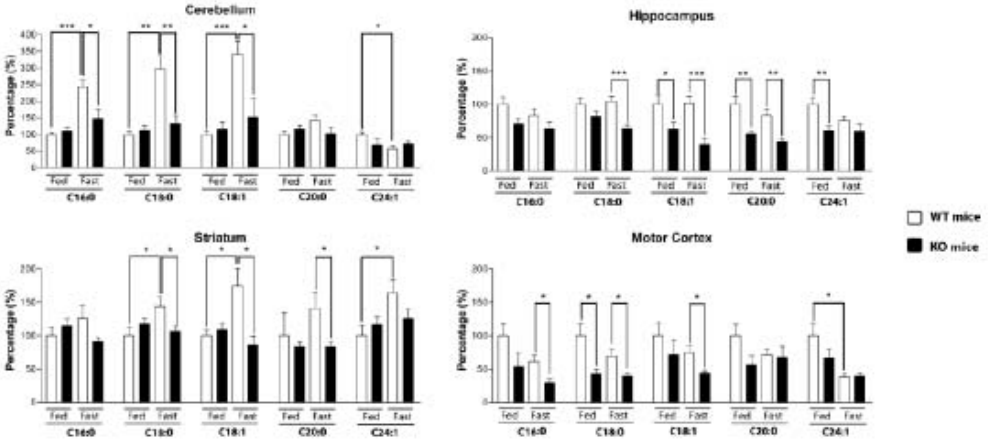
Cerebellum
Hippocampus
Striatum
Motor Cortex
Percentage (%)
Fed
Fast
C16:0
C18:0
C18:1
C20:0
C24:1
WT mice
KO mice

Figure 4

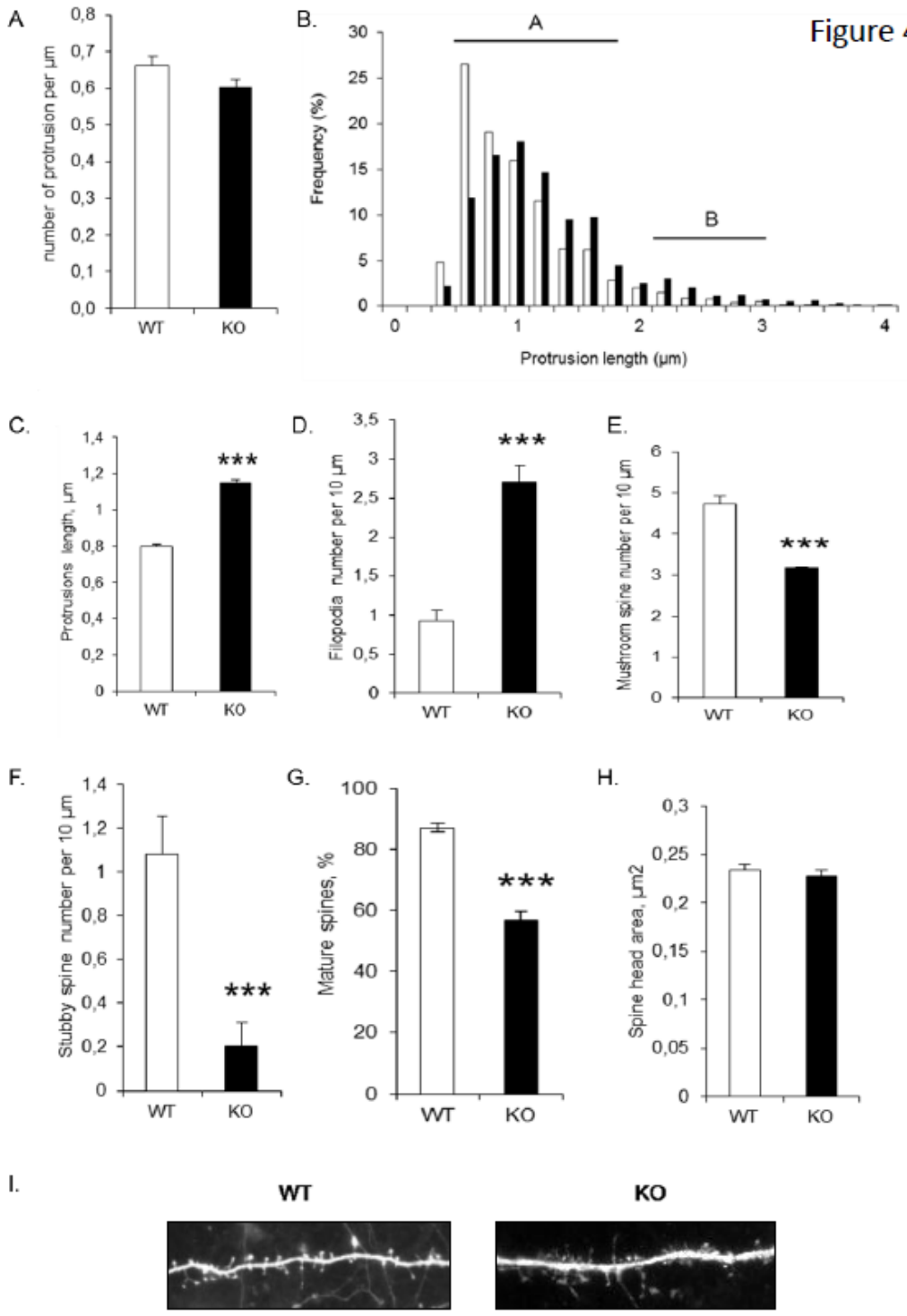
A
number of protrusion per µm
0,8
0,7
0,6
0,5
0,4
0,3
0,2
0,1
0,0
WT
KO
B.
A
B
Frequency (%)
30
25
20
15
10
5
0
0
1
2
3
4
Protrusion length (µm)
C.
Protrusions length, µm
1,4
1,2
1
0,8
0,6
0,4
0,2
0
***
WT
KO
D.
Filopodia number per 10 µm
3,5
3
2,5
2
1,5
1
0,5
0
***
WT
KO
E.
Mushroom spine number per 10 µm
6
5
4
3
2
1
0
***
WT
KO
F.
Stubby spine number per 10 µm
1,4
1,2
1
0,8
0,6
0,4
0,2
0
***
WT
KO
G.
Mature spines, %
100
80
60
40
20
0
***
WT
KO
H.
Spine head area, µm2
0,3
0,25
0,2
0,15
0,1
0,05
0
WT
KO
I.
WT
KO

Figure 5

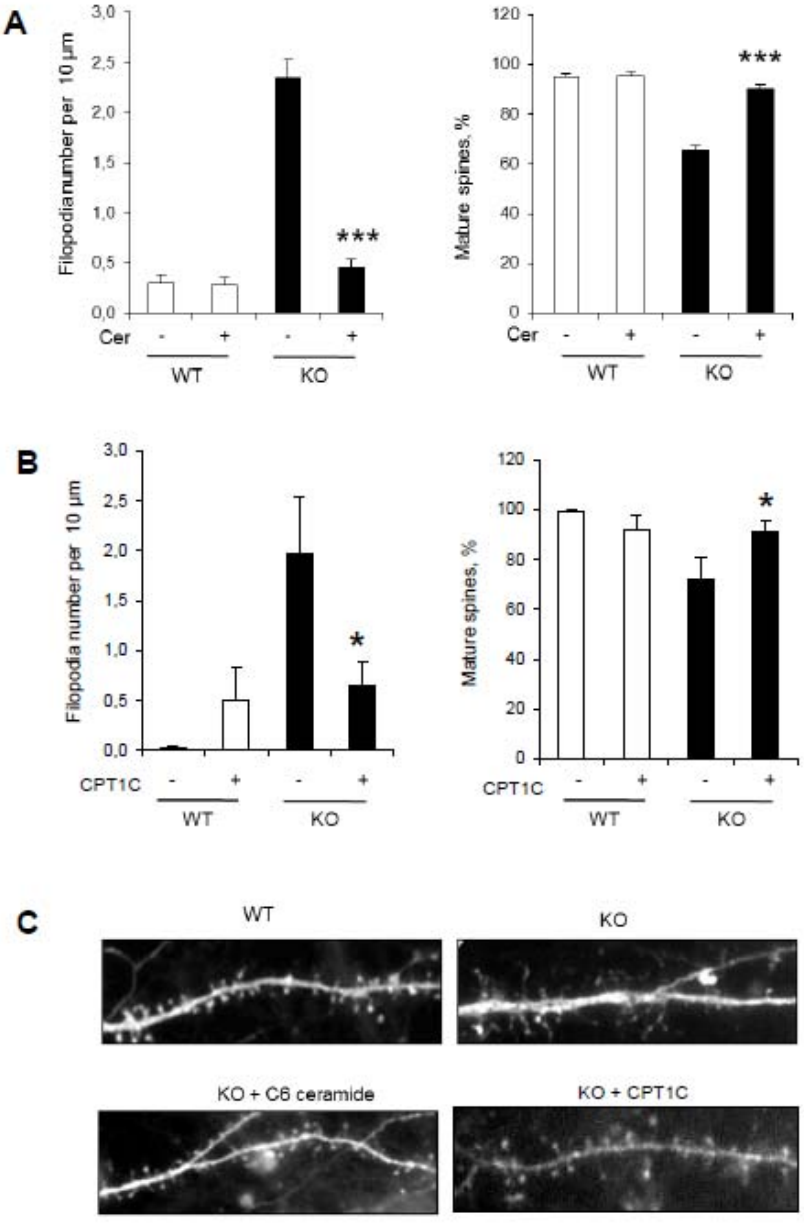
A
Filopodia number per 10 µm
3,0
2,5
2,0
1,5
1,0
0,5
0,0
***
Cer - + - +
WT
KO
Mature spines, %
120
100
80
60
40
20
0
***
Cer - + - +
WT
KO
B
Filopodia number per 10 µm
3,0
2,5
2,0
1,5
1,0
0,5
0,0
*
CPT1C - + - +
WT
KO
Mature spines, %
120
100
80
60
40
20
0
*
CPT1C - + - +
WT
KO
C
WT
KO
KO + C6 ceramide
KO + CPT1C

Figure 6

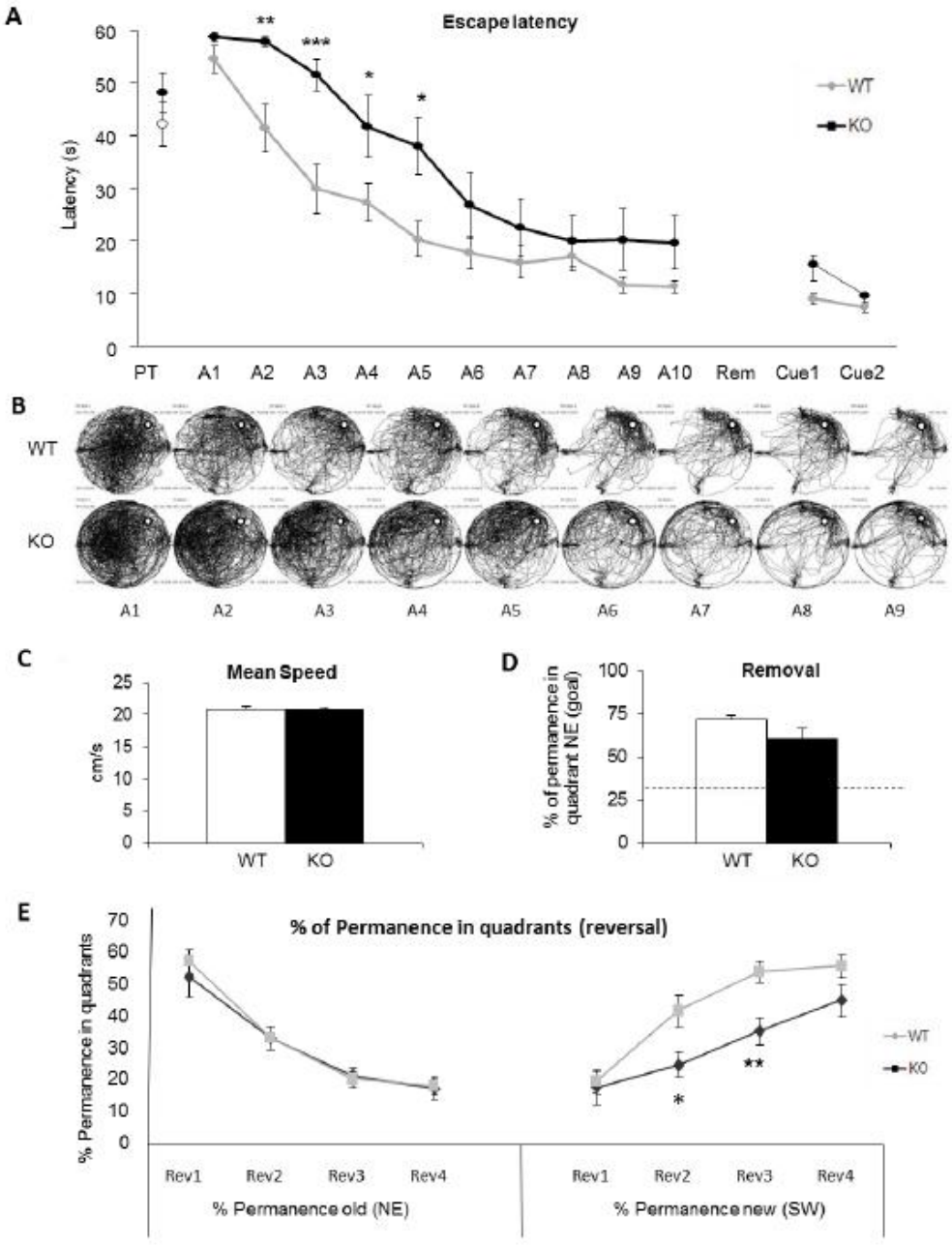
A
Escape latency
Latency (s)
WT
KO
PT
A1
A2
A3
A4
A5
A6
A7
A8
A9
A10
Rem
Cue1
Cue2
B
WT
KO
C
Mean Speed
cm/s
D
Removal
% of permanence in quadrant NE (goal)
E
% of Permanence in quadrants (reversal)
% Permanence in quadrants
Rev1
Rev2
Rev3
Rev4
% Permanence old (NE)
% Permanence new (SW)